THE UNIVERSITY
of EDINBURGH

The Cycling of Dissolved and Particulate Organic Matter in the Ocean West of the Antarctic Peninsula

Ribanna Dittrich

Thesis submitted for the degree of Doctor of Philosophy

School of Geosciences

The University of Edinburgh

2019

Declaration

I certify that this thesis has been composed solely by myself and that it has not been submitted, in whole or in part, in any previous application for a degree. Except where it states otherwise by reference or acknowledgment, the work presented is entirely my own.

……..……..

Ribanna Dittrich

Edinburgh, June 28th 2019

Thesis Abstract

Dissolved organic matter (DOM) in the oceans stores as much carbon as the atmosphere for thousands of years. However, our understanding of production, transformation and removal processes of DOM is still incomplete. At the West Antarctic Peninsula (WAP), rapid warming led to increased atmospheric and oceanic temperatures during the second half of the 20th century with reduced sea-ice cover and increased glacial melting. The WAP supports a productive ecosystem with intense primary production during the austral spring and summer when solar radiation is high and sea ice cover is reduced. Research on dissolved organic matter in this region is scarce. Concentrations of DOM here are low compared to lower latitudes but reasons for this remain unclear and the cycling of DOM is not fully understood. Because of the recent climate change in this region, its geographical distance from anthropogenic sources and the distinct seasonality of the ecosystem's productivity, the WAP represents an ideal location to study processes involved in autochthonous DOM dynamics.

This thesis integrates a suite of biogeochemical and physical data to develop an understanding of dissolved organic carbon (DOC) and nitrogen (DON) cycling at the WAP. Samples have been collected for spatial analysis with the U.S. led Palmer Longterm Ecological Research Program (PAL LTER) cruise team in 2017 and samples for temporal analysis are available from the UK's Rothera Research Station as part of the Rothera Time Series (RaTS) from 2013 to 2016. In combination with other available physical, biogeochemical and biological data, processes driving the distribution and cycling of DOM over a range of spatial and temporal timescales are investigated.

The temporal analysis from the RaTS data found DOC production occurring alongside particulate organic carbon production contrasting earlier studies where DOM production was found to occur later with a time lag of a few days to weeks. This thesis shows that DOC is produced and released directly by phytoplankton while DON shows more variable results. This might be due to high rates of DON cycling by both bacteria and phytoplankton.

The spatial analysis (PAL LTER) confirmed earlier studies showing low concentrations of dissolved organic carbon and nitrogen. There is more variability and slightly higher concentrations of DOM in coastal waters compared to offshore regions. This is potentially due to higher primary production and bacterial responses but could also be affected by the introduction of glacial meltwater. DON correlates well with bacterial activity while DOC can be related to either bacterial or phytoplankton activity showing the different mechanisms affecting both DOC and DON production and removal. At stations with high bacterial activity in the surface waters, DOC and DON concentrations were found to be high but decrease rapidly with increasing depth. Due to a temporal offset in the retreat of sea ice from the open ocean towards the shore, the sampled stations are found to be at different stages of the phytoplankton bloom which is reflected in the biogeochemical data including DOC and DON concentrations.

Particulate and dissolved organic matter cycling is coupled to some extent. DOC appears to be produced during the development of the first phytoplankton bloom of each season but is decoupled from direct production of POC thereafter, possibly due to bacterial removal and production processes. DOC and DON are highly decoupled throughout the investigated seasons and across the WAP shelf. The C and N isotopic compositions of particulate organic matter in both the spatial and the temporal data sets confirm intense upper-ocean recycling of organic matter with little export to greater depths. Further, the N-isotopic composition shows that nitrification plays an

important role in the upper ocean at the WAP with nitrified nitrate and potentially ammonium being produced and taken up by phytoplankton at the later stage of phytoplankton activity.

Ammonium measurements were only available for the RaTS data sets but show that the seasonal variability is intense. Increased production of ammonium in the upper ocean is related to lowered DON concentrations showing rapid ammonification.

The contribution by meltwater from both glaciers and sea ice was analysed. While direct contributions of DOM from these sources are likely, they are suggested to be minor due to intense dilution with seawater. However, indirectly, DOM dynamics are likely affected intensely by the addition of sea-ice algae, bacteria, particulate organic matter and nutrients and effects on the physical structure of the water column, all of which can affect the production, transformation and removal of DOM.

This thesis shows that processes driving DOC and DON dynamics are complex in the ocean of the WAP. There are different processes acting on DOM compounds in different regions of the WAP at different timescales. DOM produced at the WAP seems to be of a highly labile nature, supported by low DOC:DON ratios overall. High surface DOM concentrations decreased rapidly with depth which shows high rates of bacterial degradation. These findings suggest that if DOM production increases in this region, as projected by various studies due to a warming climate and increased meltwater addition, upper-ocean cycling of carbon and nitrogen might increase while carbon export decreases.

This thesis contributes to our understanding of carbon and nitrogen cycling in high-productivity Southern Ocean shelf environments with implications for the functioning of the regional biological carbon pump.

Acknowledgments

First of all, I would like to thank my supervisor Dr Sian Henley for her support and help throughout the last 3.5 years of this doctoral experience. Thank you for helping me to shape the academic in me. Thank you for making it possible to collect my own samples in Antarctica, for your guidance and help in the lab, for your readiness and willingness for discussions and probably a lot of silly questions you answered without the bat of an eyelid. I would also like to thank Prof Hugh Ducklow for making my precious time in the field possible and for his valuable contributions and support via e-mail but especially for coming to Edinburgh for some intense data discussions.

I further thank Prof Raja Ganeshram for his support and help to steer my data interpretations into the right directions. Thanks also go to Dr Greg Cowie for his help in the processes involved in the lab and the open discussions about the possibilities of analyses in his lab. Mike Meredith – Thank you for providing some very useful and important data and help and for always replying to my e-mails incredibly promptly.

From here, I extent my gratitude to Steve Mowbray and Colin Chilcott who devoured a lot of their instrument time – and their own – to help me analysing the endless amount of samples and for always being happy to answer a lot of questions, coming up with alternatives and giving me ideas for more. I'd also like to say thanks to Clare Peters who helped me out a lot in setting up experiments and who provided me with materials when necessary.

My gratitude goes to the National Environmental Research Council, the funding body of this whole project. Further, a big thank you goes to the U.S. National Science Foundation who made it financially and logistically possible for me to spend a field season in Antarctica. I also would like to thank the whole Palmer Station and PAL

LTER 2016 team, in particular Naomi Manahan, for all your help in the field and even after that, for answering all my questions.

Moving from the academic side of things away, the greatest thank you goes to my parents Susanne and Peter and my brother Bastian who always believe in and support what I am doing to the fullest even when some of those skype conversations might have been with a very grumpy and tired Ph.D. student.

I would like to thank my friends, especially Imke, for being there for me whenever I needed an ear to listen or just to get distracted. Luci, the same is for you: Thank you for endless skype conversations, motivation and even Ph.D. related discussions. I am not sure what I would have done without you two!

Last but not least, a big thank you also goes to my Edinburgh people, particularly Rachel, Berta, Ivana, Paula, James, Ed and Ibi. You always listened, knew what to say, how to motivate or distract me. A special thanks to Ed for patiently helping me out with all my statistics and coding questions.

Table of Contents

CHAPTER 1 INTRODUCTION

Thesis Overview

This Ph.D. thesis investigates the role of dissolved organic matter (DOM) in the ocean west of the Antarctic Peninsula. Dissolved organic matter plays a vital role in the global carbon cycle, yet processes driving the cycling of DOM are still poorly understood. DOM is produced, transformed, and removed within the ocean by a series of biotic and abiotic mechanisms. Marine DOM can originate from three distinct sources: allochthonous such as terrestrial DOM derived from plants, anthropogenic or autochthonous, i.e. produced *in situ* by primary producers. Within the study region of this thesis, the west Antarctic Peninsula (WAP), the dynamics of DOM are clearly distinguished from those found in other continental shelf seas. Here, allochthonous and anthropogenic sources are negligible due to minimum terrestrial river runoff or human impact so that the only source remaining is *in situ* production. The Southern Ocean is subject to considerable seasonality, clearly delineating periods of low and high productivity which provides ideal conditions to study cycling of autochthonous DOM. Understanding this cycling and the role different processes play will enhance our ability to quantify this part of the global carbon cycle.

Furthermore, during the second half of the 20th century, the WAP underwent rapid warming. Studying the dynamics of this region may provide insight into possible future course of ocean dynamics and improve our understanding of high-latitude climate change. The first chapter of this thesis will introduce the reader to the existing research and understanding related to dissolved organic matter cycling in marine systems. It will then focus on the study region at hand by giving an introduction to the Southern Ocean, and its physical and biogeochemical importance in the world's oceans and climate. This is followed by a review of the west Antarctic Peninsula itself,

discussing the physical settings, the recent climate change of the region, and its responses to this climate change in the context of dissolved organic matter cycling. These brief introductions will provide the basis and context for the key objectives of this thesis which are outlined at the end of the introductory chapter.

1.1 Dissolved organic matter

1.1.1 Definition of dissolved organic matter

Dissolved organic matter (DOM) is defined as the fraction of organic matter passing through 0.1-0.7 µM glass fibre filters (Mostofa et al., 2013).

Residence times of DOM are highly variable and range from minutes-to-days, months-to-years, or centuries-to-millennia, and are referred to as labile, semi-labile, or refractory, respectively (Carlson & Ducklow 1995; Carlson 2002). Refractory DOM holds about 642 Pg C in the deep ocean over long timescales (> 4,000 years) which is equivalent in size to the atmospheric CO_2 reservoir (Hansell, 2013). The division of DOM into these pools is controlled by various biotic and abiotic factors, such as microbial composition and degradation rates, metabolic capacity, or abiotic transformation by solar irradiance, among others (Koch et al., 2014).

In surface waters, multiple processes can affect DOM, for instance, solar radiation, uptake by phytoplankton, or bacterial degradation (figure 1.1). In the deep sea, microbial activity dominates processes affecting DOM.

From a chemical perspective, DOM compounds may consist of a wide range of organic molecular structures from simple biochemicals such as simple sugars, vitamins, fatty and amino acids to more complex compounds such as proteins and polysaccharides. The characterisation of these compounds is methodologically difficult and depends on the progress of compound isolation from seawater. It is estimated that less than 10% of DOM have been characterised (Repeta, 2015).

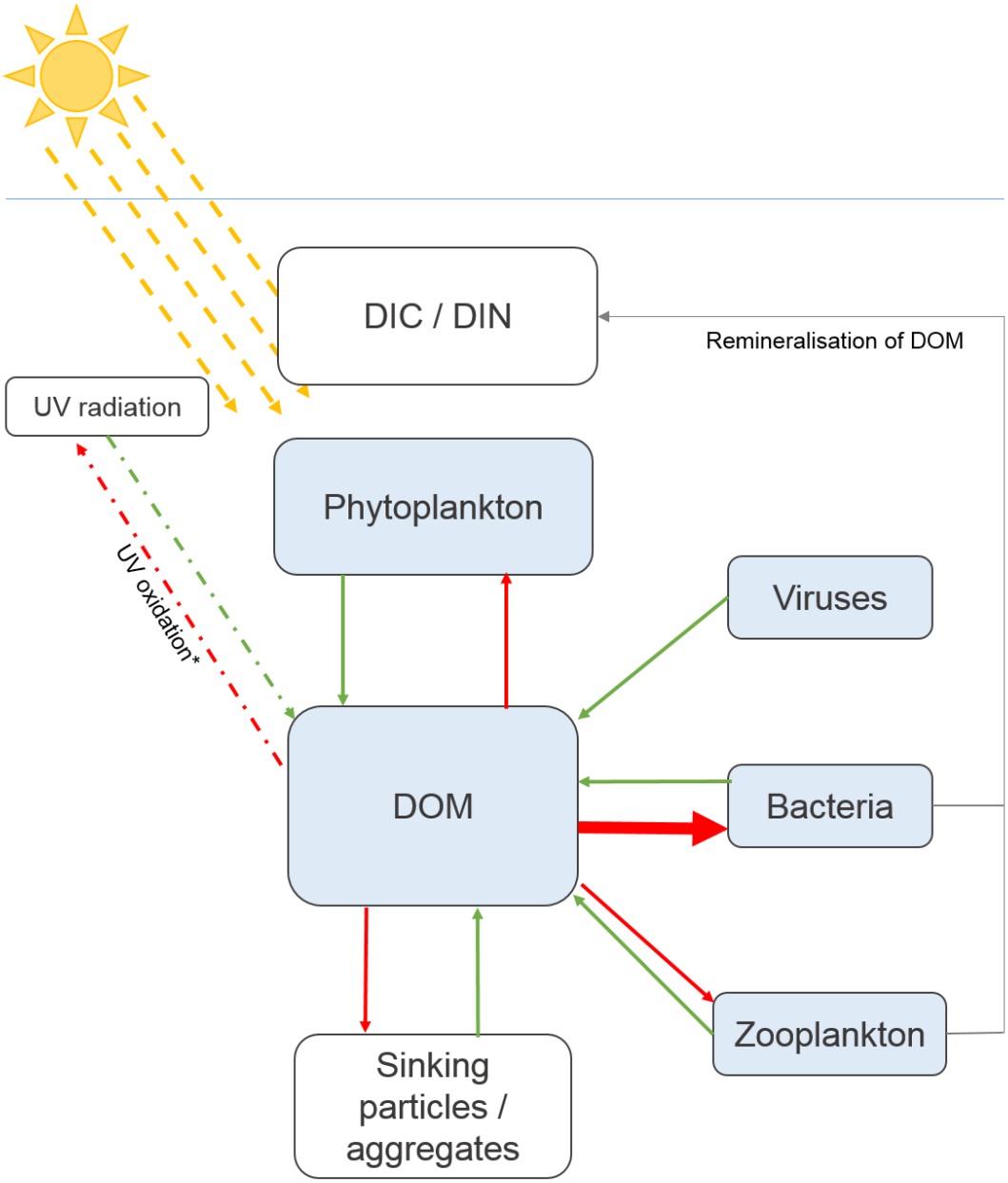

*Figure 1.1: Production and Consumption processes of DOM in marine systems. The blue boxes show biological contributors, the white boxes are abiotic contributors. The green arrows represent DOM production, the red arrows DOM consumption with the big red arrow for bacteria depicting the dominant biogenic removal process. *UV oxidation can transform DOM compounds into inorganic forms but also refractory DOM into labile DOM compounds.*

1.1.2 Sources of dissolved organic matter

The composition of DOM is highly variable due to different organisms and their varying strategies and pathways for DOM production and release.

In the open ocean, most DOM is produced in the euphotic zone. However, the amount of DOM production depends on various biotic and abiotic factors so that the proportion of DOM in the total organic carbon pool can range from less than 11% (Ross Sea; Tang et al. 2008) to more than 86% (e.g. Sargasso Sea; Carlson et al. 1998). Phytoplankton represent a direct source of DOM via a number of processes, such as extracellular release. Stress, including nutrient limitation, may cause increased extracelluar DOM release and autocatalytic cell death in which altered biochemical pathways lead to morphological changes and eventually the dissolution of the cell.

DOM can also be released as a result of sloppy feeding by grazers, excretion and egestion, viral lysis, solubilisation, bacterial transformation and release, and chemoautotrophic production and release (Sherr and Sherr 1988; Calbet 2001).

Microzooplankton graze on bacteria and release significant amounts of DOM (Nagata & Kirchman, 1999). Bacterial cell growth and metabolism, and viral lysis also release bacterial DOM (Kawasaki & Benner, 2006). As bacteria are smaller than phytoplankton and therefore have a larger surface-to-volume ratio, extracellular release is greater (Kawasaki & Benner, 2006) and is estimated to range from 14-31% of assimilated carbon (in comparison to 2-10% for phytoplankton; Nagata 2000). Viruses themselves, due to their small size, are considered a part of the DOM pool (Bronk, 2002; Karl & Björkman, 2015; Wilhelm et al., 1999). Viruses exceed bacterial abundance in seawater by 3-5 orders of magnitude with 10^9 - 10^{11} particles L^{-1} (Carlson, 2002). They are estimated to be responsible for approximately 10-50 % of bacterial mortality (Carlson, 2002). Viral lysis of bacterial and phytoplankton cells is

considered to release highly labile DOM compounds due to the nature of the DOM released originating from a recently healthy organism.

The transformation of POM to DOM via hydrolysis by bacteria is referred to as particle solubilisation. Bacteria attach to aggregations of organic material which tend to have low C:N ratios with increasing molecular size (Alldredge, 1998; Müller-Niklas et al., 1994). These attached bacterial assemblages produce extracellular enzymes and the concurrent solubilisation of POM can result in intense DOM release (Kiørboe & Jackson, 2001) which, in turn, increases the activity of free-living bacteria in the surrounding water (Azam, 1998; Long & Azam, 2001; Reinthaler et al., 2006).

1.1.3 Sinks of dissolved organic matter

Marine heterotrophic bacteria are responsible for most of the labile DOM degradation in surface and subsurface waters. They are present with approximately 10^6 cells L^{-1} (Carlson & Hansell, 2015) and are also responsible for the transformation of POM to DOM and for the regeneration of nutrients (Caron et al. 1985; Goldman & Dennett 2000; Pomeroy et al. 2007; Jiao et al. 2010, 2011). Due to their small size, bacteria are limited in their capability of taking in DOM to low-molecular weight (LMW) compounds. The degradation of high-molecular weight (HMW) compounds requires hydrolysis. Bacteria are controlled by a series of external factors such as nutrient limitation, UV radiation, temperature, pH, grazing pressure, and viral lysis. All of which affect the role of bacteria in the biogeochemical cycling of nutrients and DOM.

Labile HMW DOM compounds can be ingested by phytoplankton as an additional nitrogen source. This process has been observed predominantly in situations of light or nutrient limitation (First & Hollibaugh, 2009; Sherr & Sherr, 1988; Tranvik, 1993).

Abiotic processes that remove DOM from surface waters are the vertical export to the deep ocean, and sorption onto particles (which is estimated to account for ~ 1.4 - 2.8 nmol C kg^{-1} yr^{-1}) with subsequent export to the deep ocean (Carlson & Hansell, 2015). UV radiation can photo-oxidise refractory DOM compounds in surface waters to CO_2 and CO but also to labile DOM compounds which are then available for bacteria and phytoplankton (Carlson & Hansell, 2015; Mopper & Kieber, 2002; Stubbins et al., 2012). From these processes, nitrogen-rich compounds such as ammonium or amino acids can also be released fuelling microbial activity (Moran & Zepp, 2000).

Sorption processes by which DOM compounds attach to sinking POM compounds have been estimated to remove a small but substantial amount of DOM from surface waters and can affect refractory compounds as much as labile compounds. Studies on this process are limited but a $\delta^{14}C$ study shows that about 14% of suspended POC in the deep sea might originate from the sorption of old DOC compounds (Druffel & Williams, 1990). Ionic and polyionic DOM compounds assemble to form marine microgels which can form particles of such high density that they sink rapidly (Verdugo, 2011).

1.1.4 Global distributions of dissolved organic matter

Global marine DOC concentrations vary from deep-ocean lows of approximately 34 µmol C L^{-1} to surface maxima of > 90 µmol C L^{-1} (Hansell, 2002). Global mean DON concentrations range from 2 to 7 µM N with a mean of 4.4 ± 0.5 µM N (Sipler & Bronk, 2015). The C:N:P ratio of DOM in surface samples is 300:22:1 indicating a depletion of N and P relative to average marine plankton C:N:P.

The distribution of refractory DOM, particularly in the deep ocean, is relatively uniform across the world's oceans with ~ 38 µmol C L^{-1} (Lechtenfeld et al., 2014) with a slight

decrease following the thermohaline circulation. Highest deep-ocean DOC concentrations are found in the Eurasian Basin of the Arctic with > 50 µmol C L^{-1} which likely originates from refractory terrestrial DOC (Opsahl et al., 1999; Wheeler et al., 1997).

Highest surface [DOC] are generally found in low to mid latitudes of the Indian and Pacific Ocean. Highest [DOC] with > 70 µM C are found in the surface water of the Western Pacific Warm Pool (Hansell, 2002).

[DOC] generally decreases vertically from surface to the deep ocean as well as with decreasing temperature poleward. Upwelling sites tend to show low surface [DOC] even though primary production may be high, e.g. along the northwest African coast and the Oman coast (Hansell & Peltzer, 1998) due to the upwelling of and dilution with low deep-sea [DOC]. Oligotrophic systems, as well as subtropical and tropical regions show minimal seasonal variability in both DOC and DON (Hansell, 2002). Most seasonal influence can be observed in coastal, estuarine, and high-latitude systems.

1.2 The Southern Ocean

1.2.1 Physical oceanography

The Southern Ocean (SO) comprises the oceanic region south of ~ 44 ° S, varying with longitude (Lenton et al., 2013). It is the only ocean with free boundaries to the North connecting it to the Atlantic, Pacific and Indian Ocean.

The two major ocean current systems of the SO are the Antarctic Circumpolar Current (ACC) flowing clockwise and the Antarctic Coastal Current flowing anticlockwise

(Cochlan, 2008). The ACC plays an important role as part of the global thermohaline circulation transporting heat, nutrients and gases. The narrowest passage is the Drake Passage between the Antarctic Peninsula and Chile where the full-depth transport of the ACC is estimated to be 154 ± 38 Sverdrup (Firing et al., 2011). The major sites of deep and bottom water formation through sea-ice formation in the SO are the Weddell Sea and the Ross Sea (figure 1.1) from where the cold Antarctic Bottom Water (AABW) moves North (Carlson et al., 1998; Convey et al., 2014). In the Atlantic sector, warm and saline North Atlantic Deep Water (NADW) flows southward, mixing with the Antarctic water masses and contributing to the properties of the ACC (Foldvik & Gammelsrød 1988; Carlson et al. 1998). Antarctic surface water (AASW) reaches depths of about 100 m and extends from the continental shelf to the Polar Front. It is relatively fresh (salinity of 34.0-34.3 on the practical salinity scale) and close to freezing temperature except near the Front, where temperatures can be as high as 2.5 °C (Emery & Meincke, 1986).

Circumpolar Deep Water (CDW) is the most voluminous water mass in the SO. CDW is a mixture of NADW and deep and bottom water from the Weddell Sea, the Indian and Pacific Oceans (Santoso et al., 2006). It can extend to depths between approximately 1,400 and 3,500 m in the open Southern Ocean. The temperature of CDW ranges between 1 and 2 °C and salinity between 34.57 and 34.75 (Emery & Meincke, 1986; Martinson & McKee, 2012). CDW comprises Lower CDW and Upper CDW. LCDW reflects the input of NADW with salinity ranging from 34.70-34.75 (Carter et al., 2008) while UCDW salinity ranges from 34.57 to 34.69 (Martinson et al., 2008).

Typical UCDW signatures are elevated nutrient concentrations and an oxygen minimum reflecting the contribution of Indian and Pacific water (Carter et al. 2008). Upwelling of CDW by coastal Ekman circulation or mixing of CDW with overlying water

masses introduces high nutrient concentrations to the surface waters of the SO (Pollard et al. 2006; Sigman et al. 1999). Through this upwelling, an important connection between deep water and atmosphere is created. Because of both major upwelling and downwelling mechanisms, the SO represents a vital link between surface and deep ocean as well as high and low latitude regions in terms of heat and gas exchange but also transport of nutrients and carbon cycling.

1.2.2 Sea ice in the Southern Ocean

During austral winter, when there is no to little solar radiation, the area of Antarctic winter sea ice can expand to up to 15.2 x 10^6 km^2 (Comiso et al., 2016) which is approximately equivalent to the size of the Antarctic continent itself (Convey et al., 2014). With the onset of summer, Antarctic sea ice mostly disappears (approximately ~ 3 x 10^6 km^2 sea ice; Comiso et al. 2016). This highly dynamic seasonal cycling drives the productivity in Antarctic marine systems.

High and long sea-ice cover in winter preconditions the water column so that the melting of sea ice leads to stratification which shallows the mixed layer in spring/summer. The stability and depth of the mixed layer are important for successful primary production. In a stable and shallow mixed layer, phytoplankton are kept in the well-lit upper ocean and can photosynthesise more efficiently. Further, melting of sea ice supplies potential nutrients and sea-ice algae to water column phytoplankton and thus increase water column productivity (Lizotte, 2006; Selz et al., 2018). Low winter sea-ice cover, on the other hand, allows for early mixing of the water column by winds and introduces less freshwater so that stratification is less stable and the mixed layer is usually deeper causing deeper mixing of phytoplankton reducing overall primary production efficiency (Rozema et al., 2016; Venables, et al., 2013).

During sea-ice formation, nutrients are expelled from the ice. However, organisms living in the sea ice contribute to organic-matter formation and thus to sea ice being an overall nutrient sink. It is still uncertain whether this sea-ice derived organic matter is degraded completely within the sea ice or whether it contributes to export production in the Southern Ocean (Fripiat et al., 2017). Ice algae, ice-associated bacteria and organic and inorganic nutrients seed the upper ocean during sea-ice decay periods and initiate or enhance productivity.

1.2.3 Carbon in the Southern Ocean

Even though the SO only covers 20 % of the world oceans, it is estimated to be responsible for 30% of the annual carbon uptake (Ducklow, 2009; Gruber et al., 2009; Lenton et al., 2013; Takahashi et al., 2009). Dissolved Inorganic Carbon (DIC) uptake estimations in the SO are complicated due to the highly complex hydrography, disparate behaviour in the different regions of the SO, and because it remains one of the most poorly sampled regions in the world. Estimates range from 270 ± 130 Tg C yr^{-1} to 420 ± 70 Tg C yr^{-1} (Lenton et al., 2013).

The vertical mixing of water masses in the Southern Ocean allow for ventilation of deep-ocean CO_2 creating a net source of CO_2 to the atmosphere which dominates during the austral winter. However, the uptake of atmospheric CO_2 by summer primary production is estimated to be higher than the net SO source so that overall, the Southern Ocean is considered a CO_2 sink. However, it is proposed that the SO's potential as a net CO_2 sink will decrease due to increasing atmospheric CO_2 concentrations, ocean temperatures, changes in wind pattern and strength, as well as an overall reduction in biological uptake and export. In addition to this, it is also proposed that the SO will become more acidic with severe effects on $CaCO_3$ forming

organisms and, as such, whole food webs (Constable et al., 2014; Hauri et al., 2015). Recent models can reconstruct DIC fluxes in the subpolar regions, however, the reconstruction of high-latitude DIC fluxes and biogeochemical cycles remains challenging and inaccurate, highlighting our incomplete understanding of local biogeochemical and physical processes (Sallée et al., 2012).

The contribution to biological productivity in the Southern Ocean varies greatly between SO sectors. Most of the open-ocean SO is considered a low productivity system despite high nutrient concentrations (High Nutrient Low Chlorophyll regions, HNLC). Several studies have shown growth limitation by iron, in combination with effects of deep mixing (e.g. Tagliabue et al. 2014; Coale 2004; Bowie et al. 2001; Boyd et al. 2007; Boyd & Ellwood 2010). Intense upwelling of macronutrient-rich waters dilute iron concentrations in the surface waters. Iron is essential for photosynthesis. Iron fertilisation experiments in the SO could confirm the hypothesis of iron limitation in HNLC regions (Bowie et al., 2001; Oliver et al., 2004). The limited primary production has major impacts on the system's biological pump with limited organic matter formation and hence, minimum carbon export to the deep sea, transfer to higher trophic levels or utilisation through the microbial loop. An increase in nutrient uptake in the SO has been shown to drive a strong decline in atmospheric ρCO_2 so that studies suggest that the productivity of the SO, possibly due to changes in iron availability, has been a major control on atmospheric ρCO_2 variations over past glacial-interglacial cycles (Sigman et al. 2010, Martin 1990). Iron is supplied to the Southern Ocean by a multitude of processes such as glacial meltwater influx, resuspended sediments, atmospheric dust, or interactions with bathymetry and hydrothermal vents, all of which make iron more available in the shelf waters of the Antarctic continent or around islands like Kerguelen (Annett et al., 2015; Blain et al., 2007; Duce & Tindale, 1991; Trull et al., 2008).

Primary production in the Southern Ocean is limited in time but can exceed lower latitude phytoplankton blooms in magnitude, particularly in shelf waters where macro- and micro-nutrients are plentifully available. Intense phytoplankton blooms occur during spring and summer. Particulate organic matter (POM) produced during these blooms is generally of high quality (low C:N ratio) and represents the base of the food web in the system. High grazing rates of zooplankton, in particular Antarctic krill, on this organic matter is thought to be responsible for high carbon export in some regions of the SO while in naturally Fe-fertilised regions, efficient upper-ocean cycling tends to reduce the carbon export (Tremblay et al., 2015). Highest productivity is found in sea-ice zones and continental shelf regions. However, because these regions are small in size, the pelagic SO is overall more productive at 3912 Tg C yr^{-1} (Arrigo, 1999).

1.2.4 Dissolved organic matter in the Southern Ocean

Due to negligible terrestrial input, DOM in the open SO is exclusively of autochthonous nature. In contrast to lower-latitude DOM, concentrations in the SO make up a relatively small proportion of the total *in situ* organic matter pool (Billen & Becquevort, 1991).

Deep-water [DOC] range between 34 and 40 µmol C L^{-1} (Kähler et al., 1997; Ogawa et al., 1999) and mostly represent the refractory background concentrations which are introduced to the surface waters by upwelling. However, DON surface minima point to the breakdown of upwelled DOM so that it is suggested that the deep-water refractory DOM is not necessarily stable under surface conditions where high solar radiation can lead to photo-oxidation (Kähler et al., 1997).

Globally, Southern Ocean [DOM] are the lowest despite highly productive blooms in the austral summer (Lechtenfeld et al., 2014). In the Australian Sector, summer DOC concentrations range from 45 to 55 µmol C L^{-1} and highest values coincide with low nitrate concentrations indicating newly produced OM (Ogawa et al. 1999). DON values in these waters are 12 ± 4 % of total dissolved nitrogen which varies between 24 and 42 µmol N L^{-1} in the surface waters and show larger horizontal and vertical variation than DOC (Ogawa et al., 1999). This can be due to either large analytical errors arising from high nitrate concentrations or to biological effects.

It has been hypothesised that more OM of the total pool is partitioned into the particulate pool rather than the DOM pool and that efficient grazing by zooplankton leaves only little DOM in the water column (Kirchman et al. 2009; Carlson et al. 1998; Kähler et al. 1997). DOC:DON ratios are lower in the SO surface waters (5-15) than in other oceanic sites (20-25) which indicates either selective degradation or nitrogen-rich DOM production in these waters (Ogawa et al., 1999).

Over the last decade, focus has been on the bacterial activity in Antarctic waters in response to DOM. Bacterial production is hypothesised to be limited by DOM availability and quality and a possible co-limitation by iron (Church et al., 2000; Ducklow et al., 2001; Hall & Safi, 2001). In bacterial-response experiments in the HNLC regions of the Southern Ocean, bacterial production was highest with the addition of glucose + iron which indicates co-limitation by iron (Church et al., 2000). Similar results are shown in the SOFeX experiment: Bacterial abundance increased by 60 to 110% as a response to phytoplankton fertilisation with iron with a significant correlation with available POC (Oliver et al., 2004). Kähler et al. (1997) analysed bacterial production in SO surface waters vs. SO deep water and showed a strong correlation between the amount of initial DOC and bacterial growth in surface waters while in deep water, bacterial growth was minimal.

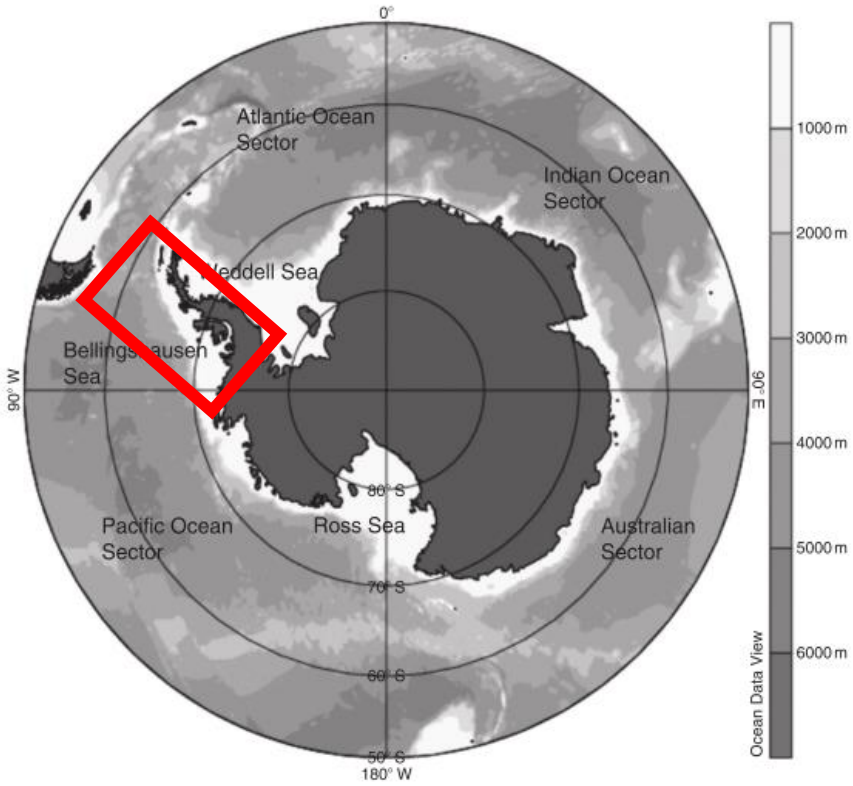

Figure 1.1: Sectors of the Southern Ocean showing the west Antarctic Peninsula in the red box. Source: Post et al. (2014).

1.3 The West Antarctic Peninsula

1.3.1 *Physical oceanography*

The shelf west of the Antarctic Peninsula extends approximately 200 km offshore with complex bathymetry, a steep continental slope and deep, glacially scoured canyons. On average, it is 430 m deep (Ducklow et al. 2007).

The ACC lies directly adjacent to the WAP. The Southern boundary of the ACC is located on the upper continental slope between 750 and 1000 m depth. This leads to regular and persistent onshelf intrusions of UCDW introducing heat (~1.7°C;

Martinson & McKee 2012) and high nutrient concentrations (NO_3^- = 32-34 µmol N L^{-1}, $Si(OH)_4^-$ = 100-105 µmol Si L^{-1}; Klinck et al. 2004; Prezelin et al. 2000).

UCDW is usually found at depths between 200 and 400 m along the WAP shelves (figure 1.2). It intrudes the shelf along deep canyons and by eddies. Once on the shelf, it mixes with Antarctic Surface Water (AASW) forming a modified version of UCDW (Smith et al., 1999). Effective vertical mixing provides the WAP surface waters with heat, salinity and nutrients (Meredith et al., 2013). LCDW is present in the outer shelf regions and depressions of the WAP, such as the Marguerite Trough, and is an important source of silicic acid to WAP shelf waters (Klinck et al., 2004).

The AASW overlying the CDW has a deep mixed layer in winter and is comparatively saline and cold due to winter cooling and sea-ice formation. During spring and summer, the surface waters become fresher and warmer - due to sea-ice melting and solar radiation - so that the winter AASW, also known as Winter Water (WW), becomes separated and exists as a remnant WW layer usually between 50 and 150 m depth (Meredith et al., 2013). There is a permanent pycnocline between WW and UCDW (Martinson & McKee, 2012).

The Antarctic Peninsula Coastal Current (APCC) flows southwestwards along the coast. This current is buoyancy and wind forced and is only present seasonally during summer and autumn (Moffat et al., 2008).

Like other Antarctic regions, the WAP experiences extreme seasonality with pronounced changes in solar irradiance; sea-ice cover, extent and duration; primary production; and vertical mixing. Unlike other regions of Antarctica, the WAP rarely experiences cold, katabatic winds from the continent (Meredith et al., 2013). Wind stresses mostly from North/Northwest so that the atmospheric temperature is rarely influenced by the continental temperatures and wind patterns (Meredith et al., 2013).

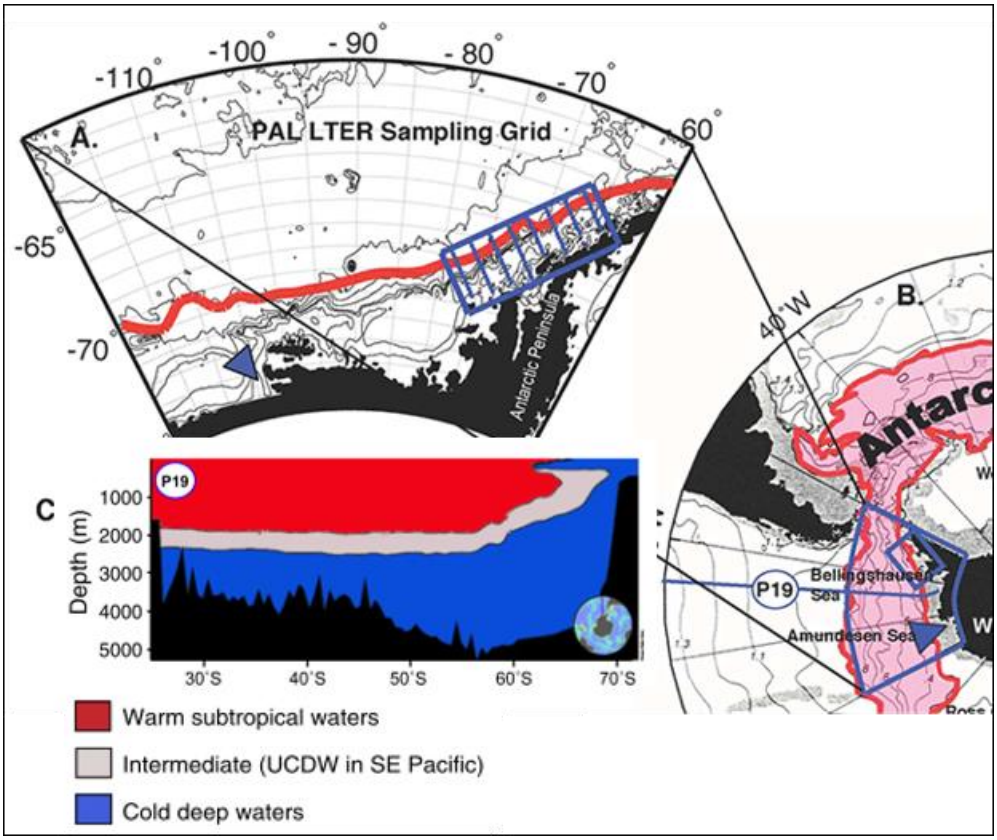

Figure 1.2 Simplified version of West Antarctic Peninsula hydrography (bottom left) and the PAL LTER annual sampling grid (upper left). Source: Ducklow et al. 2015; Martinson & McKee 2012

1.3.2 Climate change at the WAP in the second half of the 20th century

During the second half of the 20th century, the WAP experienced pronounced warming. Winter atmospheric temperatures have risen by 6 °C (> 5 times the global average) with the upper and deep ocean showing significant warming (Meredith & King, 2005; Smith et al., 1996; Van Wessem et al., 2015; Vaughan et al., 2003). The sea-ice extent decreased by 30% and the duration of sea-ice cover has declined by about 85 days since 1978 (Stammerjohn et al., 2008). 90% of the WAP glaciers are in retreat (Cook et al. 2005, 2016) which is the reason for significant freshening of the surface waters in coastal regions (Meredith & King, 2005).

The trends of regional warming slowed down since the late 1990's and have since been plateauing with increasing sea-ice cover since the late 1990's (Figure 1.3; Stammerjohn et al., 2008; 2008 (a); Turner et al., 2016). These reversals in climatic trends are likely short-termed and reflect natural internal variability (Hobbs et al., 2016).

The climatic trends at the WAP are controlled by large-scale atmospheric circulation patterns. Changes in the Amundsen Sea Low (ASL) in particular, which is a persistent low-pressure system located between the WAP and the Ross Sea, affect wind strength and patterns over the WAP which are the primary control on sea-ice dynamics (Turner et al., 2013). During the second half of the 20th century, the ASL deepened, forcing stronger north-to-northwesterly winds advecting warm and moist air towards the WAP and pushing sea ice further south. The ASL is influenced by changes in the Southern Annular Mode (SAM) and the El Nino Southern Oscillation (ENSO) (Lachlan-Cope et al., 2001; Raphael et al., 2016; Turner et al., 2013). A deepening of the ASL is associated with more positive SAM phases while more negative SAM phases force more cold east-to-southeasterly winds from the Antarctic continent over the WAP which has been observed since the 1990's.

The intense climatic variability with its effects on sea-ice cover, glacial melt and local winds has a strong impact on the local ecosystem with high interannual variability in primary production and community composition.

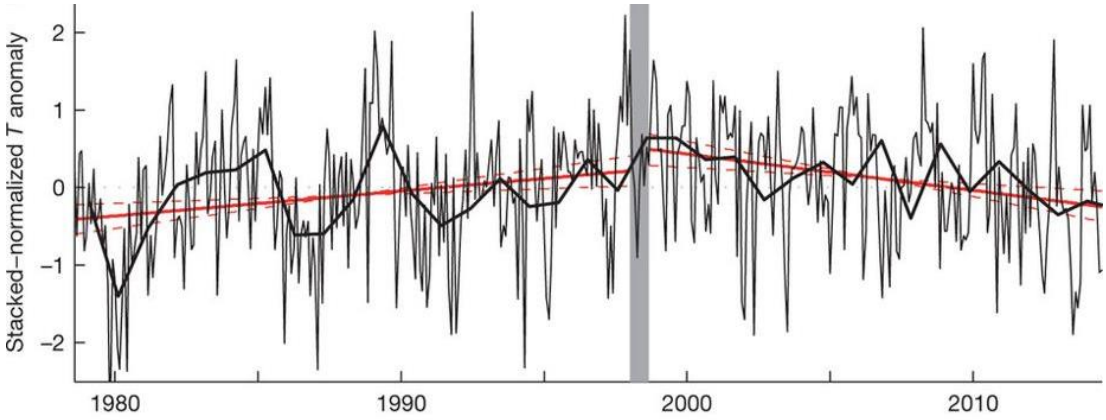

Figure 1.3: Stacked-normalised temperature anomalies for 1979 – 2014 at the WAP showing a warming trend until the late 1990's after which temperatures decreased slightly. Figure from Turner et al. (2016).

1.3.3 Phytoplankton and primary production at the WAP

The cycling of organic carbon is closely linked to the observed high-latitude seasonality with particulate C fluxes up to four orders of magnitude higher during the summer (Karl et al. 1991; 1996) than during the ice-covered and dark winter (Buesseler et al. 2010). Phytoplankton blooms and subsequent particle flux peak shortly after ice retreat in the summer. Primary production at the WAP is controlled by upper-ocean physics, light, and the supply of macro and micronutrients. A strong gradient in primary productivity can be observed from coastal regions (~ 1,000 mg C m^{-2} d^{-1}) to the open ocean (~ 100 mg C m^{-2} d^{-1}) (Vernet et al., 2008) with production starting first in the open and following sea-ice retreat towards the coast (Arrigo et al., 2017). The primary control on primary production is exerted by sea-ice dynamics. High-ice years lead to decreased wind-induced mixing over winter and the higher amounts of meltwater upon warming lead to a more stable water column supporting high rates of primary production in favourable light conditions. In years of low sea-ice cover, the upper water column experiences intense wind-induced mixing and the smaller meltwater input leads to a deeper mixed layer which leads to phytoplankton

being mixed to greater depths out of ideal photosynthetic conditions (Moline, 1998; Vernet et al., 2008).

Since the 1970s, phytoplankton biomass has experienced an overall decrease with differing magnitudes in the Northern and Southern parts of the WAP (Fraser et al., 2013). In the North, an increase in cloud cover and spring and summer winds plus decreasing sea-ice cover and duration has led to increased upward mixing of nutrients on the one hand, but also to an increased mixed layer depth so that phytoplankton are mixed out of the euphotic zone - where photosynthetically active radiation is highest - which ultimately leads to less phytoplankton biomass overall (Montes-Hugo et al., 2009; Saba et al., 2014).

In the Southern part of the WAP, however, a decrease in sea-ice cover, cloudiness and winds led to more open water with less stratification but no intense deepening of the mixed layer so that in total, there is more time, space and irradiance for phytoplankton, primarily diatoms, to reproduce (Montes-Hugo et al., 2009). Phytoplankton blooms occur earlier in the North than in the South. The decrease in Northern WAP phytoplankton biomass is postulated to be the reason for decreases in krill abundance and biomass (Montes-Hugo et al., 2009).

WAP phytoplankton blooms are mostly dominated by diatoms but other taxa are increasingly recognised as important components of the phytoplankton species composition (Saba et al., 2014). Low-ice years are often associated with a dominance of cryptophytes and haptophytes in the WAP ecosystem with haptophytes being more prominent particularly in the South (Rozema et al., 2016). Cryptophytes utilise less CO_2 per unit chlorophyll than diatoms so that it is hypothesised that an increase in cryptophytes could lead to reduced carbon uptake (Schofield et al., 2017). Phaeocystis, a haptophyte genus, are well-known for producing mucus-like layers of carbon-rich exopolymeric substances (EPS) (Nichols et al., 2005). EPS plays an

important role in carbon cycling, both particulate and dissolved carbon, due to its gel-like and usually poly-anionic structure binding trace metals and serving as a nutritious substrate for bacterial growth (Meiners & Michel, 2016; Riedel et al., 2006). In Marguerite Bay, *Phaeocystis antarctica* are more prominent than cryptophytes (Garibotti et al., 2003; Kozlowski et al., 2011; Rozema et al., 2016; Stefels et al., 2018).

Primary production in sea ice is highly variable and an important carbon source in winter for species such as juvenile krill. Algae from sea ice can seed pelagic primary production with high seasonal variability. Release in early spring leads to early under-ice phytoplankton blooms (Lizotte, 2006; Selz et al., 2018) while later in the season, release of sea-ice algae is more likely consumed by higher trophic levels (Riebesell et al., 1991). Sea-ice associated release of organic carbon is highly related to the dynamics of sea-ice retreat and the composition of the organic matter (Norkko et al., 2007; Wing et al., 2012).

1.3.4 Nutrient dynamics at the WAP

The CDW is the primary source of macronutrients to the WAP shelf region. CDW intrudes the WAP shelf from the ACC and introduces nutrients and heat which is mixed upwards by the bathymetry and eddies (Klinck et al., 2004; Prézelin et al., 2000). Phytoplankton biomass is found to be higher in the surface waters above deeply scoured canyons due to increased supply with cross-shelf CDW transport in these regions. Typical CDW nitrate and silicate concentrations are 32-34 µmol N L^{-1} and 100-105 µmol Si L^{-1}, respectively (Klinck et al., 2004; Prézelin et al., 2000). Even though nutrient concentrations in the WAP are usually replete, intense phytoplankton blooms can drive nutrient levels towards depletion over short periods of time

especially in coastal areas where higher rates of primary production control the surface nutrient availability in summer (Pedulli et al., 2014). N:P uptake ratios cover a range of approximately 13 to 21 indicating diatom and non-diatom dominated areas, respectively (Clarke et al., 2008; Henley et al., 2017). A Si:N uptake ratio of 1 or lower indicates diatom dominance in the Southern part of the WAP (Henley et al., 2017). Nutrient uptake and uptake ratios vary intensely across the shelf and throughout the season due to sea-ice conditions and changes in the phytoplankton communities. Nitrification occurs in the deeper layers of the water column (Henley et al., 2018). Regenerated nitrate and phosphate can account to up to one third of the surface-available nutrients in the summer (Henley et al., 2018).

1.3.4.1 Dynamics of carbon and nitrogen stable isotopes

Stable isotopes of carbon and nitrogen are a useful tool for tracing and quantifying processes involved in nutrient and organic matter cycling. Nitrate introduced to the WAP surface from CDW carries a specific $\delta^{15}N_{NO3}$ composition of 4.8-5.3 ‰ (e.g. Henley 2013; Henley et al. 2018; Sigman et al. 2000). Upon nitrate assimilation by phytoplankton, $\delta^{15}N_{NO3}$ increases due to the preferential uptake of the lighter ^{14}N isotope by phytoplankton. Consequently, the N-isotopic composition of organic matter ($\delta^{15}N_{PN}$) is lighter than $\delta^{15}N_{NO3}$. This process is known as kinetic fractionation. The WAP nitrogen cycle can be considered a closed system (Rayleigh) as nutrients are replenished in winter but the nutrient pool is depleted over the austral summer growing season. The isotope effect (Ɛ) is defined by the difference in rate constants of the ^{14}N and ^{15}N isotopes from the reactant to the product:

$$\varepsilon(‰) = ({}^{14}k/{}^{15}k - 1)\ x\ 1000$$

where ^{14}k and ^{15}k are the rate coefficients of ^{14}N and ^{15}N, respectively. ε is between 4 and 5 ‰ at the WAP (Henley et al., 2018, 2017; Rafter et al., 2013; Sigman et al., 2000; Smart et al., 2015). This means that organic matter produced instantaneously from a specific nitrate pool of $\delta^{15}N_{NO3}$ = x ‰ will be x-4 ‰ to x-5 ‰ lighter than $\delta^{15}N_{NO3}$ (figure 1.3.4.1). The nitrate pool itself will become depleted and therefore isotopically enriched over time as the lighter isotope is removed. With complete consumption of the nitrate pool, uptake and remineralisation leave no net effect on subsurface $\delta^{15}N_{NO3}$. However, in waters with incomplete nitrate consumption such as the Southern Ocean, $\delta^{15}N_{NO3}$ and $\delta^{15}N_{PN}$ and deviations from the modelled values are indicative of physical or biogeochemical processes at work (Figure 1.3.4.1). PN is being degraded with a currently unknown isotope effect in WAP waters, with DON and DIN being formed. Due to these mechanisms, nitrate resulting from nitrification processes in the subsurface, thus being the product of PN degradation, carries a lighter $\delta^{15}N$. Ammonification and nitrification of organic nitrogen closes the cycle of nitrogen in the system, however, these parts of the nitrogen cycle are not quantified in terms of their N-isotopic composition yet.

At the WAP, there has been a strong focus on the $\delta^{15}N_{NO3}$ in order to understand the cycling of nitrogen in the upper ocean. Regenerated nitrate can make up to 30% of the nitrate in WAP surface waters being utilised by phytoplankton during a phytoplankton bloom which has important implications for the net CO_2 uptake and carbon export (Henley et al., 2018). Isotope studies of Antarctic sea ice show intense cycling of nitrogen within sea ice indicating high microbial activity (Fripiat et al., 2015).

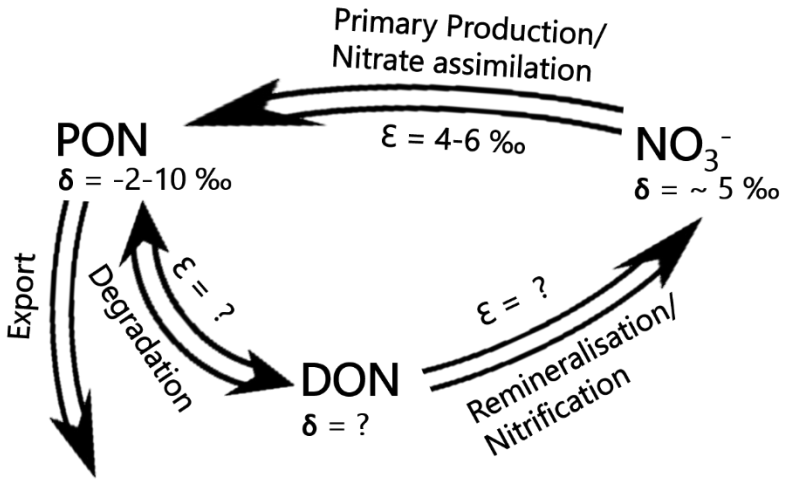

Figure 1.3.4.1: Simplified systematic model of N isotope effects (ε) and isotopic ratios ($\delta^{15}N$) of the nitrogen cycling in the WAP marine environment. Upper Circumpolar Deep Water introduces NO_3^- to the WAP with a specific $\delta^{15}N$ of ~5 ‰. During primary production, nitrate is assimilated with a ε of 4-5 ‰ which leaves particulate organic nitrogen (PN) of a modified $\delta^{15}N$. Remineralisation, rapid export and grazing by zooplankton affect $\delta^{15}N$.

The biological fractionation of carbon is driven by different mechanisms than nitrogen. C fractionation consists of three major steps which determine the C-isotopic composition of POC ($\delta^{13}C_{POC}$): (i) the intracellular diffusion of CO_2, (ii) fractionation through the carboxylation reaction as one of the first chemical steps of photosynthesis and (iii) the translocation of C isotopes within the cell. Consequently, C fractionation can be used to identify carbon concentration mechanisms (CCMs) employed by different phytoplankton species (Henley et al. 2012). These different fractionation mechanisms represent useful tools to assess POM formation and remineralisation processes.

1.3.5 Microbial processes at the WAP

Bacterioplankton across the WAP shelf is coupled to phytoplankton dynamics and highly influenced by physical and biogeochemical controls (Ducklow et al., 2012;

Morán et al., 2001; Ortega-Retuerta et al., 2008). The abundance of bacterial cells increases from North to South and from the open ocean to the coast, broadly replicating phytoplankton distributions (Ducklow et al., 2012a; Henley et al., 2019). Despite high primary production rates, bacterial abundance is up to one order of magnitude lower than in temperate regions. The ratio of bacterial to phytoplankton production is low with approximately 4% which is unique to the Southern Ocean (Ducklow et al., 2012a). Low DOM availability has been argued to be the reason for low bacterial production in the region. Low temperatures in high-latitude systems have been suggested to limit bacterial productivity (Pomeroy & Wiebe, 2001), however, there is no significant relationship between temperature and bacterial activity found in WAP waters. However, temperature might play an indirect role influencing other bacteria-controlling processes such as viral infection and microzooplankton activity.

Striking differences between summer and winter assemblages of bacteria and archaea were found in surface as well as deep waters pointing out different metabolic and energy transfer pathways. While summer assemblages showed pathways for oxygenic phototrophy, chemolithoautotrophy was supported in the winter months (Williams et al., 2012). The summer remnant of WW at 50-150 m depth showed a similar composition of bacteria and archaea as winter surface water (Bowman & Ducklow, 2015; Church et al., 2003; Luria et al., 2014). Bacterial diversity seems to be higher in the winter and decreases with the onset of summer (Luria et al., 2014). While the relative success of bacteria in summer surface waters may be due to labile OM availability, high abundance of archaea in deeper water shows adaption to environments of restricted OM and light and increased nutrient concentrations (Church et al., 2003). Summer surface archaeal abundance is low showing the inability of chemolithoautotrophs to successfully compete under conditions favourable

for heterotrophy (Luria et al., 2014). Because archaea are not analysed as part of this study, the term “bacteria” will be used to encompass both bacteria and archaea.

1.3.6 Dissolved organic matter at the WAP

Summer [DOC] at the WAP is elevated compared to winter [DOC] which represents the refractory DOC from the deep sea (Williams et al., 2012). While there are not many reliable measurements, surface [DON] is slightly elevated from background concentrations at 5-6 µmol N L^{-1} in this region (Ducklow et al. 2011 *and references therein*).

Even when primary production is high with chlorophyll *a* levels exceeding 20 mg m^{-3} in WAP waters, the proportion of DOM to the total OM pool is lower than in comparable lower latitude regions. Studies show that it might not be unique to the Antarctic ocean but to Polar regions, with similarly low BP:PP ratios and [DOM] in the Arctic Chukchi Sea (Wheeler et al., 1997). Another factor playing a role in the low proportion of DOM may be the negligible fraction of zooplankton other than krill grazing on phytoplankton. Krill ingest whole diatom cells and there is only little grazing by other zooplankton which could result in sloppy feeding and the subsequent release of DOM (Bird & Karl, 1999). Even in highly productive regions, such as the Gerlache Strait in the WAP, the absence or minimal abundance of grazers during phytoplankton blooms coincide with a lack of microbial activity (Bird & Karl, 1999).

Ducklow et al. (2011) suggest the quantity of released DOM to be a reason for the time lag between the onset of primary and bacterial production as labile [DOC] remain low until early December and only thereafter increase to concentrations utilisable for bacteria.

Karl et al. (1996) suggested that Antarctic diatoms are adapted to the high seasonality of Polar Regions by the capability to assimilate amino acids rapidly as an energy source. This would make DON an important source of nutrition for Antarctic phytoplankton. Further, the recycling of DON compounds would reduce the export of OM out of the euphotic zone (Karl et al., 1991).

The most recent warming trend at the WAP led to impacts on the WAP ecosystem structure with a shift to phytoplankton blooms dominated by smaller phytoplankton cells. Smaller phytoplankton cells take up less carbon during primary production, thus potentially reducing the overall carbon uptake during primary production. Furthermore, krill are less adapted to ingesting small phytoplankton cells so that there has already been an observable shift to an increasing number of salps with cascading effects on higher trophic levels as salps are not being eaten readily by penguins, seals, or whales. However, at the same time, microzooplankton could increase in numbers grazing on the smaller phytoplankton cells and adding a trophic level between phytoplankton and krill. This could increase carbon export by the production of faecal pellets which can sink rapidly or are ingested by larger zooplankton and repacked into larger faecal pellets.

On the other hand, a shift to an ecosystem dominated by smaller cells potentially increases the microbial response as there will likely be more DOM production at the same time. Future projections estimate that such a shift on a long-term scale can lead to 40-65 % less carbon being transferred to higher trophic levels with a subsequent higher DOM flux and an increase in microbial activity (Moline et al. 2004). Ultimately, intense microbial recycling of *in situ* produced DOM compounds will likely enhance upper-ocean carbon cycling and as such reduce carbon export.

For a better quantification of the carbon cycled in the form of DOM, it is critical to understand processes that control the production, transformation, and loss of DOM,

as well as the organisms involved. This knowledge will contribute to a better understanding and quantification of Southern Ocean carbon and nutrient biogeochemical cycling.

1.4 Key objectives and hypotheses of this thesis

This Ph.D. project is intended to augment our understanding of organic carbon and nitrogen cycling in the upper ocean along the West Antarctic Peninsula. As such, it is the first project to collect DON data to complement the PAL LTER data library. By resolving the cycling of DOC and DON, we will enhance our understanding of regional dissolved organic matter cycling. As DOM in these waters is mostly produced autochthonously and is likely recycled by marine heterotrophic bacteria, it is important to quantify how much carbon and nitrogen in the dissolved organic form is taken up by bacteria and possibly regenerated in the surface waters.

Based on the existing literature, this thesis will test the following four hypotheses.

1) Firstly, it is hypothesised that little to no DOM is produced and released by *in situ* phytoplankton production. In support of this hypothesis are the generally low DOM concentrations in the surface waters during phytoplankton blooms with high POM concentrations.
2) Furthermore, it is hypothesised that most DOM results from the bacterial degradation of particulate organic matter in the surface waters. Therefore, DOM production occurs with a temporal offset of a few days to weeks after primary production peaks due to the bacterial response.
3) Because of the generally low concentrations of DOM in Southern Ocean waters with low C:N ratios, it is further hypothesised that the bioavailable DOM is rapidly degraded and recycled in the upper ocean. For this hypothesis to be

true, DOC and DON concentrations were to decrease rapidly after DOM production, particularly when C:N ratios are lower.

4) Changing physical (e.g. temperature, salinity, meltwater contribution) and biogeochemical (e.g. phytoplankton composition, nutrient availability) parameters are hypothesised to influence DOC and DON concentrations, distribution and cycling.

In order to test these hypotheses, DOC and DON data were collected and analysed over three consecutive austral summer seasons at the UK Rothera research station and spatially along the U.S. PAL LTER WAP sampling region during one research cruise. Additionally, other biogeochemical and physical data were collected which will be used in this thesis to establish relationships between DOM and other biogeochemical parameters at the WAP.

The UK Rothera research station is located at the South-Eastern tip of the PAL LTER sampling grid (see figure 1.4 for a map and *Chapter 2: Methodology* for a site description). All available physical and biogeochemical data are involved to identify production and removal processes of both DOC and DON. Biogeochemical data include phytoplankton parameters such as chlorophyll-*a*, primary production (PAL LTER only), pigmentation data (RaTS only); inorganic nutrients (NO_3^-, PO_4^{3-}, SO_4^{3-}), the N-isotopic composition of nitrate, microbial data (PAL LTER only) such as bacterial activity, bacterial abundance, HNA and LNA abundance, particulate organic carbon and nitrogen and their stable isotopic compositions. Physical data collected include salinity, temperature, density, oxygen, sea-ice cover in % (PAL LTER) and sea-ice scores (Rothera), and $\delta^{18}O\text{-}H_2O$. The $\delta^{18}O$ composition of water is a useful and effective tool to separate the contribution of different water masses, particularly meltwater, in a water column. With this, seawater can be distinguished from sea-ice

meltwater and meteoric or glacial meltwater (see Chapter 2: Methodology for more detail).

The following three chapters discuss and interpret the four available data sets by first looking at the temporal data from Rothera in order to understand the seasonal development of DOC and DON in the coastal surface waters of the WAP. Following this chapter, the spatial data are analysed and put into context with the data from the previous chapter. Chapter 5 investigates the coupling processes between POM and DOM as well as between DOC and DON and POC and PN of both temporal and spatial data. Further, C and N stable isotopic data are introduced to pinpoint processes directly involved in the cycling of organic carbon and nitrogen.

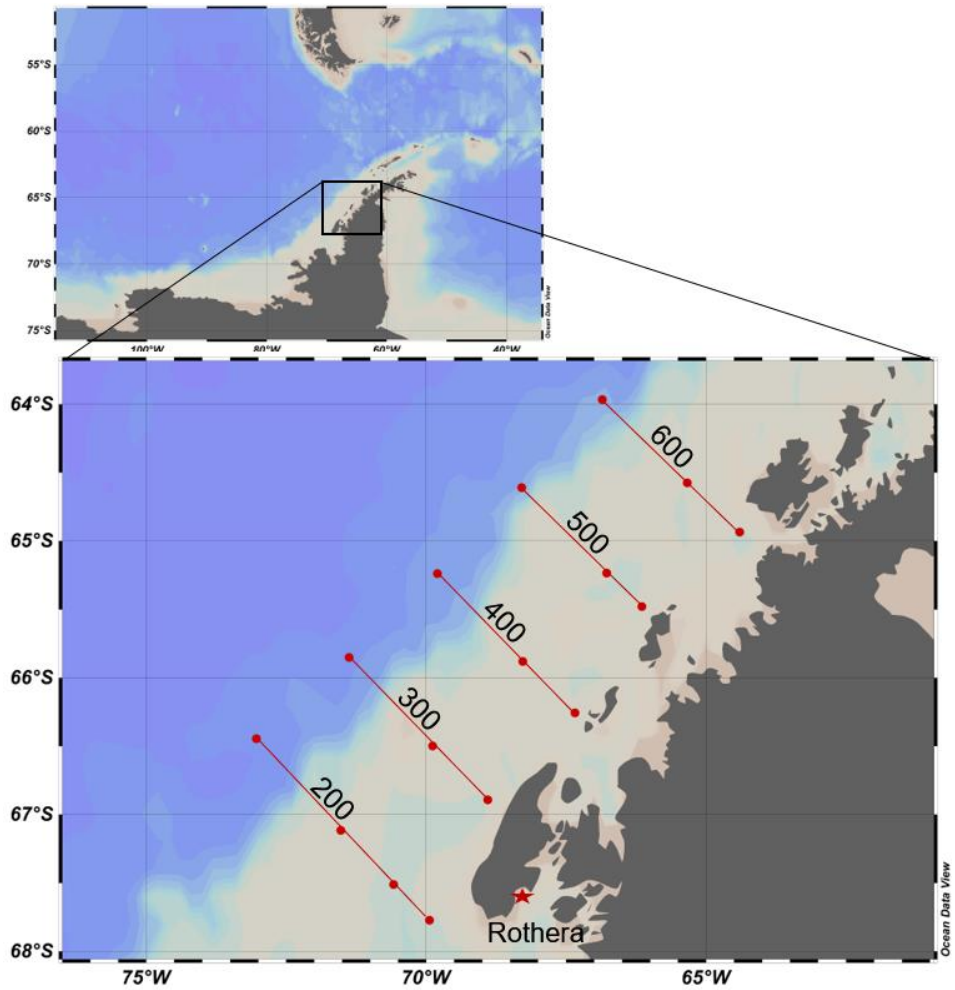

Figure 1.4: The sampling grid of the U.S. PAL LTER programme along the West Antarctic Peninsula on a zoomed-in map. Sampling stations (red dots) are along pre-defined lines orthogonal to the coast. The UK Rothera research station is located at the south-eastern tip of the sampling grid in Marguerite Bay (red star).

CHAPTER 2

Methodology

Samples were collected from the PAL LTER cruise 2017 and the UK Rothera Research Station and analysed for dissolved organic carbon and total dissolved nitrogen (2.2), particulate organic carbon, nitrogen and the C- and N-isotopic composition (2.3) and the N-isotopic composition of nitrate (2.4). All other data were analysed by colleagues from both the PAL LTER and RaTS programmes. A list of the laboratories and researchers involved is in appendix I. The sampling and the analyses conducted for each programme (PAL LTER and RaTS) follow the protocols established at the sites.

2.1 Field work

Field work for this Ph.D. project was conducted both ship and research-station based. For temporal analysis, samples were collected by Dr Sian Henley during three austral summer seasons at the UK Rothera research station as part of the British Antarctic Survey Rothera Oceanographic and Biolocial Time Series (RaTS) in 2013/14, 2014/15 and 2015/16. For spatial analysis, samples were collected during an austral summer research cruise (January 2017) as part of the U.S. Palmer Long Term Ecological Research project (PAL LTER).

2.1.1 Sample Collection at the UK Rothera Research Station on Adelaide Island 2013-2016

At the RaTS site, seawater samples were collected in Ryder Bay at a fixed location (67° 35' 8" S, 68° 7' 59" W). Ryder Bay is a small bay within the larger Marguerite Bay

south of Adelaide Island, west of the Antarctic Peninsula. The sampling location is approximately 4 km offshore with a water depth of approximately 520 m. Marguerite Trough is a glacially-scoured canyon within the WAP shelf system which is highly effective in transporting UCDW from the ACC into the inshore regions such as Marguerite Bay. Samples were collected twice a week from a small boat. If sea-ice or weather conditions would not allow access to this site, sampling was conducted at an alternative site which has been shown to represent similar conditions with the same water masses (Clarke et al. 2008).

Samples at the RaTS site were collected at fixed depths (surface, 5 m, 15 m, 25 m, and 40 m and if possible, at 75 and 100 m) using Niskin bottles. The 15-m depth interval represents the long-term mean depth for the fluorescence maximum so that this depth is sampled more frequently and samples for phytoplankton composition (HPLC) and $\delta^{18}O_{H2O}$ are collected at this depth. On a few sampling days, samples were also taken at greater depths (100 or 130 m) to establish background nutrient concentrations.

The sampling procedures follow the protocol established by RaTS research staff. Samples at the surface were collected with a 12-V electric bilge pump into acid-cleaned polyethylene containers for processing at the Rothera laboratories. All other sample depths were collected using 5-L Niskin bottles and a hand-operated winch.
DOC/TDN samples were filtered through pre-combusted GF/F filters (nominal pore size 0.7 µm) into acid-cleaned and combusted glass conical flasks under a gentle vacuum. On land, samples were transferred to acid-clean HDPE bottles and frozen at – 20 °C until analysis.
Sea-ice cores were collected from landfast sea ice in Hangar Cove to the north of Rothera for inorganic and organic nutrient analysis in 2014/15. The cores were collected using a 90-mm diameter rotary ice corer. After collection, the cores were

sectioned into slices between 5 and 15 cm thickness with a clean steel hand saw which were thawed in the dark at + 4 °C.

Inorganic macronutrient samples were filtered through Acrodisc PF syringe filters with 0.2 µm Supor membranes and immediately stored at – 80 °C for 12 hours after which they were stored at – 20 °C until analysis.

Ammonium samples were sealed immediately and kept at + 4 °C until processing.

Phytoplankton pigmentation samples were collected at 15 m depth in 2 to 10 L Niskin bottles. Particles were collected on GF/F filters (Whatman 47mm ø) by vacuum-filtering 1 L of collected seawater. Filters were snap-frozen in liquid nitrogen and stored at – 80 °C.

$\delta^{18}O_{H2O}$ samples were collected at the surface and 15 m depth in 150-ml medical flat bottles, sealed with rubber bands and parafilm until analysis.

2.1.2 Sampling sites and sample collection – U.S. Palmer Long Term Ecological Research Program Annual Cruise 2017

The PAL LTER samples for this thesis were collected on-board the *ARSV Laurence M Gould* (LMG) during research cruise LMG1701 from January 6th to February 1st 2017. Samples were collected with a SeaBird 911 Plus Conductivity-Temperature-Depth instrument attached to a rosette containing 24 Niskin bottles of which two were fired at each depth to provide enough seawater for all research conducted. Seawater was collected for the analysis of particulate organic carbon and nitrogen and their isotopic compositions, dissolved inorganic nutrients, dissolved organic carbon and nitrogen, primary production and chlorophyll *a*, microbial measurements such as bacterial cell count and activity. Sea-ice data are derived from satellite observations *of NASA's Scanning Multichannel Microwave Radiometer* and the *Defense*

Meteorological Satellite Program's Special Sensor Microwave/Imager. Data of all PAL LTER cruises since 1990 are available at http://pal.lternet.edu.

Samples for DOC/TDN and inorganic nutrient analysis were collected following the Joint Global Ocean Flux Study protocols (JGOFS, Knap et al. 1996). 60-ml HDPE bottles were acid-washed (24 hours in 10% HCl) and rinsed three times with deionised water. Nitrile gloves were worn for the sampling. Before collecting the sample, the sample bottles and lids were rinsed with the sample water three times. Sample seawater was directly gravity-filtered from the Niskin bottles through pre-combusted GF/F filters (Whatman 0.7 µm 47 mm Ø; combustion at 450 °C for 5 hours in methanol-cleaned tin foil) and the sample bottles were filled just below the bottle neck. The samples were immediately transferred to a – 80 °C freezer before being stored at – 20 °C. The majority of samples collected during the 2017 PAL LTER research cruise were delivered to the UK Rothera research station from where they were transported to the UK on a research vessel ensuring constant storage at -20 °C. Samples collected after delivery to the UK research station were transported in a Styrofoam box surrounded by dry ice with a temperature probe to ensure no major temperature change.

Samples for POCN analysis were collected on pre-combusted (450 °C for 5 hours) GF/F filters (Whatman 0.7 µm GF/F 25mm Ø). 4 L of seawater were collected directly from the Niskin bottles into acid-cleaned (24 hours in 10% HCl and 3x DIW-rinsed) brown HDPE bottles and filtered. Filters were transferred into cryovials and frozen at – 80 °C before being stored at – 20 °C. The amount of water filtered was noted in those cases the filter was clogged prior to a complete 4-L filtration.

Samples for inorganic nutrient (NO_3^-, PO_4^-, $Si(OH)_4^-$) were collected into acid-cleaned 60-ml HDPE bottles following the PAL LTER protocol which samples with the same procedure as DOC/TDN sample collection.

Samples for $\delta^{18}O_{H2O}$ were collected during the PAL LTER research cruises at every sampling depth in 50-ml glass bottles which were crimp-sealed.

2.2 Dissolved Organic Matter - Sample Analysis

DOC/TDN analysis was conducted at the School of GeoSciences at the University of Edinburgh (see *table 1 in the appendix* for an overview of all conducted analyses and analysts) via high temperature combustion on a *Shimadzu TOC-V analyser* with an attached *TNM1 Total Nitrogen Measuring unit*. Samples were thawed for approximately 3 hours before analysis. 10 ml of each sample was transferred into acid-cleaned and combusted glass vials using an acid-cleaned 5 ml pipette for analysis. Between samples, the pipette was rinsed with sample water of the following sample. The vials were closed with Teflon-coated screw caps. Milli-Q blanks and replicates were analysed throughout each run. Certified Reference Material (CRM; Hansell Deep Sea Reference Batch #15 Lot 1-15; Florida Strait 750 m DOC 42.00-45.00 µmol C L^{-1}, TDN 31.00-33.00 µmol N L^{-1}) was analysed before and after each batch of samples. The instrument automatically analyses each sample 3-5 times depending on in-run reproducibility. Deep-sea samples were re-analysed with Deep Sea Reference Batch #18 Lot 08-18 (DOC 41.0 – 45.8 µmol C L^{-1}, TDN 31.6 – 35.0 µmol N L^{-1}). CRMs were intercompared to ensure linearity of the instrument throughout the period of analysis. The CRM DOC values were checked to lie within 5% of the consensus value prior to each sample run. If this was not the case, more CRMs were analysed until the results were within the range. Detection limits are 0.04 µmol C L^{-1} for DOC and 0.36 µmol N L^{-1} for TDN and analytical precision for DOC was ± 1.09 µmol C $L^{-1}$and for TDN ± 0.51 µmol N L^{-1}.

While dissolved inorganic carbon can be removed efficiently through acid treatment prior to high temperature combustion, there is no such method currently available for the removal of dissolved inorganic nitrogen compounds (nitrate NO_3^-, nitrite NO_2^-, ammonium NH_4^+). In order to determine the concentration of dissolved organic nitrogen in a sample, all inorganic compounds have to be analysed and subtracted from the measured total dissolved nitrogen concentration. Due to logistical constraints, the PAL LTER program does not measure NH_4^+ concentrations so that all DON concentrations stated in chapter 4 are a combination of DON and NH_4^+. NH_4^+ concentrations across WAP surface waters have been shown to be minimal, however, when NH_4^+ concentrations might be of importance, they will be mentioned in the discussion. At the RaTS study site, NH_4^+ is analysed in the upper 25 m so that in chapter 3, stated DON concentrations are DON only unless stated otherwise.

2.3 Particulate Organic Carbon and Nitrogen

Particulate organic carbon and nitrogen and their specific C- and N-isotopic composition have been analysed at the School of GeoSciences at the University of Edinburgh (appendix table 1). Filters for POCN analysis were removed from freezing conditions and dried overnight in acid-cleaned and pre-combusted glass vials (24 hours in 10 % HCl, combusted at 450 °C for 5 hours) in a drying oven at 60 °C. To remove inorganic carbon, the filters were moistened carefully by pipetting DI water onto them and stored in a borosilicate glass vacuum desiccator with concentrated HCl overnight. After another overnight drying period in the drying oven at 60°C, filters were folded and transferred into tin capsules ready for analysis.

Samples were analysed on a *CE Instruments NA2500 Elemental Analyser* connected to a *Thermo Electron Delta+ Advantage* stable isotope ratio mass spectrometer. Both

instrument are linked through a *Finnigan ConFlo III Universal Interface* to allow for simultaneous carbon and nitrogen analysis. 12-14 mg of the sediment standard PACS-2 ($\delta^{15}N$ 5.215 ‰, $\delta^{13}C$ -22.228 ‰) were analysed as isotopic CRM along each sample run. Acetanilide standard is used for the determination of the elemental composition (71.09 % C, 10.36 % N).

The C- and N-isotopic compositions are stated as the ratio of relative difference in isotopic abundance in a sample compared to a standard with the general formula

$$\delta\ in\ ‰ = \frac{R(sample) - R(standard)}{R(standard)} * 1000$$

where R represents the isotopic ratio of each element. Carbon isotopic values are compared to the standard Pee Dee Belemnite with an accepted $^{13}C/^{12}C$ ratio of 11,237.2 ± 2.9 (Craig, 1957). The nitrogen standard is atmospheric N_2 with an accepted $^{15}N/^{14}N$ ratio of 3676.5 ± 8.1 (Junk & Svec, 1958).

2.4 The N-isotopic composition of nitrate

The N-isotopic composition of nitrate was analysed at the School of GeoSciences at the University of Edinburgh using the denitrifier method developed by Sigman et al. (2001), Casciotti et al. (2002) and Tuerena et al. (2015). The denitrifier method makes use of denitrifying bacteria (*Pseudomonas aureofaciens*) which lack N_2O reductase. These bacteria convert nitrate to nitrous oxide gas (N_2O) which can be analysed in an isotope ratio mass spectrometer (IRMS). *Pseudomonas aureofaciens* utilises a copper-type nitrite reductase which, unlike other denitrifying bacteria, does not incorporate oxygen from water but from nitrate into the N_2O molecules so that both nitrogen and oxygen can be analysed isotopically. Cultures of the bacterium are grown on tryptic soy agar plates from single colonies between 24 and 48 hours. A

single colony is selected and added to 120 ml of tryptic soy broth with 10 mM KNO_3, 2 mM $(NH_4)_2SO_4$ and 36 mM KH_2PO_4 to be grown in 160-ml butyl rubber-stopper bottles on a reciprocal shaker table in the dark at room temperature for approximately 7 days. After seven days, the media is tested for its nirate content using Griess reagents. Once all nitrate is consumed by the bacteria, the bacterial cultures are concentrated by centrifugation and resuspended in nitrate-free media. After resuspension, 3 ml of the bacterial medium is injected into 20 ml headspace vials which are crimp-sealed and purged with N_2 gas for three hours on a custom-built manifold. After purging, the sample is injected with an acid-cleaned and gas-tight syringe. Each sample volume is adjusted to contain 30 nmol nitrate. Samples are stored overnight in an overhead position to prevent atmospheric gases from entering. On the following day, 0.2 ml of 10 M NaOH is added to each sample and standard to lyse the bacteria.

In the IRMS, He acts as the carrier stream. After removing water vapour by sending the stream through an ethanol trap at - 60 °C, the sample travels through a stainless steel loop immersed in liquid N_2 to condense N_2O gas. Gas chromatography separates the sample into distinct N_2O and CO_2 streams before the sample is led into the *Thermo Fisher Scientific Delta+ Advantage* stable IRMS. Raw $\delta^{15}N$ data are corrected to atmospheric N_2 gas and precision and accuracy are measured with isotopic CRM as stated in table 2.1. Detection limits of the IRMS are better than 0.5 ‰ and the methodological analytical precision is 0.2 ‰ for $\delta^{15}N_{NO3}$. The N-isotopic composition is stated as the ratio of relative difference in isotopic abundance in a sample compared to a standard with the general formula

$$\delta\ in\ ‰ = \frac{R(sample) - R(standard)}{R(standard)} * 1000$$

where R represents the isotopic ratio of each element. The nitrogen standard is atmospheric N_2 with an accepted $^{15}N/^{14}N$ ratio of 3676.5 ± 8.1 (Junk & Svec, 1958).

Table 2.1: Isotopic values for reference materials used with the denitrifier method.

Reference material	*Chemical formula*	*‰ air N_2*	*Standard deviation*
IAEA-NO3	KNO_3	+4.7	0.2
USGS-32	KNO_3	+180	1.0
USGS-34	KNO_3	-1.8	0.2

2.5 Auxiliary data – laboratory analysis

2.5.1 PAL LTER Dissolved Inorganic Nutrient analysis

PAL LTER dissolved inorganic nutrients (Nitrate+nitrite, Silicate and Phosphate) were analysed using a *Seal Analytical* segmented flow autoanalyser (Mequon, WI, Seal AutoAnalyzer AA3). Methods for each analysis followed the protocols recommended in the Seal Customer Support Manual. Nitrate analysis was conducted via reduction to nitrite in a copper-cadmium column and a further reaction with N-1-naphthylethylene diamine dihydrochloride to form a purple azo dye which is then analysed colorimetrically. Phosphate analysis follows the Murphy and Riley method (Murphy & Riley, 1962). The determination of silicate is based on the reaction between silico-molybdate to molybdenum blue by ascorbic acid. Standards for each analysis were sodium nitrite and potassium nitrate, potassium dihydrogen phosphate and sodium meta-silicate nonahydrate. A deep-sea sample collected during each year's cruise at 3,000 m was analysed as an internal reference standard. Detection limits for nitrate+nitrite were 0.015 µmol N L^{-1}, for phosphate 0.0021 µmol P L^{-1} and for silicate 0.03 µmol Si L^{-1}.

2.5.2 RaTS Dissolved Inorganic Nutrient Analysis

RaTS inorganic nutrient samples were analysed at the Plymouth Marine Laboratory, UK. Samples were thawed for 48 hours to allow for complete dissolution of silicate precipitates to silicic acid. A *Technicon AAII* segmented flow autoanalyser was used for the analysis of nitrate+nitrite, nitrite, phosphate and silicate concentrations. Raw data were corrected to certified reference material (KANSO Ltd. Japan), ambient ocean salinity and pH. Analytical reproducibility was usually better than 0.2 µmol N l^{-1} for nitrate+nitrite, 0.01 µmol N L^{-1} for nitrite, 0.02 µmol P L^{-1} for phosphate and 0.6 µmol Si L^{-1} for silicate.

Ammonium concentrations were analysed with a fluorometric method using orthophthaldialdehyde (OPA) following Holmes et al. (1999). Samples were processed within 4 hours of sample collection. The working reagent was made from OPA, sodium sulphite and borate buffer and the samples were incubated along with the working reagent overnight. The combination of OPA and sodium sulphite creates coloured polymers with an intensity according to NH_4^+ concentrations which can be analysed via fluorescence. The fluorescence was measured within 24 hours on a Turner Designs 700 fluorometer. Ammonium chloride was used as calibration standard and the instrument was calibrated before and after analysis of every batch of samples using the low value of green fluorescence 7000-922. The detection limit of this method was 0.01 µmol L^{-1}.

2.5.3 Phytoplankton primary production (PAL LTER) and phytoplankton pigmentation (RaTS)

Primary production rates and chlorophyll-*a* concentrations have been gathered throughout the PAL LTER cruise by the research group of Oscar Schofield.

Primary production rates, measured as daily carbon uptake in mg C m^{-3} day^{-1}, are measured with incubation experiments. 100 ml of seawater sample were inoculated with 1 µCi of ^{14}C-radio-labelled $NaHCO_3$ in borosilicate bottles. The bottles were incubated for 24 hours at *in situ* light levels and ambient temperatures. After the 24-hour incubation period, the seawater samples were filtered through GF/F filters, the filters were washed with 10 % HCl, dried and counted in a scintillation counter.

Chlorophyll *a* samples were filtered onto GF/F filters and kept frozen at – 80 °C stored in cryovials. Analysis was conducted at Palmer Station through acetone extraction and measurement of the extract on a Turner 10AU Fluorometer.

Chlorophyll-*a* concentrations at the RaTS site were determined by fluorometry as part of the CTD deployments. Phytoplankton-pigmentation samples from the RaTS site were analysed at the University of Groningen using high-performance liquid chromatography (HPLC). Prior to analysis, the filters were freeze-dried for 48 hours in the dark and incubated in 90% acetone for pigment extraction at 4 °C. Pigment separation was conducted on a *Waters 2695 HPLC* system with a *Zorbax Eclipse XDB-C8* column (3.5 µm particle size) following van Heukelem & Thomas, (2001) and Perl (2009). Retention time and diode array spectroscopy type 996 (Waters) were used for the manual identification of pigments. Standards (DHI Lab Products) of the following compounds were run alongside for calibration purposes: chlorophyll c3, c2, peridin, 19'-butanoyloxyfucoxanthin, fucoxanthin, neoxanthin, prasinoxanthin, 19'-hexanoyloxyfucoxanthin, alloxanthin, lutein, chlorophyll b and chlorophyll a1. The CHEMTAX v1.95 (Mackey et al., 1996) programme was used to calculate the varying

abundance of phytoplankton groups. The pigment data were separated into the 6 most represented phytoplankton classes in the Southern Ocean (Rozema et al., 2016; Wright et al., 2010): prasinophytes, chlorophytes, dinoflagellates, cryptophytes, haptophytes and diatoms. The detection limit is 0.25 µg L^{-1} Chl *a*. Pigment data is stated as % of total pigments measured.

2.5.4 PAL LTER Microbial data

Bacterial abundance, production and HNA/LNA (high nucleic and low nucleic acid content) were analysed onboard the LMG. Bacterial abundance and HNA and LNA were analysed within two hours after collection via flow cytometry with SYBR-Green staining following Gasol & Del Giorgio (2000). Total abundance was counted by adding 1 µm microspheres and 5 µm of SYBR-Green to 0.5 mL of a seawater sample. After a 30-minute dark incubation, bacterial cells were analysed for 2 minutes at a slow flow rate. Numbers were determined in cytograms of green fluorescence recorded at 530 ± 30 nm versus side angle light scatter. HNA and LNA subgroups were separated by gating the cytogram and discriminating by their respective green fluorescence.

Bacterial production rates were determined via incorporation of ^{3}H-radio-labelled leucine following a modified protocol by Smith & Azam (1992). Samples were treated in triplication. Control samples were spiked immediately after sampling with 200 µL formalin in order to stop any biological activity. Each 1.5 mL sample was spiked with ^{3}H-leucine (MP Biomedical, Santa Ana, CA; >100 Ci/mmol, 20-25 nM final concentration) and incubated for 3 hours at 0.5 °C. At the end of the incubation period, 200 µL formalin was added to the samples. After concentration by centrifugation, the

samples were rinsed with 5 % trichloroacetic acid and 70 % ethanol and air-dried overnight before analysis by liquid scintillation counting in an Ultima Gold cocktail.

2.5.5 $\delta^{18}O_{H2O}$ analysis

The samples for the $\delta^{18}O_{H2O}$ composition were analysed at the Natural Environmental Research Council Isotope Geosciences Laboratory at the British Geological Survey. Samples were analysed on a *VG Isoprep 18* and *SIRA 10* mass spectrometer with random samples analysed in duplication for precision which is usually better than ± 0.02 ‰. The oxygen isotopic composition of seawater ($\delta^{18}O_{H2O}$) is determined by the comparison of the ratio of $^{18}O/^{16}O$ of a sample to that of a standard. For oxygen isotope measurements, this standard is Vienna-Standard mean ocean water (V-SMOW). The $\delta^{18}O_{H2O}$ is expressed as

$$\delta^{18}O(sample) = \left[\frac{\left(\frac{18O}{16O}\right)sample}{\left(\frac{18O}{16O}\right)VSMOW} - 1\right] x\ 1000‰$$

The method followed the equilibrium method for carbon dioxide established by Epstein & Mayeda (1953).

2.5.6 PAL LTER Dissolved Inorganic Carbon

Dissolved inorganic carbon (DIC) samples were collected from the surface and the deepest niskin bottles and preserved with 200 uL saturated $HgCl_2$ before being sealed and transported to the Ducklow laboratory at the Lamont-Doherty Earth Observatory for analysis. Analysis followed the WOCE-JGOFS recommendations (Dickson &

Goyet, 1992; Knap et al., 1996). The average standard deviation for replicate samples was 0.15%.

2.6 Calculations and statistical analysis

2.6.1 Depth-integrated standing stocks and nutrient uptake

Organic matter standing stocks and nutrient uptake were integrated over the upper 50 m for samples from the PAL LTER sampling grid, in agreement with other studies finding that most biogeochemical parameters fall back to background levels or show only little variability below 50 m in the WAP region (Ducklow et al., 2012) and most activity happening within the mixed layer which for all stations is within this range. Further, most biological and biogeochemical measurements, such as primary production, chlorophyll *a* and POC and PN are only collected at the uppermost 6 depths at each station during the PAL LTER cruise.

For RaTS data, the upper 40 m were depth-integrated as data density was best and highest in all seasons in the upper 40 m and samples were collected less frequently at deeper depths.

Depth-integrated standing stocks of particulate and dissolved organic carbon, nitrogen, inorganic nutrients, chlorophyll-*a* and rates of primary production and bacterial production were calculated by trapezoidal integration. At stations with no 50 m (40 m) measurement, the 50 m (40 m) value was interpolated. Results are listed in the appendix table 8.

2.6.2 $\delta^{18}O_{H2O}$ fractions of CDW, sea ice and meteoric origin

The contributions of sea ice and glacial meltwater to the surface waters of the WAP PAL LTER grid were calculated from $\delta^{18}O_{H2O}$ measurements. A three-endmember

mass balance developed by Östlund & Hut (1984) and adapted to WAP conditions is used to separate the freshwater contribution from sea-ice and meteoric meltwater from CDW seawater:

$$\begin{pmatrix} sim + fmet + fcdw = 1 \\ fsim \,.\, fsim + Smet \,.\, fmet + Scdw \,.\, fcdw = S \\ \delta sim \,.\, fsim + \delta met \,.\, fmet + \delta cdw \,.\, fcdw = \delta \end{pmatrix}$$

Where *f*sim, *f*met and *f*cdw are the fractions of sea ice, meteoric water and CDW, respectively; Ssim, Smet and Scdw are the salinities of sea ice, meteoric water and CDW and δsim, δmet, δcdw their corresponding $\delta^{18}O$ values. The $\delta^{18}O$ and salinity endmember values, respectively, are + 0.1 ‰ and 34.73 for CDW, + 2.1 ‰ and 7 for sea ice and – 16 ‰ and 0 for meteoric water (Meredith et al., 2008, 2010).

2.6.3 Mixed layer depth

The mixed layer depth (MLD) is defined as the depth at which $\sigma_t > 0.05$ kg m^{-3} from surface measurements of the CTD downcast data in agreement with other Southern Ocean studies (Long et al., 2012; Mitchell & Holm-Hansen, 1991; Venables et al., 2013).

2.6.4 Statistical analyses

Statistical analyses were conducted in the statistical software R version 3.4.3 (R Core Team, 2017). Surface and depth contour plots were drawn in Ocean Data View 4 (Schlitzer, 2017) using weighted-average gridding. Statistical differences were calculated using two-sample t-tests ($\alpha = 0.05$). Relationships between variables were

established through linear regression analysis. Further, stepwise regression was conducted to establish temporal and spatial trends. The temporal datasets were statistically analysed with lags in time and depth in order to investigate potential offsets in time and space. The significance of established relationships was evaluated at $p < 0.05$.

CHAPTER 3

Temporal Variability and Physical and Biological Controls of Dissolved Organic Carbon and Nitrogen West of the Antarctic Peninsula

3.1 Introduction

Dissolved organic matter (DOM) represents a large pool of oceanic carbon which is potentially exportable to deep waters. Identifying processes involved in DOM cycling is important to fully understand the global marine carbon cycle. Processes driving the production and removal of dissolved organic carbon (DOC) and dissolved organic nitrogen (DON) at the West Antarctic Peninsula (WAP) on seasonal and inter-annual time scales have not been investigated to this date. DOC concentrations are stated in several Southern Ocean studies (e.g. Carlson et al., 1998; Doval et al., 2002; Kähler et al. 1997; Wedborg et al. 1998; Wiebinga et al., 1998), however, there is little research on the production and recycling of DOC or DON in the WAP upper ocean. There is a general agreement that only little DOM is being produced in the Southern Ocean (Carlson et al., 1998; Kähler et al., 1997, Doval et al., 2002; Ducklow et al., 2012; Wang et al., 2010). However, temporarily high accumulation of DOC during phytoplankton blooms in the Southern Ocean could be shown in some of those mentioned studies.

The WAP represents a shelf region different from other regions in Antarctica for two main reasons: Firstly, it is in close proximity of the Antarctic Circumpolar Current (Hofmann et al., 1996; Martinson et al., 2008) which allows for intrusions of relatively warm and nutrient-rich Upper Circumpolar Deep Water (UCDW) nourishing the shelf waters with nutrients essential for primary production.

Secondly, during the second half of the 20th century, the WAP underwent rapid warming with increases in atmospheric and oceanic temperatures along with increased glacial melting and decreases in sea-ice coverage and duration (Marshall et al., 2006; Meredith & King, 2005; Vaughan et al., 2003).

At the UK Rothera Research Station, located on Adelaide Island in the Southern part of the WAP shelf (67°35'8"S, 68°7'59"W, Figure 3.1.1), the local marine ecosystem has been studied since 1997 with year-round quasi-weekly sample collection in Ryder Bay. Due to its proximity to the glaciated coast, there is frequent and high influx of glacial meltwater influencing the local ecosystem. During spring, light availability and sea-ice melt increase which allow for phytoplankton growth with high rates of primary production. The ecosystem at the RaTS site highly depends on climatic changes with the greatest influence being sea-ice cover and duration as well as wind patterns (e.g. Smith & Comiso, 2008; Vernet et al., 2008). In the North of the WAP, recent climate change led to a combination of increased cloud cover and winds with a decrease in sea-ice cover and duration which causes a deepening of the mixed layer with the effect of decreased phytoplankton biomass. In the South, a decrease in sea-ice cover led to decreased stratification, which ultimately caused a decrease in primary production in the coastal region of the South. At the same time, in the open ocean areas, decreasing cloud cover and winds caused less mixing so that there is more space, radiation and time available for phytoplankton primary production (Montes-Hugo et al., 2009; Saba et al., 2014). Despite these striking difference within the WAP region, major biogeochemical processes have been found to be relatively uniform in the North and the South (Ducklow et al., 2015). Glacial meltwater supports stratification in coastal regions, such as Ryder Bay, and has been shown to introduce micronutrients to the surface waters enhancing primary production (Annett et al., 2015; Eveleth et al., 2017). The effect of sea-ice melt and glacial meltwater on stratification has cascading effects on primary production: Diatoms, dominating WAP

phytoplankton blooms, have been shown to grow more efficiently in shallower mixed layers due to enhanced irradiance while haptophytes are often associated with areas of strongly mixed surface waters (Arrigo, 1999) and cryptophytes occur with high glacial meltwater input (Moline et al. 2004). While particulate organic matter (POM) is a direct product of primary production, DOM is not only the product of primary production. Many physical and biogeochemical processes affect DOM production and removal on different timescales. Quantitative estimates for direct DOM excretion by phytoplankton are difficult to establish. However, multiple studies show direct DOC release ranging from 2 to 60% of photosynthetic carbon assimilation with varying effects from nutrient limitation, phytoplankton species composition and the stage of the phytoplankton bloom (Fisher & Rochelle-Newall, 2002; Myklestad, 2001; Van den Meersche et al., 2004; Wetz & Wheeler, 2003). Further, some phytoplankton species utilise dissolved organic nitrogen as a nutrient source (Bradley et al., 2010; Bronk et al., 2007; Zhang et al., 2015), complicating the scenario of DOM production and removal processes. Due to above mentioned regional differences in warming and varying degrees of freshwater influx, phytoplankton community composition and biomass vary in space and time along the WAP (Garibotti et al., 2003, 2005; Prézelin et al., 2000; Saba et al., 2014).

DOC measurements have been collected at the RaTS site since 1997 (Clarke et al., 2008). However, neither these nor DON measurements have yet been the main focus of research. For this study, samples have been collected over three consecutive austral summer seasons at the RaTS site (2013/14, 2014/15, 2015/16) in order to establish an understanding of the seasonal cycling of DOC and DON as well as interannual variability.

In this study, it is hypothesised that DOC and DON are not being released directly from phytoplankton during a phytoplankton bloom but with a temporal offset which is

due to bacterial degradation of particulate organic matter. Further, it is tested whether DOC and DON concentrations change in response to physical (e.g. salinity, temperature, meltwater fraction) and biological changes (e.g. phytoplankton community and bacterial composition). It is additionally hypothesised that the major driver of bioavailable DOM accumulation in the WAP surface waters ultimately is the phytoplankton community composition and the timing of phytoplankton blooms.

DOM measurements are available for the complete austral summer season of 2013/14. 2014/15 samples cover the onset of spring/summer conditions up to the first phytoplankton bloom maximum and 2015/16 data collection started in early-bloom conditions in January. The focus of this study will therefore be on the 2013/14 season and the data of the other two seasons will be used to investigate differences in DOM dynamics and possible reasons behind those and to establish an understanding of interannual variability.

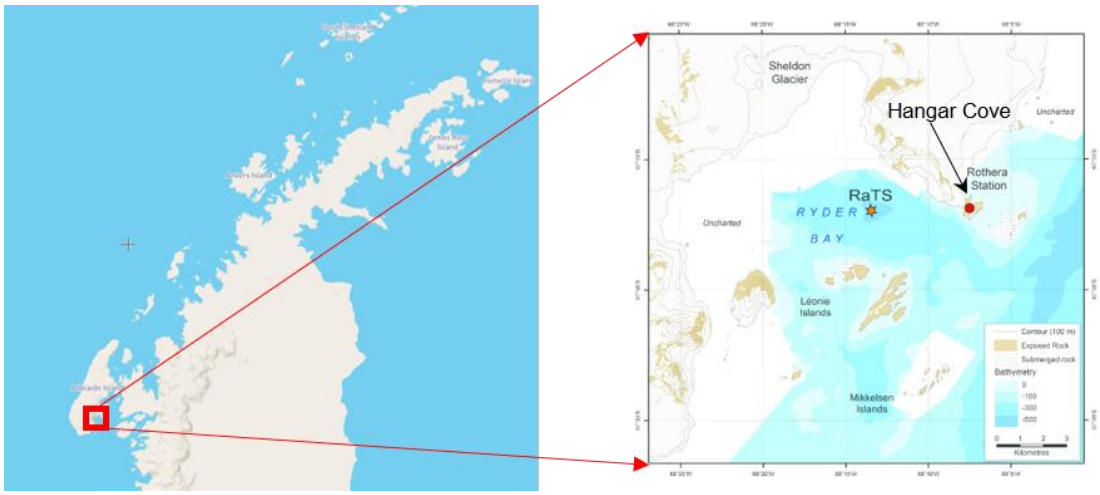

Figure 3.1.1: Location of RaTS sampling site in Ryder Bay and Hangar Cove (sea-ice sampling) in northern Marguerite Bay, Adelaide Island at the West Antarctic Peninsula (map adapted from Bown et al., 2016).

3.2 Methods

3.2.1 Sampling site and sample collection

Seawater samples were collected at the Rothera Time Series (RaTS) site in Ryder Bay, a small bay within the larger Marguerite Bay south of Adelaide Island, west of the Antarctic Peninsula (Figure 3.1.1). The sampling location is approximately 4 km offshore with a water depth of approximately 520 m. Marguerite Trough is a glacially-scoured canyon within the WAP shelf system which is highly effective in transporting UCDW from the ACC into the inshore regions such as Marguerite Bay.

Samples were collected twice a week from a small boat. If sea-ice or weather conditions would not allow access to this site, sampling was conducted at an alternative site which has been shown to represent similar conditions with the same water masses (Clarke et al., 2008). Samples were collected at fixed depths (surface, 5m, 15m, 25, and 40m and if possible, at 75, and 100m) using Niskin bottles. For DOC/TDN, samples were filtered through pre-combusted GF/F filters (nominal pore size 0.7 µm) into acid-cleaned and combusted glass conical flasks under a gentle vacuum. Samples were transferred to acid-clean HDPE bottles and frozen at -20°C until analysis. In 2013/14, samples were collected from mid-November 2013 to the end of February 2014. The 2014/15 season was sampled from mid-November 2014 until the end of December 2014 with additional samples collected mid-January 2015. The 2015/16 season was sampled from early January 2016 to the end of March 2016. During all sampling events, a conductivity-temperature-depth instrument was deployed for measurements of temperature, pressure, salinity, photosynthetically active radiation (PAR) and fluorescence. The data were logged at 1m-resolution. The mixed layer depth (MLD) was defined as the depth at which σ_t is 0.05 kg m^{-3} greater than σ_t at the surface.

Sea-ice cores were collected from landfast sea ice in Hangar Cove to the north of Rothera (Figure 3.1.1) for inorganic and organic nutrient analysis in 2014/15. The cores were collected using a 90-mm Ø rotary ice corer. After collection, the cores were sectioned into slices between 5 and 15cm thickness with a clean steel hand saw and thawed in the dark at + 4 °C. Samples for organic nutrient analysis were filtered through pre-combusted Whatman GF/F filters and stored at -20 °C for further analysis. Samples for inorganic nutrient analysis were filtered through 0.2 µm nucleopore filters, snap frozen at -80 ° C and stored at -20 °C until analysis. The sea-ice core samples were then analysed along seawater samples.

Table 1 in the appendix lists all relevant data analyses, the methodologies applied and the institute at which these analyses were conducted.

3.2.2 Analysis of dissolved organic carbon and total dissolved nitrogen

DOC/TDN analysis was conducted at the School of GeoSciences at the University of Edinburgh via high-temperature combustion on a *Shimadzu TOC-V analyser* with an attached *TNM1 Total Nitrogen Measuring unit*. Samples were thawed for approximately 3 hours before analysis. 10 ml of each sample was transferred into acid-cleaned and combusted glass vials using an acid-cleaned 5 ml pipette for analysis.

Sample replicates were analysed in each run for precision. Certified Reference Material (CRM; Hansell Deep Sea Reference Batch #15 Lot 1-15; Florida Strait 750 m DOC 42.00-45.00 µmol C L^{-1}, TDN 31.00-33.00 µmol N L^{-1}) was analysed before and after each batch of samples for accuracy. Deep-sea samples were re-analysed with Deep Sea Reference Batch #18 Lot 08-18 (DOC 41.0 – 45.8 µmol C L^{-1}, TDN 31.6 – 35.0 µmol N L^{-1}). CRMs were intercompared to ensure linearity of the

instrument throughout the period of analysis. The CRM DOC values was checked to lie within 5% of the consensus value. If this was not the case, more CRMs were analysed until the results were within the range before each sample run. Detection limits are 0.04 µmol C L^{-1} for DOC and 0.36 µmol N L^{-1} for TDN and analytical precision for DOC was ± 1.09 µmol C $L^{-1}$and for TDN ± 0.51 µmol N L^{-1}.

3.2.3 Analysis of particulate organic carbon and nitrogen

Particulate organic carbon and nitrogen concentrations were analysed at the School of GeoSciences at the University of Edinburgh. Filters for POC:N analysis were prepared following a method adapted from Lourey et al. (2004). In brief, filters were decarbonated by wetting them with Milli-Q and fumed with 70% HCl overnight before drying and carefully folding them into clean tin capsules. Samples were analysed on a *CE Instruments NA2500 Elemental Analyser* connected to a *Thermo Finnigan Delta+ Advantage stable isotope ratio mass spectrometer*. Both instruments are linked through a *Finnigan ConFlo III Universal Interface* to allow for simultaneous carbon and nitrogen analysis. The CRMs PACS-2 and acetanilide were analysed for the isotopic composition and carbon and nitrogen concentrations, respectively. The analytical reproducibility was better than 1.0% for POC and better than 1.1% for PN.

3.2.4 Analysis of auxiliary samples

3.2.4.1 Inorganic nutrients

Inorganic macronutrient samples were filtered through Acrodisc PF syringe filters with 0.2 µm Supor membranes and immediately stored at – 80 °C for 12 hours after which they were stored at – 20 °C until analysis (except for ammonium samples). In the Plymouth Marine Laboratory, UK, samples were thawed for 48 hours to allow for

complete redissolution of silicate precipitates to silicic acid. A *Technicon AAII* segmented flow autoanalyser was used for the analysis of nitrate+nitrite, nitrite, phosphate and silicate concentrations. Raw data were corrected to certified reference material (KANSO Ltd. Japan), ambient ocean salinity and pH. Analytical precision was usually better than 0.2 µmol N L^{-1} for nitrate+nitrite, 0.01 µmol N L^{-1} for nitrite, 0.02 µmol P L^{-1} for phosphate and 0.6 µmol Si L^{-1} for silicate.

Ammonium concentrations were analysed at the Rothera laboratories by reaction with orthophthal-dialdehyde (OPA) overnight and analysis by fluorometry following Holmes et al (1999). Ammonium samples were incubated overnight with the working reagent (OPA, sodium sulphite and borate buffer). The fluorescence was measured within 24 hours of incubation using a Turner Designs 700 fluorometer. Ammonium chloride was used as a standard. The fluorometer was calibrated at the beginning and the end of each batch using the low value of green fluorescence standard 7000-922. The detection limit is 0.01 µmol N L^{-1}. Sample processing was carried out within four hours after sample collection to minimise changes to ammonium concentrations during sample storage.

3.2.4.2 Phytoplankton pigment analysis

Phytoplankton pigmentation analysis was conducted at the University of Groningen using high-performance liquid chromatography. Samples were collected in 2 to 10 L Niskin bottles at 15m depth since this depth is the overall long-term fluorescence maximum. Particles were collected on GF/F filters (Whatman 47mm Ø) by vacuum-filtering 1 L of collected seawater. Filters were snap-frozen in liquid nitrogen and stored at – 80 °C. Prior to analysis, the filters were freeze-dried for 48 hours in the dark and incubated in 90% acetone for pigment extraction at 4 ˚C. Pigment separation was conducted on a *Waters 2695 HPLC system* with *a Zorbax Eclipse XDB-C8*

column (3.5 µm particle size) following van Heukelem & Thomas (2001) and Perl (2009). Pigment data is stated as % of total pigments measured.

3.2.4.3 The $\delta^{18}O$ composition of seawater

Samples for $\delta^{18}O_{H2O}$ were collected from the surface and 15 m depth in 150-ml medical flat bottles, sealed with rubber bands and parafilm. The samples were analysed at the Natural Environmental Research Council Isotope Geosciences Laboratory at the British Geological Survey. Samples were analysed on a *VG Isoprep 18 and SIRA 10* mass spectrometer with random samples analysed in duplicate which showed an average precision better than ± 0.02‰. The method followed the equilibrium method for carbon dioxide established by Epstein & Mayeda (1953). The contribution of sea ice and glacial meltwater were calculated using a three end-member mass balance approach following Meredith et al. (2016) who adopted the method from (Östlund & Hut, 1984).

3.2.4.4 Sea-ice observations

At the RaTS site, sea ice cover was observed visually, and a weighting scheme is employed for conversion to an overall sea-ice score ranging from 0 to 10. A score of 0 marks ice-free conditions while a score of 10 represents full ice cover.

3.2.4.5 Statistical analysis and data integration and interpolation

Statistical analyses were conducted in the statistical software *R* version 3.4.3 (R Core Team, 2017). Depth contour plots were drawn in *Ocean Data View 4* (Schlitzer, 2017) using weighted-average gridding. Statistical differences were calculated using two-

sample t-tests ($\alpha = 0.05$). Relationships between variables were established through linear regression analysis. Further, stepwise regression was conducted to establish temporal and spatial trends. All RaTS datasets were statistically analysed with lags in time and depth in order to investigate potential offsets in time and space. The significance of established relationships was evaluated at a $p < 0.05$.

3.3 Results

The available data vary greatly between seasons. While the 2013/14 dataset is the most complete and covers the entire season from November until the end of February, both 2014/15 and 2015/16 are limited: The 2014/15 data set captures pre-bloom conditions and the build-up phase of the first phytoplankton bloom. 2015/16 covers the period from mid-January until mid-March. Other biogeochemical parameters have been measured throughout the 2015/16 season showing that phytoplankton did not start forming blooms until early January so that the first phytoplankton bloom maximum is captured in the data available. All contour plots are drawn with Ocean Data View (Schlitzer, 2017). Tables with all data presented here are listed in the appendix of the thesis.

3.3.1 Oceanographic setting

All three seasons were preceded by winters of full sea-ice cover (> ice score 7) lasting between 3 (2013) and 4.5 months (2015) (Figure 3.3.1). Sea ice retreated earliest in 2013 on November 21st, and in 2014 on December 18th. The 2015/16 season shows more variability in sea-ice cover. Based on Stammerjohn et al. (2008), sea-ice retreat days are defined as the number of days since the first day that sea-ice cover is < 15 % for more than 5 consecutive days prior to sampling. For this study, a threshold of 20 % is applied due to the different approach of sea-ice observations at the RaTS site where a sea-ice score of 2 accounts for 20% sea-ice cover. In October 2015, there is at first a longer duration of sea-ice free conditions, but sea ice then returns to the area again with >20% until early January 2016.

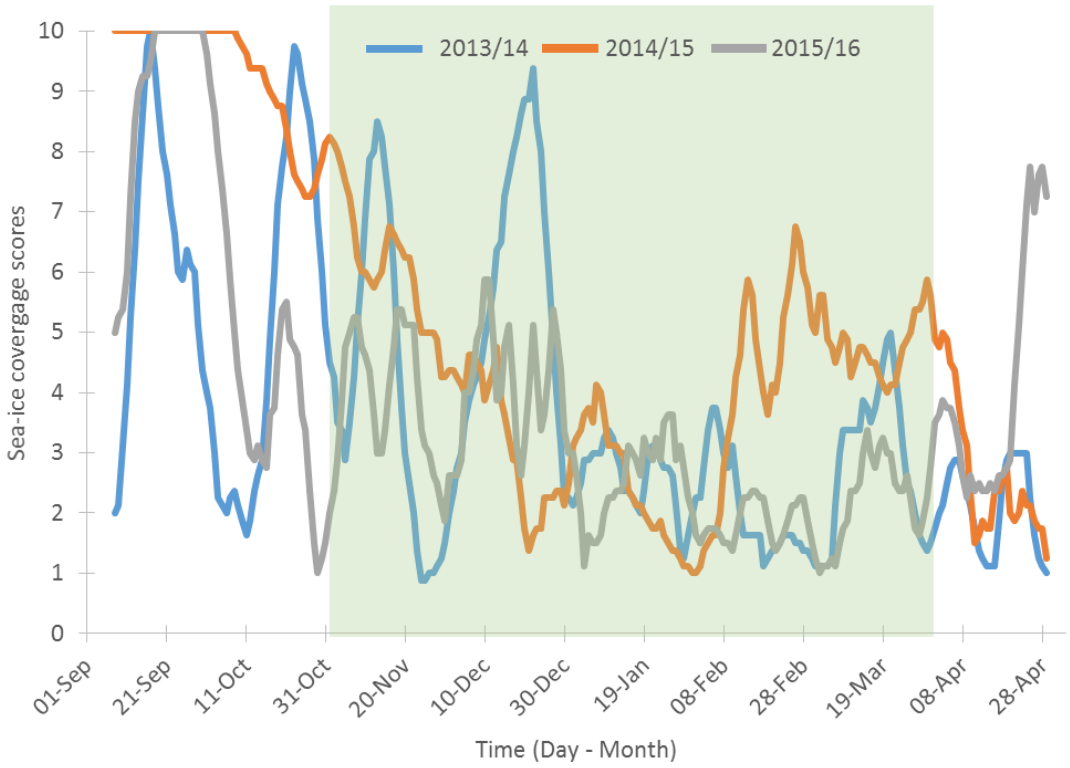

Figure 3.3.1: 8-day moving average of sea-ice coverage at the RaTS sampling site in Ryder Bay for September to April for the three investigated seasons 2013/14 (blue), 2014/15 (orange) and 2015/16 (grey). The green area depicts the spring/summer period.

The mixed layer was shallowest and most stable in 2013/14 remaining shallower than 10 m throughout the sampling period (Figure 3.3.2). In 2014/15, salinity starts to decrease during December with a concurrent increase in temperature leading to a shallowing of the mixed layer which, prior to this point, was variable between 2 and 40 m (Figure 3.3.3). In 2015/16, the situation is similar with a strong decrease in salinity in early January which promotes formation of a shallow mixed layer (Figure 3.3.4).

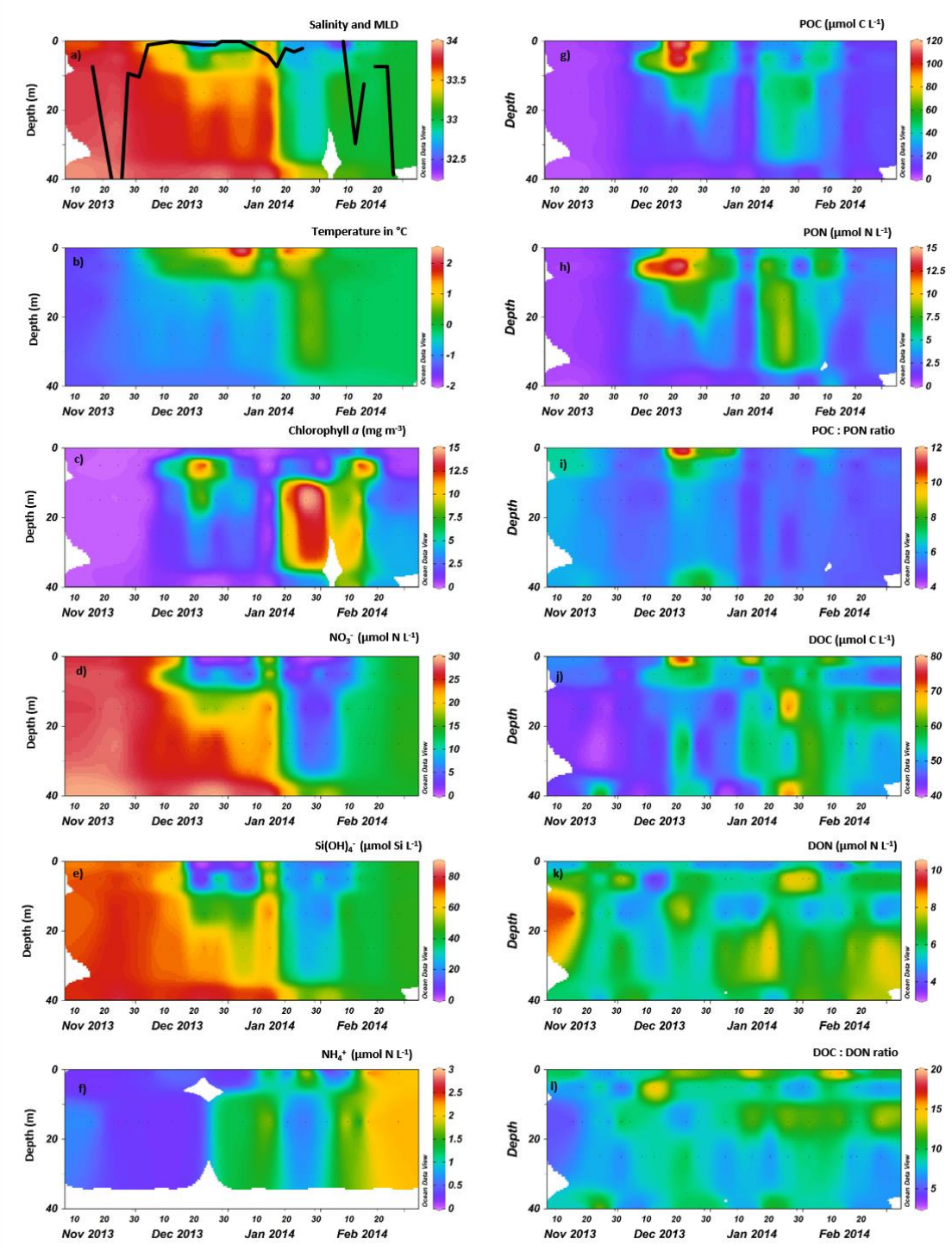

Figure 3.3.2: Distribution of physical and biogeochemical parameters at the RaTS sampling site from November 2013 to February 2014 in the upper 40 meters. In a) the salinity distribution is overlaid by the mixed layer depth (MLD, black line). b) shows the temperature, c)-f) chlorophyll a concentrations and inorganic nutrient concentrations. g)-l) particulate and dissolved organic matter and their molecular ratios, respectively.

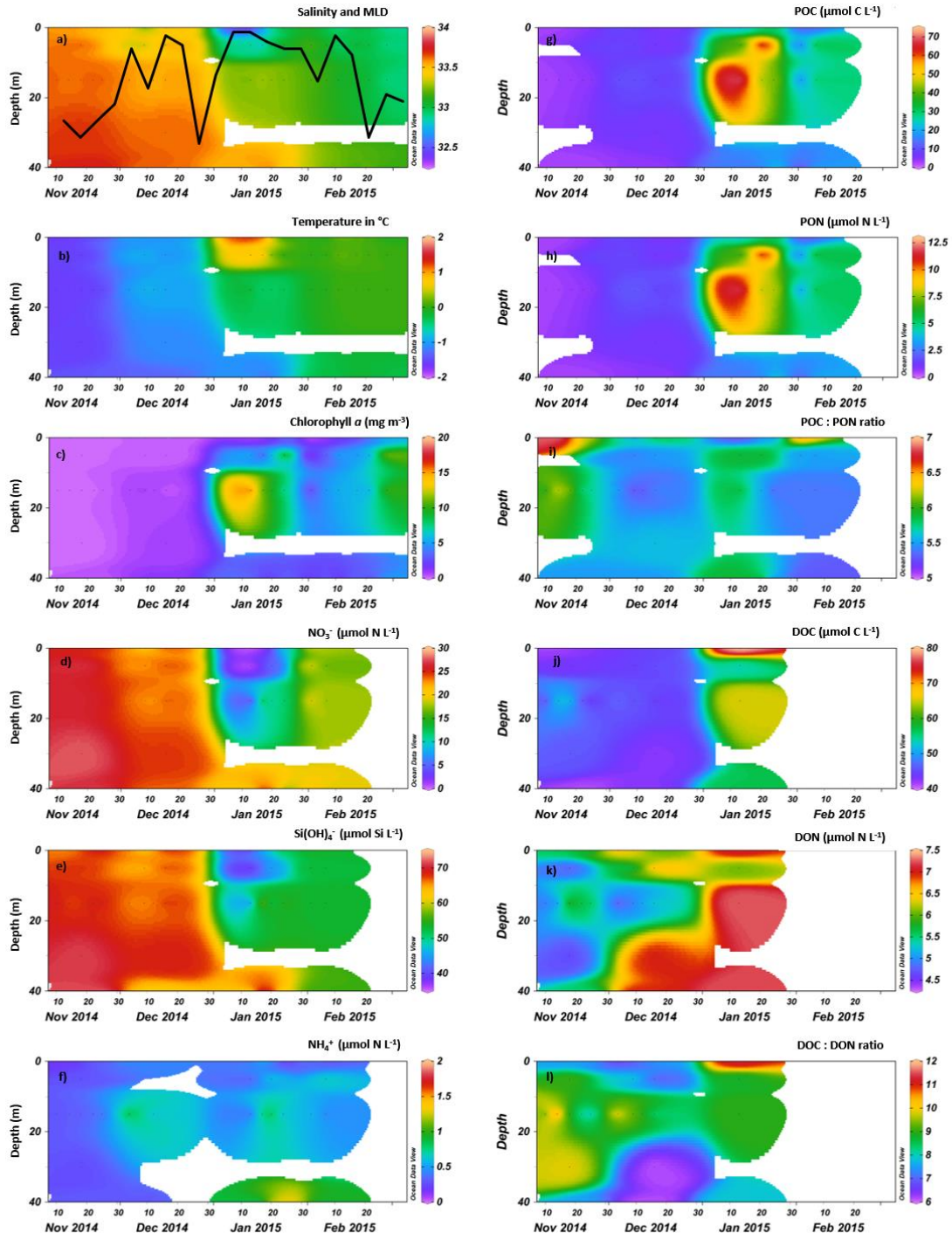

Figure 3.3.3: Distribution of physical and biogeochemical parameters at the RaTS sampling side from November 2014 to February 2015 in the upper 40 meters. In a) the salinity distribution is overlaid by the mixed layer depth (MLD, black line). b) shows the temperature, c)-f) chlorophyll a concentrations and inorganic nutrients. g)-l) particulate and dissolved organic matter and their molecular ratios, respectively.

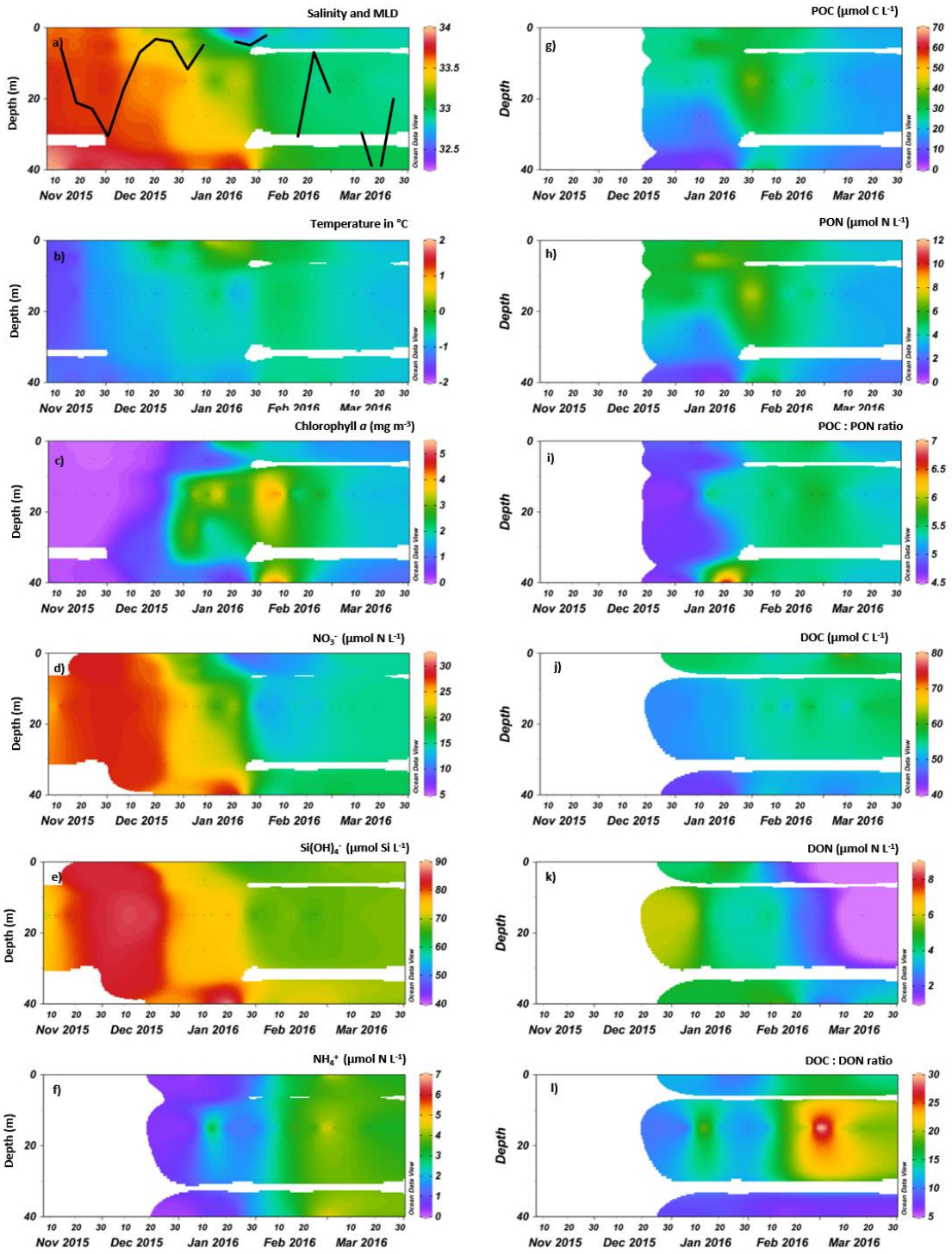

Figure 3.3.4: Distribution of physical and biogeochemical parameters at the RaTS sampling site from November 2015-March 2016 in the upper 40 meters. In a) the salinity distribution is overlaid by the mixed layer depth (MLD, black line). b) shows the temperature, c)-f) chlorophyll a concentrations and inorganic nutrients. g)-l) particulate and dissolved organic matter and their molecular ratios, respectively.

3.3.2 Phytoplankton, POM and nutrient dynamics

In all three investigated seasons, and in agreement with other studies (Baker et al., 1996; Ducklow et al., 2007; Martinson et al., 2008; Smith et al., 1995), the retreating sea ice in spring leads to a shallowing and stabilisation of the mixed layer at the RaTS site. In addition to increasing solar radiation, conditions for phytoplankton-bloom development are created. The phytoplankton blooms build up to a maximum of chlorophyll *a* (2013/14 14.92 mg Chl-*a* m^{-3}, 2014/15 19.86 mg Chl-*a* m^{-3}, 2015/16 5.15 mg Chl-*a* m^{-3}) and POM concentrations (2013/14 166.77 µmol C L^{-1}, 18.79 µmol N L^{-1}; 2014/15 71.42 µmol C L^{-1}, 12.12 µmol N L^{-1}; 2015/16 43.40 µmol C L^{-1}, 8.12 µmol N L^{-1}) after which POM concentrations decrease rapidly (Figures 3.3.2, 3.3.3, 3.3.4). POM and chlorophyll-*a* concentrations overall remain at elevated concentrations after the onset of the first phytoplankton bloom with distinct peaks of strongly increased chlorophyll-*a* in all three seasons.

Daily depth-integrated (40m) chlorophyll-*a* concentrations are maximal 481 mg m^{-2} in 2013/14 (Figure 3.3.5). In 2014/15, maximum depth-integrated chlorophyll *a* is measured on January 3rd 2015 with 484.6 mg m^{-2} and in 2015/16, maximum chlorophyll concentration was 180 mg m^{-2}. The phytoplankton peak in 2014/15 occurred during the period of no sample collection as shown in the chlorophyll-*a* data. For 2015/16, chlorophyll-*a* data are available for the entire spring/summer and no increased chlorophyll-*a* values are observed prior to the measured blooms. Whilst depth-integrated chlorophyll-*a* stocks vary intensely between years, depth-integrated POM standing stocks show less variability with a range of maximum values from 1478 mmol C m^{-2} (2015/16) to 1890 mmol C m^{-2} (2013/14) and 275 mmol N m^{-2} (2014/15) to 290 mmol N L^{-2} (2013/14). In 2013/14, highest depth-integrated POC occurs during the first phytoplankton bloom while PN is higher in the second peak at the end of January. The integrated POC:N ratio is higher than the Redfield ratio during the 1st

bloom (7.6) and lower than Redfield in the second bloom (5.2). In 2014/15, all OM concentrations peak at the same time on January 13th (Figure 3.3.5 and 3.3.6).

In 2015/16, the second peak in primary production brings highest depth-integrated POC and PN concentrations. Depth-integrated chlorophyll-*a* maxima appear to be less stable and occur only over short periods of times with a rapid build-up and rapid degradation afterwards. However, chlorophyll-*a* concentrations remain elevated in the upper 15 m after the first increase for the entire sampling period with maxima lower than in the previous two seasons (Figure 3.3.4).

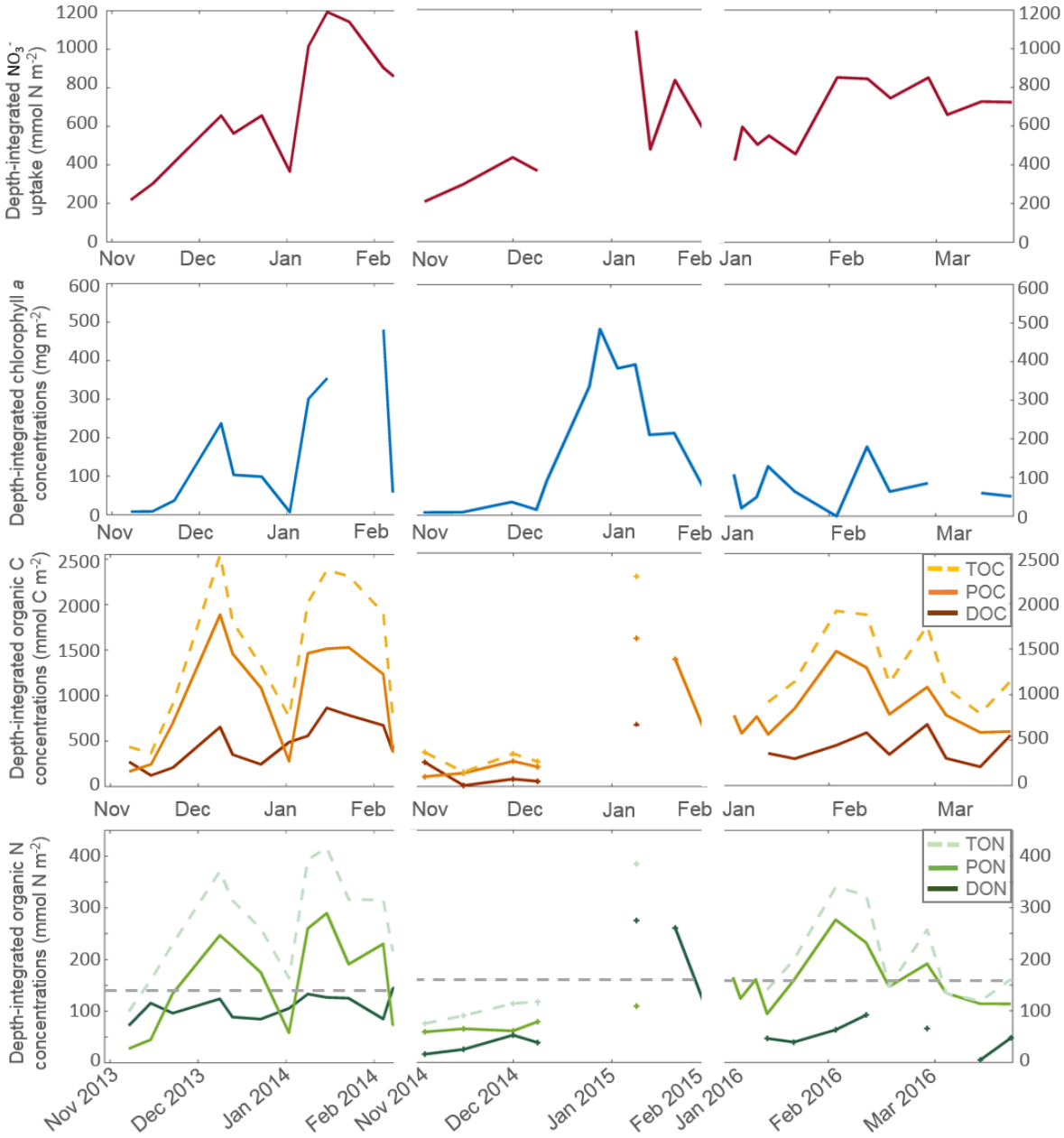

Figure 3.3.5: Depth-integrated (upper 40m) nitrate uptake, chlorophyll a and organic carbon and nitrogen for all three RaTS seasons in comparison. Data are most complete for 2013/14. The data collected show strongest phytoplankton blooms with highest POM concentrations in 2013/14 and lowest in 2015/16. The grey dashed line in the organic nitrogen plot shows integrated deep-sea DON (calculated from the deepest measurements which are considered CDW background over 50m). Calculated values above the line indicate DON production and values below DON consumption.*
** Nitrate uptake is calculated as the difference of the deepest measured nitrate concentrations and the subsequent upper ocean depth.*

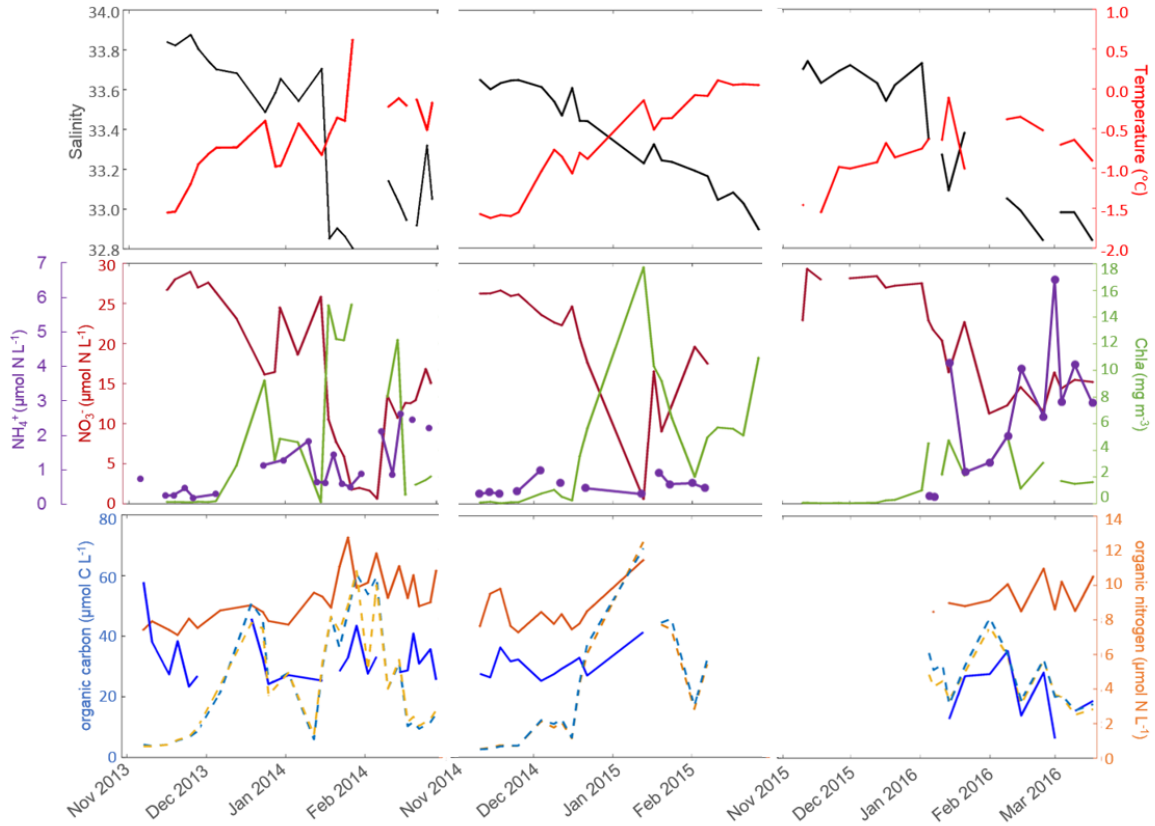

Figure 3.3.6: Salinity, temperature, nitrate and chlorophyll a concentrations and POM and DOM in a time series plot from November to March for all three seasons 2013/14, 2014/15, 2015/16 measured at 15m at the RaTS sampling site in Ryder Bay, Adelaide Island,west of the Antarctic Peninsula. In the lower panel, particulate organic carbon is shown with a dashed blue line and particulate organic nitrogen with a dashed yellow line. Please note the varying time periods on the x axis per season.

The HPLC analyses show that in all three seasons, the peaks of phytoplankton blooms are dominated by > 80% diatoms (Figure 3.3.7). There is a seasonal progression of the phytoplankton community with other phytoplankton groups such as haptophytes and cryptophytes showing higher contributions to the phytoplankton community composition during the bloom-development phase or during degradation. In the late stage of the second bloom of 2013/14, the phytoplankton assemblage consists of approximately 35% cryptophytes, 29% haptophytes and 29% diatoms with the remaining 7% being a mixed assemblage of prasinophytes, chlorophytes and dinoflagellates. In 2014/15, during pre- and early bloom conditions, haptophytes, and

to some extent prasinophytes contribute significantly to the phytoplankton assemblage with up to 32 and 15%, respectively. In late 2015/16 bloom conditions, cryptophytes dominate with 40-60% of the total phytoplankton assemblage.

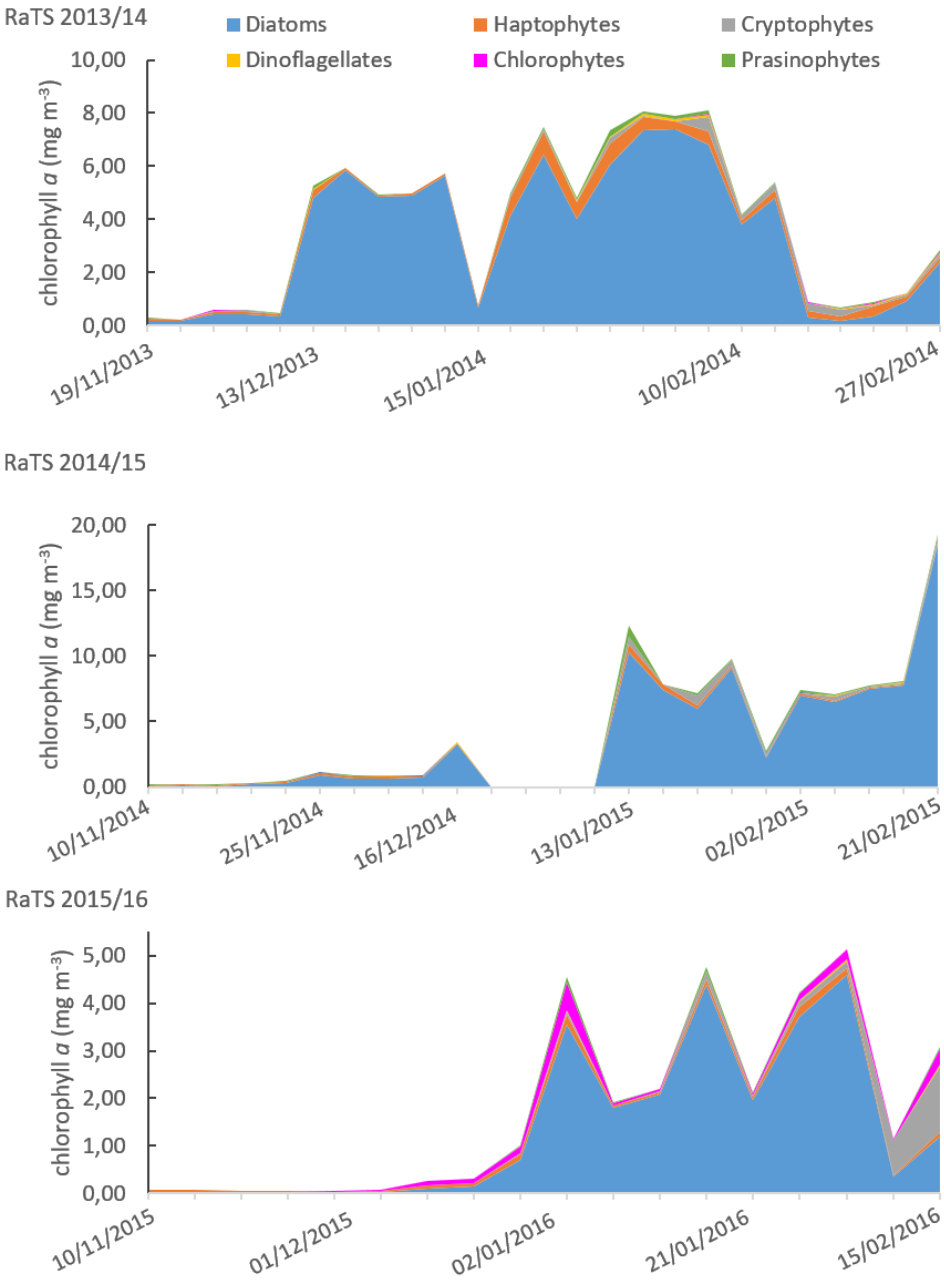

Figure 3.3.7: Phytoplankton species contribution to total chlorophyll calculated as percentage contribution. The total represents chlorophyll a measurements. All data measured at 15m at the RaTS sampling site 2013-2016. Please take note of the different scales on y axes due to large differences between seasons.

During the first phytoplankton peak from late December 2013 to early January 2014 (Figure 3.3.2), nitrate concentrations in the surface are near depletion (< 0.05 µmol N L^{-1}) which occurs again down to 5 m depth during the second phytoplankton production maximum during January. $Si(OH)_4^-$ concentrations approach depletion during the first bloom but not during the second.

NH_4^+ concentrations are highly variable between years (figure 3.3.2f, 3.3.3f, 3.3.4f). In 2013/14 maximum concentrations do not exceed 3 µmol N L^{-1}, in 2014/15, maximum concentrations are 1.4 µmol N L^{-1} and in 2015/16, maximum concentrations are 6.56 µmol N L^{-1}. Ammonium concentrations are higher than in the other two seasons throughout the water column in 2015/16. Due to the high interannual and seasonal variability, [NH_4^+] for 40 m in 2013/14 have not been interpolated. However, both 2013/14 and 2014/15 data show a trend of NH_4^+ accumulation over time at all depths. Therefore, DON concentrations at 40 m in January 2014 can be expected to comprise between 1 and 2 µmol N L^{-1} from NH_4^+ and in February, the NH_4^+ contribution to DON might have increased to approximately 2-3 µmol N L^{-1}. In 2015/16, NH_4^+ concentrations are < 1.00 µmol N L^{-1} at the beginning of the phytoplankton bloom in early January and are elevated throughout thereafter. Both 2013/14 and 2014/15 only show increased values (> 1 µmol N L^{-1}) later in the season (late January to early February). In 2014/15, these high concentrations only occur at the 40 m sampling interval.

3.3.3 Dissolved Organic Matter

In 2013/14, both DOC and DON concentrations tend to follow POC and PN concentrations to some extent with accumulation and maximum concentrations (DOC 88.65 µmol C L^{-1}, DON 8.46 µmol N L^{-1}) either with or shortly after the POC and PN

maxima of the first phytoplankton bloom. Both show large variability thereafter (Figure 3.3.5 and 3.3.6).

At 15 m, DOC concentrations remain elevated (> 51 µmol C L^{-1}) after the second bloom, but with strong variability over time. At the surface and at 5 m, [DOC] increases with the build-up of the first phytoplankton bloom and quickly decreases after. There is no net accumulation at these depth during the second bloom. Elevated DOC concentrations coincide with the peak of the first phytoplankton bloom at the surface and occur after the second POC maximum at 15 and 40 m depth. Concentrations > 60 µmol C L^{-1} are generally found in the upper 40m only. DON concentrations range from 3.38 to 10.13 µmol N L^{-1}.

The DOC:DON ratio shows large variability over a range from 4.16 to 18.09. Highest ratios occur at the surface and at 15m depth towards the end of the season.

The deepest DOC measurements available in 2013/14 were collected at 100m and have a mean of 42.63 ± 1.17 µmol C L^{-1}. The lowest DOC concentration of 40.54 µmol C L^{-1} is found at the end of November in the surface waters and is likely upwelled refractory DOC. DOC concentrations remain low through the entire season below 75 m. Deep DON concentrations in 2013/14 are 5.65 ± 0.74 µmol N L^{-1} (100m) and 5.61 µmol N L^{-1} (130m).

2014/15 DOC measurements for > 40 m are available for 50 and 75 m with 2 samples taken at each depth. The mean DOC concentration here is 44.94 ± 6.22 µmol C L^{-1} and for DON 6.24 ± 0.83 µmol N L^{-1}.

In 2013/14, highest depth-integrated DOC concentrations occur with the second phytoplankton peak at the end of January while depth-integrated DON peaks after the second peak in February (Figure 3.3.5). Both depth-integrated DOC and DON peak at the same time as POM in the 2014/15 data set. In 2015/16, the second primary

production peak is higher in depth-integrated POM while both DOC and DON peak later. Highest depth-integrated DON is found 8 days after the POM peak and DOC peaks 14 days after the DON maximum. This DOC maximum co-occurs with elevated depth-integrated POC and PN which is, however, not as high as the first peak.

3.3.4 Sea-ice core dissolved organic matter, nitrate and ammonium concentrations

The sea-ice cores collected in 2014/15 cover the period from November 4th 2014 to December 22nd 2014. They show high spatial and temporal variability in DOC and DON concentrations with ranges for DOC from 29 µmol C L^{-1} to 1.04 mmol C L^{-1} (median = 70.49 µmol C L^{-1}) and for DON 1.9 to 159.0 µmol N L^{-1} (median = 4.75 µmol N L^{-1}), Figure 3.3.8. The DOC:DON ratio lies between 7.5 and 56.8 with a median of 14.7. Highest DOC and DON concentrations are found on December 22nd in the bottom 5 cm slice with DOC being approximately 11 times higher and DON being 24 times higher than the early-to-mid-November mean (DOC mean from Nov 4th – Nov 18th = 93.52 ± 22.56 µmol C L^{-1} and DON mean = 6.59 ± 1.09 µmol N L^{-1}).

Except for two ice-core slices, nitrate concentrations are very low (35 out of 42 samples < 1.0 µmol N L^{-1}, data in the appendix). Highest NO_3^- concentrations (9.13 – 13.61 µmol N L^{-1}) are most commonly found in the bottom 5 cm of each ice core except for two cores in November in which they are in the section 20-35 cm from the ice-water interface (0.58 and 2.77 µmol N L^{-1}).

Ammonium concentrations in the analysed sea-ice cores is consistently below 2 µmol N L^{-1}. Highest concentrations (> 1 µmol N L^{-1}), except for one ice core, are only found in those sea-ice core slices in which both DOC and DON concentrations are elevated compared to the other slices.

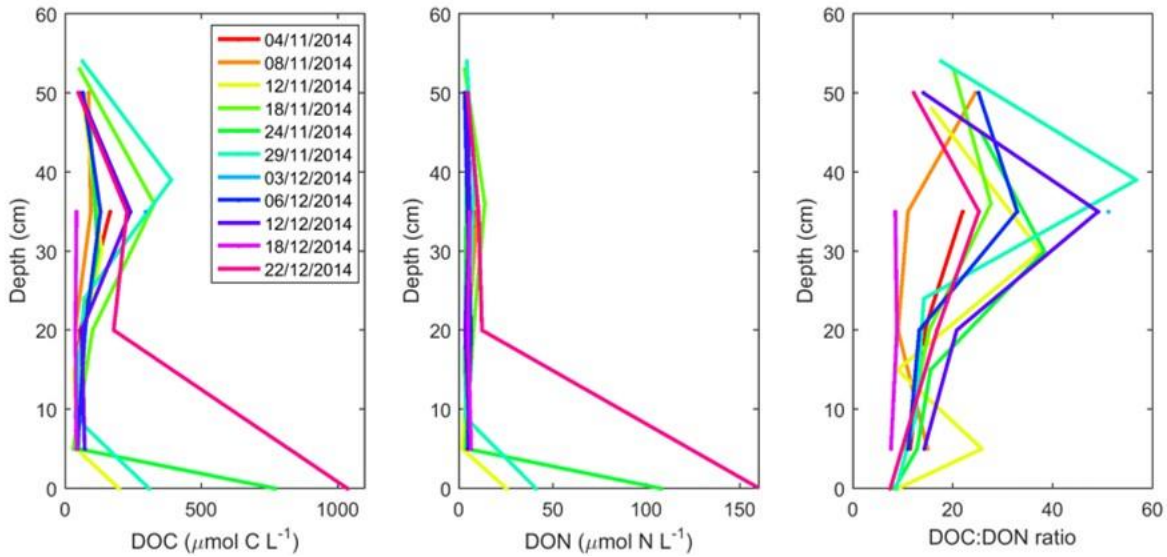

Figure 3.3.8: Concentrations of DOC and DON and the DOC:DON ratio in the 2014/15 sea-ice cores collected at Hangar Cove. 0cm depth represents the interface between seawater and sea ice.

3.4 Discussion

In all three seasons, phytoplankton biomass increases shortly after the decline of sea ice, an increase in light availability and a shallowing of the mixed layer. Nutrient concentrations are well-mixed throughout the water column at the beginning of each season. POM concentrations increase with the onset of phytoplankton bloom activity shown by increasing chlorophyll-*a* concentrations and nutrient drawdown in the upper ocean. There are two distinct blooms in the 2013/14 season with varying intensity. POC and PN concentrations are highest in the upper 5m during the first bloom and at 15m during the second. At the surface, the POC:N ratio increases rapidly during the first bloom to a peak of 11.8 while at 15m, it remains mostly below Redfield and varies between 4.7 and 6.7 with a mean of 5.77 ± 1.12. During the second bloom, primary production at the surface is much lower than during the first which indicates a shift in phytoplankton species composition. Even though diatoms are still dominant during the second bloom, their contribution decreases from >95% to 85-90% and cryptophytes increase in numbers. The C:N ratio of POM remains mostly below Redfield ranging from 4.7 to 6.7 in the upper 15m. These low C:N ratios show that phytoplankton are not limited by nitrogen in these waters. However, nitrate concentrations come close to depletion levels during both blooms in the upper 15 m. The following discussion will focus on the role of DOC and DON in these conditions in the WAP shelf biogeochemical cycling over an austral summer season.

3.4.1 Distribution of DOC and DON in 2013/14, 2014/15 and 2015/16

DOM concentrations in the analysed seasons makes up only a small fraction of *in situ* total organic matter concentrations compared to lower-latitude systems where DOC makes up > 80% of TOC (Carlson et al., 1998; Osterholz et al., 2016): With

background levels of approximately 40 µmol C L^{-1} and 3 - 4 µmol N L^{-1} DOC and DON, respectively, freshly produced DOM in all three seasons covers a range from 0.3 µmol C L^{-1} to maxima between 30 and 45 µmol C L^{-1} and 0.05 to 6.75 µmol N L^{-1}. High DOC and DON concentrations in 2013/14 and 2014/15 occur in the surface at the same time of POC maxima. DON concentrations in 2013/14 are highest with the start of observations in November (10.13 µmol N L^{-1}). However, it is unclear what caused these increased concentrations due to no preceding available data. A possible reason is direct release from melting sea ice which showed 100% cover between November 8th and 11th and decreased to 50% within a few days before sampling. On January 15th 2014, a mixing event introduced water of higher salinity, lower temperature, and higher nutrients to the surface. Chlorophyll *a* and POM concentrations are diluted minimally or mixed downwards. DOC concentrations show a slight increase in the surface while there is no observable effect on DON.

The vertical distribution of DOC and DON is variable in all seasons. Overall, the upper 25 m show most variability in every season which is likely due to processes of both production and removal taking place in the upper ocean. In 2015/16, DOC concentrations decrease with depth throughout all sample days. DON shows more variability and will be discussed in section 3.4.3.

When data are available below 40 m, DOC concentrations mostly decrease back to approximately background levels. However, there are only seven measurements below 40 m available for the entire 2013/14 season, four for 2014/15 and none for 2015/16 so that deeper processes cannot be inferred. DON concentrations are elevated throughout the 2013/14 season at depths below 40 m. There are no measurements available below 130 m so that it is unclear whether concentrations remain elevated with depth or where they decrease to known background concentrations. The 75-m measurements for 2014/15 show similar results to 2013/14:

DOC concentrations are close to deep-sea background concentrations while DON concentrations are slightly elevated below 40 m. The higher DON concentrations at depth are likely the result of bacterial degradation of PN or grazing by zooplankton with high production of NH_4^+ which, at this depth, are included in the DON measurements and are discussed in the following section.

3.4.2 The role of NH_4^+ in WAP waters

Previous studies showed that ammonium accumulation in WAP shelf waters occurs in late summer/early autumn and, thus, concentrations would remain low during the austral spring and summer months during the most productive season due to rapid cycling during primary production (Henley et al., 2018; Serebrennikova, 2005; Serebrennikova & Fanning, 2004). The available RaTS data show that NH_4^+ concentrations can increase intensely during phases of high rates of primary production. 2015/16 shows NH_4^+ concentrations higher than DON concentrations with [NH_4^+] ranging from 0.25 to 6.56 µmol N L^{-1}. High concentrations (>2 µmol N L^{-1}) occur already at the beginning of the phytoplankton bloom in January and remain high until the end of measurements. These high concentrations are found at all sampled depths, however, at the surface, high concentrations only occur at a later stage. The other two seasons show lower concentrations (2014/15: 0.18 - 1.4 µmol N L^{-1}; 2013/14: 0.1 - 2.82 µmol N L^{-1}). The high variability between depths and in the other two seasons does not allow for interpolation at the 40m-interval in 2013/14. Increased upper ocean NH_4^+ concentrations in 2013/14 mostly occur towards the end of the bloom. In 2014/15, concentrations remain low and full-depth measurements end with the onset of the second phytoplankton bloom. These two seasons, in contrast to 2015/16, support the findings of above-mentioned previous studies of NH_4^+ accumulation towards the end of the phytoplankton growing season. In February 2014, DON

concentrations at 40m range from 6.00 to 7.63 µmol N L^{-1}. It is likely that these DON concentrations are increased due to contributions from ammonium of 2-3 µmol N L^{-1} which has not been measured at this depth. Bacteria degrade DON to NH_4^+ (ammonification, e.g. Berman et al., 1999) which occurs before nitrification (conversion of ammonium to nitrate via nitrite). This conversion occurs rapidly over short time scales. Hence, even though the fraction of NH_4^+ in DON cannot be quantified based on the available data, DON+NH_4^+ concentrations can still be used in order to determine processes within the nitrogen cycle of the system.

The full available data set for 2015/16 shows a strong correlation between DON and NH_4^+ (r= -0.87, $p = 1.74*10^{-6}$), indicating intense ammonification taking place. Further, it shows that DON in Ryder Bay is cycled rapidly to inorganic compounds with little to no DON being exported. The correlation between DON and NH_4^+ is not as strong in 2014/15 which is probably due to the stage in time of the growing season. All seasons show a decrease in NH_4^+ concentrations during the time of high chlorophyll-*a* suggesting preferential NH_4^+ consumption over NO_3^-. This rapid NH_4^+ consumption leads to accumulation only after peak production periods but also to a less strong and less straightforward relationship between NH_4^+ and DON in 2013/14 and 2014/15. For 2013/14, there are not enough data available after the peak of the second phytoplankton bloom (3 data points at 15m), so that this relationship cannot be established.

3.4.3 DOC as a direct product of WAP primary production

Multiple studies show a time lag between phytoplankton and bacterioplankton blooms along the WAP which can last from a few days to weeks (Billen & Becquevort, 1991; Kim & Ducklow, 2016; Lancelot et al., 1991). One hypothesis for this lag was argued to be caused by insufficient dissolved organic matter being produced directly by phytoplankton and thereby limiting bacterial growth (Billen & Becquevort, 1991; Ducklow et al., 2012; Ghiglione & Murray, 2012; Piquet et al., 2011; Rozema et al., 2016). This study confirms that the amount of labile DOM being produced is low and that production occurs only over a short period of time, during phytoplankton bloom activity. However, it does show intensive *in situ* release during phytoplankton bloom conditions with DOC concentrations higher than reported in previous studies.

The focus in the following is on the 2013/14 season. The strong correlations between DOC, inorganic nutrients, POM and chlorophyll-*a* suggest *in situ* DOC production and release by phytoplankton alongside POC production (table 3.4.3.1). Diatoms are thought to produce small amounts of DOM directly (Norrman et al., 1995) with smaller phytoplankton producing and releasing DOM at higher rates than diatoms (Malinsky-Rushansky & Legrand, 1996). Even though the fraction of smaller phytoplankton seems to be minor in the 2013/14 season, they might contribute significant amounts of DOM. A negative correlation between DOC and the Si:N uptake ratio ($r = -0.75$, $p = 8.96*10^{-6}$) supports this suggestion. Lower Si:N ratios are associated with less diatom-dominated phytoplankton blooms which, in this case, correlate with an increased release of DOC. Haptophytes, especially *Phaeocystis*, produce and release large amounts of exopolymeric substances (EPS) which can be in a dissolved or particulate form. EPS compounds are rich in DOC (Arrigo, 1999; DiTullio et al., 2000; Schoemann et al., 2005). Haptophytes do not dominate the blooms in 2013/14, but they show an important contribution throughout the season.

Step-wise regression analyses show that DOC correlates best with other biogeochemical and physical parameters measured contemporaneously (table 3.4.3.1). Further, DOC correlates mostly with biogeochemical parameters in the upper 25 m and other processes appear to be influencing DOC dynamics at greater depths.

At each sampling depth of the upper 25 m (surface, 5 m, 15 m, 25 m), DOC correlates negatively with all inorganic nutrients, and positively with both POC and PN. These correlations are strongest at 15m depth, table 3.4.3.1.

Table 3.4.3.1: Statistical correlation results for both DOC and DON vs. various parameters divided by depth intervals for 2013/14.

		DOC		DON	
		r	p	r	p
0m	NO_3^-	-0.55	0.018	0.10	0.696
	PO_4^-	-0.56	0.015	0.14	0.583
	$Si(OH)_4^-$	-0.49	0.037	0.17	0.510
	POC	0.85	$8.44*10^{-6}$	0.26	0.291
	PN	0.82	$2.89*10^{-5}$	0.16	0.534
	POC:N	0.63	0.005	0.25	0.323
5m	NO_3^-	-0.73	0.0005	-0.15	0.546
	PO_4^-	-0.72	0.0005	-0.07	0.767
	$Si(OH)_4^-$	-0.63	0.004	-0.21	0.377
	POC	0.62	0.004	-0.17	0.479
	PN	0.67	0.003	-0.33	0.183
	POC:N	0.28	0.256	-0.10	0.697
15m	NO_3^-	-0.80	$1.05*10^{-6}$	0.01	0.951
	PO_4^-	-0.77	$3.82*10^{-6}$	0.04	0.851
	$Si(OH)_4^-$	-0.75	$1.07*10^{-5}$	0.01	0.956
	POC	0.53	0.005	0.07	0.760
	PN	0.57	0.002	0.08	0.730
	POC:N	-0.002	0.990	0.41	0.060

Contradicting previous studies (Billen & Becquevort, 1991; Ducklow et al., 2012; Ghiglione & Murray, 2012; Piquet et al., 2011; Rozema et al., 2016), it appears here

that DOC is directly produced along with POM during phytoplankton blooms within the upper ocean. DOC and DON are decoupled. While DON concentrations show a similar development over time until the first phytoplankton bloom peak, there are no good correlations with any biogeochemical parameters (Table 3.4.3.1) without the consideration of time or depth offsets. DON concentrations tend to show the best fit with a time lag of 12 - 22 days (4 sampling days). The decoupled processes indicate that DON undergoes different mechanisms of production and removal than DOC, possibly also representing a nutrient source for both bacteria and phytoplankton and is likely being rapidly cycled in the surface waters at the RaTS site. DON has been shown to be taken up by some phytoplankton species as a preferred nitrogen source in the Arctic (Bradley et al., 2010) and other environments (Bronk et al., 2007; Zhang et al., 2015) with comparable phytoplankton compositions. Some phytoplankton species can switch between inorganic and organic nitrogen sources in order to maintain their nitrogen levels (Bronk et al., 2007; Mulholland et al., 1998, 2003). Once nitrate approaches depletion levels, phytoplankton in Ryder Bay might start utilising available DON compounds in the surrounding water.

The proposed time offset between bacterial and phytoplankton bloom discussed earlier is likely the reason for neither DOC nor DON closely following POM concentrations during the second bloom. During the first bloom, which builds up from November to its peak between December 13th 2013 and January 6th 2014, DOC appears to be driven by the same mechanisms as POM production with strong relationships to physical and biogeochemical parameters (Figure 3.4.1). After splitting the bloom into phases of build-up (start of the bloom until peak) and degradation (after peak until end) (table 3.4.3.2), it becomes clear that these correlations are established within the build-up phase. There are no significant relationships with any of those parameters after the peak of the phytoplankton bloom. This explains temporal

processes throughout the season: The seasonal onset of primary production, and therefore nutrient drawdown and organic matter production, is ultimately driven by light availability, sea-ice melt and co-occurring changes in the system's physical state, the later bloom is not initiated by these physical changes but by nutrient replenishment through mixing events and nutrient recycling.

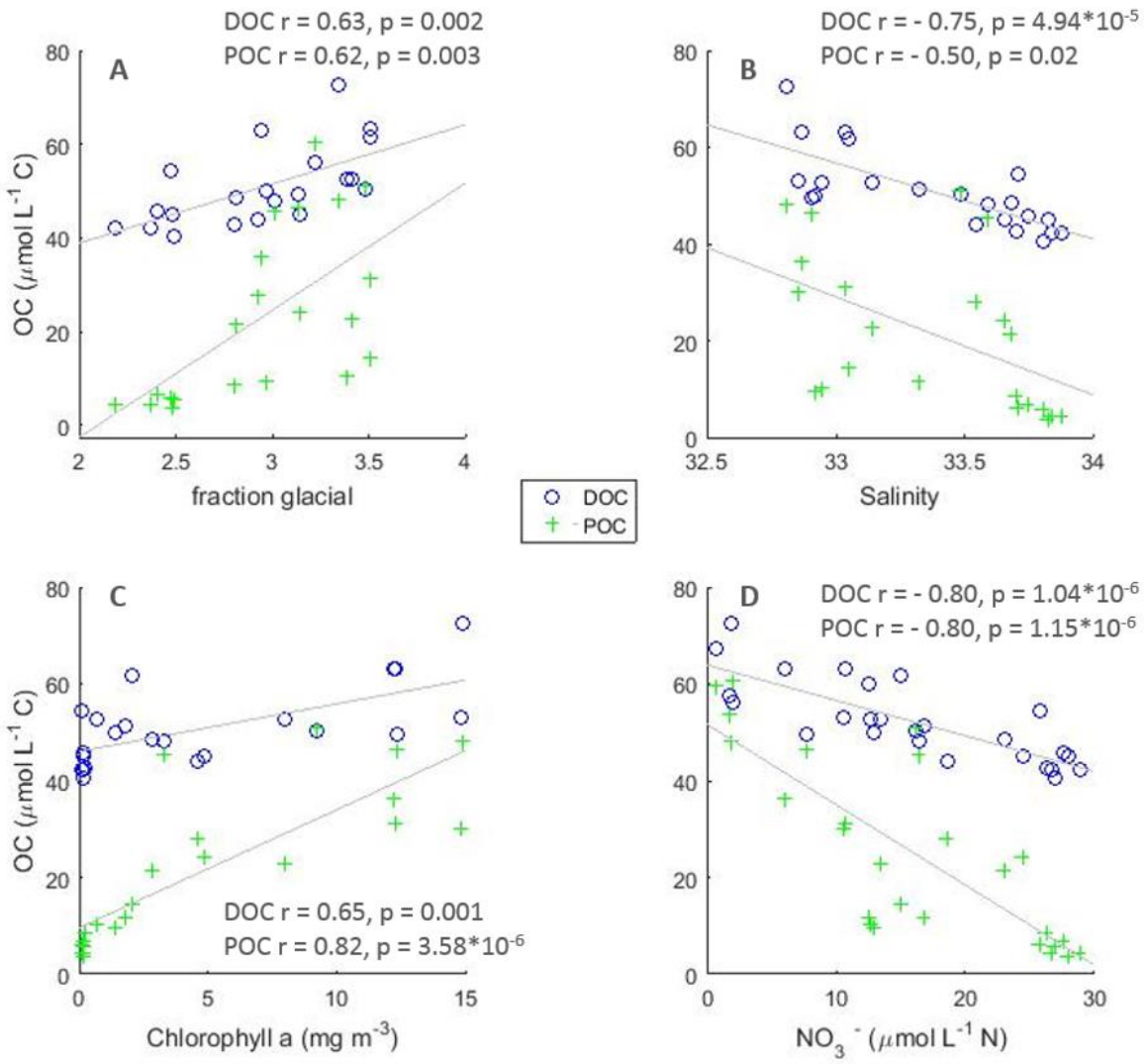

Figure 3.4.1: Correlations of organic carbon (DOC and POC) at 15 m with physical parameters in 2013/14. (A) glacial meltwater fraction, and (B) salinity and biological parameters (C) chlorophyll a and (D) nitrate showing that DOC is likely co-produced during POC formation as a result of physical changes of the water column which allow for primary production.

Multiple studies show that during the growth phase of a phytoplankton bloom and particularly towards the end of it, DOC production and release tend to occur at higher rates and synchronously with POC synthesis (Biddanda & Benner, 1997; Soendergaard et al., 2000; Zlotnik & Dubinsky, 1989). A likely scenario for the 2013/14 season is that DOC accumulated during the first bloom while bacteria increased in abundance and activity. For the duration of the second bloom, bacteria degrade available “first-bloom” DOC along with freshly produced DOM from the second bloom while at the same time, more DOC is being produced. In support of this are the linear regression results in table 3.4.3.2. First of all, DOC correlates significantly with inorganic nutrients as well as POC during the first bloom. Even more, DOC correlates well with physical parameters such as salinity and $\delta^{18}O_{H2O\text{-}seaice}$. DON does not correlate with any parameters in this bloom. The second bloom shows only weak correlations between DOC and inorganic nutrients. Further, there are no correlations with any physical parameters and weak correlations with POC, supporting the three scenarios discussed: (i) physical changes prime the conditions for POM and co-occurring DOM production during the first bloom, (ii) DOC is an *in situ* product of primary production, and (iii) bioavailable DOC is degraded during and after the second bloom. The lack of significant correlations during the degradation phase supports the idea of direct production of DOC during phytoplankton blooms with emphasis on the build-up phase and subsequent degradation by bacteria and possibly other micro grazers in the system.

Table 3.4.3.2: Linear regression results for subdivisions of the 2013/14 data into phytoplankton bloom, the bloom build-up phase and the degradation phase. Correlations between DOC and biogeochemical and physical parameters are good in the first bloom but show improvement after separating the build-up phase from the degradation phase of both blooms. f_{sim} = fraction of sea-ice melt determined by the $\delta^{18}O_{H2O}$.

		DOC		DON	
		r^2	*P*	r^2	*p*
First bloom	NO_3^-	0.49	$1.7*10^{-5}$	0.00	0.887
	$Si(OH)_4^-$	0.35	$5.8*10^{-4}$	0.00	0.870
	POC	0.79	$6.8*10^{-11}$	0.00	0.920
	Chl*a*	0.12	0.077	0.00	0.855
	Salinity	0.59	$1.6*10^{-6}$	0.05	0.264
	Temp.	0.25	0.007	0.11	0.088
	f_{sim}	0.49	0.001	0.01	0.681
Second bloom	NO_3^-	0.14	0.033	0.03	0.333
	$Si(OH)_4^-$	0.12	0.048	0.04	0.271
	POC	0.22	0.006	0.00	0.919
	Chl*a*	0.08	0.181	0.02	0.564
	Salinity	0.03	0.378	0.01	0.616
	Temp.	0.03	0.429	0.03	0.444
	f_{sim}	0.00	0.981	0.24	0.075

		DOC		DON	
		r^2	*p*	r^2	*p*
Bloom build-up	NO_3^-	0.69	$8.8*10^{-8}$	0.00	0.844
	$Si(OH)_4^-$	0.70	$5.0*10^{-8}$	0.00	0.853
	POC	0.69	$7.8*10^{-8}$	0.01	0.733
	Chl*a*	0.45	0.001	0.06	0.290
	Salinity	0.60	$2.2*10^{-5}$	0.05	0.333
	Temp.	0.35	0.004	0.05	0.322
	f_{sim}	0.64	$1.9*10^{-4}$	0.04	0.484
Bloom degradation	NO_3^-	0.01	0.636	0.00	0.943
	$Si(OH)_4^-$	0.00	0.933	0.00	0.975
	POC	0.03	0.411	0.17	0.055
	Chl*a*	0.01	0.720	0.01	0.656
	Salinity	0.04	0.438	0.00	0.851
	Temp.	0.00	0.919	0.01	0.742
	f_{sim}	0.03	0.588	0.05	0.491

There are good correlations between DON and inorganic nutrients (NO_3^-, PO_4^-, $Si(OH)_4^-$) all $r < -0.85$, $p < 0.05$ and PN ($r = 0.76$, $p = 0.005$) when time-lagged by 4 sampling days and with a depth offset between 25 and 40m, which do not exist with any shorter time lags. Even though the number of data points is small (n = 8) due to the lag imposed, the relationships are strong. Because these relationships do not exist for contemporaneous measurements or with any other lag in depth or time, it is likely that PN was produced at shallower depths and degradation processes by zooplankton and bacteria lead to decreasing PN concentrations with depth while at the same time DON is released.

3.4.4 Comparison to 2014/15 and 2015/16

The dynamics of DOM in 2014/15 are similar to 2013/14. Even though no overall conclusion about DOM dynamics in this season can be drawn, some of the reported observations in 2013/14 can be supported here: Both DOC and DON concentrations increase with increasing POM concentrations and show highest values in January during the recorded phytoplankton bloom maximum. Surface DOC appears to be driven by the same factors as POM production correlating well with nutrient uptake (DOC ~ NO_3^- r = -0.98, p = 0.0004) and POC concentrations (DOC ~ POC r = 0.92, p = 0.01). In this season, DON also seems to be directly produced by phytoplankton shown by surface DON concentrations strongly correlating with PN (r = 0.92, p = 0.009) and a negative correlation between DON and NO_3^- in the upper 15m (r = -0.54, p = 0.009). In 2014/15, nutrients do not approach depletion levels to the same extent as in 2013/14.

The 2015/16 data show a dissimilar pattern with differences in both POM and DOM dynamics. As in the other two investigated seasons, the DOC maximum concentrations in 2015/16 occur in the surface but approximately two weeks after POM starts to decline. Surface DOC concentrations are elevated from background concentrations from the start of observations indicating a previous elevation in organic matter production which can be seen in slightly increased POC production a week before DOM observations are available. This early period of POM production despite low chlorophyll-*a* levels is potentially due to the release of DOM and POM from sea-ice melting (see section 3.4.6).

Surface DON concentrations follow PN concentrations closely for the duration of the first POM peak after which they decline until late March. Compared to the elevated DOC concentrations, DON surface concentrations remain low which is reflected in comparatively high DOC:DON ratios ranging from 9.7 to 17.7 in the surface waters.

Highest DON concentrations are found at the start of the phytoplankton bloom early January. On some dates, DON concentrations at 15m and 40m are below background DON concentrations. High NH_4^+ concentrations at the same time point towards ammonification of semi-labile or even refractory DON compounds at these depths. A priming process like this has been suggested by Bianchi (2011) and Tremblay et al. (2015): High concentrations of labile DOM stimulate the activity of bacteria to such extent that they become capable of degrading refractory organic matter. The degradation of organic matter leads to the eventual release of refractory DOM of highly diverse molecules which accumulate in the ocean and are not degraded any further. This refractory DOM can only be further degraded or transformed under suitable environmental conditions such as UV radiation or priming by highly bioavailable DOM but also through well-adapted clades of bacteria in microhabitats (Shen & Benner, 2018).

Because POM is a direct product of phytoplankton production, there is generally a good correlation between nutrient uptake and POM concentrations (Figure 3.4.2). In 2015/16, with the onset of the first phytoplankton bloom, however, nitrate does not appear to be drawn down linearly with POM formation. Both nitrate and PN concentrations are elevated which leads to an insignificant relationship ($p > 0.05$). Without this short period of simultaneous high nitrate and high PN concentrations, the relationship between these two remains as strong as expected (Figure 3.4.2). These dates coincide with increased meltwater input by sea ice after a short period of net sea-ice formation. It is likely that algae and POM are being released from sea ice which would explain the high POM concentrations prior to increasing primary production and nutrient drawdown.

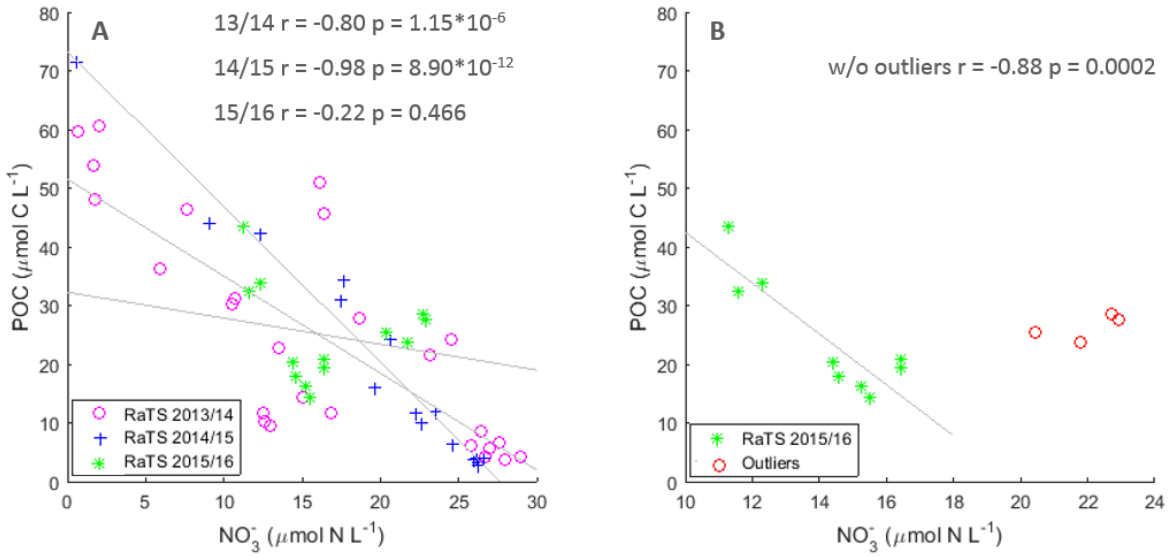

Figure 3.4.2: (A) shows strong correlations between NO_3^- and POC concentrations for the seasons 2013/14 and 2014/15, however, not for 2015/16. As shown in (B), the non-correlation in 2015/16 is due to a period of high nitrate and POC concentrations at the same time without which the correlation between NO_3^- and POC remains strong.

Minimum DON concentrations are lower than typical background levels measuring only 1.14 µmol N L^{-1} in post-bloom conditions. This is surprising because background DOM is considered refractory. UV light is known to being able to transform refractory into labile compounds and vice versa (Kähler et al., 1997; Ortega-Retuerta et al., 2010). However, measured PAR is not particularly high on this date or on any of the preceding sampling days. Even though DOC concentrations also decrease on this date, the decrease is not comparable to that of DON. The DOC:DON ratio increases to 43 showing highly N-depleted DOM. This is the highest ratio measured throughout all three investigated seasons. Overall, DOC:DON ratios range from 5 to 15 but are mostly close around the Redfield C:N ratio.

Only in 2015/16 there is a strong negative correlation between NH_4^+ and DON ($r = -0.87$, $p = 1.74*10^{-6}$) in the upper 15m throughout the sampling period. This negative relationship in combination with the simultaneous decrease of both PN and DON

indicates remineralisation and ammonification. However, it has been shown that along the WAP, the accumulation of NH_4^+ occurs mostly after the productive spring and summer (Henley et al., 2017). A possible explanation for elevated NH_4^+ concentrations throughout the sampling period is high grazing by zooplankton. Antarctic krill have been associated with high release rates of ammonium in Antarctic waters (Whitehouse et al., 2011). But also other zooplankton have been shown to be responsible for high ammonium production rates (Molina et al., 2012). Zooplankton research along the WAP has mostly focused on macro-species such as krill and salps. Microzooplankton, such as ciliates, heterotrophic dinoflagellates, and larval stages of larger zooplankton are understudied in this region. In lower latitude regions, these represent the major grazers of phytoplankton blooms. Garzio et al. (2013) show high microzooplankton biomass particularly in the Southern part of the WAP in 2010/11, with higher abundance in high-chlorophyll *a* hotspots such as Marguerite Bay. These findings plus the simultaneous decrease of PN and DON with increasing ammonium concentrations in this study and the higher contribution of other phytoplankton than diatoms in this season support the idea of high abundance and grazing by microzooplankton and bacteria which can explain both the increase in ammonium and the decrease in organic nitrogen concentrations.

The rapid cycling of organic matter by microzooplankton creates an important link in the Antarctic food web: If there is going to be a shift to an ecosystem dominated by smaller cells, as suggested in multiple studies (e.g. Moline et al., 2004; Montes-Hugo et al., 2009; Schofield et al., 2017), microzooplankton will potentially be dominating the grazing level on phytoplankton. However, they will also be able to package organic matter into such form that krill and salps could potentially be able to feed on, thus creating rapidly sinking faecal pellets and supporting export (Ducklow et al., 2015). At the same time, with the increase of smaller cells, it is likely that the production of labile DOM will increase which, on the one hand, as shown here, can create an additional

nutrient source for phytoplankton and bacterioplankton. But on the other hand, it might also support higher bacterial respiration in the upper ocean of the WAP leading to increasing *in situ* production of CO_2 and reduced carbon export.

3.4.5 DOM as a product of phytoplankton stress

Direct release of DOM by phytoplankton can be increased by stress, e.g. nutrient limitation or sudden environmental changes (Carlson & Hansell, 2015; Conan et al., 2007; Goldberg et al., 2009; Wear et al., 2015; Williams, 1995). Physical stress on phytoplankton cells can be caused by rapid changes in salinity or temperature. Hernando et al. (2015) show that rapid salinity changes increase respiration rates and inhibit photosynthetic activity for a short period of time in Antarctic diatoms. In order to reduce the osmotic stress on the cell, diatoms respond with increased extracellular release of dissolved organic matter (Rijstenbil et al., 1989). In all three seasons, there are surface freshwater influx events during which salinity and temperature change rapidly. These events are used here to investigate physical stress situations such as osmotic cell stress. In 2013/14, rapid freshening and warming of the water on January 18th and the following days coincide with highest DOC concentrations. Overall, there is increasing DOC with decreasing salinity and increasing temperature (DOC ~ Salinity r = - 0.75, $p = 4.95*10^{-5}$, DOC ~ Temperature r = 0.77, $p = 2.375*10^{-5}$). In 2014/15, there is also a negative correlation between DOC and salinity (r = -0.61, p = 0.036). Interestingly, it is not the freshest waters of the season coinciding with highest DOC concentrations but the water after a rapid freshening and warming event so that a stress-related DOC release is possible here. While there is no significant relationship between DOC and temperature in the 2014/15 data (p= 0.2), the trend follows this pattern and highest DOC concentrations are found after temperatures increased rapidly. For 2015/16, rapid freshening occurs just before samples were

collected so that this observation cannot be confirmed for the third season. However, there is a trend of increasing DOC concentrations with decreasing salinities.

Along the WAP, nutrient depletion does not occur often or over long periods of time, however, high nutrient drawdown close to depletion occurred in 2013/14 and 2014/15. In combination with the 2015/16 season which does not show nutrient depletion, these situations were used to test whether there is increased DOM production during situations that could cause stress to phytoplankton (Figure 3.4.3). In all three seasons, lowest NO_3^- concentrations coincide with highest DOC concentrations. The relationship between NO_3^- uptake and DOC production is strongest in 2013/14 ($r = 0.80$, $p = 1.043*10^{-6}$) when low NO_3^- concentrations were observed most often and for the longest period of all three investigated seasons. The strength of the correlation is weaker in 2014/15 ($r = - 0.69$, $p = 0.014$) and, while the same trend shows in 2015/16, the correlation between NO_3^- and DOC concentrations is statistically insignificant ($p = 0.08$). All three seasons combined show a correlation of $r = - 0.63$ and $p = 2.2*10^{-16}$. While stress related to nutrient-depletion potentially occurred in 2013/14 and 2014/15, these data do not exclusively show that nutrient limitation can cause phytoplankton to release more DOM. However, previous studies have shown increased release of DOM by phytoplankton when nutrient limited and also during the late growth phase of phytoplankton (Biddanda & Benner, 1997; Soendergaard et al., 2000) both of which cause high DOC concentrations coinciding with the nutrient minimum.

Increased DOC concentrations can be the result of a multitude of reasons in addition to a phytoplankton-stress response, e.g. a shift in phytoplankton community structure with freshening of surface waters. In 2013/14, the presence of haptophytes is growing with the freshening event. However, their contribution to the phytoplankton community is much higher later when there is no increased DOC release observed. These data

suggest that stress-related release by phytoplankton is a more likely source of enhanced DOM release.

While nutrient-depletion scenarios are less likely to occur frequently in the WAP region, these data show that short-lived nutrient depletion scenarios are related to increased *in situ* DOC release. Stress situations of rapid freshening or warming of water masses are more likely to occur more frequently with a warming climate particularly in the WAP coastal regions in proximity of the glaciated coast and an overall decrease in sea-ice duration and cover. Both glaciers and sea ice are sources of freshwater which can enter the surface ocean in rapid impulses and thus cause rapid changes of the physical state of the surface ocean including rapid freshening and strong stratification. As shown here, freshening events can potentially cause stress situations for phytoplankton which can lead to increased DOM production.

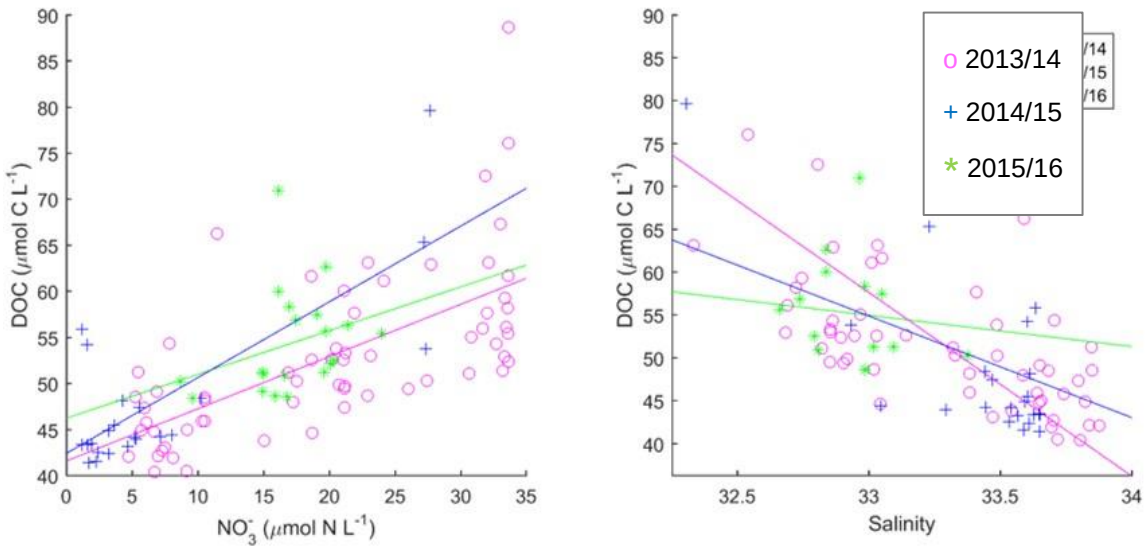

Figure 3.4.3: DOC correlates well with both nitrate and salinity in the upper 15m showing highest DOC concentrations with highest nitrate uptake and lowest salinities in all three seasons. In 2013/14 and 2014/15, those events can be considered stress situations as nitrate is close to depletion and the freshening of the water column occurred suddenly.

3.4.6 Effect of glacial or sea-ice melt

Even though there are good relationships between DOC and both the fraction of sea ice and glacial melt in 2013/14, the separation into blooms shows that this effect is only true for the first bloom. Correlations with the meltwater fractions for all other biogeochemical parameters such as nutrients and POM are either just as strong as or stronger than those for DOC, so that the relationship between DOM and meltwater is more likely an indirect effect on DOM caused by a combination of other factors.

In 2014/15, DOC correlates well with the sea-ice melt fraction and salinity. These correlations still exist after salinity-normalising DOC concentrations which excludes conservative mixing of DOC. Considering the apparent rapid DON cycling in both 2013/14 and 2014/15, direct labile DOM release from sea ice is possible which is also rapidly cycled in the upper ocean.

Sea-ice samples were collected in the 2014/15 season and analysed for nutrients and DOM. Overall, nitrate is depleted in all cores except for the lower 5 cm. DOC and DON concentrations are higher than water column DOM concentrations with an average C:N ratio >15. The highest concentrations for DOC and DON are found in the lower 5cm of every core. Even though these high concentrations of DOC and DON would be introduced to the upper ocean upon sea-ice melting, the contribution of sea-ice derived freshwater in the surface in 2014/15 is small due to net sea-ice formation (more formation than melting), shown by negative $\delta^{18}O_{H2Oseaice}$, for most of the overlapping sampling period for sea ice and organic matter.

Considering the only two dates of net sea-ice melt within the sampling period (November 25th and December 9th 2014), the contribution of sea-ice meltwater to the surface is 0.02 and 0.79 %, respectively. From a simple mass-balance equation based

on the ice cores sampled just before those dates, DOC and DON concentrations in the surface waters would be diluted to such levels that they would lie within the error of DOC and DON measurements (DOC < 48 nmol C L^{-1}, DON < 5.4 nmol N L^{-1}) with a similar C:N ratio (8.74) to that found in the surface waters at these dates. However, the DOC and DON concentrations in sea ice show high variability among sampling dates and vertical position within a single core. Taking the highest sea-ice derived freshwater contribution of the 2014/15 season (2.94%) and highest average DOM concentrations from the sea-ice cores (372.54 µmol C L^{-1} and 46.98 µmol N L^{-1}), this would translate to a maximum additional 10.95 µmol C L^{-1} and 1.38 µmol N L^{-1} to the surface waters from sea ice (DOC:DON ratio 7.93) which would show in surface water DOC and DON concentrations.

In a study on Antarctic sea-ice DOM, Stedmon et al. (2011) characterised three distinct pools of DOM in sea ice. For DOC:DON ratios <30, the majority of DOM was characterised as amino acids which would represent a highly bioavailable pool of DOM. Based on these findings, the majority of DOM from the analysed ice cores of 2014/15 would fall into this category and would represent a highly labile DOM pool which potentially presents an early trigger mechanism for bacterial activity and also a source of (sea ice) bacteria. However, the quality of sea-ice DOM highly depends on formation processes and ambient water characteristics (Stedmon et al., 2011). The surface waters in the 2014/15 season show constant fluctuations of net sea-ice formation and melt with varying effects on the melting process at the ice-ocean interface. Further, strong winds control the movement and the amount of sea ice in a specific location with intense variability between days. While overall, the high concentrations of DOC and DON suggest high contribution to the surface waters upon sea-ice melt, the rate of melt and the motion of the ice ultimately control how much organic matter is released by sea ice within a given period at a specific location.

In the 2015/16 data set, there is no apparent direct effect from sea-ice or glacial melt on DOM concentrations. This is surprising because it is the season with the highest influx of both sea ice and glacial melt fractions with maxima of 3.15 and 5.09%, respectively. However, the lack of data in the early season might be the reason why a direct impact cannot be observed.

3.5 Summary and future implications

The three seasons investigated show high seasonal and interannual variability agreeing with previous studies with high variability between years mostly depending on climatic conditions and subsequent development of phytoplankton activity. It appears that DOM dynamics in Ryder Bay are mostly driven by biological and biogeochemical interactions which, in turn, are controlled by physical changes. 2013/14 and 2014/15 show relatively similar behaviour. It was shown that DOC is very likely a direct product of primary production and is released at the same time as POC, disproving the first hypothesis of this study. This hypothesis was based on previous studies showing negligible *in situ* release of DOM during primary production. However, production of DOC is decoupled from POC after the first phytoplankton bloom which is likely due to the onset of high bacterial degradation and possibly grazing by zooplankton.

The release of DOM as a stress response by phytoplankton has not been tested in WAP waters before. However, the results of this chapter show that stress-related release of DOC potentially plays an important role in the WAP waters. Highest concentrations of DOC were found at or shortly after events that can potentially put phytoplankton under stress, such as sudden changes in salinity and temperature or nutrient limitation.

The lack of relationships between DON and other biogeochemical parameters lead to the suggestion of DON having another source and/or being rapidly cycled in Ryder Bay and potentially also playing a role as N source for phytoplankton. 2015/16 showed a dissimilar pattern for DOC and DON with maximum concentrations not coinciding with POM maxima and DON concentrations being more depleted at shallower depths while higher concentrations are found at the greatest measured depth.

In all investigated seasons, DOC concentrations decrease back to background concentrations with depth. However, DON concentrations remain slightly elevated. Mesopelagic processes cannot be inferred from the available data as no measurements are available below 130m. However, the available NH_4^+ data indicate that the measured increased DON concentrations contain a substantial contribution from NH_4^+ at depth particularly towards the later stage of the phytoplankton bloom. The fact that overall, DOC:DON ratios are low at the RaTS study site suggests DOM of high lability which supports the hypothesis of active and efficient upper-ocean DOM cycling. The dissimilar pattern of DOM in 2015/16 shows high interannual variability in DOM dynamics.

DOM contribution from meltwater was shown to be likely but small. Even though sea-ice cores collected in 2014/15 show high DOM content of increased DOC:DON ratios throughout the season, a rapid melting event would be necessary to introduce all this DOM to the surface waters. The measured minor fractions of sea-ice meltwater present in the surface waters in 2014/15 would not affect seawater DOM concentrations. However, the high vertical variability of DOM in sea ice infers that high amounts of DOM can be released at any given melting event. This DOM would be highly labile and possibly lead to high bacterial activity.

Previous studies suggested high partitioning of organic matter into the particulate pool during primary production and negligible direct release of DOM from phytoplankton.

This study shows direct and sporadically high release of DOC by phytoplankton during primary production adding complexity to our understanding of the DOM dynamics in the WAP ecosystem.

The importance of carbon in the dissolved pool has only been recognised relatively recently with the dissolved organic nitrogen being even less investigated. Focussed studies on specific DOM compounds, the microbes responsible for the cycling of specific compounds and physical conditions and their effects on DOC and DON are rare, particularly in the remote regions of Antarctica. A combination of long-term field and laboratory studies on DOC and DON concentrations, specific DOM compounds, release and consumption mechanisms under ambient and stress conditions is required to improve our understanding of the processes involved in DOC and DON cycling in the upper ocean of the WAP shelf.

Under current projection scenarios of ongoing climate change in the WAP region, above described patterns and behaviour of DOM cycling will likely be highly affected. This study shows that shifts in phytoplankton species composition, decreases in surface salinity due to increased melting, shifts in the specialised bacterial clades and possibly in ambient zooplankton species will all affect both the production and the cycling of carbon and nitrogen at the WAP in the dissolved form.

CHAPTER 4

Spatial Variability and Physical and Biological Controls of Dissolved Organic Carbon and Nitrogen West of the Antarctic Peninsula

4.1 Introduction

The role of dissolved organic carbon (DOC) in the global marine carbon cycle is still not entirely understood. Processes such as DOC production, transformation and removal all involve a variety of different mechanisms which makes resolving the cycling of dissolved organic matter in the oceans difficult. Production of marine DOM occurs through different mechanisms such as *in situ* production and release during phytoplankton blooms (Carlson, 2002; López-Sandoval et al., 2011; Marañón et al., 2005; Nagata, 2000), sloppy feeding by zooplankton, excretion and egestion processes(Carlson, 2002; Møller, 2005; Saba et al., 2009, 2011; Steinberg & Saba, 2008). Marine heterotrophic microbes are the primary consumers of DOM and are responsible for most of the transformation and removal processes (e.g. Azam et al., 1983; Ducklow et al., 1986; Goldman & Dennett, 2000; Jiao et al., 2011; Pomeroy et al., 2007). Further, inactive, such as gravity-driven sinking of particles, and active vertical transport processes, e.g. from vertically migrating zooplankton releasing OM at depth, can act as sinks exporting DOM from the surface waters. However, it has also been shown that DOM can act as an organic nutrient source for primary producers and other trophic levels (Granéli et al., 1999; Karl et al., 1996). Bacterial processing of labile DOM leaves refractory DOM compounds which are not readily degraded creating a carbon reservoir similar in size to the atmospheric carbon reservoir. The microbial cycling of organic matter is referred to as the microbial carbon pump and was first described as such by Jiao et al., (2010). The oceanic refractory

carbon reservoir stores carbon up to millennia (e.g. Hansell, 2013; Hansell et al., 2009).

While in lower latitude open-ocean systems, DOM is produced directly during phytoplankton blooms and makes up the majority of the total organic matter stock (particulate plus dissolved), high-latitude systems tend to show much lower concentrations of DOM in surface waters with little direct contribution by phytoplankton (Bird & Karl, 1999; Ducklow et al., 2011; Straza et al., 2010). Further, several studies at the West Antarctic Peninsula (WAP) have shown that the ratio of bacterial production (BP) to primary production (PP) is low and BP often does not exceed 4% of primary production indicating insufficient supply of bioavailable material for BP (Bird & Karl, 1999; Kim & Ducklow, 2016). Low temperatures were suggested to hamper bacterial production (Pomeroy & Wiebe, 2001), however, Straza et al. (2010) found that temperature alone does not control bacterial activity. Seawater collected in the shelf waters of the west Antarctic Peninsula enriched with glucose increased bacterial production supporting the idea of limited bioavailable DOM being responsible for low BP in Antarctic waters (Ducklow et al. 2011). BP shows a better relationship to chlorophyll-*a* than to PP suggesting that bacteria feed on organic matter originating from PP but which has already undergone degradation processes such as grazing by higher trophic levels (Kim & Ducklow, 2016). However, at present, there is no study looking into the fate of DOM in the WAP shelf waters directly. It remains unclear how much DOM is being produced, recycled in the upper ocean and how much or if any is exported to the deep ocean. In Antarctic open water, the primary source of DOM is primary production as there is no riverine runoff high in DOM and the Southern Ocean is far away from any anthropogenic sources.

While there has been some research on the interaction between bacteria and dissolved organic matter in the Southern Ocean (Church et al., 2000; Ducklow, 2003;

Ducklow et al., 2012; Kähler et al., 1997), the questions as to why DOM concentrations are lower than in low latitudes and how DOM is processed in the Southern Ocean remain unanswered. Further, most studies focus on dissolved organic carbon. The analysis of dissolved organic nitrogen (DON) is more challenging and therefore often disregarded. DON is measured by analysing total dissolved nitrogen (TDN), which contains organic and inorganic nitrogen species (NO_3^-, NO_2^-, NH_4^+). The concentrations of the inorganic species are subtracted from TDN to gain DON concentrations so that these carry the error of the analyses of inorganic nutrients plus the TDN analysis itself. Nonetheless, to fully understand processes involved, DON is a useful measure as C:N ratios might indicate lability of DOM which is suggested to play a more important role in bacterial growth efficiency than the quantity of the substrate itself (Church et al., 2000; Goldman et al., 1987; Goldman & Dennett, 1991). Even though the DOC:DON ratio, unlike the POC:N ratio, should not be used to draw conclusions of source or fate and cannot be used as a proxy for either DOC or DON (Kähler & Koeve, 2001), it is a useful tool to investigate N-enriched and therefore likely more labile DOM in the region. Because DON contains both carbon and nitrogen, DON compounds tend to be sites of high bacterial activity as they represent a source for both required elements. Concentrations of DOC, DON and the C:N ratio are used in combination with microbial parameters such as bacterial abundance and activity in order to understand processes involved in DOM cycling. Both bacterial activity and cell counts have long been a standard measurement of the PAL LTER program.

Particulate organic matter (POM) in the WAP shelf waters is produced during primary production by phytoplankton in the surface. Intense POM accumulation during the short period of productivity forms the base of the local food web. New production estimates in the WAP region are larger than export which is likely the result of passive

transport like diffusion and advection (Stukel et al., 2015; Stukel & Ducklow, 2017) but also indicates intense recycling in surface waters. The ratio of C:N in POM highly depends on the phytoplankton species composition in each bloom but generally, C:N ratios in high-latitude regions are lower than in lower latitudes which has been attributed to a dominance by diatoms (e.g. Annett et al. 2010) and low temperatures which lead to a higher enzyme expression (Young et al., 2015). High abundance of krill and other zooplankton and bacterial degradation lead to rapid degradation of POM with depth.

The WAP is a pelagic marine ecosystem which was subject to rapid warming in the second half of the 20th century with increases in atmospheric and oceanic temperatures; changes in precipitation; a decline in sea-ice extent and duration; and increasing glacial melting in the area (Marshall et al., 2006; Smith et al., 1996; Van Wessem et al., 2015; Vaughan et al., 2003). All ecological processes in the area ultimately depend on sea-ice dynamics so that the WAP ecosystem is subject to large inter- and intra-annual variability. Sea-ice cover and duration in the WAP are controlled by climatic variability, in particular by the Amundsen Sea Low (ASL), a low-pressure system between the Ross Sea and the WAP. The ASL is controlled by a combination of two large-scale climate modes, the El Niño-Southern Oscillation (ENSO) and the Southern Annular Mode (SAM). In brief, changes in the ASL affect wind strength and patterns at the WAP which is the primary control on sea ice (Saba et al., 2014; Stammerjohn et al., 2008; Vaughan et al., 2003). A deepening of the ASL has been observed in the second half of the 20th century leading to warmer and more moisture-laden air being steered towards the WAP while more recently, this warming period has plateaued which is likely due to natural internal variability.

This study focusses on the continental shelf west of the Antarctic Peninsula studied by the U.S. Palmer Antarctic Long-Term Ecological Research (PAL LTER) program

since 1990 (see map in figure 4.2.1). Each year in January, the PAL LTER cruise covers a defined sampling grid to study spatial and inter-annual physical, ecological and biogeochemical processes of the region.

It is hypothesised that DOC and DON concentrations are low throughout the study region and that DOM is being produced with a temporal offset after the start of a phytoplankton bloom. Further, it is hypothesised that increased DOM concentrations, particularly those of low C:N ratios, occur in regions of high bacterial productivity. In addition, this study investigates the effect of freshwater contribution from sea-ice and glacial meltwater on DOM concentrations and the response by phytoplankton and bacteria.

In order to address the above hypotheses, DOC and DON concentrations were measured along with other biogeochemical parameters as part of the 2017 PAL LTER cruise. This is the first time any PAL LTER samples have been analysed for DON. Spatial patterns and variations of DOC and DON distributions are brought into context by comparing those to physical, biological and biogeochemical changes throughout the sampled area. By comparing the open ocean to the shelf area of the WAP, different mechanisms responsible for spatial variability in DOM cycling are identified. This study will investigate potential DOM sources other than primary production and the efficiency of bacterial degradation of bioavailable DOM along the WAP.

4.2 Methods

4.2.1 Sample site

The sample region west of the Antarctic Peninsula covers an area of 900 x 200 km. The sampling locations are the same for each annual cruise and follow a pattern of lines orthogonal to the coast approximately 100 km apart (see figure 4.2.1). The number of lines and stations sampled highly depends on accessibility due to sea-ice cover. For this study, samples were collected along lines 200 to 600 from January 6th to January 31st 2017 on board the *ARSV Laurence M. Gould* (LMG).

The sampling scheme on each annual cruise involves deployments of a SeaBird 911+ conductivity-temperature-depth instrument attached to a rosette with 24 niskin bottles. Samples are collected from niskin bottles closed at specific depths in the water column for particulate organic carbon and nitrogen and their isotopic compositions, dissolved inorganic nutrients, dissolved organic carbon (and nitrogen), primary production, chlorophyll-*a*, and bacterial measurements. Sea-ice data are derived from satellite observations from *NASA's Scanning Multichannel Microwave Radiometer* and *the Defense Meteorological Satellite Program's Special Sensor Microwave/Imager*.

Table 1 in the appendix lists all relevant data analyses, the methodologies applied and the institutes involved.

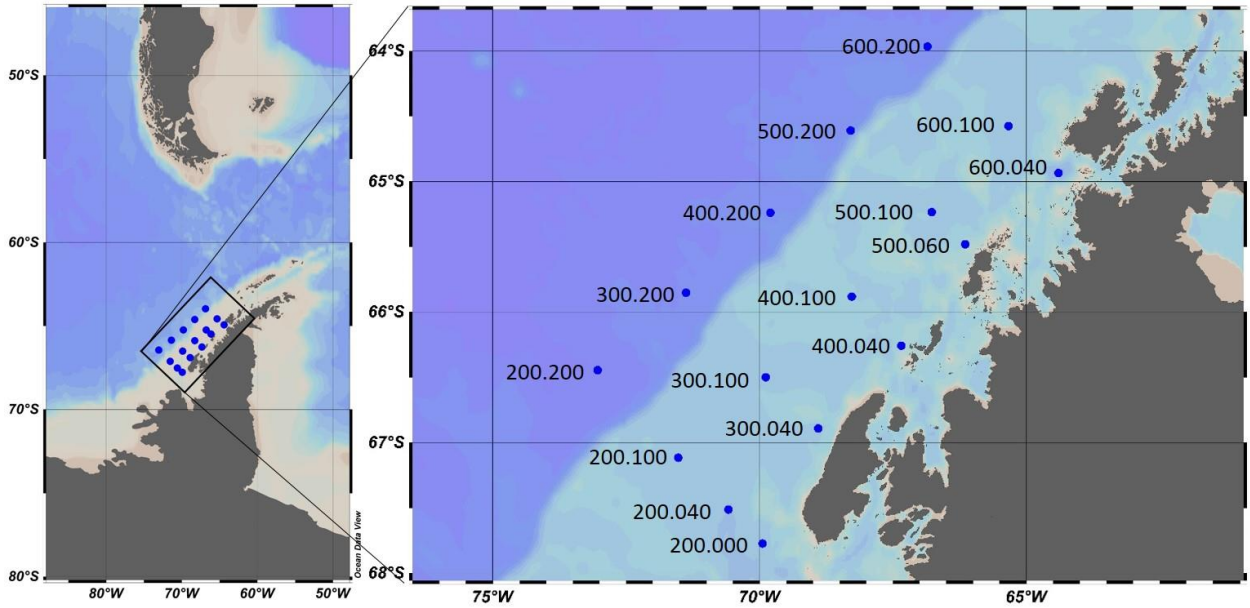

Figure 4.2.1: Map of the west Antarctic Peninsula and zoom on PAL LTER sampling grid west of the Antarctic Peninsula showing all stations sampled in 2017.

4.2.2 Sample Collection

Samples for DOC and TDN analysis were collected in acid-cleaned (24 hours in 10 % HCl, 3x DIW-rinsed and baked for 5 hours at 450 °C) 60-ml HDPE bottles. Prior to sample collection, each bottle and lid were rinsed three times with the sampled seawater. Sample seawater was gravity-filtered directly from the niskin bottles through pre-combusted GF/F filters (Whatman 0.7 µm 47 mm Ø; precombusted at 450 °C for 5 hours in methanol-cleaned tin foil) and immediately transferred to a -80 °C freezer.

POM samples were collected by filtering up to 4 L of collected seawater through pre-combusted GF/F filters (Whatman 0.7 µm GF/F 25 mm Ø). The filters were stored in cryovials at -80 °C.

4.2.3 Analysis of DOC and TDN

DOC/TDN analysis was conducted via high-temperature combustion on a *Shimadzu TOC-V analyser* with an attached *TNM1 Total Nitrogen Measuring unit*. Samples were thawed for approximately 3 hours before analysis. 10 ml of each sample was transferred into acid-cleaned and combusted glass vials using an acid-cleaned 5 ml pipette for analysis.

Sample replicates were analysed in each run for precision. Certified Reference Material (CRM; Hansell Deep Sea Reference Batch #15 Lot 1-15; Florida Strait 750 m DOC 42.00-45.00 µmol C L^{-1}, TDN 31.00-33.00 µmol N L^{-1}) was analysed before and after each batch of samples for accuracy. The instrument automatically analyses each sample 3-5 times depending on in-run reproducibility. Deep-sea samples were re-analysed with Deep Sea Reference Batch #18 Lot 08-18 (DOC 41.0 – 45.8 µmol C L^{-1}, TDN 31.6 – 35.0 µmol N L^{-1}). CRMs were intercompared to ensure linearity of the instrument throughout the period of analysis. The CRM DOC values was checked to lie within 5% of the consensus value before each sample run. If this was not the case, more CRMs were analysed until the results were within the range. Detection limits are 0.04 µmol C L^{-1} for DOC and 0.36 µmol N L^{-1} for TDN and analytical precision for DOC was ± 1.09 µmol C $L^{-1}$and for TDN ± 0.51 µmol N L^{-1}.

Due to logistical constrains, only the inorganic nitrogen species NO_2^- and NO_3^- were analysed so that DON concentrations stated contain NH_4^+. NH_4^+ concentrations across WAP surface waters have been shown to be minimal, however, when NH_4^+ concentrations might be of importance, they will be mentioned in the discussion.

4.2.4 Analysis of particulate organic carbon and nitrogen

Particulate organic carbon and nitrogen were analysed at the School of GeoSciences at the University of Edinburgh. Filters for POC:N analysis were prepared following a method adapted from Lourey et al. (2004). In brief, filters were decarbonated by wetting them with Milli-Q and fumed with 70% HCl overnight before drying and carefully folding them into clean tin capsules. Samples were analysed on a *CE Instruments NA2500 Elemental Analyser* connected to a *Thermo Finnigan Delta+ Advantage stable isotope ratio mass spectrometer*. Both instruments are linked through a *Finnigan ConFlo III Universal Interface* to allow for simultaneous carbon and nitrogen analysis. The CRMs PACS-2 and acetanilide were analysed for the isotopic composition and carbon and nitrogen concentrations, respectively. The analytical reproducibility was better than 1.0% for POC and better than 1.1% for PN.

4.2.5 Analysis of inorganic nutrients

Dissolved inorganic nutrients (Nitrate+nitrite, Silicate and Phosphate) were analysed using a *Seal Analytical* segmented flow autoanalyser (Mequon, WI, Seal AutoAnalyzer AA3). Methods for each analysis followed the protocols recommended in the Seal Customer Support Manual. Nitrate analysis was conducted via reduction to nitrite in a copper-cadmium column and a further reaction with N-1-naphthylethylene diamine dihydrochloride to form a purple azo dye which is then analysed colorimetrically. Phosphate analysis follows the Murphy and Riley method (Murphy & Riley, 1962). The determination of silicate is based on the reaction between silico-molybdate to molybdenum blue by ascorbic acid. Standards for each analysis were sodium nitrite and potassium nitrate, potassium dihydrogen phosphate and sodium meta-silicate nonahydrate. A deep-sea sample collected during each year's

cruise at 3,000 m is analysed as an internal reference standard. Detection limits for nitrate+nitrite were 0.015 µmol N L^{-1}, for phosphate 0.0021 µmol P L^{-1} and for silicate 0.03 µmol Si L^{-1}.

4.2.6 Analysis of bacterial data

Bacterial abundance, production and HNA/LNA (high nucleic and low nucleic acid content) were analysed onboard the LMG. Bacterial abundance and HNA and LNA were analysed within two hours after collection via flow cytometry following Gasol & Del Giorgio (2000) with SYBR-Green staining. Total abundance was counted by adding 1 µm microspheres and 5 µm of SYBR-Green to 0.5 mL of a seawater sample. After a 30-minute dark incubation, bacterial cells were analysed for 2 minutes at a slow flow rate. Numbers were determined in cytograms of green fluorescence recorded at 530 ± 30 nm versus side angle light scatter. HNA and LNA subgroups were separated by gating the cytogram and discriminating by their respective green fluorescence.

Bacterial production rates were determined via incorporation of ^{3}H-radio-labelled leucine following a modified protocol by Smith & Azam (1992). Samples were treated in triplication. Control samples were spiked immediately after sampling with 200 µL formalin in order to stop any biological activity. Each 1.5 mL sample was spiked with ^{3}H-leucine (MP Biomedical, Santa Ana, CA; >100 Ci/mmol, 20-25 nM final concentration) and incubated for 3 hours at 0.5 °C. At the end of the incubation period, 200 µL formalin was added to the samples. After concentration by centrifugation, the samples were rinsed with 5 % trichloroacetic acid and 70 % ethanol and air-dried overnight before analysis by liquid scintillation counting in an Ultima Gold cocktail.

4.2.7 Analysis of other auxiliary data

4.2.7.1 Primary production and chlorophyll-a

Primary production rates and chlorophyll-*a* concentrations have been gathered throughout the PAL LTER cruise by the research group of Oscar Schofield.

Primary production rates, measured as daily carbon uptake in mg C m^{-3} day^{-1}, are measured with incubation experiments. 100 ml of seawater sample were inoculated with 1 µCi of ^{14}C-radio-labelled $NaHCO_3$ in borosilicate bottles. The bottles were incubated for 24 hours at *in situ* light levels and ambient temperatures. After the 24-hour incubation period, the seawater samples were filtered through GF/F filters, the filters were washed with 10 % HCl, dried and counted in a scintillation counter.

Chlorophyll *a* samples were filtered onto GF/F filters and kept frozen at – 80 °C stored in cryovials. Analysis was conducted at Palmer Station through acetone extraction and measurement of the extract on a Turner 10AU Fluorometer.

4.2.7.2 $\delta^{18}O_{H2O}$ analysis

The samples for the $\delta^{18}O_{H2O}$ composition were analysed at the Natural Environmental Research Council Isotope Geosciences Laboratory at the British Geological Survey. Samples were analysed on a *VG Isoprep 18* and *SIRA 10* mass spectrometer with random samples analysed in duplication for precision which is usually better than ± 0.02 ‰. The oxygen isotopic composition of seawater ($\delta^{18}O_{H2O}$) is determined by the comparison of the ratio of $^{18}O/^{16}O$ of a sample to that of a standard. For oxygen isotope measurements, this standard is Vienna-Standard mean ocean water (V-SMOW). The $\delta^{18}O_{H2O}$ is expressed as

$$\delta^{18}O(sample) = \left[\frac{\left(\frac{18O}{16O}\right)sample}{\left(\frac{18O}{16O}\right)VSMOW} - 1\right] x\ 1000‰$$

The method followed the equilibrium method for carbon dioxide established by Epstein & Mayeda (1953).

4.2.7.3 PAL LTER Dissolved Inorganic Carbon

Samples were collected from the surface and the deepest niskin bottles and preserved with 200 uL saturated $HgCl_2$ before being sealed and transported to the Ducklow laboratory at the Lamont-Doherty Earth Observatory for analysis. Analysis followed the WOCE-JGOFS recommendations (Dickson & Goyet, 1992; Knap et al., 1996). The average standard deviation for replicate samples was 0.15%.

4.2.8 Calculations

4.2.8.1 Depth-integrated standing stocks and nutrient uptake

Organic matter standing stocks and nutrient uptake were integrated over the upper 50 m, in agreement with other studies finding that most biogeochemical parameters fall back to background levels or show only little variability below 50 m in the WAP region (Ducklow et al., 2012) and most activity happening within the mixed layer which for all stations is within this range. Further, most biological and biogeochemical measurements, such as primary production, chlorophyll-*a* and POC and PN are only collected at the uppermost 6 depths at each station during the PAL LTER cruises.

Standing stocks of particulate and dissolved organic carbon, nitrogen and inorganic nutrients were calculated by trapezoidal integration. At stations with no 50-m measurement, the 50 m value was interpolated. Results are listed in table 8 in the appendix.

4.2.8.2 $\delta^{18}O_{H2O}$ fractions of CDW, sea ice and meteoric origin

Samples for $\delta^{18}O_{H2O}$ were collected during the PAL LTER research cruises at every sampling station in 50-ml glass bottles which were crimp-sealed. The samples were analysed at the Natural Environmental Research Council Isotope Geosciences Laboratory at the British Geological Survey. Samples were analysed on a *VG Isoprep 18 and SIRA 10* mass spectrometer with random samples analysed in duplicate which showed an average precision better than ± 0.02‰. The method followed the equilibrium method for CO_2 established by Epstein & Mayeda (1953). The contribution of sea ice and glacial meltwater were calculated using simultaneous equations following Meredith et al. (2016) who adopted the method from (Östlund & Hut, 1984). A description is given in *Chapter 2: Methods*.

4.2.8.3 Mixed layer depth

The mixed layer depth (MLD) is defined as the depth at which σ_t is 0.05 kg m^{-3} greater than σ_t at the surface from CTD downcast data in agreement with other Southern Ocean studies (Long et al., 2012; Mitchell & Holm-Hansen, 1991; Venables et al., 2013).

4.2.8.4 Nutrient Uptake Ratio Calculations

The nutrient uptake ratios were calculated as the ratio of the difference of the nutrient concentrations measured from deep UCDW measurements (which represent background nutrient concentrations) of each station and the subsequent upper ocean depth.

4.3 Results

From the observations of the data presented here, the depth profiles and later discussions are divided into open ocean and shelf+coast stations. Open ocean stations describe stations 200.200, 300.200, 400.200, 500.200 and 600.200 and are those off the shelf region of the WAP (see Figure 4.2.1). Shelf and coast stations show a similar behaviour to each other with more variability along the coast. All surface contour plots are drawn with Ocean Data View (Schlitzer, 2017). Tables with all data presented here are listed in the appendix of the thesis.

4.3.1 Sea ice and hydrography

The study area is characterised by highly variable sea-ice coverage and glacial meltwater influence. All physical parameters are shown in figure 4.3.1 a and b. Salinity in the sampling grid ranges from 32.64 at the surface to 34.73 at depth. Most variation in salinity is found in the upper 100m with sharp decreases in surface salinity and higher variability at the stations closer to the shore. Temperature ranges from -1.71 °C to 2.93 °C. Winter water is present at all stations between 10 and 200m with a temperature range from -1.71 °C to 0.00 °C. Surface waters are warmest at the coastal station 500.060 (2.9 °C) and coldest at 200.040 (1.07 °C) while the rest of the surface sampling grid ranges from 1.32 to 2.68 °C.

The MLD is shallow but highly variable along the sampled stations varying from 8 m at 600.040 to 38 m at 400.200. The MLD correlates strongly with the number of days since sea-ice retreat ($r = 0.68$, $p = 0.005$), i.e. the longer a station has been sea-ice free, the deeper the MLD. Sea-ice retreat days (SIRD) are defined as the number of days between the first day of sea-ice concentration <15% for at least 5 consecutive days and the sampling day (Stammerjohn et al., 2008). As shown in figure 4.3.1a, sea

ice retreated earliest in the region off shelf (125 days at 200.200) and persisted longest towards the shore (6 days since sea-ice retreat at 200.000) except for station 600.200 which was still sea-ice covered on the day of sampling.

The $\delta^{18}O_{H2O}$ data show the contribution of freshwater, which along the WAP consists mostly of sea-ice and meteoric water, which are isotopically lighter than seawater. Meteoric water mainly consists of glacial meltwater, but a small fraction originates from precipitation. While the open-ocean stations are less influenced by freshwater, the coastal stations and, to some extent, the shelf stations show the influence of meteoric water in the surface. The South-eastern part of the sampling grid (including stations 400.040, 300.040, 300.100, 200.100, 200.040 and 200.000) shows highest freshwater contributions with its minimum $\delta^{18}O_{H2O}$ value at 300.040.

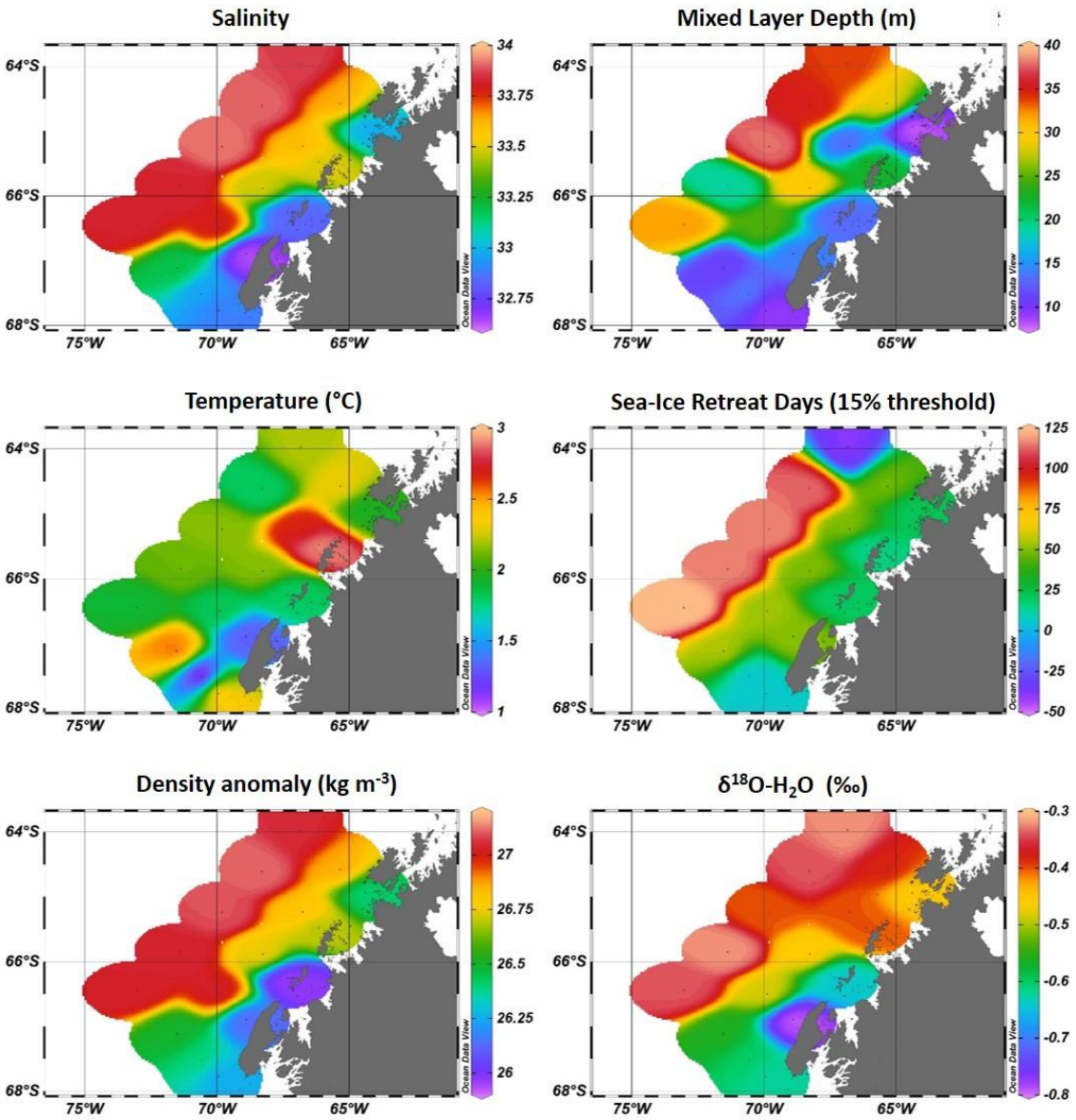

Figure 4.3.1a: Surface physical conditions along the WAP during PAL LTER 2017 showing high variability along the sampling grid with a distinct onshore-to-offshore trend in all parameters.

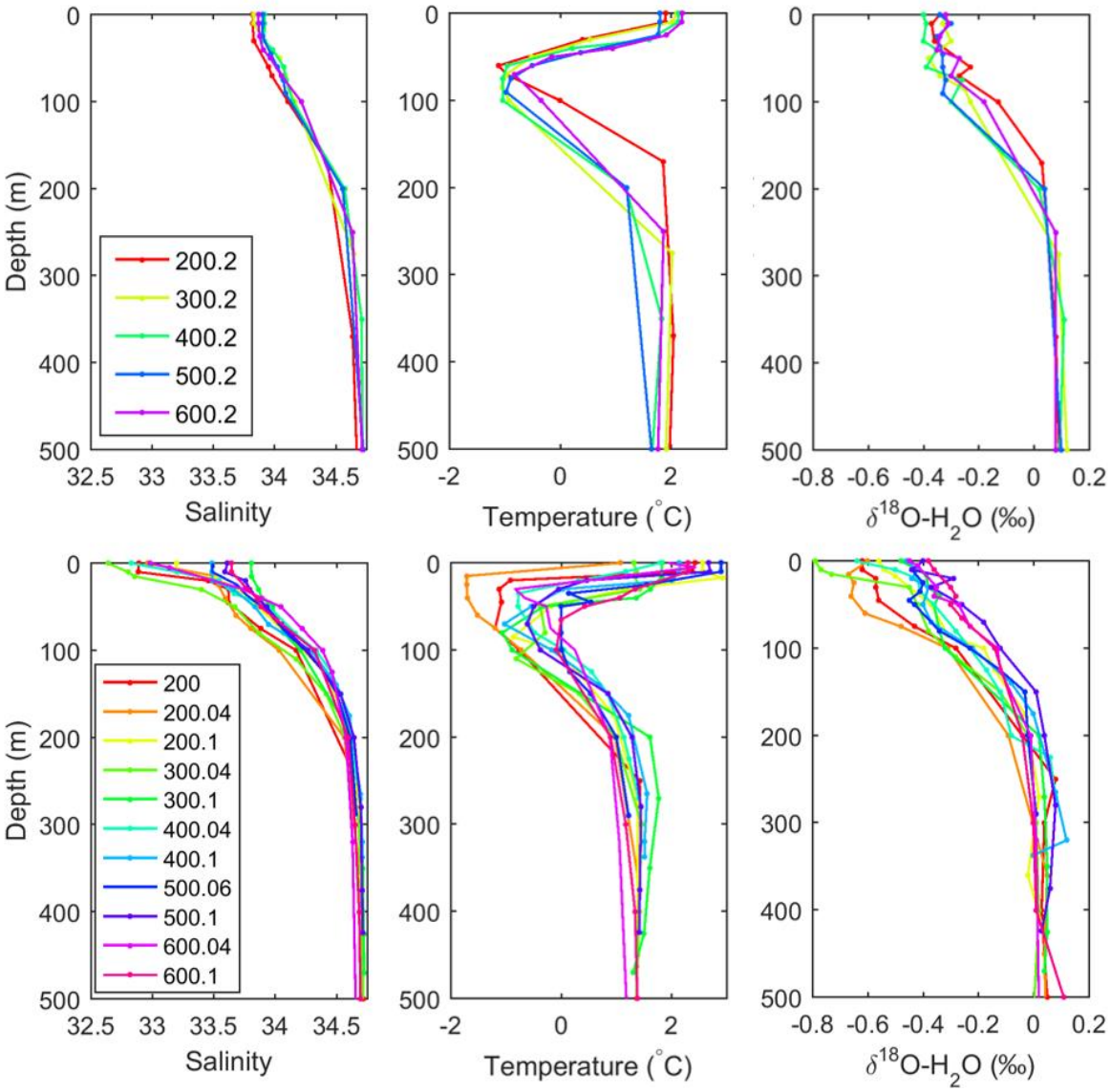

Figure 4.3.1b: Depth profiles of physical parameters over the upper 150m during PAL LTER cruise 2017. The data are divided into Open Ocean stations on the top row and shelf+coast at the bottom. The colours represent each sampled station according to the legend.

4.3.2 The distribution of inorganic nutrients along the WAP

The surface distribution of nutrients across the sampling grid reflects the above described physical conditions (figure 4.3.2a, b). At depths > 200 m, NO_3^- concentrations have a mean of 33.15 ± 1.21 µmol N L^{-1} representing NO_3^- concentrations in CDW being transported across the WAP shelf. Above 100 m, NO_3^- concentrations decrease towards the surface. Surface NO_3^- concentrations range from 0.77 µmol N L^{-1} at 300.040 to 25.45 µmol N L^{-1} at 200.200. The open ocean stations show higher surface concentrations (24.52 ± 1.26 µmol N L^{-1}) in comparison to shelf waters (19.34 ± 1.86 µmol N L^{-1}) and coastal stations (12.85 ± 6.6 µmol N L^{-1}). The higher standard deviation at the coastal stations shows more variable NO_3^- uptake in these waters with more depleted surface waters at the southernmost stations. Figure 4.3.2b shows the depth distribution of nutrients. Surface PO_4^{3-} and DIC concentrations follow the NO_3^- distribution closely. The N:P uptake ratio in the surface waters ranges from 11.5 to 16.0 with an average 14.2 ± 1.5 (table 4.3.1) being slightly below Redfield conditions in agreement with other studies (Pedulli et al. 2014; Henley et al. 2017). Si:N uptake ratios also vary strongly between open and coastal conditions: In the open, the Si:N uptake ratios range between 2.1 and 3.8 with a mean of 2.9 ± 0.7, along the shelf 1.4 ± 0.3 and across the coastal stations 0.9 ± 0.2 (table 4.3.1). DIC measurements are only taken at the surface so that uptake and ratios cannot be calculated.

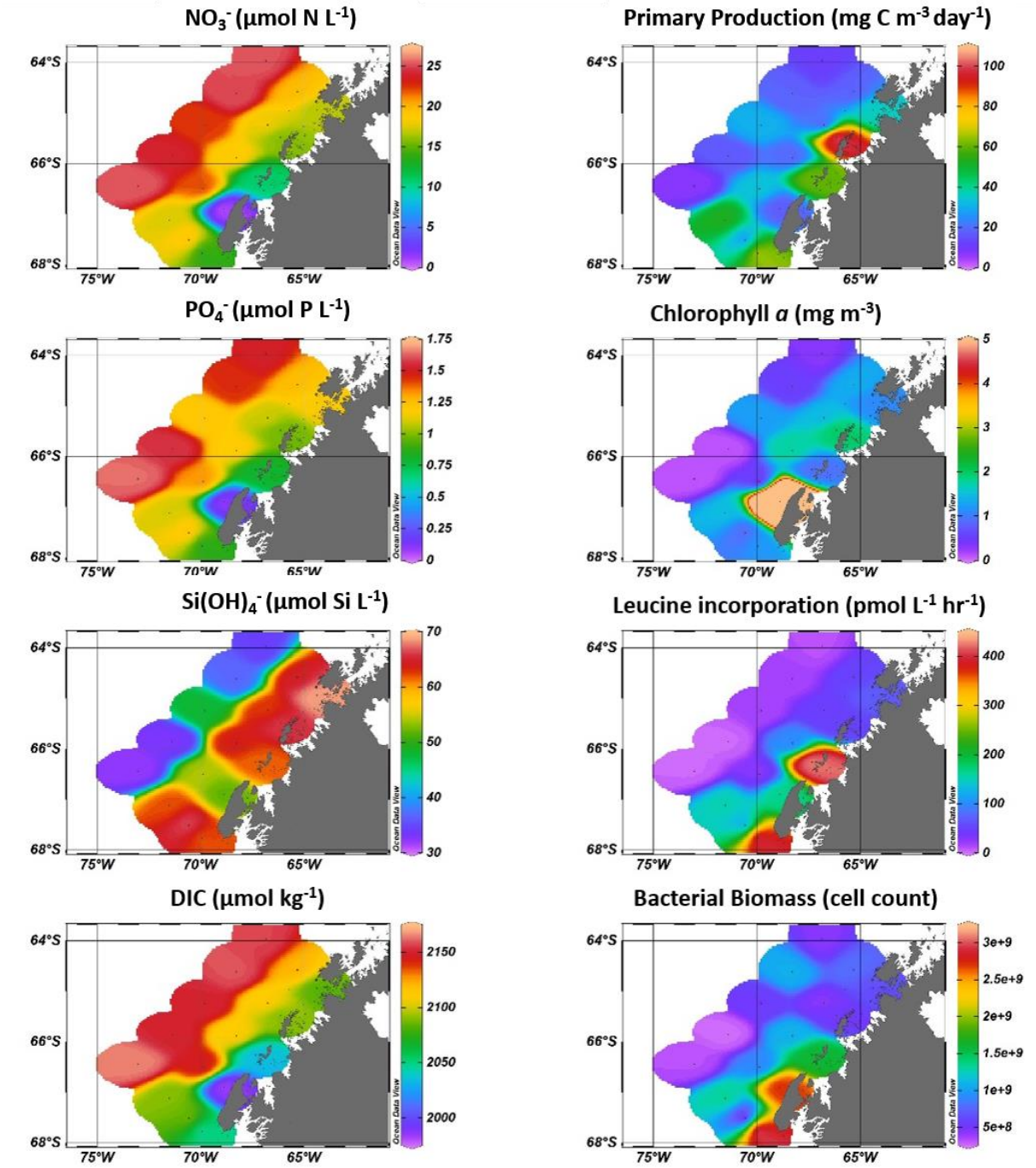

Figure 4.3.2a: Surface distribution of inorganic nutrient concentrations, phytoplankton and microbial parameters during the PAL LTER cruise 2017.

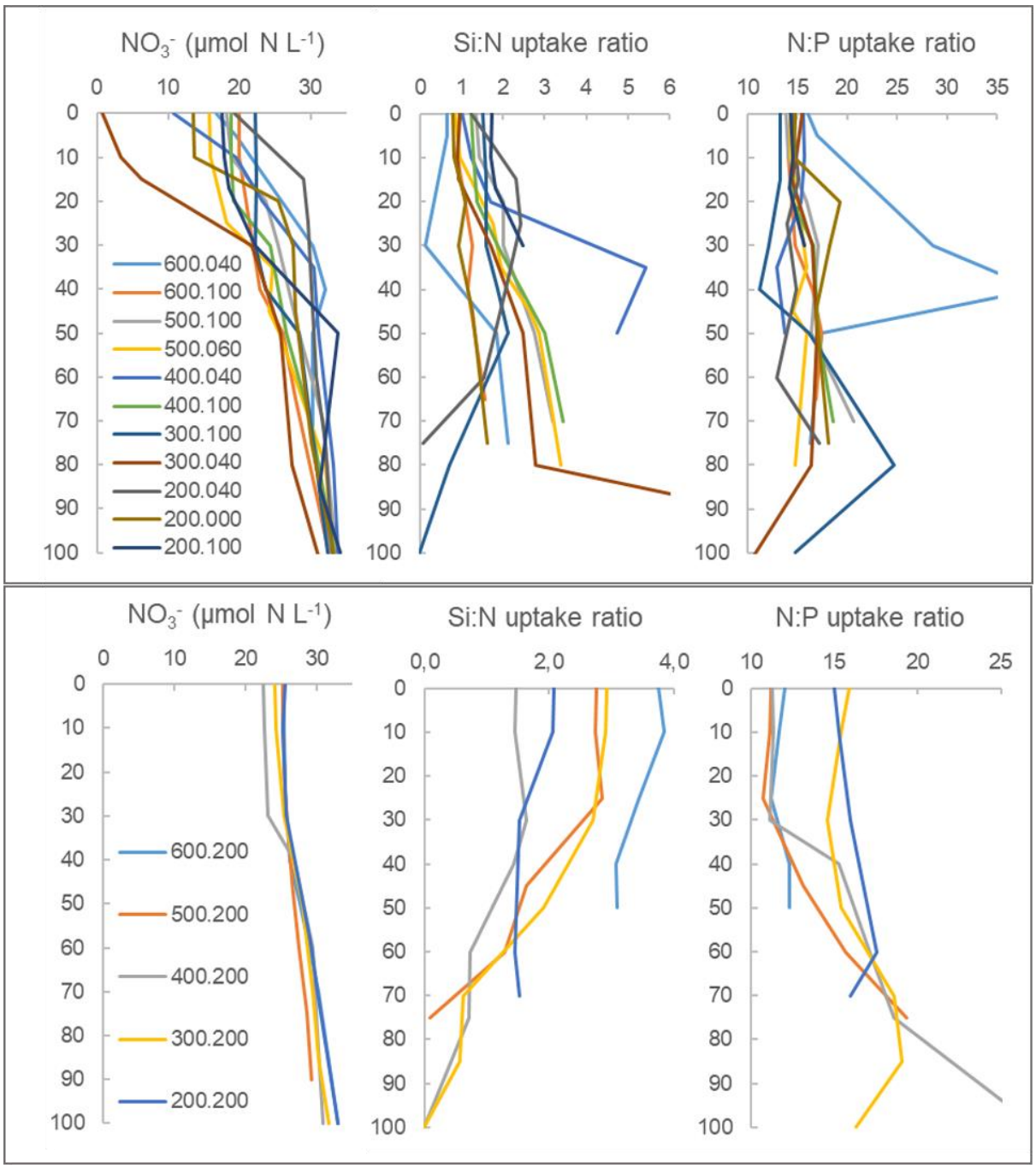

Figure 4.3.2b: Depth profiles of nutrients over the upper 100m during PAL LTER cruise 2017. The data are divided into shelf+coastal stations (top) and open ocean stations (bottom) and coloured by station number as per legend.

4.3.3 The distribution of phytoplankton parameters along the WAP

Primary production and chlorophyll-*a* show strong variability across the sampling grid (Figure 4.3.2a). Primary production is mostly low except for the coastal region with a peak of 102 mg C m^{-3} day^{-1} at 500.060. Primary production peaks are found at the surface and in the subsurface down to 70 m (see figure 4.3.3).

Chlorophyll-*a* concentrations range from 0.1 to 2.0 mg m^{-3} except for station 300.040 (surface chlorophyll-*a* concentration = 17.0 mg m^{-3}). Among the other 15 stations, mean surface chlorophyll-*a* was 1.0 ± 0.6 mg m^{-3}.

Depth-integrated primary production and chlorophyll-a concentrations are stated in table 4.3.1 along with nutrient uptake ratios. Highest variability and values are found along the coast, generally decreasing towards the open ocean.

Table 4.3.1: Si:N and N:P uptake ratios for integrated nutrient uptake of the top 50m, maximum primary production rates and integrated Chlorophyll-a concentrations. Stations listed North to South and subdivided into coast, shelf and open ocean.

	Station	Si:N uptake	N:P uptake	PP (mg m^{-3} day^{-1})	Chl*a* (mg m^{-3})
Coast	600.040	0.64	18.17	46.76	17.22
	500.060	1.53	14.88	101.95	69.97
	400.040	1.76	15.24	61.3	35.3
	300.040	1.23	15.35	17.19	331.67
	200.040	1.82	14.45	45.43	19.24
	200.000	0.95	14.94	66.72	29.81
Shelf	600.100	1.08	14.91	17.83	61.93
	500.100	1.80	15.28	16.67	41.49
	400.100	1.65	15.33	55.14	57.18
	300.100	1.66	12.63	50.09	62.66
	200.100	1.40	14.71	53.31	43.6
Open	600.200	3.47	11.72	11.74	19.78
	500.200	2.45	11.56	18.08	26.62
	400.200	1.48	11.84	41.84	46.32
	300.200	2.69	15.11	16.56	6.86
	200.200	1.76	15.79	12.3	9.71

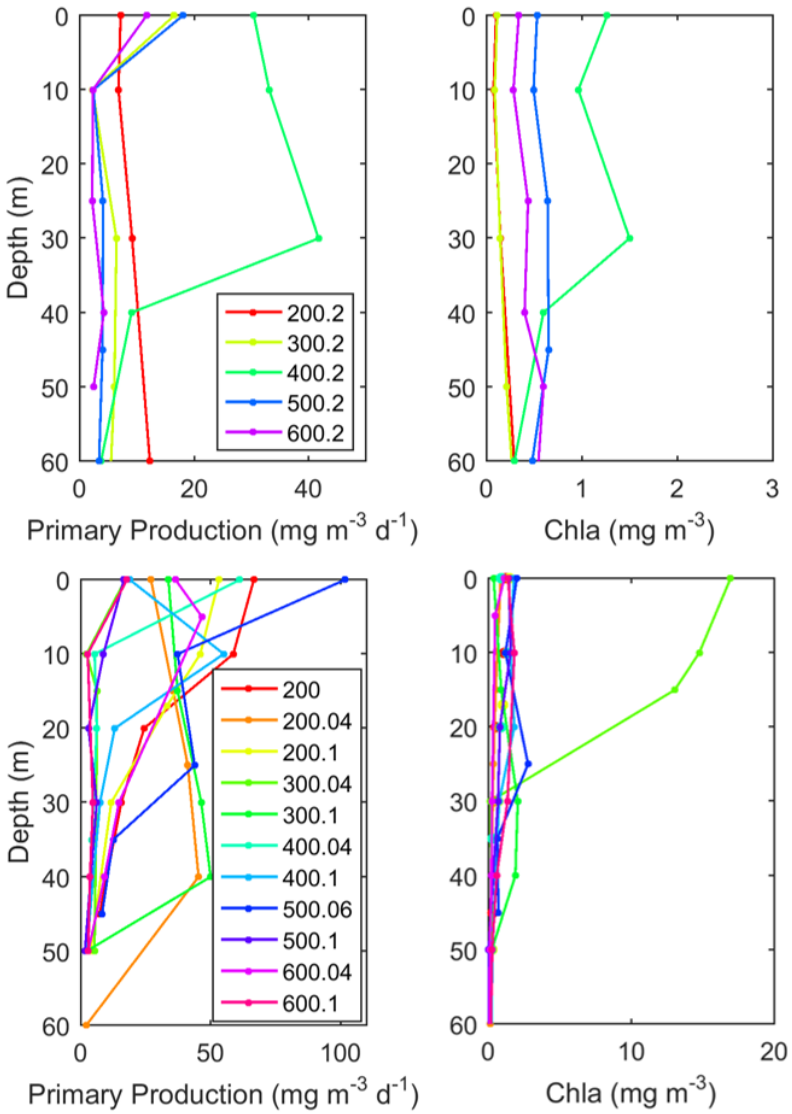

Figure 4.3.3: Depth profiles of phytoplankton parameters over the upper 60m during PAL LTER cruise 2017. The data are divided into Open Ocean stations and shelf+coast stations.

4.3.4 The distribution of microbial parameters along the WAP

As with the aforementioned physical and biogeochemical parameters, both bacterial abundance and bacterial activity reflect similar patterns with highest leucine incorporation rates (bacterial activity) at the coastal stations and rates decreasing towards the open ocean and North (figure 4.3.2a). Bacterial abundance peaks at 200.000 and 300.040 while bacterial activity peaks at 400.040 and 200.000. In relation to the rest of the sampling grid, the bacterial activity maxima at these stations are extremely high at > 400 pmol leu hr $^{-1}$ L $^{-1}$. The rest of the surface values shows high variability ranging from leucine incorporation rates as low as 3.65 pmol leu hr $^{-1}$ L $^{-1}$ at 200.200 to 168.3 pmol leu hr $^{-1}$ L $^{-1}$ at 300.040. Bacterial abundance ranges from 4.4x10^{8} cells L^{-1} at 500.100 to 3.1x10^{9} cells L^{-1} at 200.000. Bacterial activity at the open-ocean stations is 10 to 100 times lower than coastal bacterial activity. All open-ocean stations show bacterial activity maxima at depths between 25 and 30 m while, except for 300.040, at all coastal stations, maxima are found at the surface. Bacterial abundance maxima are found mostly between 15m and 60m with a few exceptions of surface maxima (figure 4.3.4).

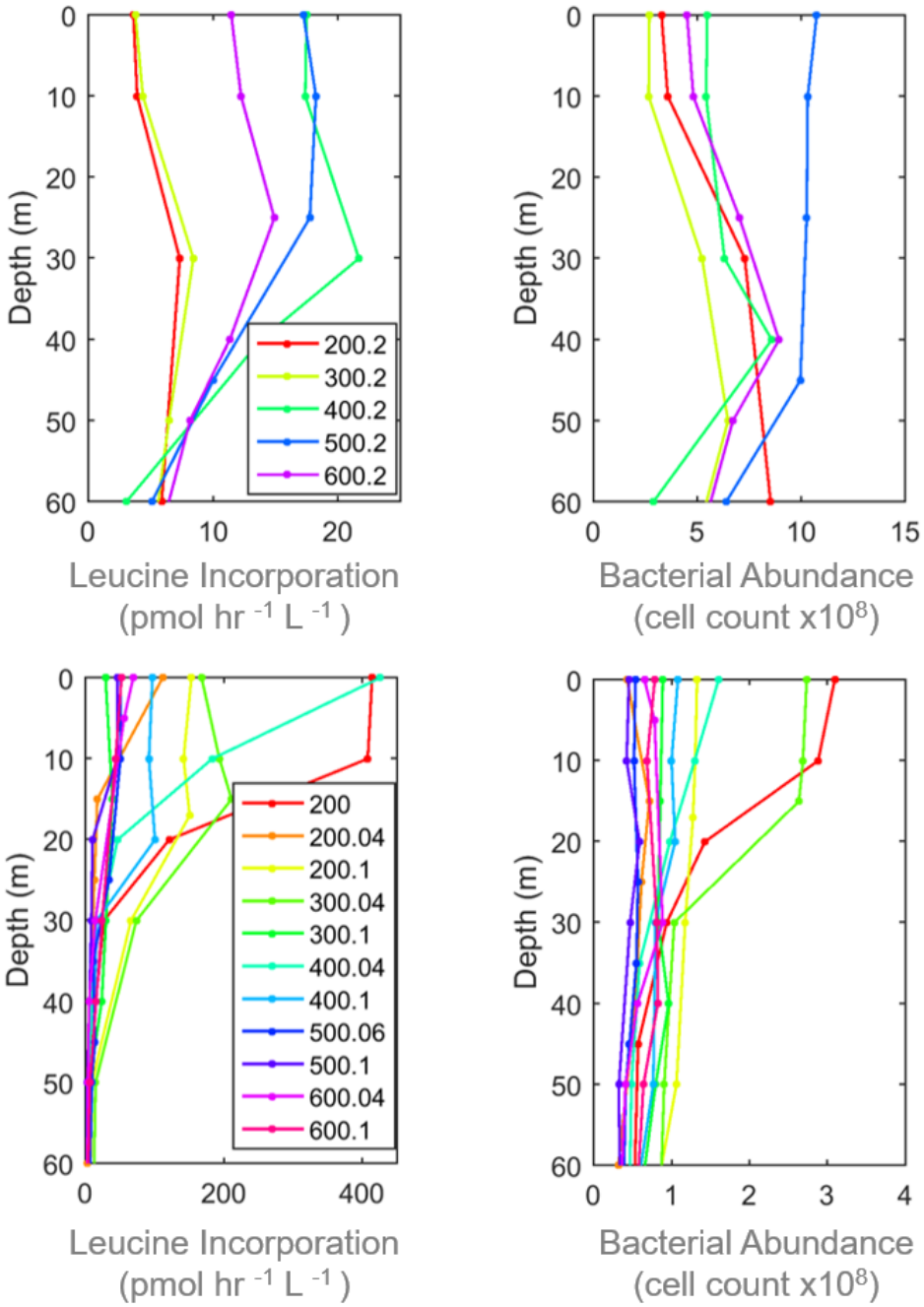

Figure 4.3.4: Depth profiles of microbial parameters over the upper 60m during PAL LTER cruise 2017. The data are divided into Open Ocean stations and shelf+coast at the bottom.

4.3.5 The distribution of organic matter along the WAP

4.3.5.1 Particulate organic matter

Particulate organic matter is a direct product of primary production, and thus, agrees well with the observations of chlorophyll-*a*. Both POC and PN peak at station 300.040 along with chlorophyll-*a*. Lowest concentrations are found at the open-ocean stations 200.200 and 300.200 and elevated surface concentrations are seen along stations 600.100 and 500.060 (see surface plots in figure 4.3.5a). In general, highest concentrations are found at the surface for both POC and PN. However, at some stations, POC and PN maxima are between 10 and 30m in agreement with chlorophyll-*a* peaks (figure 4.3.5b).

Surface POC:N ratios averages 7.34 ± 1.98. Stations 600.100 and 600.200 show elevated ratios of 13.0 and 10.3 in surface waters, respectively. Excluding these two stations, the shelf mean POC:N ratio is 6.34 ±0.42 and the open stations 6.49 ±0.56. The coastal station mean POC:N ratio is 7.10 ± 1.38. With depth, both POC and PN concentrations decrease along with increasing POC:N ratios.

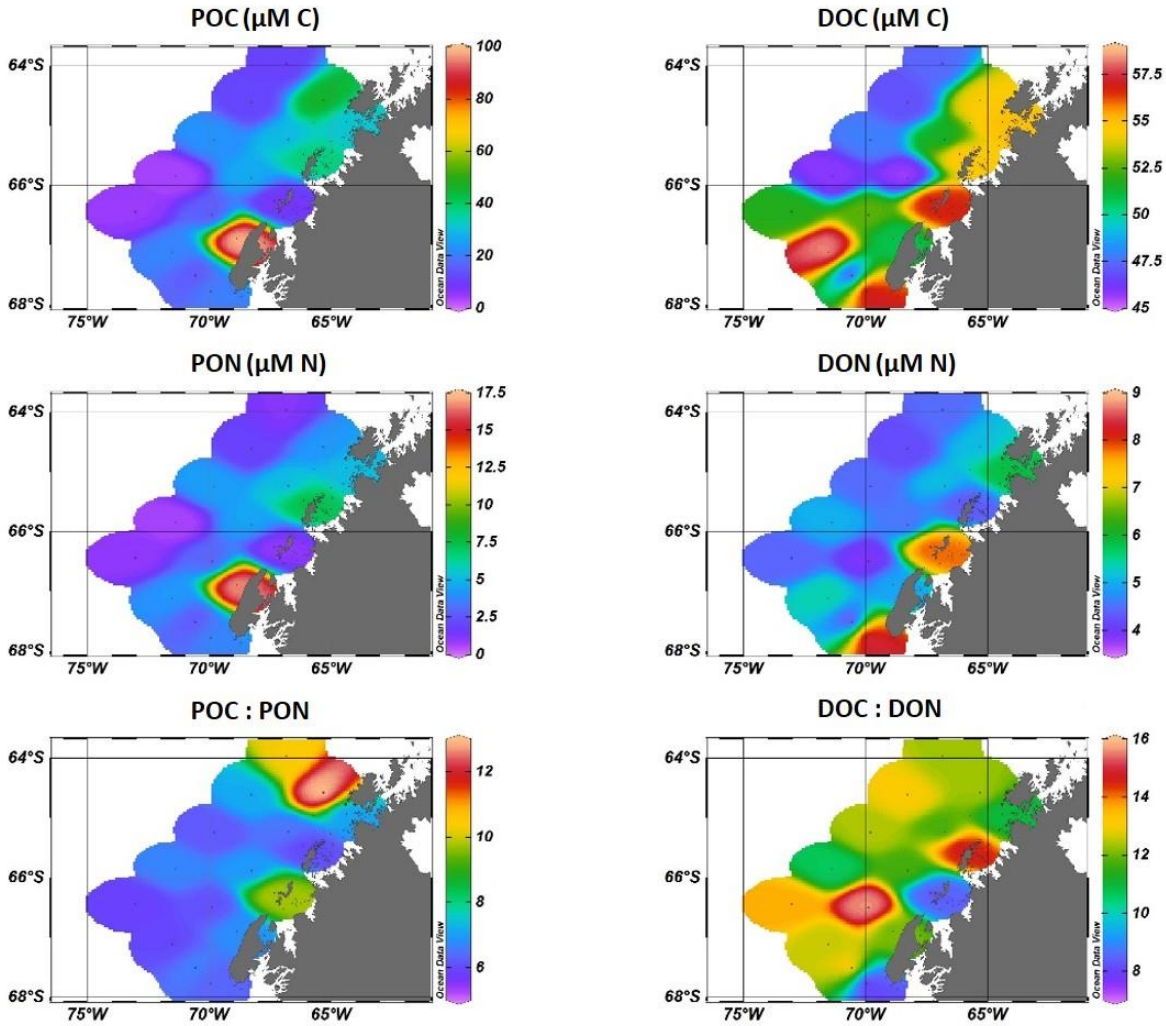

Figure 4.3.5a: Surface distribution of particulate and dissolved organic matter and their C:N ratios, respectively, during PAL LTER cruise 2017.

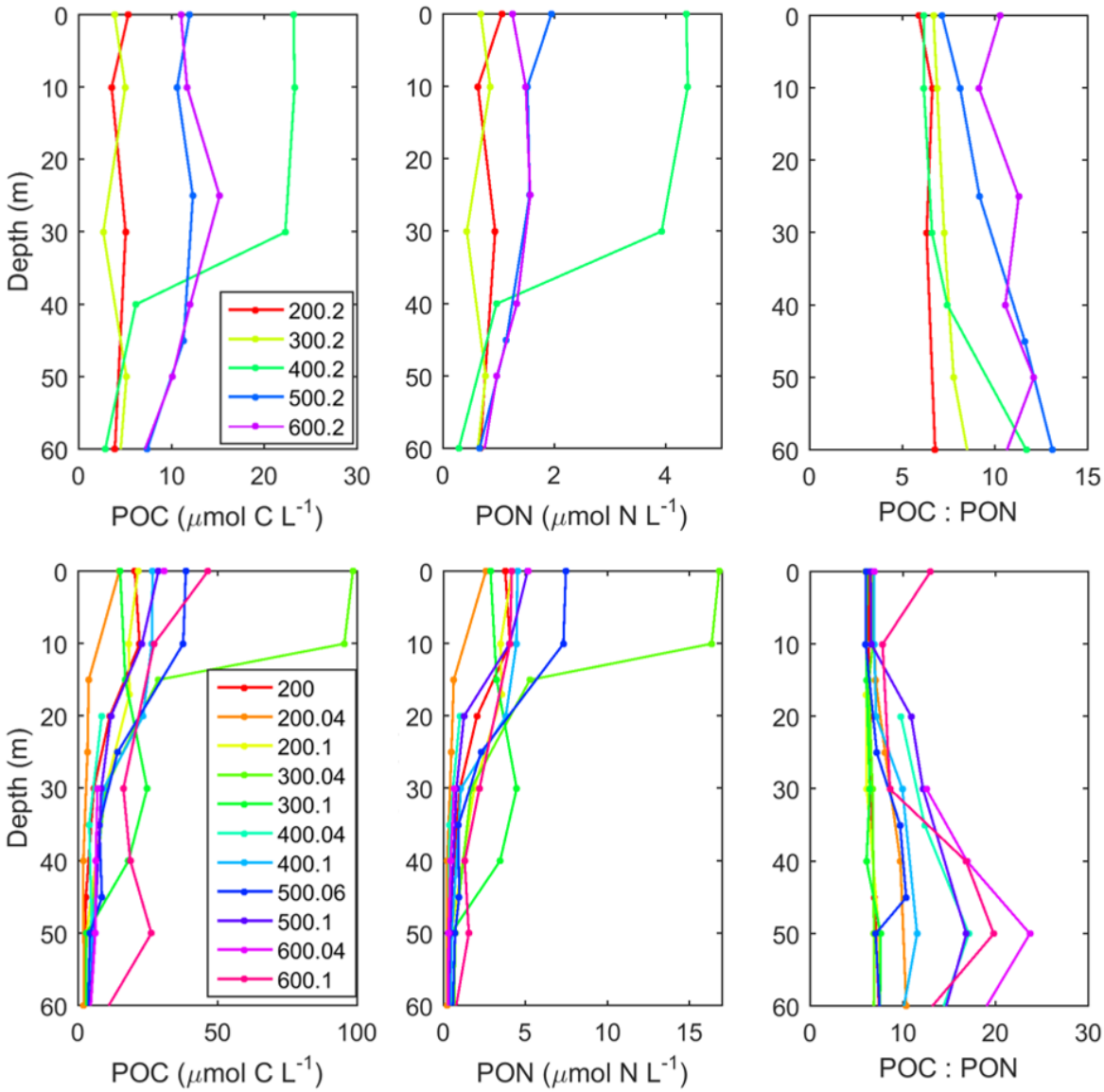

Figure 4.3.5b: Depth profiles of particulate organic carbon, nitrogen, and the POC:N ratio over the upper 60m during PAL LTER cruise 2017. The data are divided into Open Ocean stations and shelf+coast at the bottom.

4.3.5.2 Dissolved organic matter

Dissolved organic matter concentrations show high variability but are low overall and cover a small range compared to lower latitudes. Highest variability of DOC concentrations is found in the upper 80 m ranging from 38.13 µmol C L^{-1} to 60.47 µmol C L^{-1}. Below 500 m, the range narrows down to 38.87 – 43.50 µmol C L^{-1}.

DON shows a similar behaviour with highest concentrations in the top 100 m ranging from 1.70 µmol N L^{-1} to 10.52 µmol N L^{-1}. Highest concentrations (> 8.5 µmol N L^{-1}) are exclusively found in the upper 50 m. Below 500 m, [DON] have a mean of 4.25 ± 0.78 µmol N L^{-1}. See figure 4.3.5a for surface distributions of DOC and DON.

In the upper 50 m of the open-ocean stations, [DOC] range from 42.99 µmol C L^{-1} to 60.22 µmol C L^{-1}. DON in this region ranges from 2.9 µmol N L^{-1} to 7.12 µmol N L^{-1} (figure 4.3.6).

In the shelf waters, [DOC] range from 44.33 µmol C L^{-1} to 58.45 µmol C L^{-1}. [DON] is more heterogeneously distributed than DOC and ranges from 3.65 µmol N L^{-1} to 8.12 µmol N L^{-1}. Compared to [DOC], [DON] is more variable both horizontally and vertically in this area.

Coastal waters have surface DOC concentrations averaging 54.23 ± 4.28 µmol C L^{-1} with a range from 42.51 µmol C L^{-1} to 60.41 µmol C L^{-1}. Most elevated concentrations are found in the upper 10 m of 200.000 (57.64 and 58.28 µmol C L^{-1}). Upper ocean [DON] ranges from 1.7 µmol N L^{-1} at 500.060 to 10.52 µmol N L^{-1} at 200.000 which is the highest [DON] in the entire sampling grid. [DON] decreases with depth but shows high variability in the upper 50-80 m.

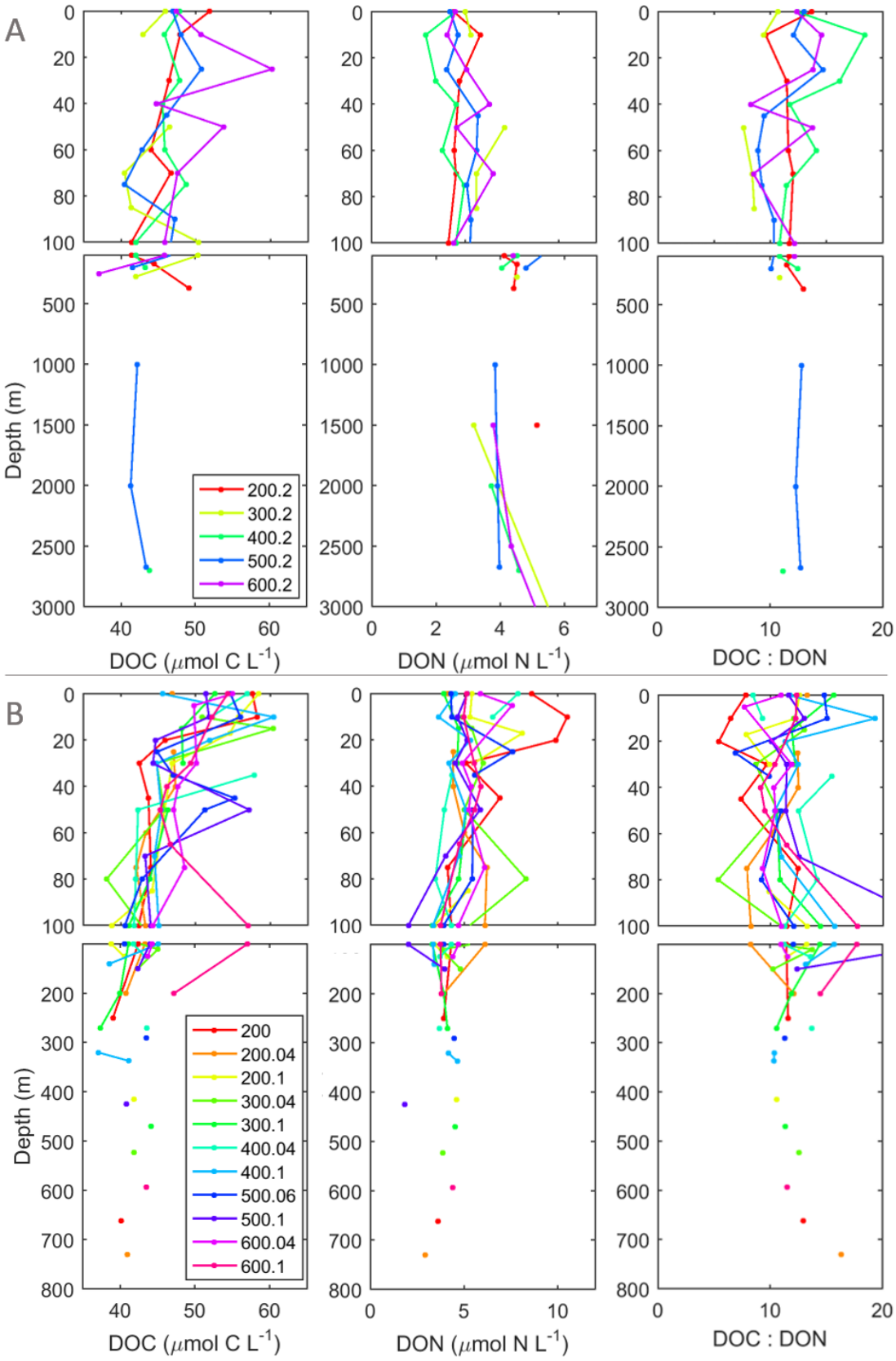

Figure 4.3.6: Full depth profiles of dissolved organic carbon, nitrogen and the DOC:DON ratio with expansion of the upper 60m PAL LTER cruise 2017. A = Open Ocean, B = Shelf+Coast.

4.4 Discussion

4.4.1 Oceanographic and biogeochemical setting of WAP conditions during PAL LTER cruise 2017

The data in this study represent a snapshot in time of the biogeochemical dynamics at the West Antarctic Peninsula. Sea-ice retreat varies from 5 to 126 days setting the scene for the whole area. Stratification in the WAP region has been shown to be largely driven by sea-ice conditions (e.g. Kim et al., 2016; Venables et al., 2013) and is also reflected in this study with a positive correlation between MLD and sea-ice retreat days (SIRD; r = 0.68, p = 0.005). While in the open ocean, sea ice retreated > 100 days prior to sampling and conditions for phytoplankton blooms were initiated shortly after, the conditions on shelf are at a different stage in time. Here, sea ice retreated between a few days to weeks prior to sampling so that primary production rates are higher and more variable. In the coastal region, the addition of glacial meltwater plays a supplementary role and increases stratification, which allows for increased biological production due to favourable conditions for phytoplankton species. A highly stratified water column hinders phytoplankton cells from sinking below the well-lit zone of the upper ocean (Garibotti et al., 2005) and glacial meltwater introduces micronutrients to the upper ocean (Annett et al., 2015; Eveleth et al., 2017). As described above, the addition of meltwater is indicated by a low $\delta^{18}O_{H2O}$ isotopic composition in water and is most prominent in coastal areas. These physical characteristics of the WAP region control biological processes of the water column which is reflected in the biogeochemical parameters shown in this study: Primary production is higher closer to the shore and correlates with SIRD (PP_{max} ~ SIRD r = -0.558, p = 0.02). The negative correlation between PP and SIRD shows that PP is strongest where sea-ice retreated the latest and has declined already in areas of higher SIRD which agrees with previous studies (Kim et al. 2016, 2018; Schofield et

al. 2018) and can further be supported by correlations between nutrients uptake concentrations with SIRD (r = -0.58 and -0.53, $p < 0.05$ for NO_3^- and PO_4^-, respectively).

Bacterial activity correlates negatively with SIRD and is highest where sea ice retreated only recently (r = -0.58, $p = 0.02$). This is surprising because previous studies show a significant time lag of several days to 3-4 weeks between phytoplankton and microbial blooms (Billen & Becquevort, 1991; Kim & Ducklow, 2016; Lancelot et al., 1991). These lags in time have been shown to be the result of varying degrees of DOM production and quality which, in turn, appear to be a function of phytoplankton assemblages and the responding bacterial clades (Kim & Ducklow, 2016; Straza et al., 2009; Nikrad et al., 2014). There are no phytoplankton pigmentation data for the 2017 PAL LTER cruise available, however, the Si:N uptake ratio is a useful tool for identifying diatom-dominated phytoplankton blooms. Diatoms are thought to produce small amounts of DOM which has been shown experimentally (Norrman et al., 1995). A Si:N ratio > 1.5 is considered to represent diatom-dominated phytoplankton blooms but also Fe-deplete conditions in which diatoms accumulate more silicic acid than NO_3^- (Hutchins, 1998). Open-ocean stations generally show higher Si:N ratios than coastal stations indicating a higher contribution of diatoms but also likely limitation by iron. Nutrient uptake ratios, primary production and chlorophyll-*a* maxima are shown in table 4.3.1. Possible reasons for high bacterial activity at the southernmost and most recently sea-ice free stations will be discussed in more detail in section 4.4.3.

4.4.2 Dynamics of dissolved organic matter with regard to biogeochemical and biophysical properties

Overall, dissolved organic carbon and nitrogen distributions show intense spatial heterogeneity. Deep-sea background levels of DOC (refractory DOC) average 41.5 ± 2.2 µmol C L^{-1} and surface concentrations do not exceed 61 µmol C L^{-1} agreeing well with Southern Ocean deep-sea and surface values measured in other studies (e.g. Carlson et al., 2000; Hansell & Carlson, 1998; Lechtenfeld et al., 2014; Nikrad et al., 2014; Ogawa et al., 1999; Wang et al., 2010). For DON, deep-sea background values average 4.26 µmol N L^{-1} with a range from 2.92 to 5.59 µmol N L^{-1} which also agrees with other Southern Ocean studies (Hubberten et al., 1995; Sanders & Jickells, 2000).

Over the whole PAL LTER grid, DON correlates significantly with DIC ($r = -0.77$, $p = 0.0008$) and shows a weak yet significant positive correlation with bacterial activity ($r = 0.48$, $p = 1.6 * 10^{-5}$) (figure 4.4.1). DOC correlates positively with POC ($r = 0.52$, $p = 4.3*10^{-6}$) and bacterial activity ($r = 0.53$, $p = 1.02*10^{-6}$), and negatively with NO_3^- ($r = -0.55$, $p = 3.8 * 10^{-7}$), and DIC ($r = -0.65$, $p = 0.009$), figure 4.4.1 and 4.4.2. The positive correlation of DOC with POC in conjunction with the negative correlation with both NO_3^- and DIC strongly suggests that DOC is to some extent produced directly by phytoplankton. However, the relative weakness of these relationships also suggests that other processes are at work leading to production and simultaneous consumption of DOM. The lacking correlation of DON with chlorophyll-*a*, primary production, NO_3^- or PN, in conjunction with a positive correlation with bacterial activity might be due to rapid removal processes of the generally more labile DON as well as an indication for DON being a product of bacterial activity rather than primary production.

Different mechanisms appear to be involved in DOM cycling, particularly DON, which lead to high variability even though concentrations are low, particularly along the coast with additional influence from increased primary production, bacterial activity and

freshwater. These mechanisms might influence DON concentrations to such extent that relationships between DON and other biogeochemical parameters are difficult to distinguish. Figure 4.4.2 shows the correlations between POC, PN, DOC, DON and NO_3^- and the lacking correlation between DON and NO_3^- uptake indicating several processes influencing DON production and removal which likely act at much shorter time scales than those influencing POM or DOC.

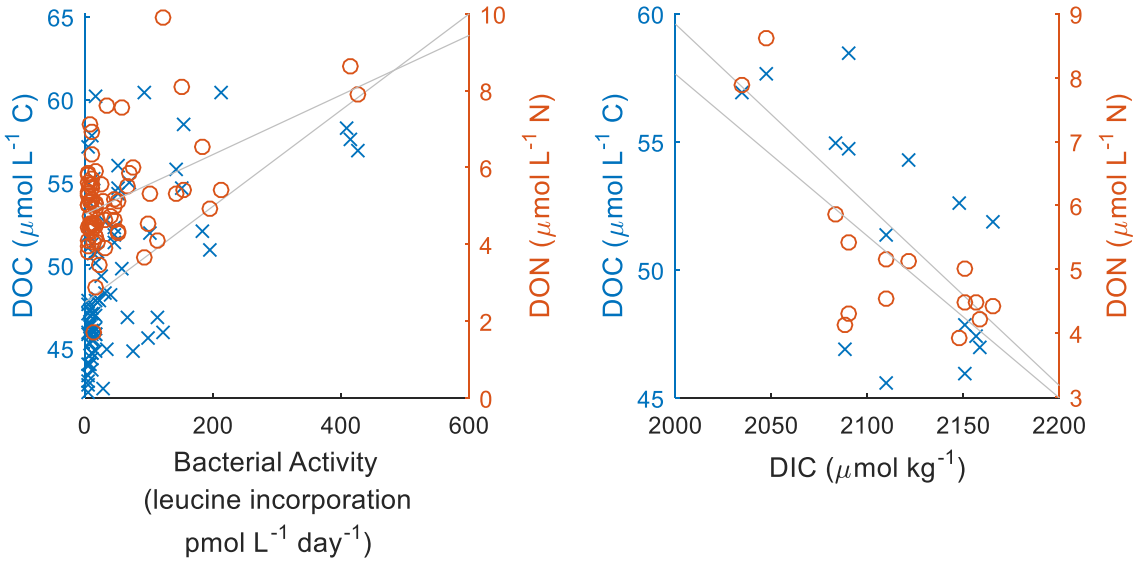

*Figure 4.4.1: DOC and DON correlate significantly with bacterial activity (DON ~ BA r = 0.48, p = 1.6 * 10^{-5}; DOC ~ BA r = 0.53, p = 1.02*10^{-6}) and DIC surface concentrations (DON ~ DIC r = -0.77, p = 0.0008, DOC ~ DIC r = -0.65, p = 0.009) in the entire PAL LTER sampling area.*

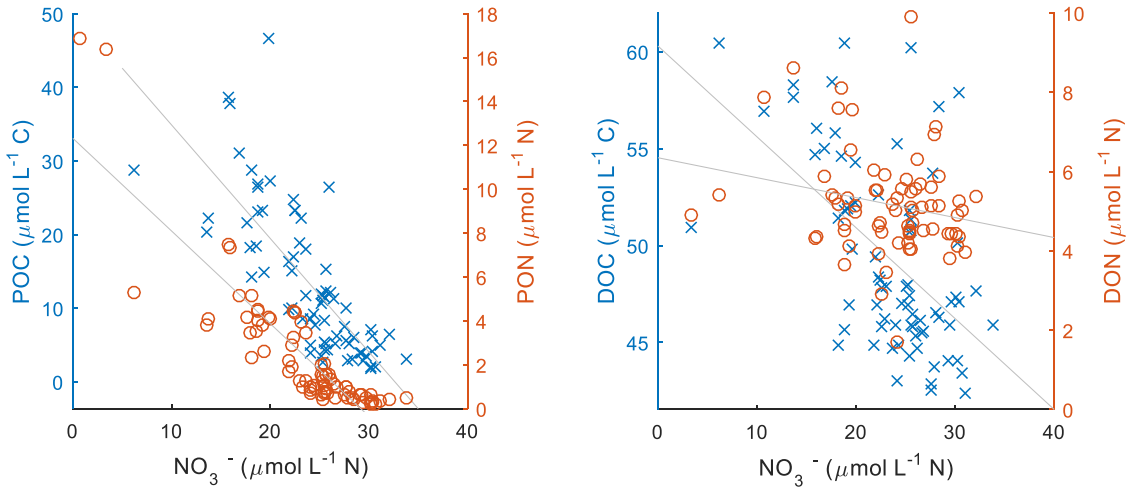

Figure 4.4.2: Upper 50 m particulate organic carbon and nitrogen show a strong negative correlation with NO_3^- concentrations indicating POM formation during phytoplankton blooms. DOC correlates with NO_3^- at a significant but weaker level ($r = -0.55$, $p = 3.8 * 10^{-7}$) while DON does not show a statistically significant relationship to NO_3^- ($p > 0.05$) indicating processes other than PP being responsible for DON production and removal.

Depth-integrated PN (PN_{int50}) and DON (DON_{int50}) show a good relationship along the open ocean stations (r = 0.91, *p* = 0.02) which does not exist for the shelf+coast stations. However, in the shelf+coast region, DON_{int50} correlates strongly with bacterial $activity_{int50}$ (r = 0.84, *p* = 0.001). DOC also correlates with POC and bacterial activity. However, for carbon, these correlations are weaker suggesting a preferential breakdown of N-enriched POM by bacteria. In the shelf+coastal waters, physical parameters play a more important role for DOM dynamics. For example, DOC correlates strongly with maximum temperatures (r = 0.86 and *p* = 0.0006) and the integrated DOC:DON ratio correlates well with the fraction of meteoric water ($DOC:DON \sim f_{glac}$ r = - 0.60, *p* = 0.05) indicating N-enriched DOM with increasing meteoric influx.

Even though previous studies have found profound differences between the North and South of the WAP in biological and biogeochemical properties, those differences are minor and insignificant for DOM dynamics, possibly because of the small amounts

of DOM concentrations overall. However, a clear difference between the open and the shelf region and an offshore-to-coast trend is shown in all available data.

4.4.2.1 Dissolved organic matter dynamics in the open ocean

Dissolved organic carbon and nitrogen concentrations remain within a low range in the open ocean. [DON] correlates significantly but weakly with chlorophyll-*a*, ($r = -0.46$, $p = 0.03$), [PN] ($r = -0.51$, $p = 0.02$), and leucine incorporation ($r = -0.46$, $p = 0.03$) in the open ocean. There is no correlation between [DOC] and any of the above parameters. Interestingly, all these correlations are negative across the open-ocean stations which could indicate a different stage of timing in the phytoplankton bloom and bacterial activity than elsewhere in the PAL LTER area: As shown above, sea ice retreated between 114 and 125 days prior to sampling at the open ocean stations (except 600.200 which was ice-covered at the time of sampling) meaning phytoplankton activity has likely peaked a first time a relatively long time ago giving bacteria time to react and form enough active biomass to break down the biologically available organic matter. In this instance, the negative correlation might show a stage at which most PN has been degraded and bacteria are now breaking down DON compounds, hence the negative relationship, also shown in the negative correlation between DON and PN. Because it is in the late stage of the bacterial bloom, bacterial abundance and activity as well as organic matter concentrations are in decline. The shelf waters, on the other hand, have just experienced the phytoplankton bloom peak so that here, bacteria have had time to form bacterial blooms starting to break down POM to DOM. Even though in this context, a spatial pattern is established, it shows the temporal development of DOM concentrations in the surface waters over the austral summer phytoplankton concentrations at the same time (see conceptual model in Figure 4.4.3).

4.4.2.2 Dissolved organic matter dynamics in the shelf and coastal region

Along the coast, DON concentrations show a good relationship with bacterial activity ($r = 0.65$, $p = 2.0*10^{-4}$). While the correlation in the open ocean is negative, i.e. [DON] decreases with increasing leucine incorporation, it is positive in the coastal waters, showing increasing bacterial activity with increasing [DON] (see conceptual model in figure 4.4.3).

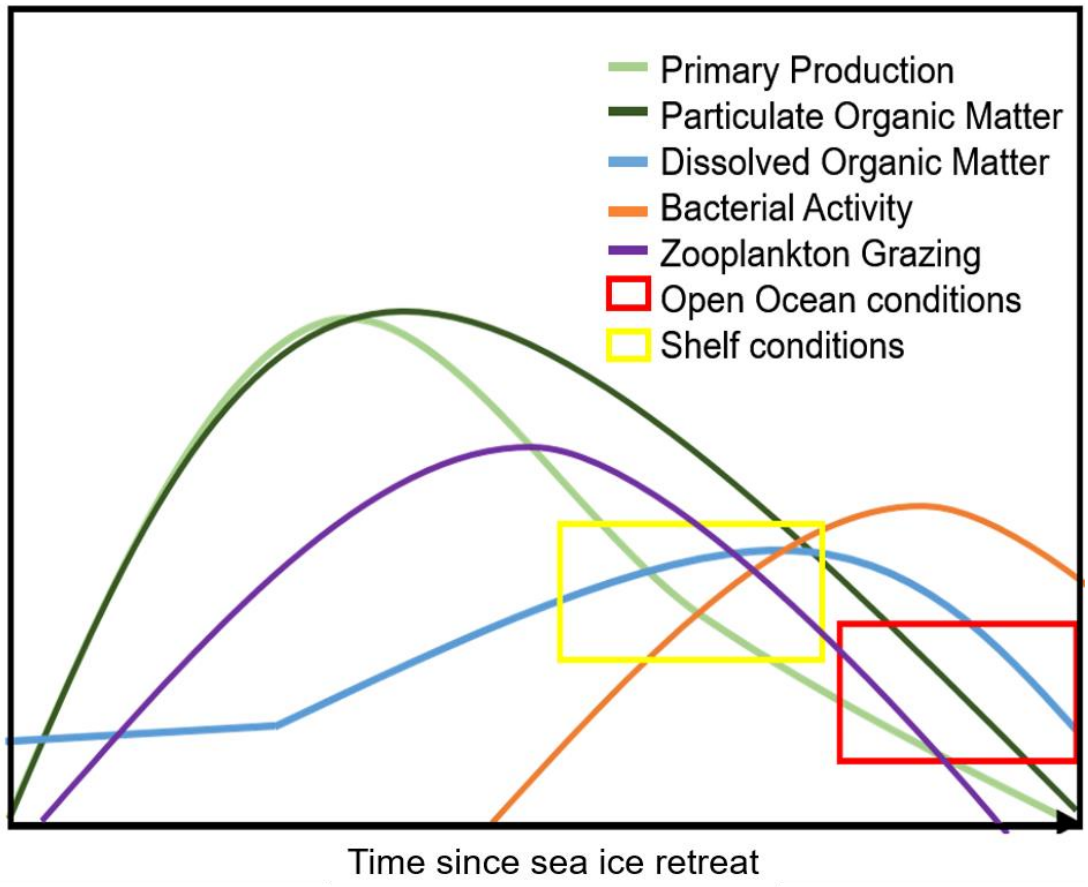

Figure 4.4.3: Conceptual model of the timing of phytoplankton and bacterial production in the PAL LTER grid: Light green = Primary production, dark green = particulate organic matter concentration; orange = bacterial activity; blue = dissolved organic matter concentration. Particulate organic matter accumulates in the surface waters during a phytoplankton bloom. Bacteria react to the available organic matter with a time lag of a few days to 3-4 weeks and break the particulate organic matter down to dissolved organic matter (note that DOM is to some extent likely also being directly produced by phytoplankton and zooplankton grazing). The yellow rectangle shows the suggested stage in time for the shelf region while the red rectangle represents the state in the open ocean explaining the negative relationship between bacterial activity and DON. This illustration does not represent actual dimensions of biogeochemical parameters.

There is a negative correlation between DOC and NO_3^- (r = -0.58, $p = 1.6*10^{-5}$) and a positive correlation between DOC and PP in the shelf+coast region (r = 0.64, p = 0.01). The positive correlations of both DON and DOC with bacterial activity (BA ~ DOC r = 0.54, $p = 2.98*10^{-5}$, BA ~ DON r = 0.60, $p = 2.61*10^{-6}$) show bacteria actively breaking down organic matter and releasing DOM. While there is no direct link between DON and *in situ* production by phytoplankton, the correlations between DOC, NO_3^- and primary production indicate that DOC is a product of *in situ* production by phytoplankton.

There are several possible reasons for DON only correlating well with bacterial activity while DOC also correlates well with chlorophyll-*a* and NO_3^-. Firstly, the presence of NH_4^+ which might be high enough at some depths to interfere. Because NH_4^+ is a direct product of organic matter degradation (Dugdale & Goering, 1967; Eppley & Peterson, 1979; Harrison, 1980), it does support the correlation between DON and bacterial activity, i.e. there is likely more NH_4^+ in areas of high bacterial activity. Further, studies have shown that phytoplankton can compete with bacteria for DON as a nitrogen source in both inorganic N replete and depleted conditions so that rapid cycling of DON might be taking place (Bradley et al., 2010; Bronk et al., 2007; Zhang et al., 2015).

Along the coast, where glacial contribution is greatest, both DON and DOC correlate positively with the meltwater fraction of both glacial and sea-ice derived meltwater ($f_{met+seaice}$) (DOC ~ $f_{met+seaice}$ r = 0.56, p = 0.002; DON ~ $f_{met+seaice}$ r = 0.46, p = 0.01) which will be discussed in section 4.4.3.

DOM concentrations drop back to background concentrations within the top 50-150 m. Even though single-point measurements of DOC and DON show high variability in the upper 50m, upper-50-m DOC and DON standing stocks show little variability. In

combination with the significant relationship with bacterial activity, this little variability suggests that DOM cycling in the upper ocean is taking place efficiently to such extent that there is no or little export to deeper depth. After dividing the water column into 50 m bins to allow for direct comparison with the depth-integrated upper ocean standing stocks (DOC_{int50} mean = 2326.3 ± 242.43 µmol C L^{-1}, DON_{int50} mean = 259.7 ± 45.45 µmol N L^{-1}), the average standing stock for DOC and DON below 50 m are 2117 ± 87.1 mmol C m^{-2} $50m^{-1}$ and 277 ± 26.1 mmol N m^{-2} $50m^{-1}$. These findings support previous studies hypothesising the WAP to be a productive ecosystem but being inefficient in organic matter export (Ducklow et al., 2018; Stukel et al., 2015; Stukel & Ducklow, 2017). Instead, upper-ocean carbon and nitrogen remineralisation appears to be efficient.

4.4.2.3 Station-specific variability along the coastal stations of the 2017 PAL LTER cruise

While most of the PAL LTER sampling grid seems to be past the major phytoplankton bloom of austral spring and bacteria have started the degradation process of the available POM, the coastal stations show high variability among each other with varying stages and degrees of phytoplankton-bloom conditions:

Station 500.060 shows highest primary-production rates in the entire sampling grid. Bacterial abundance and production are lowest at this station among all coastal stations (Bacterial abundance = 5.4 * 10^8 cells L^{-1}, bacterial activity = 50.96 pmol leu L^{-1} hr^{-1}) indicating that the existing phytoplankton bloom is likely the first one of the season in this area. Of all coastal stations, this station is least influenced by meteoric water (3.38%) which might explain the relatively deep mixed layer (23m) despite recent sea-ice retreat (14 days).

Highest chlorophyll-*a* concentrations of this study are found at station 300.040 (Chl*a* = 16.97 mg m^{-3}) in agreement with high nutrient uptake (NO_3^- uptake = 33.62 µmol N L^{-1}) and particulate organic matter production (POC = 98.62 µmol C L^{-1}; PN = 16.84 µmol N L^{-1}). It is also the station with lowest surface salinity (32.64) and highest influence of meteoric water (5.59%) all of which likely contribute to high biological activity. The high meteoric-water input is reflected in low-salinity surface waters and increased stratification. Additionally, a likely supply of micronutrients from glacial sources promotes intense phytoplankton blooms. DOC concentrations are elevated in the subsurface while DON concentrations stay at relatively low levels. DON has been shown to be a suitable source of nitrogen for phytoplankton (Berman & Bronk, 2003; Treger & Jaques, 1992). Since NO_3^- is almost completely depleted at this station, the low DON concentrations might suggest a shift in nitrogen source by the prevailing phytoplankton species.

Station 600.040, the northernmost coastal station, shows highest contribution of sea-ice melt in the surface waters (1.75%) among all stations but did not seem to exert any biological activity to a greater extent than any of other stations. The contribution of glacial meltwater is lower than at the other coastal stations (3.6%). The surface waters of 600.040, in comparison to other stations, show slightly elevated levels of DOC (54.97 µmol C L^{-1}) and DON (5.87 µmol N L^{-1}) with a comparatively high DOC:DON ratio which could be the result of DOM release from sea-ice melt. Sea-ice cores collected in 2014 at the UK Rothera Research Station support elevated sea-ice derived DOC:DON ratios (see chapter 3).

At station 200.000, sea ice had retreated shortly before the day of sampling (6 days). This station shows highest concentrations of DON (10.52 µmol N L^{-1}) in the whole sampling grid and high bacterial activity (414.83 pmol leu L^{-1} hr^{-1}) which is surprising considering bacteria have been shown to respond to primary production with a time

lag of up to several weeks in the WAP region. Primary production rates do not vary greatly from other coastal stations (66.72 mg C m^{-3} d^{-1}). 200.000 is strongly influenced by glacial water (4.6%) and by sea-ice melt (0.9%) in a similar manner to 400.040 (discussed below). While DOC and DON concentrations are highest in the surface waters at this station, POC and PN concentrations are comparatively low (20.41 µmol C L^{-1}, 3.78 µmol N L^{-1}). Thus, there is one of two mechanisms suggested to take place here: Firstly, an ice-edge bloom dominated by a phytoplankton species, such as *Phaeocystis spp.*, which produces and releases DOM directly to the surrounding water. *Phaeocystis* is a genus of haptophytes which produces high amounts of high-carbon dissolved organic matter in the form of exopolymeric substances (EPS). In Antarctic waters, they can occur in high density and dominate phytoplankton blooms temporarily (Arrigo, 1999; DiTullio et al., 2000; Schoemann et al., 2005). In support of this idea are the development of nutrient concentrations with depth which are depleted only in the upper 10m within the shallow mixed layer at this station. Below the MLD, nutrient concentrations quickly increase back to CDW values.

Secondly, the release of active bacteria, DOM and potentially other macro- and micronutrients from both sea ice and glacial water. The surface water at this station is comparatively warm, likely due to strong stratification and solar radiation heating up the surface, which might support higher bacterial activity (Kirchman et al., 2009; Pomeroy & Wiebe, 2001). Even though it has been shown that temperature *per se* does not control bacterial growth, these data show that in combination with other factors, i.e. increased stratification and external influences from meteoric water, bacterial activity can be increased at higher temperatures.

Highest bacterial activity is found at station 400.040 (426.50 pmol leu L^{-1} hr^{-1}) accompanied by high DON concentrations (7.88 µmol N L^{-1}). Even though sea ice was < 15% for 20 days prior to sampling, the influence of sea ice is still comparatively

high at 0.97%. Glacial meltwater makes up 4.7% of the sampled surface waters. Highest phytoplankton and bacterial activities take place within the mixed layer which is in the top 13 m and rapidly drop back to levels comparable to other coastal stations.

Considering the high bacterial activity and DON concentrations at 200.000 and 400.040 – both with higher influence by glacial and sea-ice meltwater than the other stations – it is likely that the bacterial response at these stations is controlled by a combination of a shallow mixed layer and an extra supply of labile dissolved organic matter from glacial and/or sea-ice sources which will be discussed in more detail in section 4.4.3.

4.4.3 Glacial and sea-ice DOM as possible source of (semi) labile DOM to WAP surface waters

DOC, DON as well as bacterial production all correlate well with $\delta^{18}O_{H2O}$ in the coastal region of the WAP despite only recent sea-ice retreat (figure 4.4.4). For that reason, the possibility of both DOM and bacteria directly originating from glaciers and/or sea ice is investigated here.

Glacial DOM is characterised by high N content and thus lower C:N ratios which makes it more readily available in downstream environments (Hood et al., 2009; McKnight et al., 1994).

Sea-ice cores from the UK Rothera research station (see chapter 3) show high concentrations of both DOC and DON with slightly elevated DOC:DON ratios.

Low DOC:DON ratios can be shown at the surface of two out of three most glacially influenced stations: 200.000 (7.8) and 400.040 (8.42), coinciding with high bacterial activity. The low C:N ratios at these stations suggest higher influence on DOM quality by glacial meltwater than by sea ice with higher C:N ratios. This leads to the

suggestion of a combination of different mechanisms which are not necessarily the same for both stations. As suggested above, a combination of recent sea-ice retreat and concurrent release of sea-ice derived organic and inorganic nutrients, phytoplankton and bacterial clades as well as meteoric water influence are likely the reason for both high DON and high bacterial activity at 200.000. At 400.040, sea-ice retreat is not as recent. Therefore, high DOM concentrations could result from high glacial influx and relatively high primary production leading to high bacterial activity and high levels of DOM. While bacterial production is similar at both 200.000 and 400.040, bacterial abundance is 1.9 times higher at 200.000. This further supports the potential fresh addition of bacteria and DOM from both sea ice and glaciers. The most prominent biological difference between the two stations is a clear difference in the bacterial structure with 200.000 showing a ratio of high nucleic acid bacteria cells (HNA) to low nucleic acid cells (LNA) of 14.6 while at 400.040 the HNA:LNA ratio is 6.6. Even though there is much debate about what qualitative information can be drawn from HNA and LNA analyses (Gasol et al, 1999; Gomes et al., 2015; Sherr et al., 2006; Vila-Costa et al., 2012; Zubkov et al., 2001), it is clear that there is a difference between these two stations which might indicate a shift in taxonomy or physiology of the present bacterial clades (Luria et al., 2017). Bowman et al. (2017) suggest that HNA may represent community physiology which might have an effect on DOM cycling. Compared to the other coastal stations, both 200.000 and 400.040 show elevated HNA numbers and might thus express a different physiological preference for specific DOM compounds. Only 300.040 shows a similarly high HNA:LNA ratio of 10.7. As it is these three stations with highest HNA:LNA ratios and highest glacial meltwater influx, it is likely that the bacterial community composition is influenced by glacial meltwater. While both stations 200.000 and 400.040 are influenced by glacial meltwater input, it is likely that 200.000 gains its high DON and bacterial activity from these inputs plus recent sea-ice melt. At 400.040, bacteria might

have reacted to the ongoing primary production due to early triggering by glacial meltwater input and further, as DOM is released directly by phytoplankton due to the bloom being at a later stage. Hence, while different mechanisms play a role at both stations, the result is similar: High bacterial production accompanies, and is potentially triggered by, high DOM availability. DOC concentrations are also elevated at both stations but not as substantially as DON concentrations indicating glacially derived DOM. At both stations, DON and DOC concentrations decrease close to background levels within the top 50 m suggesting labile DOM being rapidly cycle by bacteria in the upper ocean.

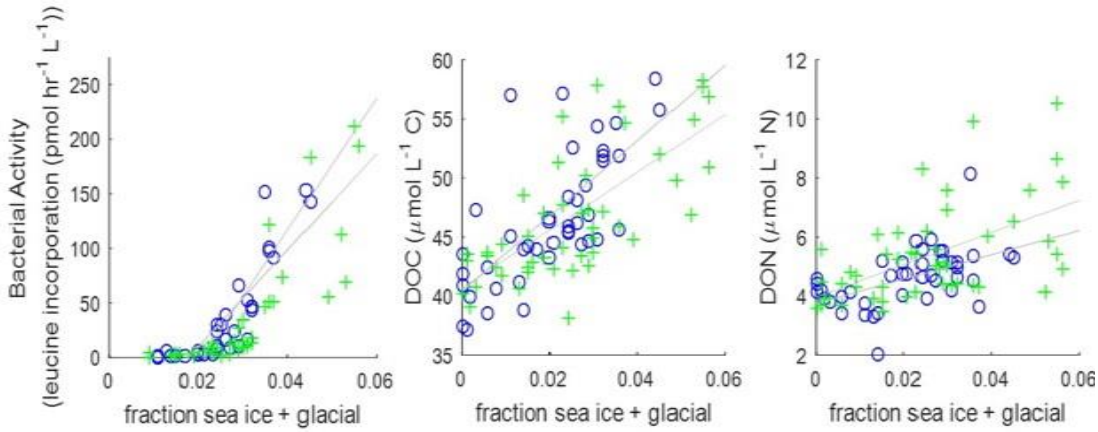

Figure 4.4.4: Bacterial activity, DOC and DON correlate well with the fraction of freshwater, here the sum of sea ice and glacial meltwater, in the shelf (o) and coast (+). All r- and p-values are stated in section 4.4.3.

Several studies show that supraglacial meltwater contains low concentrations of DOC (approximately 10-40 µmol L^{-1} C) while subglacial and basal sources can carry between 60 µmol C L^{-1} and 4 mmol C L^{-1} (Barker et al., 2006; Bhatia et al., 2010; Christner et al., 2014; Lafrenière & Sharp, 2004; Lyons et al., 2007) with varying degrees of lability. Supraglacial DOM has been found to be mainly of microbial origin while subglacial DOM originates from subglacial vegetation erosion and microbial

degradation. Bacterial abundance and activity are high in glacial environments so that glacial meltwater could not only be a source of DOM but also of active bacteria.

Sea-ice cores collected at the UK Rothera Research Station (chapter 3) show a wide range of DOC and DON concentrations but overall high DOC concentrations (29.88 – 1037.00 µmol C L^{-1}, mean = 145.15 ± 196.41 µmol C L^{-1}) and elevated DON concentrations (1.90 – 160.55 µmol N L^{-1}, mean = 12.95 ± 28.85 µmol N L^{-1}) with DOC:DON ratios ranging from 7.53 – 56.83 (mean = 19.26 ± 12.23).

Considering the dilution effect with CDW, glacial addition at station 200.000 and 400.040 with their respective meteoric water content of 4.58 and 4.71% would carry a diluted DOC signature between 2.75 and 188.4 µmol C L^{-1}. For the sea-ice fraction, which makes up 0.9% at both stations, there would be an additional DOC concentration of 0.27 – 9.33 µmol C L^{-1} and DON concentrations of 0.02 to 1.44 µmol N L^{-1}. These concentration ranges highly depend on the composition and source of the glacial flow and/or sea ice. There has not been a major phytoplankton bloom at 200.000 so that all DOM additional to the background levels of CDW could potentially come from glacial runoff and sea ice only. (Semi) labile concentrations of DOC and DON are determined by subtracting background CDW DOC (or DON) concentrations from measured surface concentrations. In order to meet the measured bioavailable DOC and DON surface concentrations at 200.000 (18.68 µmol C L^{-1} and 6.76 µmol N L^{-1}), the introduced freshwater (from both sea ice and glacial melt), when undiluted, would have to carry a signature of 340.88 µmol C L^{-1} and 123.36 µmol N L^{-1} (figure 4.4.5). These concentrations are within the range of subglacial DOC concentrations from literature and agree with the findings from the WAP sea-ice cores. However, given that there may be an additional contribution from *in situ* phytoplankton production or degradation, these estimates represent upper bounds on meltwater DOM concentrations.

Employing the same calculations for 400.040, the glacially-derived DOM component would be accounting for 271.12 µmol C L^{-1} and 69.34 µmol N L^{-1} which is less than 200.000 but still, it is within the range of known glacial and sea-ice DOM concentrations. Reasons for this difference even though concentrations of DOC and DON are similarly high might be different glacial sources plus potentially an increased contribution of phytoplankton-derived DOM at 400.040.

Even though the shelf stations show minor glacial influence still, these calculations cannot be expanded onto these stations. Phytoplankton blooms likely occurred at these stations already, making the assumption of no phytoplankton-derived DOM invalid and the labile nature of the glacially derived DOM leads to probably continued degradation with distance travelled.

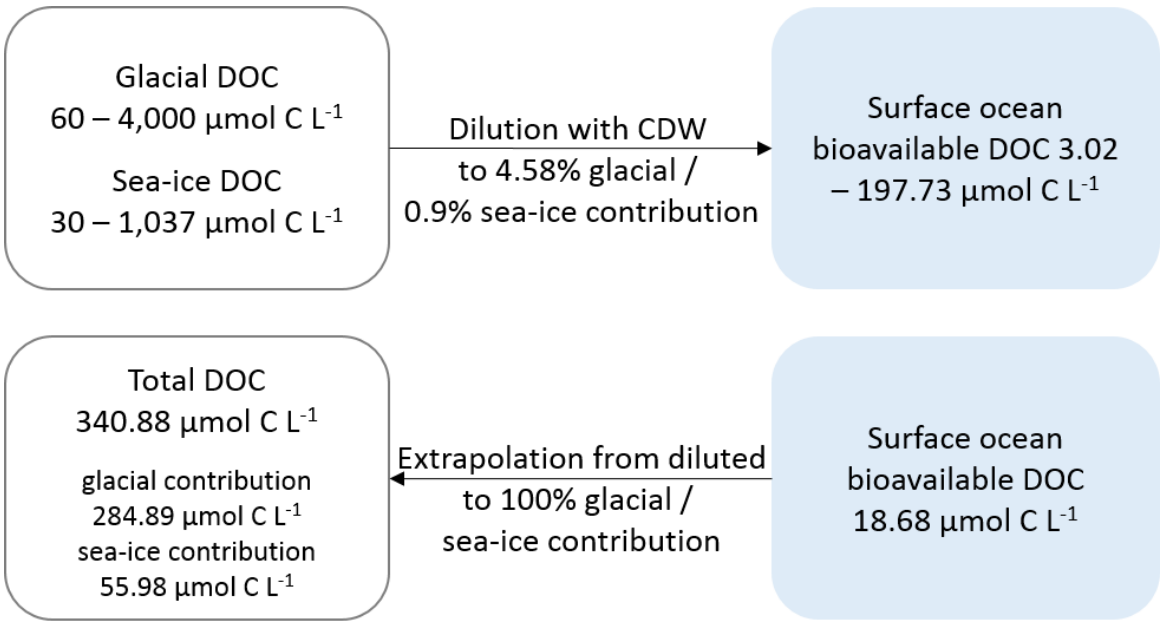

Figure 4.4.5: Meltwater contribution at station 200.000: The top shows the theoretical effect of glacial and sea-ice meltwater to surface DOC concentrations from literature values and RaTS sea-ice cores after dilution of meltwater with CDW. The bottom shows these calculations reversed: Assuming all surface bioavailable DOC measured comes from meltwater only, the glacial and sea-ice sources would have the stated DOC concentrations.

4.4.4 *Additional mechanisms potentially affecting dissolved organic matter dynamics*

Viral lysis plays a significant role in controlling bacterial abundance and activity. It leads to the release of fresh DOM from both phytoplankton and bacteria to the ambient water which, in turn, can be recycled quickly. During this process, known as the viral shunt, viruses infect a host cell, grow and lyse these, leading to the release of highly labile DOM with important effects on the biological pump (Malits et al., 2014; Weitz & Wilhelm, 2012) as more bioavailable DOM hypothetically triggers an increase in bacterial respiration and hence a reduction in organic carbon export to depth. Even though there is only little research on Southern Ocean viruses, two studies at the Kerguelen Plateau and at the WAP, respectively, have shown that viral production is particularly high during intense phytoplankton blooms and represent a reason for high bacterial mortality (Brum et al., 2015; Malits et al, 2014). While there are no viral data available for this study, viruses are likely to play an important role in regulating DOM availability and bacterial abundance and activity.

A general differentiation between (semi) labile and refractory DOM is made by subtracting deep-sea measurements from surface values which results in net production (or loss) of DOC and DON. Refractory DOM is introduced to the WAP surface waters with the intrusions of CDW. These background levels are thought to be refractory in the deep sea, however, it has been shown that UV radiation can have destructive effects on refractory DOM compounds. While a previous study by Ortega-Retuerta et al. (2010) showed a high correlation between chromophoric DOM and salinity, Chlorophyll-*a* and bacterial activity in glacially influenced waters, Kaehler et al. (1997) concluded that if UV radiation affects surface DOM in the Southern Ocean, such changes are likely undetectable due to the overall small concentrations in Southern Ocean surface waters.

4.5 Summary

The spatial distribution of DOC and DON in the upper ocean of the WAP and production and removal mechanisms

Numerous studies on physical, biological and biogeochemical processes along the WAP have shown intense interannual variability mostly dependent on climatic conditions with effects on sea ice in the region. The data presented in this study show high variability within the region west of the Antarctic Peninsula which is likely due to both sea-ice conditions and proximity to the shore of the peninsula from where meteoric water introduces micronutrients and enhanced stratification which often is in favour of increased primary production. Ducklow et al. (2018) conclude that processes such as vertical mixing, active transport by migrating zooplankton and removal by whales and birds play an important role within the WAP ecosystem and its production-export imbalance observed in numerous WAP POM export studies (Ducklow et al., 2018; Stukel et al., 2015; Stukel & Ducklow, 2017). The degradation of POM with depth is a well-established process and the increasing POC:N ratio with depth shows the preferential removal of N from POM compounds. The variability of DOM is much more complex. This study shows that there are many co-existing processes driving production and removal of DOM: This study finds generally more bioavailable DOM available in shore proximity, with likely external DOM sources being glacially and sea-ice derived DOM. This hypothesis is emphasised by significant correlations of DOC and DON as well as bacterial activity with the $\delta^{18}O_{H2O}$ composition and an absent correlation between DOM and POM in the coastal regions suggesting another DOM source than phytoplankton.

Overall, DOC and DON concentrations remain within a low range, as hypothesised, with highest concentrations in regions of increased phytoplankton (DOC) or bacterial activity (DON).

In the open ocean, sea ice retreated much earlier than in the coastal regions and meteoric water is negligible. Further, likely co-limitation by micronutrients such as iron (Annett et al., 2015) potentially leads to the blooms in this area being weaker than those occurring in the shelf waters. Here, correlations between DOM and POM and DOM and bacterial activity support the hypothesis of a preferential breakdown of N-rich POM by bacteria into DOM compounds and further utilisation of N-rich DOM. The degradation process of POM can be observed in the correlation between PN_{int50} and DON_{int50} being strongest in the open ocean and decreasing towards the coast. The negative relationships between DON and PN, and DON and bacterial activity in the open ocean suggest that the microbial bloom is already approaching declining conditions.

Due to the timing of phytoplankton blooms in the different regions, DOM production from POM might dominate relevant DOM production mechanisms in the coastal regions at a later stage. As sea ice just retreated in this area and primary production likely just started, the previously proposed direct release of DOM by phytoplankton or POM degradation at a later stage of a phytoplankton bloom is likely to occur in this area, too, and might even exceed the suggested fraction of glacial and sea-ice DOM contribution over the course of the growing season. DON concentrations were shown to be highest along the coast and could be shown to occur along high bacterial activity. At the same time, DOC concentrations were not increased so that this DOM is of low C:N ratios, supporting one of the tested hypotheses of this study. From the available data, it cannot be shown whether DON concentrations are increased due to bacterial release of DON or whether bacteria increased in number and activity due to bioavailable DON. Considering the data and likely DON sources in chapter 3, it is more likely that bacteria are the dominant source of DON along the WAP.

Overall, the following sources are suggested for bioavailable DOM along the WAP:

(i) Direct and indirect release by phytoplankton via e.g. sloppy feeding by zooplankton. This source scenario is supported by strong correlations between primary production and DON ($r = 0.81$, $p = 0.009$) and NO_3^- ($r = -0.85$, $p = 0.002$) in the surface waters.

(ii) DOM produced and released by bacteria. This has been shown with the negative correlation between DON_{int50} and PN_{int50} and DON_{max} and Leu_{max} in the open. Highest [DON] are accompanied by highest bacterial activity ($r = 0.92$, $p = 0.0002$) in the shelf+coast. However, there is no correlation between surface DON and PN concentrations so that it remains uncertain whether this DON was produced by bacteria or the bacteria are reacting to it being made available from another source. Ultimately, bacterially produced DOM derives from POM degradation.

(iii) Allochthonous material from glacial and sea-ice melt at coastal stations. Surface DON, DOC and bacterial activity correlate significantly with the meteoric water fraction $\delta^{18}O_{H2O}$ while, at the same time, neither DON or DOC show a significant correlation with phytoplankton parameters such as PP, chlorophyll-*a* or POC and PN. There is a decreasing trend in the DOC:DON ratio with increasing glacial contribution pointing towards more labile material with increasing glacial influence.

From the above discussion, it becomes clear that processes ultimately linked to DOM production, such as phytoplankton and microbial production, vary substantially between stations which is potentially the result of physical differences and varying macro- and micronutrient inputs, time since sea-ice retreat and therefore the timing and conditions of major phytoplankton blooms. In pre-bloom conditions such as at station 200.000, the influence of sea ice and/or glacial meltwater can lead to direct addition of DOM from those sources; but the freshening of the surface layer and

addition of micronutrients, and potentially phytoplankton and bacteria, can further facilitate increased DOM production. Lacking correlations of DOC and DON with POC or PN in the shelf+coastal area emphasise the different source scenarios. The good correlations with bacterial activity, on the other hand, show active and efficient bacterial breakdown of surface POM and production of DOM independent of the source.

The apparent relationships between DOC and DON and other biogeochemical parameters show complex dynamics for DOM cycling in the region likely with multiple processes occurring simultaneously driving DOM production, transformation and consumption.

The ecosystem west of the Antarctic Peninsula has been hypothesised to change to an ecosystem dominated by smaller plankton species due to the warming observed in the second half of the 20th century. Not only does this study show intense bacterial cycling of freshly produced DOM in the upper ocean of the WAP region with unknown fate of the respired carbon in these waters but also it becomes clear that possible additional DOM delivered to the surface waters from glacial or sea-ice sources undergoes the same mechanisms of degradation representing additional carbon entering the system and being respired in the upper ocean. This carbon has not been initially fixed by primary producers in the ocean and has not been considered in WAP carbon budget studies.

With the hypothesised prediction of continued warming, DOM will gain a more prominent role in the regional organic matter cycling. This study shows that the majority of DOM is being cycled efficiently in the upper ocean and that additional DOM from sea ice or glacial sources tends to be of high bioavailability and therefore is likely to undergo the same mechanisms of respiration representing an additional source of inorganic carbon to the surface waters. The results from the study show a great

likelihood of reduced carbon export and increased upper ocean respiration. Further research, considering ammonium production and uptake, and possibly incubation experiments to investigate DOM sources and sinks, are required to fully understand the cycling of DOM in this region. In addition, winter measurements are necessary to investigate chemoautotrophic production of DOM and cycling in the winter waters which have been shown to hold a higher diversity of bacterial and archaeal clades (Bowman & Ducklow, 2015; Church et al., 2003; Luria et al., 2014) which would indicate highly specialised mechanisms of carbon and nitrogen cycling through the microbial loop.

CHAPTER 5

Spatiotemporal Coupling of Organic Carbon and Nitrogen and their C- and N-isotopic composition at the West Antarctic Peninsula

5.1 Introduction

Globally, most organic matter in the open ocean originates from primary producers and can be differentiated by size into particulate and dissolved forms. As part of the local ecosystem at the western Antarctic Peninsula (WAP), particulate organic matter (POM) dynamics are ultimately controlled by light availability and climatic variations which exert control on the sea-ice dynamics of the region (Saba et al. 2014). With increasing light availability and the start of sea-ice melt in the austral spring, phytoplankton blooms high in biomass develop over the summer season (Moline and Prezelin 1996) with an increasing trend from offshore to onshore following the advance of sea-ice retreat (Arrigo et al., 2017; Li et al., 2016). The phytoplankton community at the WAP is dominated by diatoms but other phytoplankton, such as cryptophytes, can dominate the phytoplankton species assemblage with a changing climate (Moline et al., 2004; Montes-Hugo et al., 2009) and previous studies acknowledge the presence and importance of smaller phytoplankton in the WAP ecosystem (Montes-Hugo et al., 2009; Schofield et al., 2017). At the global scale, phytoplankton incorporate inorganic nutrients at a relatively constant ratio of 106C:16N (Redfield, 1958). However, there are strong latitudinal and species-driven patterns controlling this ratio at the regional scale (Li & Peng, 2002; Martiny et al., 2013). In the Southern Ocean, the C:N ratio of POM is often found to be lower than the Redfield ratio. With depth, POM concentrations decrease because of grazing by

zooplankton and bacterial remineralisation with an increase in the C:N ratio due to the preferential uptake of nitrogen by bacteria.

The cycling of dissolved organic matter (DOM) is not understood as well as the cycling of POM. Reasons for this are numerous processes being involved in every step of the production, transformation and removal of DOM which vary in time and space. DOC:DON ratios have been found to differ from the Redfield ratio due to high molecular restructuring of DOM and N-removal during bacterial degradation processes but also due to various sources of DOM which are not only from *in situ* phytoplankton production. In the Arctic, for example, most DOM is introduced via river runoff (Letscher et al., 2011; Raymond et al., 2007). Riverine DOM has a more refractory nature than marine DOM with a higher C:N ratio (Amon, 2004). In the Southern Ocean, on the other hand, terrestrial sources are scarce and distant. Here, DOM originates from phytoplankton and might have undergone transformation processes by bacteria or zooplankton. In a model study, DeVries et al. (2018) show that DOC export in subtropical gyre regions can make up to 50% of carbon export and DOC:DON ratios tend to be 2-3 times higher than the Redfield ratio. Contrastingly, Southern Ocean DOM shows low C:N ratios which is potentially due to the high contribution of diatoms (DeVries et al. 2018). Diatoms tend to produce low C:N organic matter in cold waters. Globally, reported upper-ocean DOC:N ratios range from 4.0 to 26.0 (Gobler & Sañudo-Wilhelmy, 2003; Hopkinson Jr. & Vallino, 2005; Kähler et al., 1997; Letscher et al., 2015, Ogawa et al. 1999) with the lower end of the range from Southern Ocean studies (Kähler et al. 1997; Ogawa et al., 1999).

Further, less DOM is being produced in Southern Ocean surface waters compared to lower latitudes (Carlson et al., 1998; Doval et al., 2002; Kähler et al., 1997; Wang et al., 2010). Reasons for these relatively small amounts remain unclear. Primary production in Antarctic shelf waters, even though short-lived, can occur at higher rates

than in lower latitudes. Primary producers have been suggested to partition most organic matter into the particulate pool (Carlson et al. 1998) and grazing by zooplankton is thought to be efficient so that only little DOM is being released by sloppy feeding (Kirchman et al., 2009). The Southern Ocean is mostly nitrate replete and only very rarely reaches conditions of nitrate depletion so that organic nitrogen should not represent a required pool of bioavailable nitrogen to phytoplankton. Future projections for the WAP show a possible shift to a food web in which microbial processing of organic matter plays a more important role, which would lead to higher DOM production (Saba et al., 2014). While an increase in DOM production can potentially lead to an increase in carbon export, it can also create a positive feedback mechanism by increasing upper-ocean respiration if this fresh DOM is of high bioavailability. To determine how much DOC is potentially being exported in this region and how these estimates vary and may change in the future, it is essential to understand how POC and PN, and DOC and DON are coupled in the ocean's surface waters and how they are produced and removed from the upper ocean.

To establish an understanding of the coupling processes in POM and DOM, this study addresses the following questions: 1) What are the key processes governing the cycling of (i) POM and (ii) DOM 2) To what extent do C and N decouple spatially or temporally in (i) POM and (ii) DOM? 3) How does organic matter cycling affect the C- and N-isotopic composition of POM?

To address these questions, samples for the analyses for DOC, DON, POC, PN and the C- and N-isotopic composition of POM and the N-isotopic composition of NO_3^- were collected during the PAL LTER cruise in January 2017 and at the UK Rothera research station through three consecutive austral summer seasons (2013/14, 2014/15, 2015/16). These data are investigated for spatial and temporal variability

along with other physical and biogeochemical data to put them into the wider context of the WAP ecosystem.

The isotopic compositions of carbon and nitrogen are used to examine upper ocean processes involved in the cycling of inorganic and organic compounds. By looking into the isotopic composition of nitrogen ($\delta^{15}N$), processes such as nutrient uptake, remineralisation, export, ammonium uptake or nitrification can be determined and quantified.

The uptake of the different isotopes of carbon and nitrogen underlies the principle of kinetic fractionation. For the phytoplankton cell enzymes responsible for transferring inorganic compounds into the cell interior, the uptake of the lighter isotope is energetically preferable. The fractionation of carbon in phytoplankton amongst other factors depends on the availability of pCO_2 and HCO_3^- as well as carbon concentration mechanisms (CCM) which most phytoplankton species express for a more efficient way of DIC consumption (Cassar et al., 2004).

The N-isotopic composition of POM reflects nitrogen availability, sources and remineralisation processes. With nitrate being the primary nitrogen source in WAP waters, and the assumption of Rayleigh fractionation (closed system) in the surface waters, the N-isotopic composition of surface POM would gradually become heavier with the progression of a phytoplankton bloom due to the depletion of the available ^{14}N pool as nitrate uptake proceeds. Replenishment with nutrient-rich CDW water, sea-ice melt, nitrification and remineralisation can cause deviations from this relationship.

The $\delta^{15}N$ of instantaneously produced PN, when exported efficiently without accumulating in the surface waters, is defined by the instantaneous product (Owens, 1988; Sigman et al., 2009a):

$$\delta^{15}N_{PNinst} = \delta^{15}N_{NO3-} - \varepsilon$$

where $\delta^{15}N_{PNinst}$ describes the instantaneous product, $\delta^{15}N_{NO3-}$ the measured $\delta^{15}N_{NO3-}$ composition and ε the kinetic isotope effect.

The accumulated product considers the integrated $\delta^{15}N$ of organic matter accumulation over the growing season assuming accumulation of PN in the surface waters rather than rapid export (Owens, 1988; Sigman et al., 2009a):

$$\delta^{15}N_{PNacc} = \delta^{15}N_{NO3-ini} + \varepsilon * \left(\frac{[NO_3^-]}{[NO_3^-]_{ini} - [NO_3^-]}\right) * \ln\left(\frac{[NO_3^-]}{[NO_3^-]_{ini}}\right)$$

where $\delta^{15}N_{PNacc}$ is the $\delta^{15}N_{PN}$ composition of the accumulated product, $\delta^{15}N_{NO3\text{-}ini}$ the initial $\delta^{15}N_{NO3-}$ and $[NO_3^-]$ and $[NO_3^-]_{ini}$ the *in situ* and initial NO_3^- concentrations, respectively. Deviations from these modelled values give us an insight into mechanisms other than nitrate uptake and POM formation being in place.

The PAL LTER covers the area west of the Antarctic Peninsula from the coast to open-ocean regions. The UK Rothera time series sampling site (RaTS) lies at the Southern tip of this sampling grid in Ryder Bay off Adelaide Island (see figure 5.2.1).

Chapter 3 and 4 of this thesis are concerned with the distribution of dissolved organic matter and processes that potentially drive differences on varying temporal and spatial scales. This chapter will concentrate on processes that are involved in organic matter cycling, including both particulate and dissolved fractions, how organic matter is partitioned and how carbon and nitrogen are coupled or decoupled among those fractions.

5.2 Methods

5.2.1 Sample Site and Collection

5.2.1.1 PAL LTER cruise 2017

The sampled area west of the Antarctic Peninsula covers an area of 900 x 200 km. The sampling locations are fixed and follow a pattern of lines orthogonal to the coast approximately 100 km apart (figure 5.2.1). For this study, samples were collected from January 6th to January 31st 2017 on board the *ARSV Laurence M. Gould*. The sampling scheme on each annual cruise involves deployments of a SeaBird 911+ conductivity-temperature-depth instrument attached to a rosette with 24 niskin bottles. Samples are collected from Niskin bottles closed at specific depths in the water column for particulate organic carbon and nitrogen and their isotopic compositions, dissolved inorganic nutrients, dissolved organic carbon, primary production, chlorophyll-*a*, and bacterial measurements. Sea-ice data are derived from satellite observations from *NASA's Scanning Multichannel Microwave Radiometer* and *the Defense Meteorological Satellite Program's Special Sensor Microwave/Imager*.

Samples for DOC/TDN were collected in acid-cleaned (24 hours in 10 % HCl and DIW, 3x DIW-rinsed and baked for 5 hours at 450 °C) 60-ml HDPE bottles. Prior to sample collection, each bottle and lid were rinsed three times with the sampled seawater. Sample seawater was gravity-filtered directly from the niskin bottles through pre-combusted GF/F filters (Whatman 0.7 µm 47 mm Ø; precombusted at 450 °C for 5 hours in methanol-cleaned tin foil) and immediately transferred to a -80 °C freezer. POM samples were collected by filtering up to 4 L of collected seawater through pre-combusted GF/F filters (Whatman 0.7 µm GF/F 25 mm Ø). The filters were stored in cryovials at -80 °C.

Table 1 in the appendix lists all relevant data analysis, the methodologies applied and the institute at which these analyses were conducted.

5.2.1.2 RaTS site in Ryder Bay

Seawater samples were collected at the Rothera Time Series (RaTS) site in Ryder Bay (figure 5.2.1), a small bay within the larger Marguerite Bay south of Adelaide Island, west of the Antarctic Peninsula. The sampling location is approximately 4 km offshore with a water depth of approximately 520 m. Marguerite Trough is a glacially-scoured canyon within the WAP shelf system which is highly effective in transporting UCDW from the ACC into the inshore regions like Marguerite Bay. Samples were collected twice a week from a small boat. If sea-ice conditions would not allow access to this site, sampling was conducted at an alternative site which has been shown to represent similar conditions with the same water masses (Clarke et al., 2008). Samples were collected at fixed depths (surface, 5m, 15m, 25, 40m and if possible, at 75 and 100m) using Niskin bottles. For DOC/TDN, samples were filtered through pre-combusted GF/F filters (nominal pore size 0.7 µm) into acid-cleaned and combusted glass conical flasks under a gentle vacuum. Samples were transferred to HCl-clean 60 ml HDPE bottles and frozen at -20°C until analysis. In 2013/14, samples were collected from mid-November 2013 to the end of February 2014. The 2014/15 season was sampled from mid-November 2014 until the end of December 2014 with a few additional samples mid-January 2015. The 2015/16 season was sampled from early January 2016 to the end of March 2016. During all sampling events, a conductivity-temperature-depth instrument was deployed for measurements of temperature, pressure, salinity and fluorescence. Data were logged at 1m-resolution.

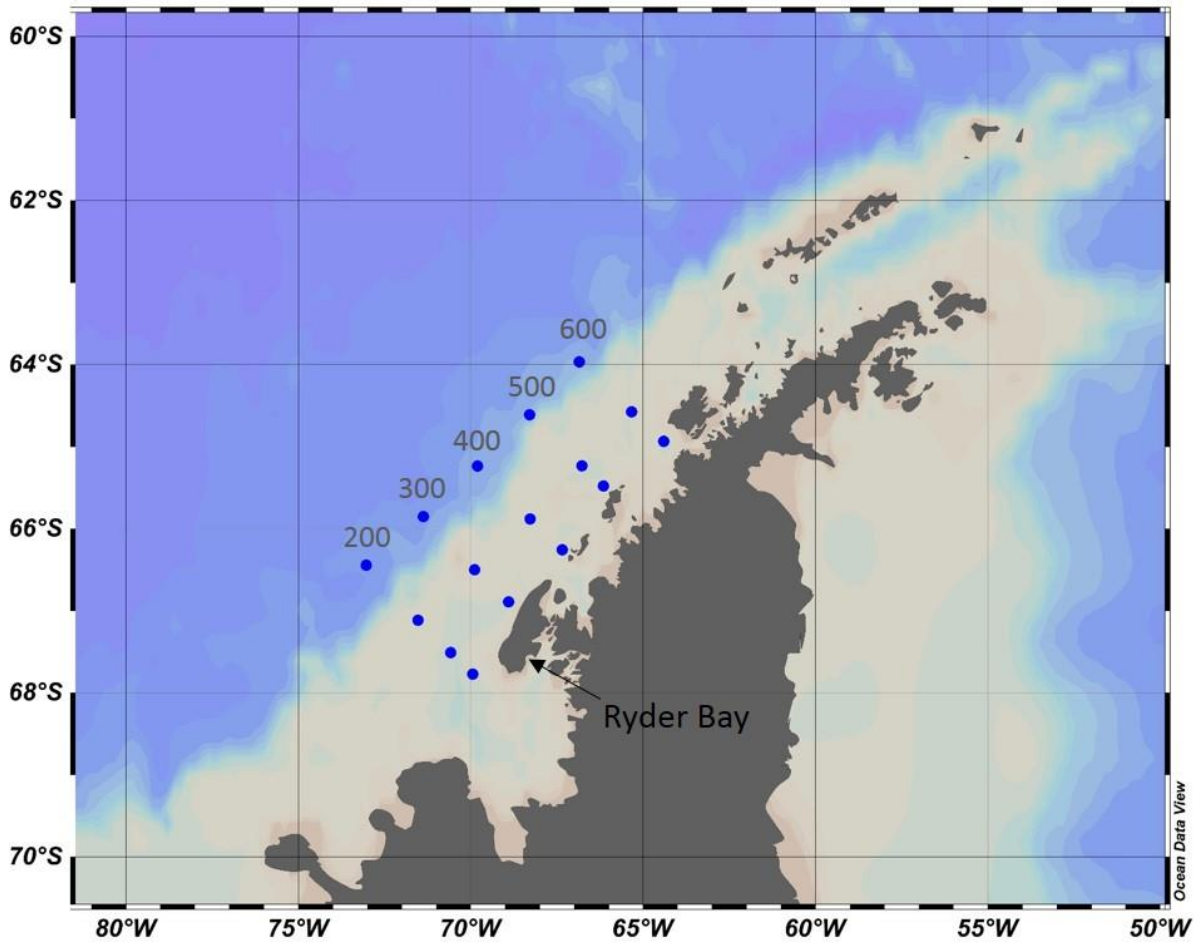

Figure 5.2.1: Map of the west Antarctic Peninsula showing the sampling grid of the PAL LTER research cruise and the sampling lines with stations. The black arrow points at Ryder Bay where samples were collected from the RaTS sampling site.

5.2.2 Particulate Organic Matter

Particulate organic carbon and nitrogen and their C- and N-isotopic composition were analysed at the School of GeoSciences at the University of Edinburgh. Filters for POC:N analysis were prepared following a method adapted from Lourey et al. (2004). In brief, filters were decarbonated by wetting them with Milli-Q and fumed with 70% HCl overnight before drying and carefully folding them into clean tin capsules. Samples were analysed on a *CE Instruments NA2500 Elemental Analyser* connected to a *Thermo Finnigan Delta+ Advantage stable isotope ratio mass spectrometer*. Both

instruments are linked through a *Finnigan ConFlo III Universal Interface* to allow for simultaneous carbon and nitrogen analysis. The CRMs PACS-2 and acetanilide were analysed for the isotopic composition and carbon and nitrogen concentrations, respectively. The analytical reproducibility was better than 1.0% for POC and better than 1.1% for PN.

5.2.3 Dissolved Organic Matter

DOC/TDN analysis was conducted via high-temperature combustion on a *Shimadzu TOC-V analyser* with an attached *TNM1 Total Nitrogen Measuring unit*. Samples were thawed for approximately 3 hours before analysis. 10 ml of each sample was transferred into acid-cleaned and combusted glass vials using an acid-cleaned 5 ml pipette for analysis.

Sample replicates were analysed in each run for precision. Certified Reference Material (CRM; Hansell Deep Sea Reference Batch #15 Lot 1-15; Florida Strait 750 m DOC 42.00-45.00 µmol C L^{-1}, TDN 31.00-33.00 µmol N L^{-1}) was analysed before and after each batch of samples for accuracy. The instrument automatically analyses each sample 3-5 times depending on in-run reproducibility. Deep-sea samples were re-analysed with Deep Sea Reference Batch #18 Lot 08-18 (DOC 41.0 – 45.8 µmol C L^{-1}, TDN 31.6 – 35.0 µmol N L^{-1}). CRMs were intercompared to ensure linearity of the instrument throughout the period of analysis. The CRM DOC values was checked to lie within 5% of the consensus value before each sample run. If this was not the case, more CRMs were analysed until the results were within the range. Detection limits are 0.04 µmol C L^{-1} for DOC and 0.36 µmol N L^{-1} for TDN and analytical precision for DOC was ± 1.09 µmol C $L^{-1}$and for TDN ± 0.51 µmol N L^{-1}.

Due to logistical constrains, samples from the PAL LTER cruise were only analysed for the inorganic nitrogen species NO_2^- and NO_3^- so that all PAL LTER DON concentrations stated contain NH_4^+. NH_4^+ concentrations across WAP surface waters have been shown to be minimal, however, when NH_4^+ concentrations might be of importance, they will be mentioned in the discussion.

5.2.4 N-isotopic composition of NO_3^- via the denitrifier method

In order to determine the N-isotopic composition of nitrate, all nitrate is converted to N_2O by denitrifying bacteria lacking N_2O reductase. After cultivating bacteria on agar plates, the bacteria are starved and purged with N_2 gas. The sample is then injected into bacterial media aliquots with the sample volume calculated from the sample NO_3^- concentration, in order to yield a nitrate content of each sample of 20 nmol N to avoid potential linearity issues with the IRMS. After one day, the bacteria are lysed by injection of NaOH. Samples are analysed by headspace analysis using a Combi PAL auto-sampler linked through a *Thermo Fisher Scientific GasBench II* to a *Thermo Fisher Scientific Delta$^+$ Advantage* stable isotope ratio mass spectrometer (IRMS). Detection limits of the IRMS are better than 0.5 ‰ and the methodological analytical precision is 0.2 ‰ for $\delta^{15}N_{NO3}$. This method is based on the method development by Sigman et al. (2001), Casciotti et al. (2002) and Tuerena et al. (2015). The N-isotopic composition is stated as the ratio of relative difference in isotopic abundance in a sample compared to a standard with the general formula

$$\delta\ in\ ‰ = \frac{R(sample) - R(standard)}{R(standard)} * 1000$$

where R represents the isotopic ratio of each element. The nitrogen standard is atmospheric N_2 with an accepted $^{15}N/^{14}N$ ratio of 3676.5 ± 8.1 (Junk & Svec, 1958).

5.2.5 Inorganic Nutrient Analysis

PAL LTER dissolved inorganic nutrients (Nitrate+nitrite, Silicate and Phosphate) were analysed using a *Seal Analytical* segmented flow autoanalyser (Mequon, WI, Seal AutoAnalyzer AA3). Methods for each analysis followed the protocols recommended in the Seal Customer Support Manual. Nitrate analysis was conducted via reduction to nitrite in a copper-cadmium column and a further reaction with N-1-naphthylethylene diamine dihydrochloride to form a purple azo dye which is then analysed colorimetrically. Phosphate analysis follows the Murphy and Riley method (Murphy & Riley, 1962). The determination of silicate is based on the reaction between silico-molybdate to molybdenum blue by ascorbic acid. Standards for each analysis were sodium nitrite and potassium nitrate, potassium dihydrogen phosphate and sodium meta-silicate nonahydrate. A deep-sea sample collected during each year's cruise at 3,000 m was analysed as an internal reference standard. Detection limits for nitrate+nitrite were 0.015 µmol N L^{-1}, for phosphate 0.0021 µmol P L^{-1} and for silicate 0.03 µmol Si L^{-1}.

The inorganic macronutrient samples from the RaTS site were filtered through Acrodisc PF syringe filters with 0.2 µm Supor membranes and immediately stored at – 80 °C for 12 hours after which they were stored at – 20 °C until analysis (except for ammonium samples). In the Plymouth Marine Laboratory, UK, samples were thawed for 48 hours to allow for complete redissolution of silicate precipitates to silicic acid. A *Technicon AAII* segmented flow autoanalyser was used for the analysis of nitrate+nitrite, nitrite, phosphate and silicate concentrations. Raw data were corrected to certified reference material (KANSO Ltd. Japan), ambient ocean salinity and pH. Analytical precision was usually better than 0.2 µmol N L^{-1} for nitrate+nitrite, 0.01 µmol N L^{-1} for nitrite, 0.02 µmol P L^{-1} for phosphate and 0.6 µmol Si L^{-1} for silicate.

Ammonium concentrations were analysed by reaction with orthophthal-dialdehyde (OPA) overnight and analysis by fluorometry following Holmes et al (1999). Ammonium samples were incubated overnight with the working reagent (OPA, sodium sulphite and borate buffer). The fluorescence was measured within 24 hours of incubation using a Turner Designs 700 fluorometer. Ammonium chloride was used as a standard. The fluorometer was calibrated at the beginning and the end of each batch using the low value of green fluorescence standard 7000-922. The detection limit is 0.01 µmol N L^{-1}. Sample processing was carried out within four hours after sample collection to minimise changes to ammonium concentrations during sample storage.

5.2.6 Primary production and chlorophyll-a

Primary production rates and chlorophyll-*a* concentrations have been gathered throughout the PAL LTER cruise by the research group of Oscar Schofield.

Primary production rates, measured as daily carbon uptake in mg C m^{-3} day^{-1}, are measured with incubation experiments. 100 ml of seawater sample were inoculated with 1 µCi of ^{14}C-radio-labelled $NaHCO_3$ in borosilicate bottles. The bottles were incubated for 24 hours at *in situ* light levels and ambient temperatures. After the 24-hour incubation period, the seawater samples were filtered through GF/F filters, the filters were washed with 10 % HCl, dried and counted in a scintillation counter.

Chlorophyll *a* samples have been filtered onto GF/F filters and kept frozen at – 80 °C stored in cryovials. Analysis was conducted at Palmer Station through acetone extraction and measurement of the extract on a Turner 10AU Fluorometer.

RaTS chlorophyll-*a* concentrations were determined by fluorometry as part of the CTD deployments.

5.2.7 Phytoplankton pigment analysis

Phytoplankton pigmentation was analysed at the University of Groningen using high-performance liquid chromatography. Samples were collected at the RaTS site at 15m depth in 2 to 10 L Niskin bottles since this depth is the overall long-term fluorescence maximum. Particles were collected on GF/F filters (Whatman 47mm Ø) by vacuum-filtering 1 L of collected seawater. Filters were snap-frozen in liquid nitrogen and stored at – 80 °C. Prior to analysis, the filters were freeze-dried for 48 hours in the dark and incubated in 90% acetone for pigment extraction at 4 ˚C. Pigment separation was conducted on a *Waters 2695 HPLC system* with *a Zorbax Eclipse XDB-C8* column (3.5 µm particle size) following van Heukelem & Thomas (2001) and Perl (2009).

5.2.8 The $\delta^{18}O$ composition of seawater

Samples for $\delta^{18}O_{H2O}$ were collected during the PAL LTER research cruises at every sampling station in 50-ml glass bottles which were crimp-sealed. RaTS samples for $\delta^{18}O_{H2O}$ were collected at the surface and 15 m depth in 150-ml medical flat bottles, sealed with rubber bands and parafilm. The samples were analysed at the Natural Environmental Research Council Isotope Geosciences Laboratory at the British Geological Survey. Samples were analysed on a *VG Isoprep 18 and SIRA 10* mass spectrometer with random samples analysed in duplicate which showed an average precision better than ± 0.02‰. The method followed the equilibrium method for CO_2 established by Epstein & Mayeda (1953). The contribution of sea ice and glacial meltwater were calculated using simultaneous equations following Meredith et al. (2016) who adopted the method from (Östlund & Hut, 1984).

5.3 Results

5.3.1 Sea ice

Sea-ice cover shows high variability along the WAP as well as throughout the investigated years. All four data sets show variable but high sea-ice coverage in the winter preceding the growing season with sea ice retreating to different extents and at different times. With 90 days of > 70 % sea-ice coverage, 2013/14 shows the lowest sea-ice coverage of all three RaTS seasons which increases to 114 days in 2014/15 and to 142 days in 2015/16. On average, sea-ice cover remains below 30 % in January and February of each season (figure 5.3.1). However, December sea-ice cover is more variable with 9 days of > 70 % sea-ice in 2013/14 and 2015/16 while in 2014/15 there is only one day with more than 70 % sea-ice.

For the PAL LTER region in 2017, there is a clear trend of sea ice having retreated from the open-ocean area earliest (> 100 days prior to sampling) and latest in the coastal regions (5 to 54 days) (figure 5.3.2). Days since sea-ice retreat are defined as the number of days since sea-ice cover < 15 % for at least 5 consecutive days, following Stammerjohn et al. (2008). For the RaTS data, a sea-ice score threshold of 2 was applied which corresponds to 20% sea-ice coverage.

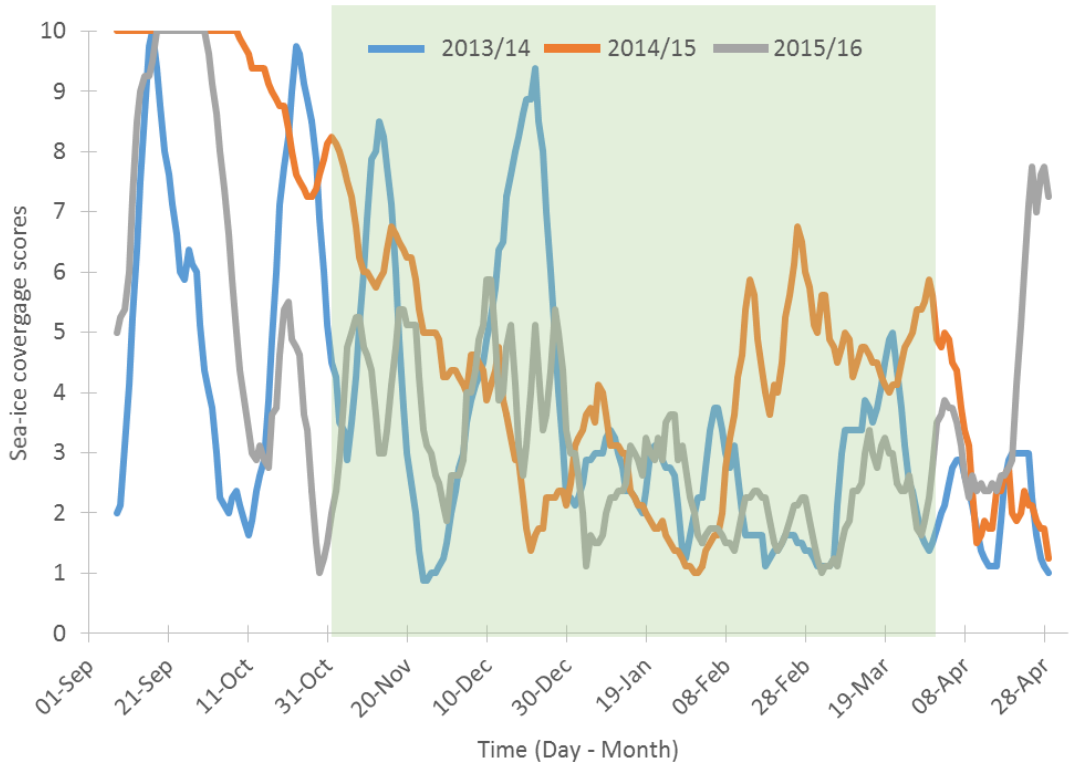

Figure 5.3.1: Moving average (8-day period) of sea-ice coverage at the RaTS sampling site in Ryder Bay for September to April for the three investigated seasons 2013/14 (blue), 2014/15 (orange) and 2015/16 (grey). The green area depicts the austral spring/summer period.

5.3.2 Hydrography

Sea-surface temperatures (SST) in the LTER grid range from 1.08 to 2.90°C with a mean of 2.10 ± 0.46°C (figure 5.3.2). Warmest SSTs are found in the North (stations 500.060 and 500.100) and coldest in the coastal South (300.040 and 200.040). Winter water is present at all stations between 10 and 200m varying in layer thickness with temperatures between -1.71 and 0.00°C.

Salinity ranges from 32.64 to 34.73 with most variability in the upper 100m where sea-ice melt and glacial meltwater influence surface water salinity. This influence is also shown by the $\delta^{18}O_{H2O}$ composition (figure 5.3.2) of the surface water. The mixed layer depth (defined as the depth at which σ_t is 0.05 kg m^{-3} greater than σ_t at the surface)

shows high variability but is shallow with a range from 8 to 40 m with deepest MLD in the offshelf northern stations and shallowest along the coast.

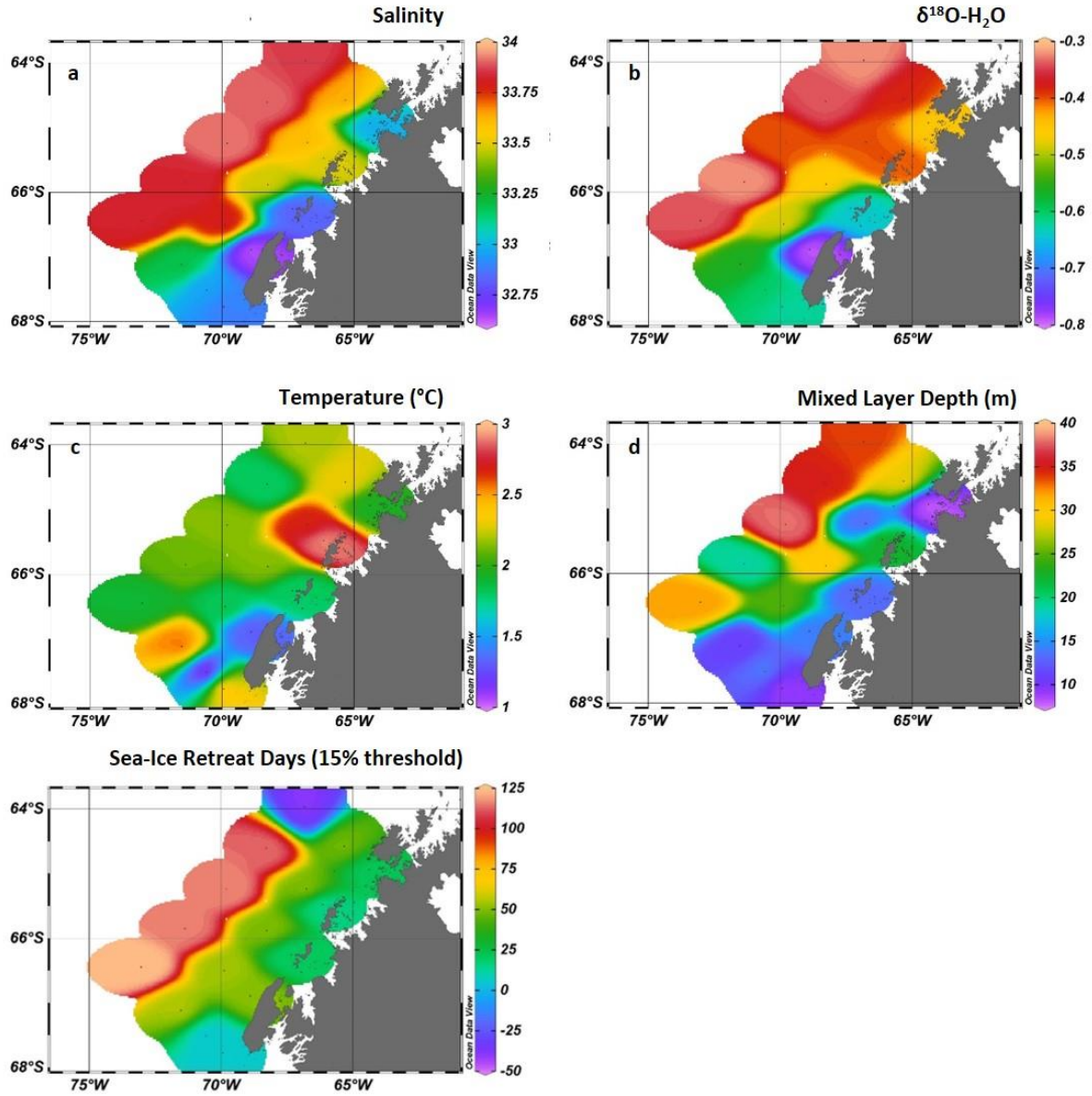

Figure 5.3.2: Surface distribution of physical parameters across the PAL LTER sampling grid in January 2017. All parameters show a general trend of freshening (a salinity), increasing meteoric water influence (b $\delta^{18}O_{H2O}$), cooling (c temperature) and shallowing of the mixed layer depth (d) from North to South and from the offshelf to coastal region.

The RaTS site shows a freshening of the surface waters in all three seasons starting between early December and January in the surface and developing to greater depths over time (figure 5.3.3). At the same time, temperatures increase in a similar manner. All three years show short intervals of fresher and warmer water for a short period of time which coincide with a higher contribution of the sea-ice meltwater fraction ($\delta^{18}O_{seaice}$) which is calculated from the $\delta^{18}O$ composition of the ambient water. On average, 2015/16 surface waters are colder than the other two seasons, figure 5.3.3.

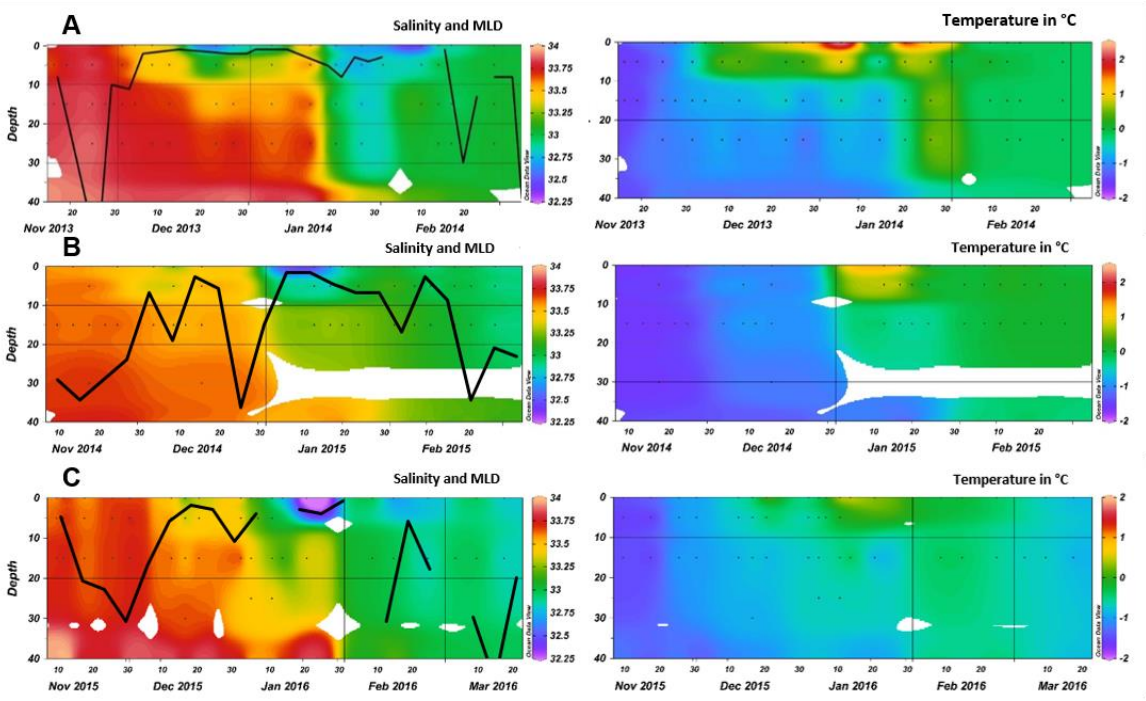

Figure 5.3.3: Contour plots of salinity and temperature development over time at the RaTS sampling site in (a) 2013/14, (b) 2014/15 and (c) 2015/16. The salinity plots show the mixed layer depth in meters.

5.3.3 Inorganic Nutrients and Phytoplankton.

Nitrate concentrations in the PAL LTER region average 33.21 ± 1.00 µmol N L^{-1} at depth > 200m. In the upper 100m, nitrate concentrations are more variable ranging from 0.77 to 33.88 µmol N L^{-1}. Highest nutrient uptake occurs in the coastal region decreasing with distance from the shore (figure 5.3.4). Among the coastal stations, nitrate is more depleted in the South than the North. The distribution of phosphate in the surface waters is similar. N:P uptake ratios in the surface waters range from 11.2 to 16.0 with less variation and ratios closer to the Redfield ratio in the South than the North. Lowest Si:N uptake ratios are found in the coastal region (0.7 – 1.0) and highest in the open ocean region (1.5 – 3.8).

The RaTS data show well-mixed water prior to the onset of freshening and sea-ice melt in all three seasons which is reflected in vertically uniform nutrient concentrations (Figure 5.3.6). In 2013/14, November nitrate averages 28.24 ± 1.71 µmol N L^{-1}, and 26.50 ± 0.70 µmol N L^{-1} in 2014/15. Nitrate is drawn down close to depletion in 2013/14 during the first phytoplankton bloom in the surface waters. During the second phytoplankton bloom, the drawdown of nitrate continues to greater depths (25m) than during the first bloom. NO_3^- concentrations recover after the second bloom in late February but remain below 20 µmol N L^{-1}. 2014/15 data show NO_3^- drawdown in the upper 15m between late December and mid-January during which surface concentrations approach depletion. In 2015/16, nitrate concentrations do not reach depletion, lowest concentrations are around 10 µmol N L^{-1}. The whole water column shows a decrease in NO_3^- concentrations to values around 15 µmol N L^{-1} with the onset of the phytoplankton bloom mid-January which remain until the end of March.

NH_4^+ concentrations are highly variable between years in the RaTS data set (figure 5.3.6). In 2013/14 maximum concentrations of NH_4^+ in the upper 15 m do not exceed 3 µmol N L^{-1}, in 2014/15, maximum concentrations are 1.4 µmol N L^{-1} (at 40 m) and

in 2015/16, maximum concentrations are 6.56 µmol N L^{-1} (at 15 m but data are available for upper 40 m). Ammonium concentrations are higher throughout the water column in 2015/16. Due to the high interannual and seasonal variability, [NH_4^+] for 40 m in 2013/14 have not been interpolated. However, both 2013/14 and 2014/15 data show a trend of NH_4^+ accumulation over time at all depths so that [NH_4^+] at 40m in 2013/14 can be expected to show a similar trend. Therefore, DON concentrations at 40m in January can be expected to comprise between 1 and 2 µmol N L^{-1} from NH_4^+ and in February, the NH_4^+ contribution to DON might have increased to approximately 2-3 µmol N L^{-1}. In 2015/16, NH_4^+ concentrations are < 1.00 µmol N L^{-1} at the beginning of the phytoplankton bloom in early January and remain high thereafter. Both 2013/14 and 2014/15 only show increased values (> 1 µmol N L^{-1}) later in the season (late January to early February). In 2014/15, these high concentrations only occur at the 40 m sampling interval.

HPLC analysis shows diatom dominance (> 80 %) for all three seasons with other species being present (figure 5.3.5). Haptophytes are the second-largest contributor in the pigment assemblage followed by cryptophytes. In the late 2015/16 bloom, cryptophytes dominate the phytoplankton species composition with a contribution of 40-60 %. There are no HPLC data available for the PAL LTER data set.

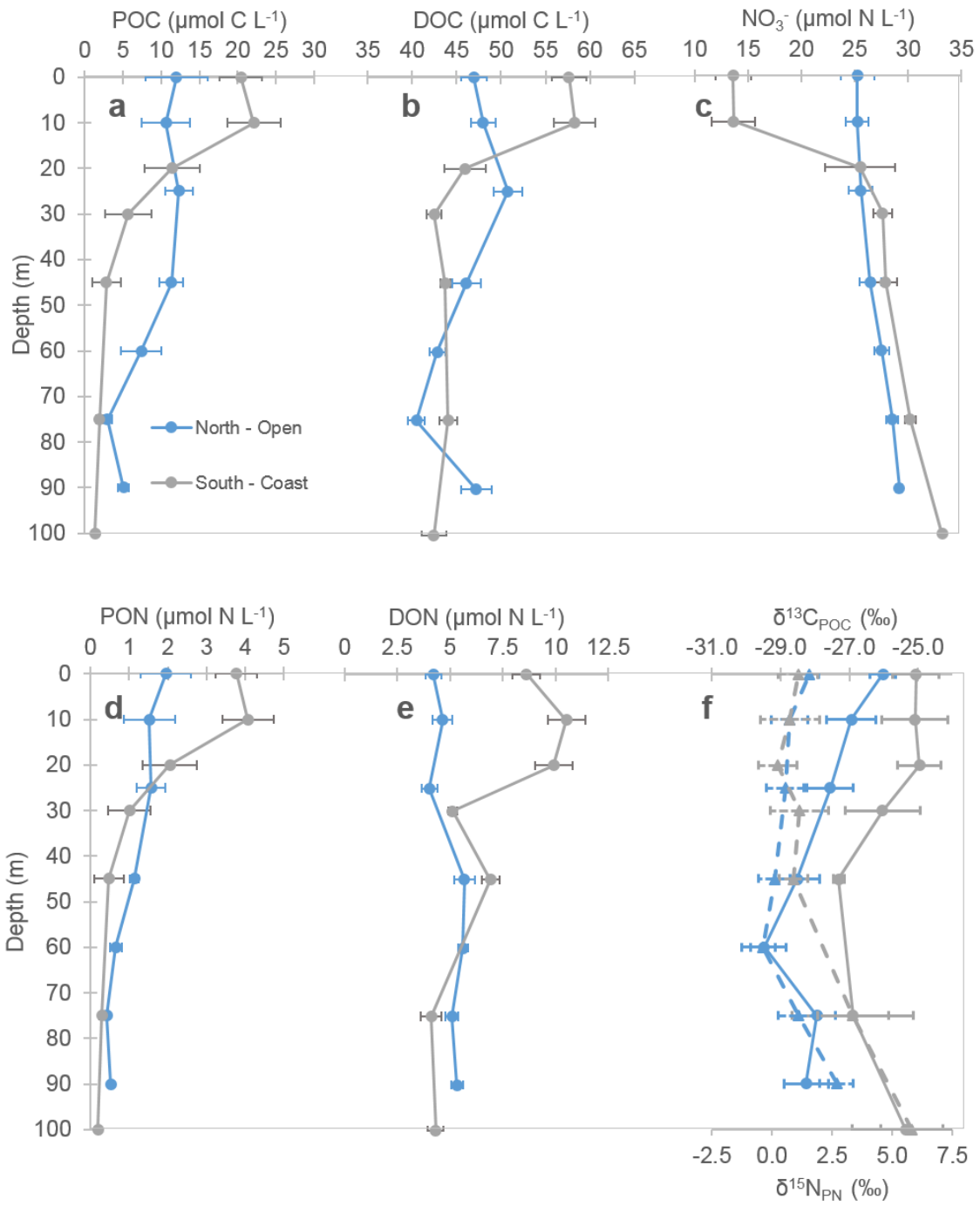

Figure 5.3.4: Biogeochemical parameters of two example sampling stations from the PAL LTER 2017 research cruise to show spatial heterogeneity. "North-Open" is station 500.200 and "South-Coast" station 200.000. (a) POC concentrations, (b) DOC concentrations, (c) nitrate concentrations. (d) PN concentrations, (e) DON concentrations and (f) C- and N-isotopic composition of POM. Solid lines show $\delta^{13}C_{POC}$, dashed lines indicate $\delta^{15}N_{PN}$. Error bars show the standard errors for all Northern / Southern stations, respectively.

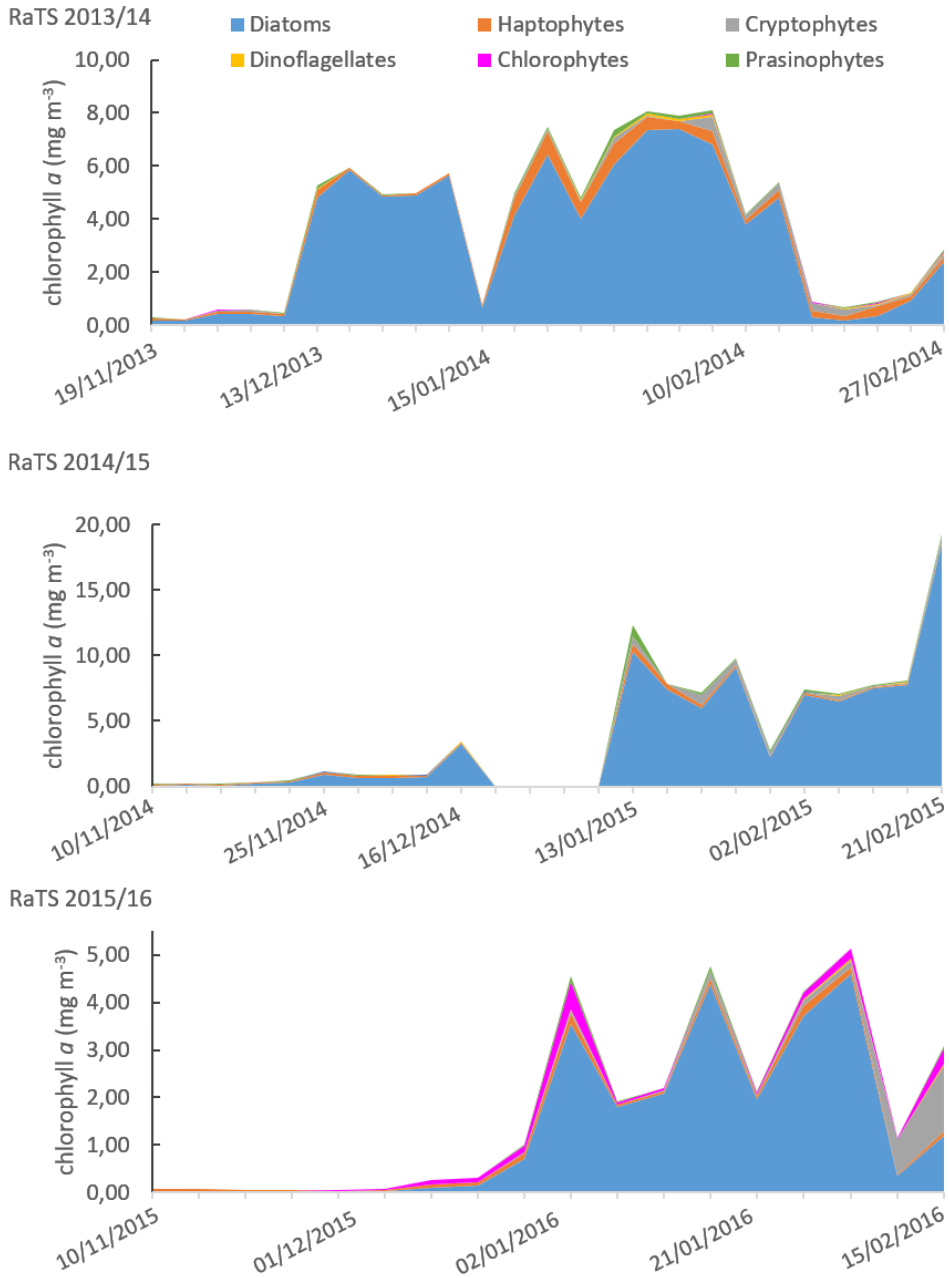

Figure 5.3.5: Phytoplankton pigmentation data from HPLC analysis as % of chlorophyll a concentration for the RaTS seasons measured at 15m depth. Please note the different scales along the y-axes.

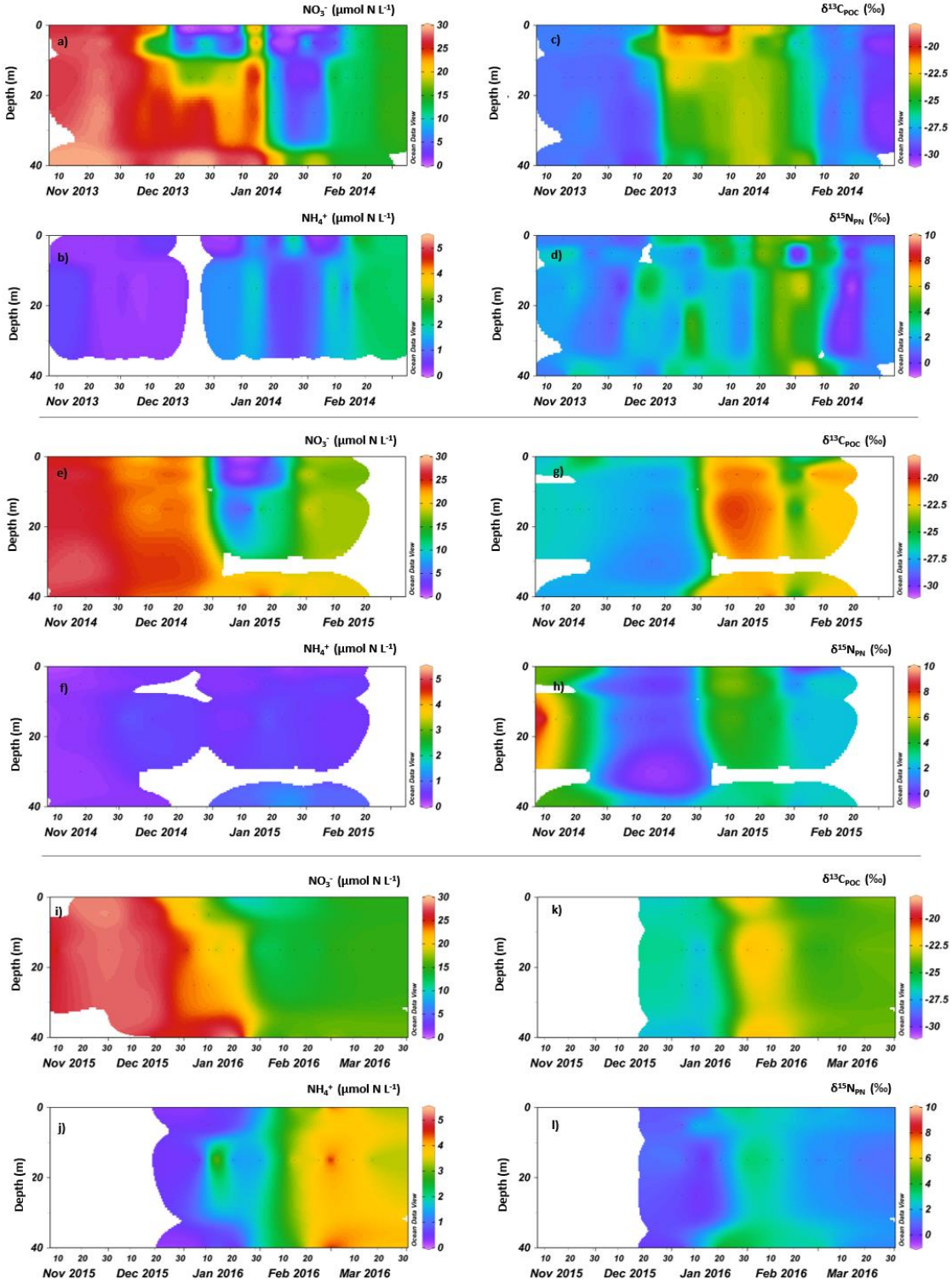

Figure 5.3.6: a-d nitrate and ammonium concentrations, $\delta^{13}C_{POC}$ and $\delta^{15}N_{PN}$ isotopic composition for 2013/14. e-h nitrate and ammonium concentrations, $\delta^{13}C_{POC}$ and $\delta^{15}N_{PN}$ isotopic composition for 2014/15. I-l nitrate and ammonium concentrations, $\delta^{13}C_{POC}$ and $\delta^{15}N_{PN}$ isotopic composition for 2015/16.

5.3.4 Particulate organic matter at the WAP

POC and PN concentrations show similar patterns at all LTER sampling grid stations with highest concentrations at the surface and an overall decrease with depth (figure 5.3.4). Except for stations 500.200, 600.200 and 600.100, stations that are northernmost and furthest from the coast, C:N ratios of POM in the upper 15 m are mostly below Redfield with a mean of 6.47 ± 0.37. Maximum POC and PN concentrations are always found at high chlorophyll-*a* concentrations, however, they are not always at the same depth as the maximum chlorophyll-*a* concentration. See table 5.3.1 for a summary of POC and PN concentrations and the POC:N ratios for the PAL LTER and RaTS data.

The RaTS POM data show a clear seasonal development with low POC and PN concentrations at the beginning of the season which start to increase with the onset of primary production. There is a short phase during the first phytoplankton bloom in 2013/14 in the upper 15m during which the POC:N ratio shows an increase to 11.8. Except for this short phase, POC:N ratios remain within a small range from 4.96 to 6.71.

In 2014/15, there is tight coupling between POC and PN throughout the pre-bloom and peak-bloom phase. The POC:N ratio remains within a small range below the Redfield ratio (5.10-6.48) throughout the observational period in the upper 15m. Maximum concentrations of POC and PN consistently occur at the same depth.

In 2015/16, the pre-bloom phase was not captured but organic matter samples are available from the first phytoplankton bloom onwards. The overall range of the POC:N ratio in the upper 15m is lower than in the previous two seasons ranging from 4.5 to 6.2. POC and PN maxima are consistently at the same depth.

Table 5.3.1: Maximum, mean and standard deviation for POC and PN concentration and the range, mean and standard deviation for the POC:N ratio for the PAL LTER 2017 data and the RaTS seasons 2013/14, 2014/15, 2015/16.

	POC (µmol C L^{-1})			PN (µmol N L^{-1})			POC:N		
	Max	Mean	SD	Max	Mean	SD	Range	Mean	SD
LTER	98.62	11.87	15.2	16.8	1.83	2.64	5.91 – 38.09	9.37	4.59
2013/14	166.26	24.25	27.2	18.8	3.83	3.6	4.67 – 11.76	5.93	1.16
2014/15	71.42	16.54	16.7	12.1	2.96	2.94	4.60 – 7.64	5.73	0.54
2015/16	43.39	20.84	10.1	8.12	4.01	1.98	4.42 – 7.22	5.27	0.52

5.3.5 $\delta^{13}C$ and $\delta^{15}N$ in POM and $\delta^{15}N$ in nitrate

Figure 5.3.7 shows surface $\delta^{15}N_{NO3}$, $\delta^{15}N_{PN}$, $\delta^{13}C_{POC}$ and nitrate concentrations during the PAL LTER 2017 cruise. Lowest nitrate concentrations are found along the coast with nitrate almost being depleted at 300.040. This pattern is reflected in the isotopic data for both C and N with highest isotopic enrichment of nitrate and POM at the coast and particularly at station 300.040.

RaTS surface $\delta^{13}C_{POC}$ and $\delta^{15}N_{PN}$ increase with the onset of phytoplankton production in all three seasons. $\delta^{13}C_{POC}$ reflects the extent of POM production more closely than $\delta^{15}N_{PN}$. The N-isotopic composition of PN shows higher variability before and during the phytoplankton blooms than $\delta^{13}C_{POC}$ (Figure 5.3.8, 5.3.9, and 5.3.10).

$\delta^{13}C_{POC}$ in Ryder Bay covers a range from -30.3 ‰ to -18.9 ‰ in all three seasons with 2013/14 showing the greatest variability. With the onset of POM accumulation, $\delta^{13}C_{POC}$ in the surface quickly increases from values around -28 ‰ to values between -18.9 and -22.5 ‰. With the onset of the second bloom, $\delta^{13}C_{POC}$ values drop back to values between -27.6 and -29.3‰. A similar pattern occurs at 15m depth while $\delta^{13}C_{POC}$ increases to values between -22.2 and -23.6‰ and the C-isotopic

composition decreases later during the second bloom. The same pattern of an increase in $\delta^{13}C_{POC}$ with increasing POC concentrations and a drop towards the end of phytoplankton bloom conditions is also observable in 2014/15 and 2015/16 data.

$\delta^{15}N_{PN}$ and $\delta^{13}C_{POC}$ in all three seasons show similar trends over time, however, $\delta^{15}N_{PN}$ shows more variability. While $\delta^{15}N_{PN}$ also starts to increase with increasing POM concentrations from values between 0.50 and 1.50 to 3.00 - 5.40 ‰ in the surface during the first phytoplankton bloom in 2013/14, it shows some excursions prior to the bloom and also during the peak bloom. In the second bloom, $\delta^{15}N_{PN}$ values are slightly higher than in the first but drop quickly in mid-February to values between -0.40 and +0.70‰. First measurements in the 2014/15 season show high $\delta^{15}N_{PN}$ (10.2‰) which decrease until early December (0.7‰). $\delta^{15}N_{PN}$ increases again with the onset of primary production and decreases after the bloom. In 2015/16, $\delta^{15}N_{PN}$ closely follows the trend of PN concentrations with only minor deviations.

In the upper 40m of the PAL LTER data set, variability of both $\delta^{13}C_{POC}$ and $\delta^{15}N_{PN}$ is highly heterogeneous (figure 5.3.4 f). Only at deeper depths, POC and PN become isotopically heavier. The depths below which the C- and N-isotopic compositions become heavier, decrease from open to shore. Among the open ocean stations, the mean depth for $\delta^{15}N_{PN}$ is 60 m which decreases to 25m along the coast whereas $\delta^{13}C_{POC}$ starts to become heavier at depths of 60 m in the open and 45m at the coastal stations.

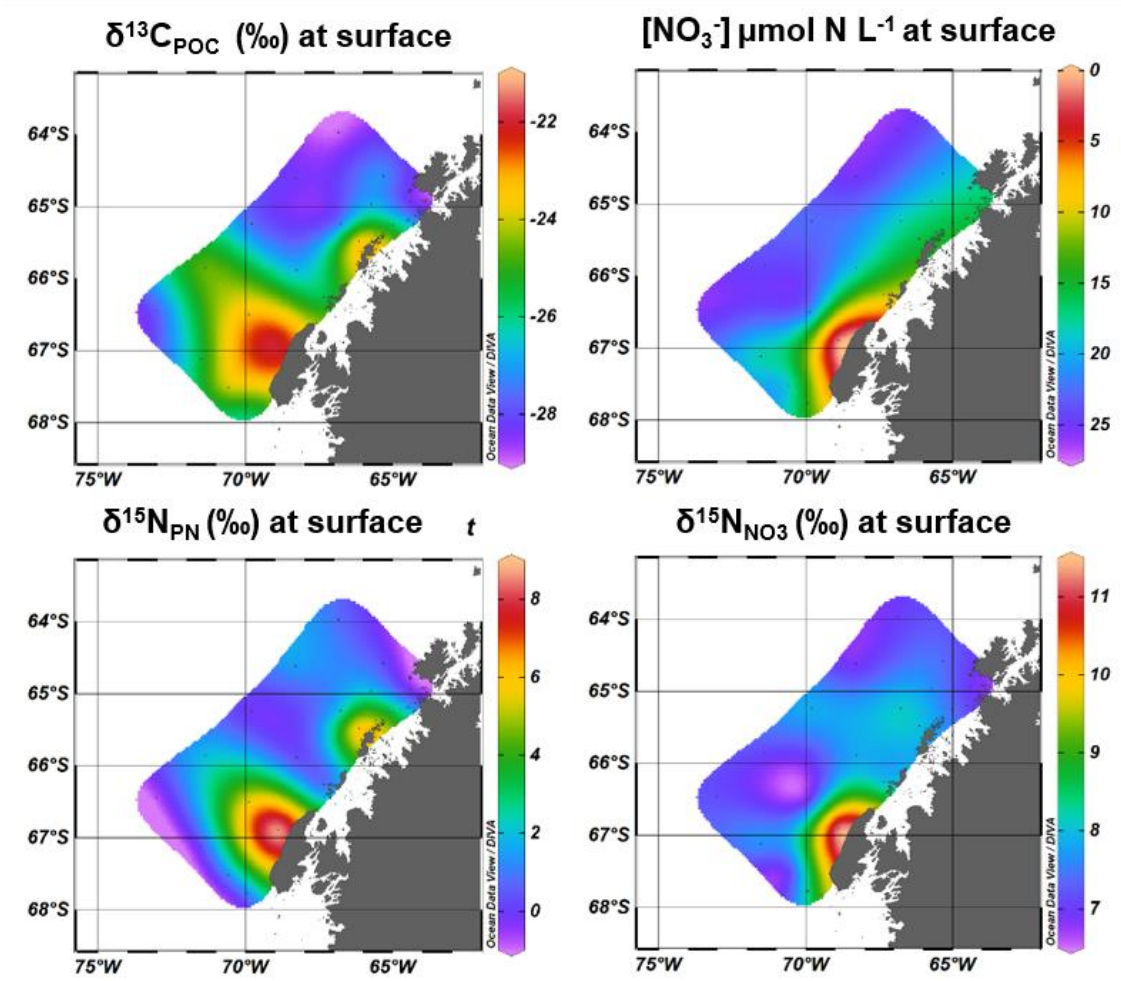

Figure 5.3.7: Surface water C and N isotopic composition of POM, nitrate concentrations (plotted in reversed colour pattern) and the N-isotopic composition of nitrate from PAL LTER cruise 2017.

In order to understand biogeochemical processes shown in the N-isotopic data, $\delta^{15}N_{PN}$ and $\delta^{15}N_{NO3}$ (only available for 2013/14), their respective concentrations and $\delta^{13}C_{POC}$ and [POC] were averaged in the upper 15 m of the water column in Ryder Bay (figure 5.3.8, 5.3.9, and 5.3.10). $\delta^{15}N_{NO3}$ increases with the drawdown of NO_3^- in the upper ocean and responds to changes in nitrate concentrations throughout the season. At the beginning of the sampling period in 2013/14, $\delta^{15}N_{NO3}$ is 5.29 ‰. $\delta^{15}N_{NO3}$ ranges from 5.29 to 8.57 ‰ over the entire sampling season and decreases towards the end when nitrate concentrations start to increase.

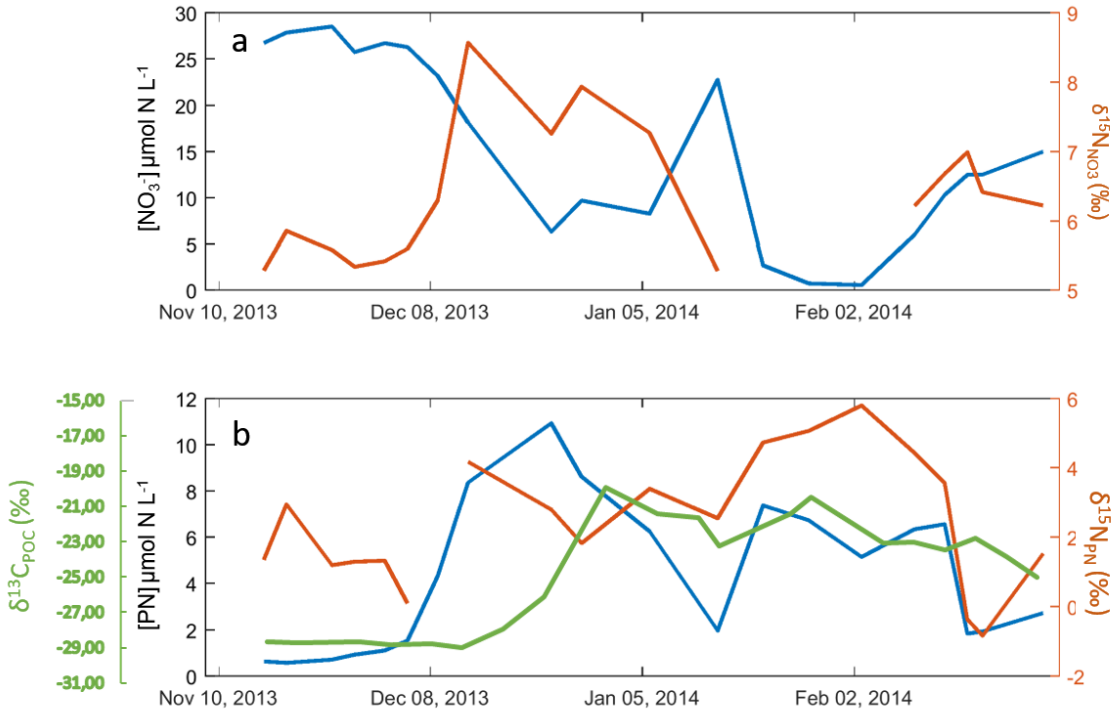

Figure 5.3.8: 2013/14 Upper 15m mean values for (a) [NO_3^-] and $\delta^{15}N_{NO3}$ and (b) [PN] (blue line), $\delta^{15}N_{PN}$ and $\delta^{13}C_{POC}$.

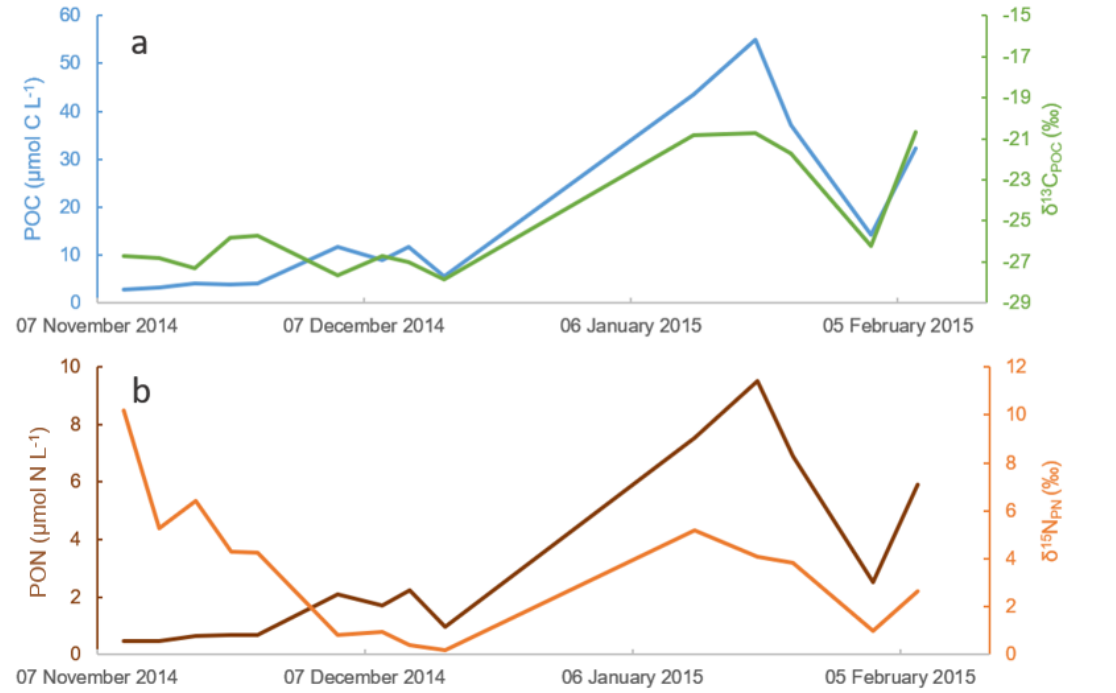

Figure 5.3.9: 2014/15 Upper 15m mean values for (a) [POC] and $\delta^{13}C_{POC}$ and (b) [PN] and $\delta^{15}N_{PN}$.

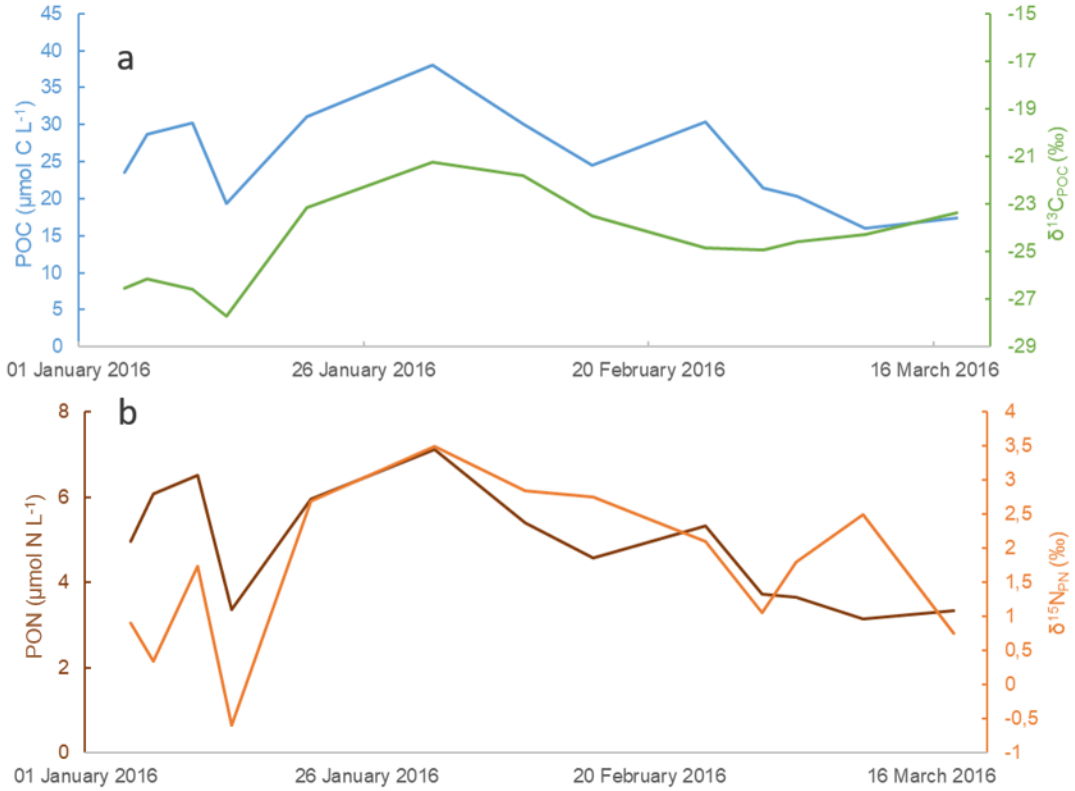

Figure 5.3.10: 2015/16 Upper 15m mean values for (a) [POC] and $\delta^{13}C_{POC}$ and (b) [PN] and $\delta^{15}N_{PN}$

5.3.6 Dissolved organic matter at the WAP

Ranges for DOC and DON concentrations and the DOC:DON ratio across the LTER grid and throughout the three sampled seasons at RaTS are stated in table 5.3.2. Highest DOC concentrations are usually found in the upper 20 m while DON maxima are distributed more variably and can occur at any sampled depth within the LTER sampling grid. The coastal stations 200.000, 300.040 and 400.040 show high DON concentrations in the surface waters.

At the RaTS site, DON concentrations are highly variable. Comparing the three RaTS seasons with the LTER grid, the RaTS site shows higher concentrations of DOC, however, the mean concentrations do not vary greatly between the seasons. Contrastingly, highest DON concentrations are found within the LTER area but again,

mean concentrations are within a narrow range. The DOC:DON ratios span a large range with the mean lying between 8.23 and 12.85 which is relatively low for DOM but ratios similar to this have been reported before for Antarctic regions (Kähler et al. 1997; Thomas et al. 2001, 2001 (b); Carlson et al. 2000).

Lowest DOC concentrations are mostly found at depths > 50 m and cover a narrow range from 38.13 to 42.27 µmol C L^{-1}. DON minima are mostly found at depths > 60m with the exceptions of stations 500.200 and 600.200 in the LTER sampling grid where DON minima are found in the upper 25m and DON maxima at 40 and 60m, respectively. All data presented here are listed in the appendix of the thesis.

Table 5.3.2: Range of DOC and DON concentrations and the DOC:DON ratio in direct comparison for PAL LTER and all three RaTS seasons.

	DOC (µmol C L^{-1}) Range	DON (µmol N L^{-1}) range	DOC:DON Range
LTER	38.13 - 60.47	1.70 - 10.52	5.34 - 37.90
2013/14	40.36 - 88.65	3.38 - 10.13	4.16 - 18.09
2014/15	40.88 - 79.66	4.39 - 7.26	6.07 - 11.69
2015/16	42.27 - 71.00	1.14 - 6.56	4.99 - 43.16

5.4 Discussion

The WAP encompasses a physically complex and environmentally dynamic ecosystem which is reflected in the data presented here and has been discussed in previous studies (e.g. Moreau et al. 2015; Trimborn et al. 2015; Arrigo et al. 2017; Ducklow et al. 2013). Increasing available solar radiation and retreating sea ice in spring lead to the onset of primary production as shown in the RaTS seasonal data. The PAL LTER data show the variability of biogeochemical dynamics across the entire sampling region west of the Antarctic Peninsula. The WAP hydrography is strongly influenced by freshwater input from glacial sources and sea ice so that freshest surface waters and consequently shallowest mixed layers are found in the coastal regions. In agreement with this spatial development are the RaTS temporal data showing a freshening and warming of the surface waters between early and late December each year which leads to a shallowing of the mixed layer and the onset of primary production. Increasing nutrient drawdown, chlorophyll-*a* and organic matter concentrations are the result.

The focus of the following discussion will be on the dynamics of particulate and dissolved organic carbon and nitrogen on varying spatial and temporal scales.

5.4.1 Dynamics of particulate organic carbon and nitrogen in the PAL LTER sampling grid and at RaTS 2013-2016

Within the PAL LTER sampling grid, primary production started earlier in the open ocean due to the earlier sea-ice retreat here. Growth limitation by micronutrients in the open-ocean regions (Annett et al., 2015; Arrigo et al., 2017) and shallower mixed layer depths along the coast lead to rates of primary production and organic matter production being higher along the coast. Highest concentrations of POC and PN along

the WAP are found in the surface waters of station 300.040 where freshwater input from glacial sources is greatest which leads to fresher and cooler surface waters with a shallow mixed layer. Here, nitrate concentrations are close to depletion and chlorophyll-*a* concentrations are highest among all sampled stations.

POC and PN decrease with depth at every station. However, all open-ocean stations and the northernmost shelf stations show a small increase in POM at depths > 30 m. Elevated chlorophyll-*a* concentrations, primary production rates and lower POC:N ratios indicate active phytoplankton blooms at depths > 30 m.

Gradients for NO_3^- and PN flux over the upper 50m were calculated to determine the amount of nitrate converted to PN:

$$\Delta PN = \frac{\delta PN}{\delta z} \quad \text{and} \quad \Delta NO_3^- = \frac{\delta NO_3^-}{\delta z}$$

The arithmetic mean of the ratio of $\Delta PN:\Delta NO_3^-$ in the entire sampling region is -0.38 ± 0.22 which shows that on average 38% of nitrate drawdown is due to PN formation in the upper 50m. It is important to keep in mind that the calculated PN gradient does not only show PN formation in the upper 50m but also includes the terms of remineralisation processes (DON formation, nitrification), and grazing so that the PN gradient includes terms of PN formation, recycling and export in the upper 50m. The ratios range from -0.02 to -0.70 demonstrating the high variability of the WAP system (table 5.4.1). Highest $\Delta PN:\Delta NO_3$ ratios are generally found in the North, and lowest in the South with an overall decrease from coastal stations to the open. A strong correlation of the vertical gradients of nitrate and PN shows that the combination of accumulation and loss of biomass is accompanied by increased NO_3^- drawdown as expected (figure 5.4.1). As the $\Delta PN:\Delta NO_3$ ratio indicates and as figure 5.4.1 shows, NO_3^- drawdown is not perfectly balanced by POM accumulation. This correlation and the above mentioned relatively low contribution of PN to nitrogen export show that

other processes such as transfer to higher trophic levels, export and conversion to DON with subsequent ammonification play important roles in the WAP nitrogen cycle.

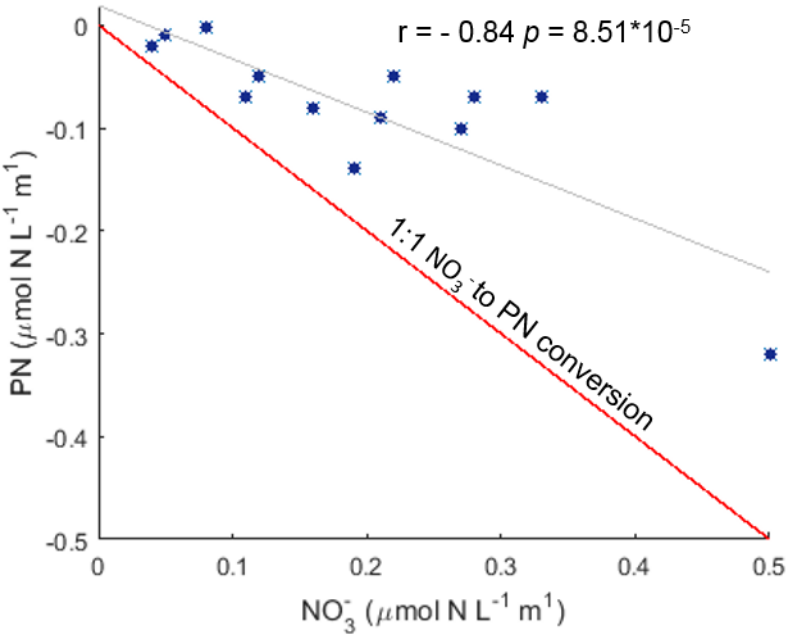

Figure 5.4.1: The good correlation between the gradients over the upper 50m for NO_3^- and PN shows that high NO_3^- drawdown is accompanied by high PN accumulation. Data along the 1:1 line would indicate high export production while the data points shown here indicate other processes such as high recycling and PN uptake in the upper ocean.

POC:N ratios in the upper 30 meters of the PAL LTER grid are close to the Redfield C:N ratio of 6.625 with a decreasing trend southward. Among almost all stations of the Southern part of the sampling grid, POC:N ratios are lower than the Redfield C:N ratio. The low ratios close to Redfield indicate direct production of POM by phytoplankton. This is also supported by the strong correlation between chlorophyll-*a* and POC and PN in the surface waters (POC ~ chlorophyll-*a* r = 0.91, $p = 2.19*10^{-6}$, PN ~ chlorophyll-*a* r = 0.94, $p = 3.01*10^{-7}$). Reasons for decreasing C:N ratios with an increase in latitude have been suggested to be changing physical conditions such as surface water temperatures and nutrient availability which results in changing phytoplankton compositions with varying nutrient demands. Young et al. (2015)

showed that in order to maintain high rates of photosynthesis in colder waters, diatoms have to produce more RuBisCO, the central enzyme necessary for photosynthesis, because water temperatures in high latitudes are often below optimal conditions for enzyme activity. This leads to a substantially increased protein content in Antarctic diatoms which, due to the high nitrogen content of proteins, leads to a decrease in the C:N ratio. The physical parameters available for the LTER 2017 research cruise (temperature, salinity, $\delta^{18}O$) show a latitudinal trend of decreasing temperature and increasing influence of glacial meltwater from North to South and open ocean to coast (figure 5.3.2) which supports the hypotheses for decreasing POC:N ratios with decreasing temperatures.

Table 5.4.1: vertical gradients of NO_3^- and PN in µmol N m^{-1}between the surface and 50 m depth and the ratio of $\partial PN/\partial NO_3^-$.

Station	ΔNO_3	ΔPN	$\Delta PN:\Delta NO_3$
600.200	0.05	-0.01	-0.12
600.100	0.12	-0.05	-0.43
600.040	0.27	-0.10	-0.36
500.200	0.04	-0.02	-0.60
500.100	0.21	-0.09	-0.46
500.060	0.19	-0.14	-0.70
400.200	0.11	-0.07	-0.67
400.100	0.16	-0.08	-0.51
300.200	0.08	0.00	-0.02
300.100	0.12	-0.05	-0.40
300.040	0.50	-0.32	-0.65
200.200	0.05	-0.01	-0.12
200.100	0.33	-0.07	-0.23
200.040	0.22	-0.05	-0.21
200.000	0.28	-0.07	-0.24

The RaTS data agree with the observations from the PAL LTER data set. Because the seasons 2014/15 and 2015/16 do not cover the entire spring/summer season, which might skew the mean POC:N ratio, POC:N ratios were compared only where chlorophyll-*a* concentrations > 1 mg m^{-3} in the upper 15 m. Through all three investigated seasons, the seasonal POC:N ratio arithmetic means in the upper 15 m are 7.52 in 2013/14, 5.70 in 2014/15 and 4.65 in 2015/16. The 2013/14 ratio is only higher than the Redfield ratio due to a short period of high ratios in the surface waters during the first phytoplankton bloom peak.

POC and PN are tightly coupled in all three seasons. There is a trend of decreasing ratios between the seasons which agrees with a trend of decreasing mean water temperature. While the C:N ratios in 2013/14 and 2014/15 are not significantly different (T-Test, t = 1.487, $p > 0.05$), 2015/16 is significantly different from 2013/14 (T-Test t = 4.067, $p = 1.07*10^{-4}$) and 2014/15 (T-Test, t = 4.221, $p = 9.38*10^{-5}$). This agrees with the observed temperature differences between the seasons in the upper 15m with no significant difference between 2013/14 and 2014/15 ($p > 0.05$) while both of those seasons differ significantly from 2015/16 (2013/14 vs. 2015/16 T-test, t = 3.07, $p = 0.003$; 2014/15 vs. 2015/16 T-test t = 3.04, $p = 0.003$). This decrease in C:N ratios can be caused by aforementioned increased RuBisCO production with decreasing temperatures, a change in phytoplankton species composition or a combination of both. The phytoplankton species composition between years varies slightly with 2015/16 again being the season which is significantly different from 2013/14 and 2014/15 (diatom fraction 2013/14 vs. 2014/15 $p > 0.05$, 2013/14 vs. 2015/16, t = 2.38, $p = 0.024$; 2014/15 vs 2015/16 t = 2.46, $p = 0.019$). Even though Young et al.'s study focused on diatom RuBisCO production, this enzyme is produced by all photosynthesising organisms so that a combination of these two factors is suggested to play a role in the changing C:N ratios found in these three seasons.

In 2013/14, POC and PN maxima are at the same depth most of the time. DOC maxima consistently coincide with POC maxima when POC and PN are decoupled which does not occur as often when POC and PN show good coupling. This could be an indication that POM is the major source for DOM which would lead to observed decoupling processes. Due to the preferred breakdown of nitrogen over carbon, the maximum concentrations of PN are found at shallower depths than POC as PN is being degraded at shallower depth with subsequent dissolved organic matter production.

During all three seasons, only a few samples were collected at depth > 40 m. All those samples show an increased POC:N ratio compared to the ratios at the shallower depths, however, most of them remain below Redfield at depth of 75 or 100 m. While those samples are not representative for all seasons, the C:N ratio close to the Redfield ratio suggests fresh POM sinking quickly to greater depths.

5.4.1.1 Nutrient utilisation and POM cycling shown by $\delta^{13}C$ of POC and $\delta^{15}N$ of PN and NO_3^-

The N-isotopic composition of NO_3^- and PN show high variability. In Figure 5.4.2 the modelled values for both the instantaneous and the accumulated product are calculated with two different isotope effects (4 and 5 ‰). There is a clear difference in the PAL LTER data set between the open, shelf and coastal stations in the N-isotopic signatures for both NO_3^- and PN (figure 5.4.2).

The PN signal along the coast shows highest variability. $\delta^{15}N_{PN}$ slightly below modelled accumulated values and generally below 3 ‰ are found for the southernmost stations 200.000 and 200.040 as well as the northernmost station 600.040. At all these stations, the phytoplankton signal is relatively low which is represented in high fractionation of nitrogen. Stations 300.040 and 500.060 show

$\delta^{15}N_{PN}$ closely around the modelled instantaneous product. Both stations show high rates of chlorophyll-*a* and primary production, respectively, which rapidly decrease with depth. The $\Delta PN:\Delta NO_3^-$ calculations (section 5.4.1) showed most intense conversion of nitrate to PN at these two stations (65 and 70% for 300.040 and 500.060, respectively) with the most intense PN gradient in the upper 50m (0.32 and 0.14 for 300.040 and 500.060, respectively). The comparatively high N-isotopic composition of PN closely following the instantaneous product confirms intense nitrogen cycling at these stations with remineralisation removing ^{14}N preferentially and leaving PN with a heavier $\delta^{15}N$ signature. $\delta^{15}N_{PN}$ at the shelf and open-ocean stations are mostly around and below values of the accumulated product and clustered together more closely than the coastal stations pointing out the high variability along the coast in this year and potentially in general. These open ocean stations are past the peak of the phytoplankton bloom which is reflected in low-productivity $\delta^{15}N_{PN}$. The N-isotopic composition of PN is likely decreased at these stations because they are at a later stage during the progression of the phytoplankton bloom which allows for higher rates of ammonium consumption. Ammonium is a product of remineralisation of ambient PN, so that $\delta^{15}N_{NH4+}$ can be assumed to be equal or lower than that of PN. Ammonium is incorporated by phytoplankton with a kinetic isotope effect between 4 and 20 ‰ (Waser et al. 1998; Sigman and Casciotti 2001; Sigman et al., 2009). A late-bloom progression in the phytoplankton species composition to a dominant smaller species which is more efficient in ammonium uptake could further this fractionation effect.

Among all available PAL LTER surface isotopic N data, there is a clear trend of an increase in the apparent fractionation factor (or kinetic isotope effect) ε from the coast (2.12 ‰) to the open (5.49 ‰). The lower fractionation factor along the coast indicates

more intense nitrification occurring in these waters which likely leads to these low values.

The RaTS data show a similar pattern in all three seasons with $\delta^{15}N_{PN}$ closely following Rayleigh PN accumulation. The $\delta^{15}N_{PN}$ shows accumulation and remineralisation of PN in surface waters indicating only little export of PN from the surface waters of Ryder Bay. These data agree with the interpretation of the calculated PAL LTER $\Delta PN:\Delta NO_3^-$ ratios in section 5.4.1 and show that the majority of PN is recycled in the upper ocean with little direct export. High recycling and nitrification have been shown to be a substantial source of recycled nutrients in the surface waters of the WAP (Henley et al., 2018) resupplying the surface waters with nutrients during the austral summer. Henley et al.'s study is based on inorganic nutrient stoichiometry and inorganic nitrate isotopic data only. This study confirms those findings utilising the isotopic composition of both inorganic nitrate and organic nitrogen.

The RaTS $\delta^{15}N_{NO3}$ values lying along the modelled values of closed-system nitrate dynamics are all in pre-bloom conditions in which nitrate concentrations are high and PN production at a minimum (Figures 5.3.8, 5.3.9, 5.4.2b). With the onset of the phytoplankton bloom, $\delta^{15}N_{NO3}$ shows only little variation even though fractionation would be expected with a fractionation factor of 4-5 ‰. The lower-than-modelled $\delta^{15}N_{NO3}$ composition indicates high rates of NH_4^+ uptake and nitrification in Ryder Bay. Nitrified nitrate is the product of remineralisation of organic matter. Because $\delta^{15}N_{PN}$ formed from CDW-nitrate is lower due to the kinetic fractionation, nitrified nitrate, which ultimately originates from low $\delta^{15}N_{PN}$ will undergo additional kinetic fractionation and show $\delta^{15}N$ equal to or less than that of its source PN. Nitrification was previously shown to play a significant role for upper-ocean biogeochemical cycling in Marguerite Bay (Henley et al., 2018, 2017). This new study indicates nitrification occurring and

affecting N cycling during phytoplankton blooms. Rapid ammonification of DON (section 5.4.2) in combination with these isotopic data strongly support these findings.

In Ryder Bay in 2013/14, N-rich surface water is present at the beginning of the growing season with $[NO_3^-] > 25$ µmol N L^{-1}. In these waters, $\delta^{15}N_{PN}$ reflects the result of minor nitrate assimilation during minimal primary production with lowest values in surface waters which increase with depth mirroring PN concentrations. Nitrate assimilation over time drives the temporal increase in $\delta^{15}N_{PN}$ throughout the season while the nitrate pool is becoming depleted (figure 5.4.3 A). Lower $\delta^{15}N_{PN}$ coincide with increased nitrate concentrations indicating replenishment of nitrate from mixing (figure 5.4.3 i and ii). Simultaneous sudden changes in salinity and temperature also suggest nitrate replenishment through vertical mixing. With the end of the phytoplankton growing season and the recovery of surface nitrate stocks, both PN concentrations and $\delta^{15}N_{PN}$ recover back to values similar to values prior to the growing season (figure 5.4.3 iii).

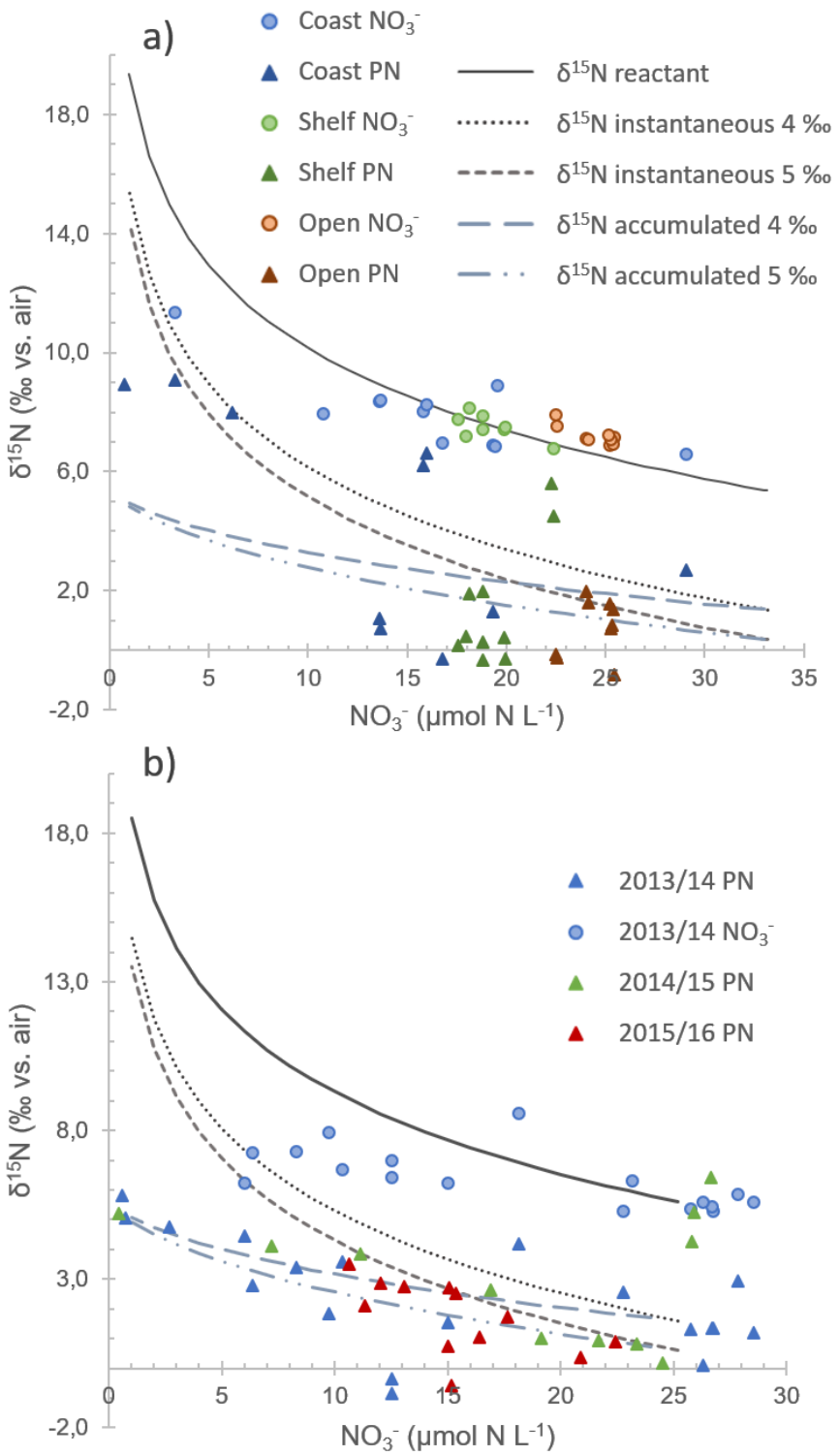

Figure 5.4.2: The N isotopic composition of particulate nitrogen and nitrate of the surface waters of a) the PAL LTER sampling grid and b) the RaTS seasons. RaTS nitrate data only available for 2013/14. The lines in both a) and b) represent the fractionation of the residual nitrate ($\delta^{15}N$ reactant), of the instantaneous product with an isotope effect of 4 and 5, respectively ($\delta^{15}N$ instantaneous) and of the accumulated product with an isotope effect of 4 and 5, respectively ($\delta^{15}N$ accumulated) following closed-system dynamics (Rayleigh).

Isotopic data for 2014/15 are scarce. The available $\delta^{15}N_{PN}$ at the start of the sampling period is high despite negligible primary production (Figure 5.3.9). Sea-ice cover is still high at this point (sea-ice scores between 5 and 8). The elevated $\delta^{15}N_{PN}$ could indicate PN being formed from sea-ice derived nitrate which usually carries a higher $\delta^{15}N$. POM being produced in sea ice, just as in the water column, preferentially incorporates the lighter ^{14}N leaving nitrate high in $\delta^{15}N$. However, in sea ice, the residual isotopically heavy NO_3^- is expelled from the sea ice through brine convection and enters the surface waters leaving.

$\delta^{13}C_{POC}$ does not show increased values reflecting the different turnover times of carbon and nitrogen and the different processes involved for each element in sea ice. The phytoplankton-species assemblage and the preferred CCM of the dominant species is indicative of changes in the C-isotopic composition (Henley et al., 2012). With the onset of the phytoplankton bloom, $\delta^{13}C_{POC}$ increases by 8 ‰ and only decreases again during the second bloom. Diatoms dominate the entire duration of bloom conditions, however, a shift in the dominating diatom species can be the reason for the substantial decrease in $\delta^{13}C_{POC}$ in mid-bloom conditions (Henley et al., 2012; Sinninghe Damsté et al., 2003). There are no specific species data available for the investigated seasons at the RaTS site, however, the diatom species *Proboscia inermis* has been shown to make up >90% of the late-season phytoplankton bloom in Ryder Bay between 2004 and 2007 (Annett et al., 2010). *P. inermis* are known for their production of ^{13}C-depleted alkanoates (Sinninghe Damsté et al., 2003) which could explain the substantial decrease in $\delta^{13}C_{POC}$ in mid-bloom conditions.

The short sampling period in 2015/16 shows an increase in $\delta^{15}N_{PN}$ along NO_3^- drawdown during the phytoplankton bloom indicating that the main driver of $\delta^{15}N_{PN}$ variability is nitrate utilisation. At the beginning of the growing season, there is a decrease in sea-ice cover and an increase in sea-ice melt which coincide with a shift

in $\delta^{15}N_{PN}$ which also occurs at the end of the growing season (figure 5.4.3 iv and v). The cycling of POM in sea ice is spatially restricted. Previous studies showed high variability of $\delta^{15}N_{PN}$ in sea ice but generally it is lowered (0 to 6‰.) compared to $\delta^{15}N_{NO3}$ (Fripiat et al., 2015). Above described expel and replacement of nitrate in sea ice with seawater nitrate of a lower $\delta^{15}N$ leads to a continuous decrease of sea ice $\delta^{15}N_{PN}$.

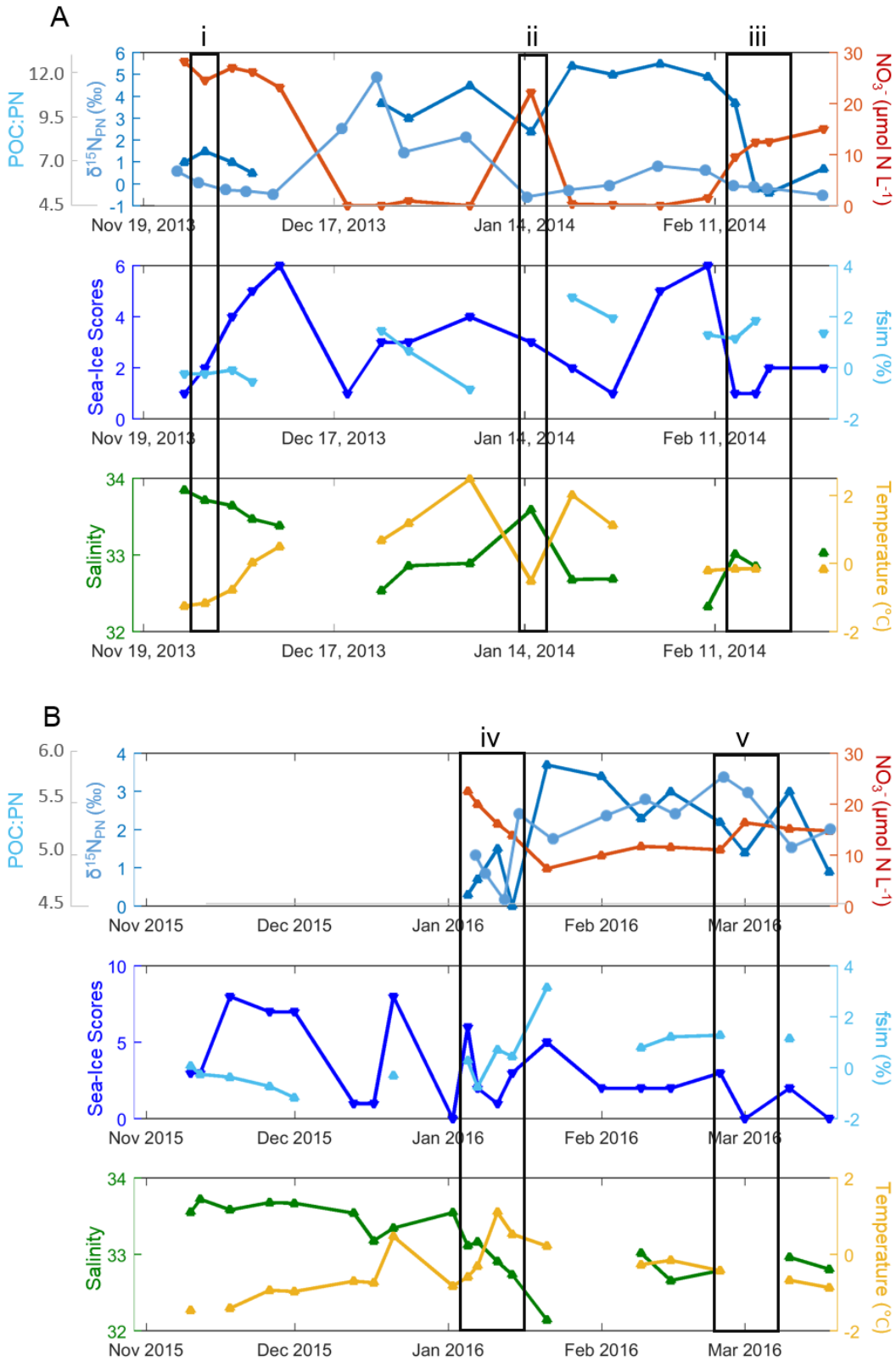

Figure 5.4.3: Surface measurements of [NO_3^-], $\delta^{15}N_{PN}$ (blue triangles), the POC:N ratio (light blue dots), sea-ice scores and the fraction of sea-ice melt, and temperature and salinity throughout the sampling seasons 2013/14 (A) and 2015/16 (B). 2014/15 is not shown here because of the restricted sampling period and gaps in measurements. The black boxes i-v are discussed in section 5.4.1.

The high variability in $\delta^{15}N_{PN}$ present in all four data sets (PAL LTER, RaTS 2013/14, 2014/15 and 2015/16) during phytoplankton bloom conditions shows the high variability of the system on spatial and temporal scales. While surface waters can be affected by sea-ice derived POM, shifts in $\delta^{15}N_{PN}$ at greater depths show the effect of preferential loss of the lighter isotope during remineralisation of organic matter with an offset in time. Both $\delta^{15}N_{PN}$ and $\delta^{13}C_{POC}$ show high variability in the upper 40m in all four data sets. While there is a limited number of data points for the RaTS site at depths > 40m, the PAL LTER data show that both $\delta^{15}N_{PN}$ and $\delta^{13}C_{POC}$ increase with increasing depths. At all PAL LTER stations, $\delta^{15}N_{PN}$ starts to increase at shallower depths than $\delta^{13}C_{POC}$ with an overall trend of decreasing depths from open-ocean to coast but no clear North-to-South trend. The earlier increase of $\delta^{15}N_{PN}$ plus the simultaneous decrease in PN concentrations are indicative of remineralisation processes with the preferential removal of (the isotopically lighter) nitrogen and is referred to as remineralisation depth intervals. The open-to-coast trend of decreasing depth of nitrate remineralisation from POM is likely due to increasing primary production and therefore bacterial activity towards the coast which leads to high rates of bacterial degradation of PN especially in the surface waters.

5.4.2 Dissolved organic carbon and nitrogen dynamics

The concentrations for both DOC and DON cover a small range in agreement with previous literature (Carlson et al., 1998; Kähler et al., 1997, Doval et al., 2002; Ducklow et al., 2012; Wang et al., 2010). Peak DOC concentrations occur alongside peak POC concentrations in two of the RaTS seasons. DOC:DON ratios in 2013/14 cover a wide range but are mostly close to the Redfield C:N ratio before the peak of the first phytoplankton bloom. After the first peak, there is an increase in both the DOC:DON ratios and their variability. In 2014/15, surface DOC:DON ratios are close

to the Redfield ratio while at 15 m, C:N ratios have a mean of 9.43. The DOC:DON ratios in 2015/16 are substantially higher in comparison with an arithmetic mean of 15.2 over the upper 40m. These high ratios are mostly due to consumption and rapid ammonification of DON which leads to concentrations below background.

Refractory dissolved organic matter remains in the deep ocean for thousands of years with relatively stable concentrations among all ocean basins. At the WAP, along with nutrients in the CDW, this refractory DOM is being upwelled and introduced into the surface waters so that there is a constant background of DOM concentrations. The measured deep-sea DOC and DON concentrations in the data sets analysed in this study are within a range of 38.13 to 40.88 µmol C L^{-1}, and 3.38 to 4.44 µmol N L^{-1}, respectively, and agree with previous DOM studies in the Southern Ocean (Carlson et al., 2000; Hansell & Carlson, 1998; Hubberten et al., 1995; Lechtenfeld et al., 2014; Nikrad et al., 2014; Sanders & Jickells, 2000; Wang et al., 2010, Ogawa et al., 1999). It is interesting to note that the DOC distribution across the entire LTER grid, covering coastal, shelf and open-ocean stations in the North and the South of the WAP, does not show much variation ($p > 0.05$ for DOC concentrations compared between open, shelf and coastal stations) even though physical, phytoplankton and bacterial dynamics are extremely variable. However, DON shows significant variability between coast and open ocean stations (t-test t = 2.161, $p = 0.035$) with higher DON at the coastal stations than at the open-ocean stations.

While there are no significant relationships between DON and phytoplankton parameters (PN, chlorophyll *a*, PP), surface [DON] show correlations with both bacterial abundance (r = 0.62, $p = 2.1*10^{-4}$) and activity (r = 0.78, $p = 2.46*10^{-7}$). Carbon is not limiting in the ocean while nitrogen can become a limiting nutrient for phytoplankton. Hence, the direct release of N-containing DOM compounds by a healthy phytoplankton cell during a photosynthetic production period is accompanied

by high energetic costs which is the reason for higher DOC than DON release by active phytoplankton (Ward & Bronk, 2001). In a DOM model study based on ^{13}C tracer experiments in a Danish fjord, Van den Meersche et al. (2004) estimated that 60 % of DOC is being released directly by phytoplankton and 40 % by bacterial processes. However, > 99 % of DON is suggested to be the product of bacteria. The PAL LTER data show that DON maxima often coincide with high bacterial activity and/or abundance and DOC maxima often coincide with either of those but more often with chlorophyll *a*. With labile DOC concentrations > 10 µmol C L^{-1}, DOC is consistently highest at the same depth as either the chlorophyll-*a* or bacterial-activity maximum which is not the case for high DON concentrations. These findings support Van der Meersche et al.'s estimations corroborating the suggestion that both phytoplankton and bacteria are involved in DOM production and consumption which affects how DOC and DON as well as DOM and POM are coupled within the water column. For DON cycling, three different scenarios can be suggested from the available data: (i) DON is released by phytoplankton directly but decoupled from POM production, e.g. at a later stage as described in chapter 4, (ii) DON is produced by either phytoplankton or bacteria and ammonified rapidly which leads to decoupling of POM and DOM, (iii) DON is a bacterial product resulting from the PN breakdown and the incorporation of inorganic nitrogen compounds into bacterial organic material.

Even though DOM exists at a continuum of different sizes, compositions and grades of lability, freshly released DOM (DOC_{lab}, DON_{lab}) can be differentiated from refractory DOM by subtracting the background DOC and DON concentrations from the measured concentrations. RaTS data were only taken into account when NH_4^+ measurements were available. The DOC:DON ratio of labile DOM ($DOC:DON_{lab}$) ratios give useful insights into sites of DOM and high DON production. The $DOC:DON_{lab}$ for all four data sets cover a wide range but are mostly lower than

Redfield showing high nitrogen content. Abiotic factors such as UV radiation, which is particularly high in the summer in high-latitude regions, can transform and decompose refractory DOM into both inorganic forms of carbon and nitrogen but also into labile forms of DOM. Unless processes like this decouple organic carbon and nitrogen by producing more inorganic forms of carbon than nitrogen, there would be no reason to assume that this could lead to decreased DOC:DON ratios.

Lowest surface $DOC:DON_{lab}$ ratios are found at coastal stations at 200.000 and 400.040 which are both associated with the highest rates of bacterial activity of the 2017 PAL LTER cruise. The low DOC:DON ratios coinciding with high bacterial activity support the aforementioned argument of bacterial activity representing the major source for DON.

Studies have shown increased phytoplankton and bacterial activity in the coastal waters due to replete macro and micronutrient concentrations and increased stratification from glacial and sea-ice melt (Ducklow et al. 2012). Micronutrients such as iron are delivered by glaciers and through upwelling (Annett et al., 2015) so that the waters close to the coast can support primary production at high rates while the region off the shelf resembles the HNLC regions of the Southern Ocean where primary production is limited by micronutrients and deeper mixed-layer depths. Hence, DOM dynamics are regulated by higher phytoplankton and bacterial activity in the coastal regions. Increased production of labile POM leads to high bacterial activity which, in turn, produces vast amounts of labile DOM and allows for increased bacterial growth efficiency which might allow bacteria to consume less labile forms of DOM as suggested by Tremblay et al. (2015). Additional DOM from sea ice or glacial meltwater could represent another source of DOM. Glacial meltwater at the WAP has been suggested to be a negligible source of DOM, however, the areas of most glacial influence also show highest DON concentrations. These increased concentrations could be the product of increased bacterial activity, which can be shown at some of

those stations. It could also come from phytoplankton of a different species composition than at the stations of less glacial influence, or which could be in a situation of osmotic stress due to the potentially rapid decrease in salinity, which could trigger increased DON release. DOM release through osmotic stress is discussed in depth in chapter 3 of this thesis and glacial influx of DOM in chapter 4.

Vertical concentrations of both DOC and DON are not clearly distributed. Maximum DOC and DON concentrations per depth profile are almost never at the same depth with DON usually being deeper. Because there are no NH_4^+ measurements available for the PAL LTER region, it is likely that DON maxima are found at depths > 40m due to increased NH_4^+ release at those depths. The available NH_4^+ data from the RaTS data show that generally there is an increase in NH_4^+ concentrations later in the season with $[NH_4^+] > 2$ µmol N L^{-1}. However, 2015/16 data show $[NH_4^+] > 6$ µmol N L^{-1} from the beginning of the phytoplankton bloom. These data clearly show that NH_4^+ can approach concentrations higher than [DON] in coastal WAP waters throughout the growing season. High rates of NH_4^+ release might be the result of high grazing activity which would also lead to increased production of DOM at those depths through sloppy feeding. The PAL LTER data do not show an increase in DOC which would be expected from DOM release by unselective sloppy feeding. Hence, increased DON concentrations at depth are likely the result of a combination of zooplankton grazing activity, NH_4^+ release by zooplankton and bacteria, and rapid cycling of labile DOM by bacteria.

The RaTS site lies in the Southern part of the LTER sampling area. Studies with different focusses have shown that Ryder Bay in Marguerite Bay is among the most productive regions at the West Antarctic Peninsula with high primary production rates, chlorophyll-*a* and POM concentrations observed in the summer seasons with strong interannual variability. The three investigated seasons show that nutrient

concentrations in Ryder Bay can come close to depletion during high rates of primary production. In these phases, DON can make up > 99% of the total dissolved nitrogen pool so that it represents the major constituent of bioavailable nitrogen which can potentially be taken up by phytoplankton cells. Additionally, bacteria consume and produce DOC and DON at the same time. The simultaneous occurrence of these mechanisms – DOM release by phytoplankton during photosynthesis, potential DON consumption by phytoplankton, DOC and DON consumption and release by bacteria – lead to decoupled dynamics of DOC and DON in Ryder Bay and potentially across the entire WAP shelf area. Vertical variation in bacterioplankton composition likely influences different rates and amounts of DOC and DON being produced and consumed. A striking difference in the bacterial community composition existed between surface waters and waters > 100m in the PAL LTER sampling grid in 2008 (Luria et al. 2014). Genetic analyses show high functional diversity among bacterial groups in WAP waters (Williams et al., 2012). These functionally diverse clades of bacteria will likely affect the preferential cycling of different DOM compounds at different depths of the water column over the seasonal cycle.

5.4.3 Coupling between particulate and dissolved organic matter phases

Total organic carbon (TOC) and total organic nitrogen (TON), the sum of particulate and dissolved organic carbon and nitrogen, respectively, and the % contribution of DOC and DON are found in table 5.4.2. Labile DOC and DON concentrations were applied in this context so that only freshly produced organic matter is considered. The majority of TOC is partitioned into the POC pool in the upper ocean which is in agreement with other Southern Ocean studies (Carlson et al. 2000; 1998; Ogawa et al., 1999). In these mentioned studies, DOC made up <30% of TOC usually during high phytoplankton production. In the four data sets available, the DOC contribution

is mostly increased during phases of low chlorophyll-*a* concentrations, so outside periods of high primary production. (figures 5.4.4).

Table 5.4.2: Total organic carbon and nitrogen and the contribution of DOC and DON, respectively. The LTER sampling area is divided into open, shelf and coast. Only the ranges are stated due to the high variability of DOM to TOM contribution.

		TOC		*TON*	
		Range	%DOC range	Range	%DON range
LTER	Open	1.3 - 33.7	0.0 - 79.7	0.1 - 4.9	2.5 - 82.6
	Shelf	1.5 - 59.2	0.0 - 72.1	0.3 - 7.7	10.5 - 81.9
	Coast	1.4 - 104.8	3.7 - 80.1	0.2 - 17.3	4.1 - 93.9
RaTS	2013/14	3.3 - 214.6	1.1 - 87.9	1.9 - 23.9	2.3 - 96.3
	2014/15	2.2 - 95.5	2.8 - 80.1	1.2 - 15.4	10.8 – 91.8
	2015/16	2.9 - 54.2	19.9 - 62.5	3.3 - 9.0	1.4 - 42.8

By comparing the LTER data to the RaTS data, the coastal LTER stations agree well with RaTS seasons 2013/14 and 2014/15 with maximum DOC contributions to TOC being in a small range between 80 and 87.90% and maximum DON contribution to TON between 91.8 and 93.3 %. However, the ranges of TOC and TON show high variability between years and areas with the RaTS season 2013/14 showing maximum TOC concentrations approximately twice as high as in the LTER coastal data or the 2014/15 season. Highest TOC concentrations across the LTER area are always found in the upper 15m. TOC concentrations < 5 µmol C L^{-1} are only found at depths > 75m except for station 200.000 where these low values are already reached at 45m. Here, DOC contributes 48% to the TOC pool. This station shows high bacterial activity in surface waters. High bacterial turnover of TOC is likely the reason for the rapid decrease with depth. The high DOC contribution supports this suggestion as this would likely trigger or increase bacterial activity.

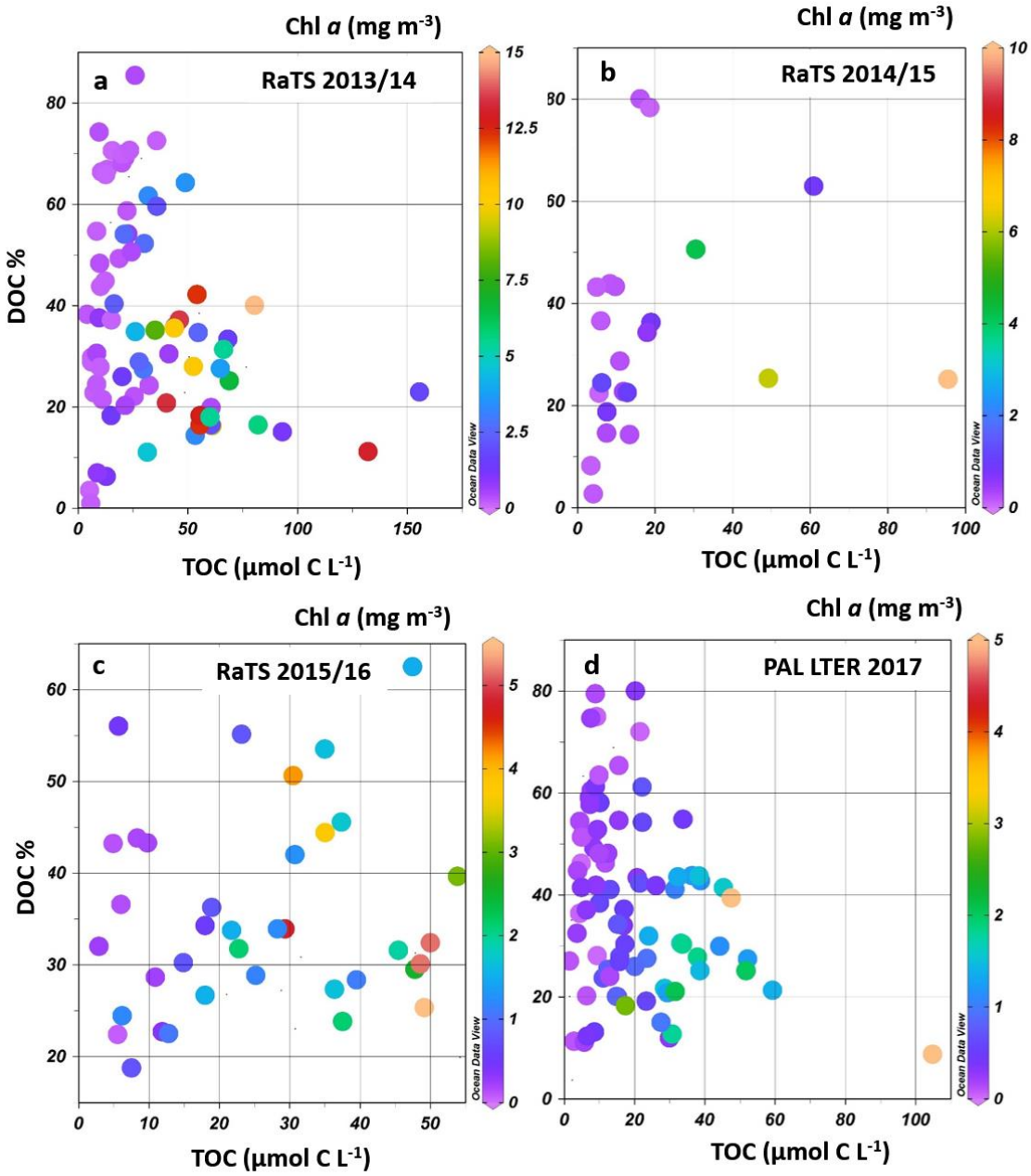

Figure 5.4.4: Upper 50m TOC (POC + labile DOC) vs. the DOC contribution in %. The chlorophyll colour-coding indicates that with increasing chlorophyll concentrations, organic carbon tends to be partitioned more into the particulate than the dissolved pool which holds true for all four data sets.(a)-(c) RaTS seasons 2013/14, 2014/15 and 2015/16, (d) PAL LTER 2017

TON shows high concentrations at almost all coastal stations, however, only at 200.000, the % of DON is between 55 and 74.3% while at stations 500.060 and 300.040, it is < 5% indicating different processes affecting DON production at 200.000

than at 300.040 or 500.060. In fact, station 200.000 shows bacterial activity much higher than any other station while stations 300.040 and 500.060 are both stations with high phytoplankton activity which indicates rapid turnover of PN with rapid DON production at station 200.000.

Strongest coupling between POC and DOC in the PAL LTER sampling area is observed in the Southern region (POC ~ DOC r = 0.81, $p = 1.14*10^{-9}$) and along the coast (POC ~ DOC r = 0.65 $p = 6.68*10^{-4}$). While the North also shows significant but less strong coupling (r = 0.36, $p = 0.02$), the division from coast to open only shows a significant relationship in the coastal region (figure 5.4.5). Possibly similar processes affect DOC and POC concentrations in the coastal and Southern stations while in the North and open ocean, POC and DOC appear to be decoupled and affected differently. On the one hand, this clearly shows spatial variability of organic matter distribution and cycling. On the other hand, however, due to the progressing sea-ice decline from open to the coast and different climatic conditions between North and South, it more likely indicates different stages of timing within the LTER sampling grid. Primary production in the open-ocean area occurred earlier than along the coast which could be the reason for the observed trends in DOC and POC. This can be supported by the RaTS data. As described above, the contribution of DOC to TOC generally decreases with increasing POC concentrations which is true for every season: Both DOC and POC concentrations increase with the onset of the first phytoplankton bloom, but at the same time, the contribution of DOC to the TOC pool decreases as more organic material is partitioned into the particulate pool. Hence, while the coastal stations and possibly the Southern station of the PAL LTER data show stages of pre- or peak bloom conditions during which POC and DOC both accumulate simultaneously but to varying extents, the open ocean and Northern stations might already be past that stage and removal processes such as zooplankton

grazing, or bacterial remineralisation could be the reason for a decoupled relationship between POC and DOC.

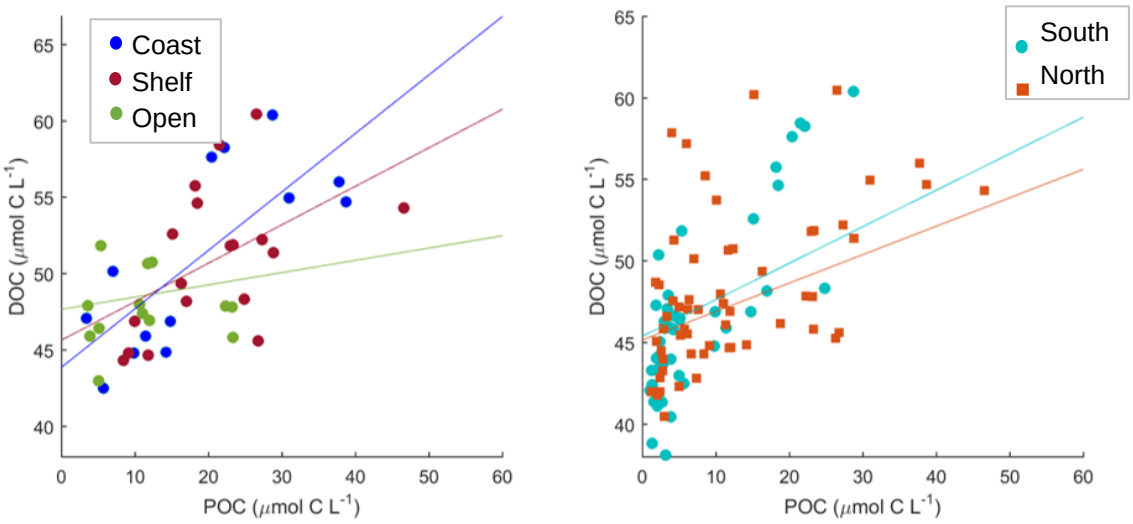

Figure 5.4.5: POC vs. DOC concentrations from PAL LTER 2017 show strongest coupling between dissolved and particulate organic carbon in the South and the coastal region of the WAP.

5.5 Summary

This study investigated the coupling of dissolved and particulate organic carbon and nitrogen at the west Antarctic Peninsula. Over a spatial sampling area and through three consecutive summer seasons, concentrations of DOC, DON, POC and PN were put in context with other biogeochemical and physical data. C- and N-isotopic data of POM and nitrate were considered to understand the cycling of carbon and nitrogen between the sources and sinks.

DOM and POM concentrations show high spatial and temporal variability in the WAP region. POM concentrations in the upper ocean are strongly correlated with chlorophyll-*a* concentrations, decrease with depth due to grazing and bacterial degradation, and PN is removed at higher rates than POC. POM concentrations are generally higher in the coastal regions than in the open and the RaTS data show a clear seasonal trend.

The spatial or temporal distribution of DOC and DON is not as clear. The PAL LTER data show a snapshot in time covering an area in which biogeochemical ecosystem dynamics are driven by different processes with a clear North-to-South and coast-to-open-ocean trends in most parameters. Overall, DOC concentrations along the WAP do not show great spatial variability and remain within a relatively narrow range with background concentrations of approximately 40 µmol C L^{-1}. Increased concentrations are found in the upper ocean and these are often in good agreement with phytoplankton or bacterial parameters. DON concentrations show more variability, especially along the coast. DON maxima co-occur with maxima of bacterial parameters and DON concentrations show better correlations with bacterial parameters than phytoplankton. This leads to the suggestion that DOC is being controlled by both phytoplankton and bacteria while DON seems to be regulated by bacteria mostly. The coinciding high DOM concentrations in surface waters of high

glacial influence could be due to glacial DOM addition, osmotic stress in phytoplankton cells which leads to additional release of N-rich DOM or a different composition of the phytoplankton and bacterial communities.

The RaTS data show the development of DOM concentrations throughout the austral spring and summer which is the period of high productivity in the region. The three consecutive seasons confirm that background (deep-sea) DOM is being upwelled with CDW water with surface concentrations reflecting those measured at deeper depths at the beginning and the end of the seasons (except for 2015/16 DON concentrations at 15m as discussed above). Moreover, they show a clear seasonal signal of DOM development with a simultaneous increase of DOC and POC concentrations and DON showing more variability. These data confirm previous findings of only small concentrations of DOC and DON being produced.

The good correlation between DOC and POC and the temporal development during the growing phase of phytoplankton blooms lead to the overall suggestion of direct DOC release by phytoplankton at least in the beginning of phytoplankton bloom development. DON concentrations do not follow the trend which points to either different mechanisms controlling DON or rapid cycling of DON in the upper ocean. Bacteria appear to be more involved in DON production than phytoplankton and possibly also in the consumption of DON. However, at times, DON can make up >99% of total dissolved nitrogen in the surface waters. At these times, it is likely that phytoplankton switch to mechanisms allowing for DON uptake instead of DIN.

The isotopic data from both the PAL LTER and the RaTS site show intense cycling of organic matter in the upper ocean. The N-isotopic data support the findings from chapter 3 and 4 of intense upper ocean remineralisation with little export and clearly show the high variability of biogeochemical processes particularly along the coast of the WAP. Further, the RaTS N- and C-isotopic data of PN and NO_3^- show the potential

addition of sea-ice derived POM and replenishment of nutrients through vertical mixing.

This study expands our knowledge of the dynamics of DOC and DON over time and space. It shows a high seasonality for DOC and co-production during phytoplankton production which contrasts with previous findings. DON concentrations respond differently and are controlled primarily by bacteria.

Further, the data presented in this chapter and in chapter 3 of this thesis show the importance of ammonium measurements. Ammonium measurements are essential to precisely calculate DON concentrations but more importantly, the high concentrations of NH_4^+ during the growth phase in 2015/16 are unexpected. While these findings agree with the high spatial and temporal variability of the WAP ecosystem, it also shows that previously suggested dynamics of NH_4^+ accumulation in late summer / early autumn cannot be generally assumed.

The data available for this study allow for suggestions of mechanisms involved but cannot define exclusively the mechanisms controlling DOM dynamics with certainty. Further research is necessary to investigate the contribution of glacial meltwater to DOM dynamics in terms of glacially-sourced DOM but more importantly of phytoplankton and bacterial response to a changing climate. A changing climate will affect the physics (temperature, salinity, sea-ice cover, glacial discharge, stratification) of the WAP ecosystem with subsequent effects on primary production, the bacterial response and the response of higher trophic levels. All these factors affect organic matter cycling in the WAP ecosystem, as shown in this study.

CHAPTER 6

Conclusion

6.1 Major Findings of This Thesis

In this doctoral thesis, the role and the dynamics of organic matter cycling at the west Antarctic Peninsula were investigated. DOC studies along the WAP are scarce and the cycling of both DOC and DON has not been investigated before. Based on these few previous studies, this thesis hypothesised that (1) no or only very little DOM is produced and released by *in situ* phytoplankton production with a temporal offset between POM and DOM. (2) This DOM has been hypothesised to be of high bioavailability due to low C:N ratios so that DOM cycling in the upper ocean is efficient and hence export is minimal. At last, it was hypothesised that (3) changing physical and biogeochemical conditions will influence DOC and DON concentrations, e.g. with allochthonous contribution of DOM from sea ice or meteoric water being negligible. Four different data sets were investigated for spatial and temporal variability in DOM dynamics to investigate these hypotheses. The data for spatial analysis were collected during an annual research cruise covering a sampling grid west of the Antarctic Peninsula as part of the US PAL LTER programme. The data for the temporal analysis were collected over three consecutive austral summer seasons (2013-2015) at the UK Rothera Research Station. The hypotheses were tested with these data sets and the following has been found:

(1) No / little DOM production and in situ *release by phytoplankton*

In conclusion, it was shown that DOC and DON concentrations spatially remain low (DOC 38.13 – 88.65 µmol C L^{-1}; DON 1.70 – 10.52 µmol N L^{-1}). The majority of *in situ*

produced organic matter is partitioned into the particulate organic matter pool during phytoplankton blooms. However, on a temporal scale, DOC and DON showed high concentrations for short periods of time which are comparable to lower-latitude systems. Even though *in situ* DOM release by phytoplankton cannot be shown with the data available, highest DOC concentrations co-occur with peaks in POC concentrations in all three temporal datasets from the UK RaTS site suggesting the same mechanisms responsible for DOC release which partially disproves this hypothesis. Significant correlations between DOC, POC, nutrient uptake and chlorophyll *a* (all $r^2 > 0.45$, $p < 0.05$) as well as C:N ratios close to the Redfield C:N ratio indicate *in situ* production and release of DOC during phytoplankton production. However, this only holds true for the build-up phase of the bloom. After the first primary production peak, DOC concentrations are not aligned with POC any longer and other mechanisms must be responsible for DOC cycling with bacterial degradation likely dominating production and removal. DON concentrations do not agree well with phytoplankton dynamics ($p > 0.05$). Therefore, it is suggested that production and removal mechanisms for DON are different from those for DOC and are likely more driven by bacteria than phytoplankton. However, periods of nutrient depletion leave DON as the predominant nitrogen species in the waters which might change the preferred nutrient source for phytoplankton from DIN to DON. These findings, however, only represent the situation of a coastal location in the Southern part of the WAP shelf sea and might not be representable for the entire WAP shelf.

(2) High bioavailability / rapid degradation of DOM in the upper ocean

In chapter 4, the PAL LTER data showed that bacterial abundance and activity are increased in the Southern coastal region of the WAP even though the first peak of primary production was not fully developed. Previous studies showed a temporal

offset between primary and bacterial production (Billen & Becquevort, 1991; Kim & Ducklow, 2016; Lancelot et al., 1991) with the hypothesised reason being low availability of bioavailable DOM for bacteria to break down. In this study, DOM of high bioavailability (low C:N) is shown to exist in areas of high bacterial activity which often coincide with regions of increased freshwater influx and stratification.

The spatial analysis of DOM variability showed that both DOC and DON concentrations decrease with depth to values of refractory DOM found in CDW which can also be shown in upper ocean depth-integrated DOC and DON data indicating efficient recycling of DOM in the upper water column. Further, bacterial activity is highest where DOM of low DOC:DON ratios is highest. This supports the hypothesis of effective DOM cycling by bacteria in the upper ocean.

The isotopic data in chapter 5 support the suggestion of different stages in timing of the progressing phytoplankton growing season in the PAL LTER sampling grid: Open-ocean and shelf stations show higher rates of nitrification and remineralisation than the coastal stations which puts these stations into a later stage of the phytoplankton bloom. $\delta^{15}N_{PN}$ at the coastal stations, on the other hand, show freshly produced PN with recent sea-ice retreat. Further, the isotopic data along with gradients of PN accumulation and nutrient drawdown in the upper ocean support this thesis' findings of intense and efficient upper ocean cycling of both particulate organic matter and labile dissolved organic matter so that only little OM is being exported to greater depths.

(3) *Effects of changing physical and biogeochemical conditions tested based on changes in (i) meltwater contribution, (ii) salinity and temperature, (iii) inorganic nutrient concentrations, (iv) phytoplankton composition or (v) bacterial activity*

Rapid freshening events in the surface and nitrate depletion events at the RaTS site were used to test for stress-related release of DOM by phytoplankton. It is shown that DOC concentrations are increased during and shortly after rapid freshening events which might be due to osmotic cell stress causing the cell to expel DOM (Rijstenbil et al. 1989). DOM concentrations are increased with nitrate depletion, but this might be due to increased organic matter production in general. Stress-related DOM release cannot be shown for nutrient depletion but is a possible additionally occurring mechanism.

By investigating the relationship of DOC and DON concentrations along the coast with the contribution of sea-ice or meteoric meltwater input and by using mass balance equations to calculate the theoretical DOM contributions from these sources, it was argued that the direct contribution from both sea ice and glaciers is minor. For glacial sources, even though DOC and DON concentrations might be high in the source material, the dilution with CDW leads to only minor contribution to the surface waters. Sea-ice melt, on the other hand, contains much higher DOC and DON concentrations which is potentially highly labile. However, due to the highly dynamic patterns of sea-ice movement and sea-ice melt vs. formation processes, the contribution of sea ice is locally minimal unless all ice melts in a limited area over a short period of time. The 2014-15 sea ice data show high concentrations of DOM in parts of the analysed sea-ice cores which could potentially be introduced to the surface ocean upon melting. However, release of high concentrations would only occur if a rapid melting event occurred with most ice melting in one location which is unlikely.

Nonetheless, surface-water seeding from sea ice, or even glacial meltwater, with DOM, POM, algae and bacteria, in addition to physical changes such as increased stratification, changes in temperature and salinity, are likely to indirectly affect upper-water column processes and DOM cycling. Both sea-ice and glacial DOM are suggested to be highly labile (Hood et al., 2009; McKnight et al., 1994) so that upon release, they could trigger an increase in bacterial activity.

DOC and DON have been shown to be decoupled spatially and temporally. While DOC is in good agreement with phytoplankton parameters such as primary production, chlorophyll-*a* and POC concentrations, DON shows different dynamics. DON shows relationships with bacterial activity so that it was assumed to that most labile DON in WAP waters is a product of bacterial production.

Ammonium concentrations measured at the RaTS site show an anti-correlation with DON supporting the idea of effective ammonification by bacteria. The ammonium released from these processes is rapidly cycled in the upper ocean as shown by the N-isotopic composition of both nitrate and PN indicating nitrification and remineralisation processes.

6.2 Implications of this study

The results of this thesis build upon the foundation of our understanding of DOC and DON dynamics at the WAP. This thesis underlines the close functional interactions between phytoplankton and bacterioplankton on a biogeochemical level with implications for the cycling of carbon and nitrogen along the WAP. Even though concentrations of DOM produced and cycled in these shelf waters are small compared to other regions, the results imply important findings for the regional carbon cycling. DOM has not been considered quantitatively in carbon budget calculations in this

region. The findings of this thesis show that a small but substantial fraction of primary production is funnelled into the DOM pool and is cycled within the upper ocean which has direct effects on the budget of carbon export and net production estimates. The overall carbon budget of the WAP cannot be completed with the data gained from this thesis. However, the findings of this thesis underline factors contributing and influencing the partitioning of organic matter into the DOM pool and what potential factors can feedback on DOC and DON cycling positively and negatively, such as changes in the physical state of the upper ocean (e.g. salinity and temperature) or biogeochemical changes (e.g. nutrient availability, phytoplankton and bacterioplankton composition). These changes are most likely to occur along the WAP with changing climatic conditions. From these findings, further research can be targeted at specific parts of the DOM cycle (see *Recommendations for future research*). To complete the WAP carbon budget, additional research into inorganic and organic carbon cycling, particularly with increasing ocean acidification and rising temperatures, is needed as well as data coverage throughout the winter season.

Only a few previous studies actively looked into dissolved organic matter along the West Antarctic Peninsula. These previous studies have found generally low concentrations of DOC in surface waters of the WAP, even during high primary production, which is reasoned with various hypotheses of which few have been tested (e.g. Ducklow et al., 2011). From these findings, other hypotheses were generated stating e.g. only small *in situ* production and release of DOC from primary producers. Further, a time lag between primary and bacterial production was argued to play an important role in DOC production and release. DON concentrations were not measured in any of these studies. There have not been any WAP studies, as of yet, quantifying how much DOM is released directly by primary producers during primary production or by bacteria during the degradation of particulate organic matter. In many

studies, allochthonous supply of DOM from e.g. glacial runoff, is stated to be negligible. However, along the WAP, concentrations of DOM in glacial runoff have not been analysed. Other studies from both the Arctic and Antarctica show that DOM concentrations in glacial meltwater can be high (Barker et al., 2006; Bhatia et al., 2010; Christner et al., 2014; Lafrenière & Sharp, 2004; Lyons et al., 2007). Even though this study shows only small *in situ* contribution of DOM from sea ice and glaciers, increasing freshwater input from e.g. increasing meltwater influx can have direct and indirect effects on DOM concentrations and cycling in the surface waters. First, the fraction of freshwater flux is projected to increase which will increase the fraction of DOM being introduced. But more importantly, increasing freshwater introduction to the WAP shelf sea will increase stratification and change the physical characteristics of the upper ocean with likely shifts in phytoplankton and bacterial species compositions.

This study shows immediately increased bacterial activity with increasing concentrations of low C:N DOM. If future projections hold true, the predicted shift in phytoplankton composition dominance to cryptophytes or haptophytes likely involves increased DOM production. Additionally, the overall carbon fixation might decrease due to lower carbon uptake by smaller phytoplankton cells. At the same time, the increasing proportion of DOM to TOM will potentially trigger increased bacterial activity and microzooplankton grazing, opposed to macrozooplankton grazing, on POM. This, in turn, could enhance upper-ocean carbon cycling and reduce carbon export.

Another important finding of this thesis are that partially DOC and DON concentrations can be lower than background concentrations indicating another important mechanism taking place in the upper ocean which requires further research: The potential breakdown of refractory DOM which has either been triggered abiotically by

UV radiation or biotically by the priming of bacteria (chapter 3). Both mechanisms are understudied in WAP waters and require further research. Considering the intense UV radiation in the Southern Ocean and the Southern Ocean being a major region of upwelling, hence, direct introduction of refractory organic matter to the surface waters, these two mechanisms stand out as an urgent area of future research.

The ammonium measurements collected at the RaTS site show that ammonium concentrations can reach concentrations higher than ambient DON concentrations early in the growing season which contradicts previous findings. Ammonium is often preferred over nitrate by phytoplankton so that these findings represent important considerations for understanding the local nitrogen cycle. The high inter-annual variability in combination with the projected continuation of a warming local climate underline the importance of implementing efforts to fully understand the WAP ecosystem.

6.3 Limitations of this study

This study gives a first insight into the dynamic and complex cycling of DOM at the WAP from bulk DOC and DON concentrations. While the methodological advances and the analytical precision for DOC measurements have improved considerably over the last few decades, DON measurements are always accompanied with a large error (see chapter 2: Methodology). Additionally, the samples collected during the PAL LTER cruise lack the ammonium component. Even though ammonium concentrations have been shown to be minor in the upper ocean during the productive season of the WAP in previous studies, the RaTS data of this thesis show that interannual variability is high and ammonium can be present at high concentrations throughout the phytoplankton growing season. DON concentrations only cover a narrow range of

mostly low concentrations so that elevated ammonium concentrations at a specific date or location can impact the results significantly.

Bulk concentrations of DOC and DON give a good first impression of cycling processes, particularly in order to quantify carbon and nitrogen being partitioned into the dissolved organic pool. Despite its common use in previous studies and this one, the simple separation of labile and semilabile fractions of DOM by subtracting the background values does not represent a precise measure of bioavailable DOM in the upper ocean. Particularly in the Southern Ocean where UV radiation during the summer months is more penetrating than elsewhere, refractory DOM upwelled from CDW might undergo abiotic transformation processes with the possible breakdown of refractory DOM to DOM compounds of higher lability or to inorganic compounds. Concentrations below background are indicative of such processes but could also be the result of highly active bacteria being able to degrade refractory material from depths. Quantitative studies on the destructive characteristics of UV radiation on refractory DOM in the region are needed to assess this effect (e.g. Medeiros et al., 2015).

This study shows that DOC and DON are undergoing different cycling processes. DOC is more likely controlled by phytoplankton and only partially by bacteria while DON is mostly controlled by bacteria. The PAL LTER and RaTS data sets complement each other by contributing microbial parameters (PAL LTER) and phytoplankton species assemblage data (RaTS). However, the patchiness of biological activity in the WAP shelf waters, especially along the coast, requires station-wise information of all these factors in order to draw more conclusive findings. Additionally, because of the high spatial and interannual variability of the system, the findings of this study cannot account for long-term changes and shifts in the

ecosystem. This is shown in the different dynamics of DOC and DON in the RaTS 2015/16 data compared to 2013/14 and 2014/15.

While there is a vast suite of analytical methods available in order to characterise the chemical composition of DOM compounds, the development and advancement of two methodological approaches need some extra attention:

First, a direct measure of DON concentrations would decrease the error that comes with TDN measurements and would increase the confidence in stating DON concentrations. In terms of the measurements conducted at the WAP, ammonium measurements should be an integrated part of the PAL LTER and RaTS research programme and cover full depth profiles.

Second, the N-isotopic composition of DON ($\delta^{15}N_{DON}$) would further our knowledge and understanding of the cycling of N within the system. Even though this study shows significant relationships between DON and bacterial parameters, the cycling of DON, including sources and sinks, cannot be reproduced. By analysing the N-isotopic compositions of all N-containing compounds present in the system (DIN, DON, PN), pathways, sinks and sources can be distinguished with more certainty and precision than with the data currently available. While there is a method available for the determination of the $\delta^{15}N_{DON}$, it suffers from the same restrictions as the analysis of bulk DON concentrations as there is no direct method for DON only. These limitations restrict the $\delta^{15}N_{DON}$ analysis to water masses in which DON concentrations are high and nitrate concentrations are low or depleted. High-nitrate low-DON waters, such as found in the Southern Ocean, represent a methodological challenge.

The development of such method was a major objective of this doctoral project. Multiple experiments were conducted in order to adapt the existing method developed by Knapp et al. (2005) for Southern Ocean water samples. The applied method is a combination of the commonly used persulfate oxidation and the denitrifier method.

Persulfate oxidation converts dissolved organic nitrogen compounds into nitrate. The denitrifier method utilises denitrifying bacteria which convert nitrate to N_2O gas which can then be analysed for its N-isotopic composition. Samples have to be treated for TDN and for nitrate separately in order to calculate the contribution of nitrate to the TDN pool. Problems already associated with the well-developed method are mainly contamination issues. Persulfate is produced under nitrogen-enriched conditions so that even low-nitrogen persulfate batches can contain concentrations of nitrogen too high for this analysis. One way to reduce contamination is the recrystallization of the persulfate reagent by boiling persulfate in DI water and recrystallizing at low temperatures multiple times. However, multiple vigilant tests have shown that contamination could be reduced but not avoided due to the multitude of analytical steps involved in the whole process from sample preparation to analysis. Further, the presence of high nitrate concentrations in combination with low DON concentrations in the waters led to results in which the error of the measurements would exceed the results and blank measurements. As long as there is no method to successfully separate DON from the TDN pool, the N-isotopic composition of DON in high-nutrient waters remains unresolvable.

6.4 Recommendations for future research

The fact that some of the results of this thesis contradict previous studies and/or deliver new findings underlines the necessity of further research in this field. This study shows that DOM cycling might be responsible for a small but substantial part of the carbon budget at the WAP. In order to fully understand the implications of DOM cycling, I recommend establishing DOM measurements as baseline measurements along with inorganic macronutrients, phytoplankton parameters such as chlorophyll concentrations, primary production rates and phytoplankton species assemblages

and microbial parameters, the least abundance and activity rates, as part of the regular sampling schemes of both the PAL LTER and the RaTS programme.

Even though DOM concentrations are low, sampling and analysing the seasonal progression in the chemical composition of DOM compounds can show major sources, sinks and transformation processes of DOM compounds. In combination with microbial genomic analysis, adaptations of bacteria to the availability of certain DOM compounds can be established and pathways of organic and inorganic nutrients can be followed in more detail. Winter measurements will show production and removal processes by bacteria and archaea with minimal phytoplankton contribution. For example, through the application of metagenomics, Bowman & Ducklow (2015) discovered that metabolic pathways of bacteria at the WAP are inherently different at surface and deeper waters and that there is a significant difference between summer and winter. Targeting the metabolic gene expressions of bacteria at the WAP will enhance our understanding of which specific DOM compounds are being rapidly cycled and which compounds might represent refractory DOM.

A separation and chemical characterisation of dissolved primary production, the photosynthates directly released during primary production by phytoplankton, could give insight into the molecular structure of these commonly highly labile compounds and could potentially indicate the paths of these compounds through the microbial loop.

In order to further our understanding of mechanisms involved in the cycling of DOC and DON along the WAP, advanced experiments and long-term observations will be helpful. Incubation experiments to establish a baseline for DOM production by local phytoplankton (e.g. Romera-Castillo et al., 2010; Sarmento et al., 2013) and bacteria and bacterial DOM consumption (e.g. Kujawinski et al., 2016) can be set up in a simple manner. These incubation experiments can be set up to also investigate

changes in DOM dynamics with rising temperatures and ocean acidification – both of which are observable changes in the Southern Ocean and both of which have been suggested to increase the bacterial degradation of DOM (Endres et al., 2014; Engel et al., 2014) but also to reduce the formation of microgels from DOM compounds (Chen et al., 2015). The contribution of sea ice and glacial meltwater can be addressed by sampling at the ice-ocean interface. Further, winter observations are urgently needed to understand if and how DOM is being cycled when there is negligible primary production. Winter sampling along the WAP certainly represents one of the biggest challenges due to high sea-ice cover, darkness and strong storms so that sampling can only occur from research stations and not from research vessels. The challenge of winter sampling is currently being faced by the development and deployment of autonomous gliders which can navigate under sea ice (e.g. Couto, 2017; Couto et al., 2017, 2016; Kohut et al., 2018; Schofield et al., 2015). Fluorescence sensors are being developed for the detection of chromophoric and fluorescent DOM and some studies show promising results (Fichot & Benner, 2012; Loginova et al., 2015; 2016). However, sensors like the MiniFluo UV (Cyr et al. 2017) are restricted to the detection of tryptophan-like and phenanthrene-like fluorophores. Tryptophan is naturally occurring but detectable concentrations are mostly found in locations of waste water entering the ocean. Phenanthrene is an anthropogenically introduced low-molecular-weight compound resulting from incomplete combustion of carbonaceous materials. Neither of these compounds are likely to be found at detectable levels in Antarctic waters. More progress has been made with the development of a sensor for the detection of chromophoric DOM (Jiang et al. 2019) so that in the near future, autonomous measurements of DOM in winter and underneath sea ice might be possible.

These advances will enhance our understanding of the cycling of carbon in the dissolved organic form at the WAP but also generally in cold regions. As such, contributions to Earth System Models may be available soon for which Southern Ocean data is still scarce. These models enhance our understanding of the global cycling of oceanic carbon (e.g. Letscher et al. 2015) which is most important in order to understand the current climate and our impacts on it.

7. Bibliography

Alldredge, A. (1998). The carbon, nitrogen and mass content of marine snow as a function of aggregate size. *Deep-Sea Research Part I: Oceanographic Research Papers*, *45*(4–5), 529–541. https://doi.org/10.1016/S0967-0637(97)00048-4

Amon, R. M. W. (2004). The Role of Dissolved Organic Matter for the Organic Carbon Cycle in the Arctic Ocean. In *The Organic Carbon Cycle in the Arctic Ocean* (pp. 83–99).

Annett, A. L., Carson, D. S., Crosta, X., Clarke, A., & Ganeshram, R. S. (2010). Seasonal progression of diatom assemblages in surface waters of Ryder Bay, Antarctica. *Polar Biology*, *33*(1), 13–29. https://doi.org/10.1007/s00300-009-0681-7

Annett, A. L., Skiba, M., Henley, S. F., Venables, H. J., Meredith, M. P., Statham, P. J., & Ganeshram, R. S. (2015). Comparative roles of upwelling and glacial iron sources in Ryder Bay, coastal western Antarctic Peninsula. *Marine Chemistry*, *176*, 21–33. https://doi.org/10.1016/j.marchem.2015.06.017

Arrigo, K. R. (1999). Phytoplankton Community Structure and the Drawdown of Nutrients and CO2 in the Southern Ocean. *Science*, *283*(5400), 365–367. https://doi.org/10.1126/science.283.5400.365

Arrigo, Kevin R., van Dijken, G. L., Alderkamp, A. C., Erickson, Z. K., Lewis, K. M., Lowry, K. E., … van de Poll, W. (2017). Early Spring Phytoplankton Dynamics in the Western Antarctic Peninsula. *Journal of Geophysical Research: Oceans*, *122*(12), 9350–9369. https://doi.org/10.1002/2017JC013281

Azam, F. (1998). Microbial control of oceanic carbon flux : Thee plot thickens. *Science*, Vol. 280, pp. 694–696. Retrieved from http://cat.inist.fr/?aModele=afficheN&cpsidt=2276299

Azam, F., Fenchel, T., Field, J. G., Gray, J. S., Meyer-Reil, L. a, & Thingstad, T. F. (1983). The Ecological Role of Water-Column Microbes in the Sea*. *Marine Ecology Progress Series*, *10*, 257–263. https://doi.org/10.3354/meps010257

Baker, K. S., Vernet, M., Fraser, W. R., Trivelpiece, W. Z., Hofmann, E. E., Klinck, J. M., … Smith, R. C. (1996). The Western Antarctic Peninsula Region: Summary of Environmental and Ecological Processes. *Foundations for Ecological Research West of the Antarctic Peninsula. Antarctic Research Series*, *70*, 437–448.

Barker, J. D., Sharp, M. J., Fitzsimons, S. J., & Turner, R. J. (2006). Abundance and Dynamics of Dissolved Organic Carbon in Glacier Systems. *Arctic, Antarctic, and Alpine Research*, *38*(2), 163–172. https://doi.org/10.1657/1523-0430(2006)38[163:AADODO]2.0.CO;2

Berman, T., Bechemin, C., & Maestrini, S. Y. (1999). Release of ammonium and urea from dissolved organic nitrogen in aquatic ecosystems. *Aquatic Microbial Ecology*, *16*, 295–302.

Berman, Tom, & Bronk, D. A. (2003). Dissolved organic nitrogen: a dynamic participant in aquatic ecosystems. *Aquatic Microbial Ecology*, *31*, 279–305.

Bhatia, M. P., Das, S. B., Longnecker, K., Charette, M. A., & Kujawinski, E. B. (2010). Molecular characterization of dissolved organic matter associated with the Greenland ice sheet. *Geochimica et Cosmochimica Acta*, *74*(13), 3768–3784. https://doi.org/10.1016/j.gca.2010.03.035

Bianchi, T. S. (2011). The role of terrestrially derived organic carbon in the coastal ocean: A changing paradigm and the priming effect. *Proceedings of the National Academy of Sciences*, *108*(49), 19473–19481. https://doi.org/10.1073/pnas.1017982108

Biddanda, B., & Benner, R. (1997). Carbon, nitrogen, and carbohydrate fluxes during the production of particulate and dissolved organic matter by marine phytoplankton. *Limnology and Oceanography*, *42*(3), 506–518. https://doi.org/10.4319/lo.1997.42.3.0506

Billen, G., & Becquevort, S. (1991). Phytoplankton Bacteria Relationship in the Antarctic Marine Ecosystem. *Polar Research*, *10*(1), 245–253. https://doi.org/10.1111/j.1751-8369.1991.tb00650.x

Bird, D. F., & Karl, D. M. (1999). Uncoupling of bacteria and phytoplankton during the austral spring bloom in Gerlache Strait, Antarctic Peninsula. *Aquatic Microbial Ecology*, *19*(1), 13–27. https://doi.org/10.3354/ame019013

Blain, S., Quéguiner, B., Armand, L., Belviso, S., Bombled, B., Bopp, L., … Wagener, T. (2007). Effect of natural iron fertilization on carbon sequestration in the Southern Ocean. *Nature*, *446*(7139), 1070–1074. https://doi.org/10.1038/nature05700

Bowie, A. R., Maldonado, M. T., Frew, R. D., Croot, P. L., Achterberg, E. P., Mantoura, R. F. C., … Boyd, P. W. (2001). The fate of added iron during a mesoscale fertilisation experiment in the Southern Ocean. *Deep-Sea Research Part II: Topical Studies in Oceanography*, *48*(11–12), 2703–2743. https://doi.org/10.1016/S0967-0645(01)00015-7

Bowman, J. S., & Ducklow, H. W. (2015). Microbial communities can be described by metabolic structure: A general framework and application to a seasonally variable, depth-stratified microbial community from the coastal West Antarctic Peninsula. *PLoS ONE*, *10*(8), 1–18. https://doi.org/10.1371/journal.pone.0135868

Bowman, Jeff S, Amaral-Zettler, L. A., J Rich, J., M Luria, C., & Ducklow, H. W. (2017). Bacterial community segmentation facilitates the prediction of ecosystem function along the coast of the western Antarctic Peninsula. *The ISME Journal*, *11*(6), 1460–1471. https://doi.org/10.1038/ismej.2016.204

Bown, J., Laan, P., Ossebaar, S., Bakker, K., Rozema, P. D., & de Baar, H. J. W. (2016). Bioactive trace metal time series during Austral summer in Ryder Bay, Western Antarctic Peninsula. *Deep Sea Research Part II: Topical Studies in Oceanography*, 1–17. https://doi.org/10.1016/j.dsr2.2016.07.004

Boyd, P. W., & Ellwood, M. J. (2010). The biogeochemical cycle of iron in the ocean. *Nature Geoscience*, *3*(10), 675–682. https://doi.org/10.1038/ngeo964

Boyd, P. W., Jickells, T. D., Law, C. S., Blain, S., Boyle, E. A., Buesseler, K. O., … Levasseur, M. (2007). *REVIEW Mesoscale Iron Enrichment Experiments 1993 – 2005: Synthesis and Future Directions*. *315*(February), 612–618.

Bradley, P. B., Sanderson, M. P., Nejstgaard, J. C., Sazhin, A. F., Frischer, M. E., Killberg-Thoreson, L. M., … Bronk, D. A. (2010). Nitrogen uptake by phytoplankton and bacteria during an induced Phaeocystis pouchetii bloom, measured using size fractionation and flow cytometric sorting. *Aquatic Microbial Ecology*, *61*(1), 89–104. https://doi.org/10.3354/ame01414

Bronk, D. A. (2002). Dynamics of DON. In *Biogeochemistry of Marine Dissolved Organic Matter* (pp. 153–247). https://doi.org/10.1016/B978-012323841-2/50007-5

Bronk, D. A., See, J. H., Bradley, P., & Killberg, L. (2007). DON as a source of bioavailable nitrogen for phytoplankton. *Biogeosciences*, *4*, 283–296. https://doi.org/10.5194/bgd-3-1247-2006

Brum, J. R., Hurwitz, B. L., Schofield, O. M. E., Ducklow, H. W., & Sullivan, M. B. (2015). Seasonal time bombs: dominant temperate viruses affect Southern Ocean microbial dynamics. *Isme J*, 1–13. https://doi.org/10.1038/ismej.2015.125

Buesseler, K. O., McDonnell, A. M. P., Schofield, O. M. E., Steinberg, D. K., & Ducklow, H. W. (2010). High particle export over the continental shelf of the west Antarctic Peninsula. *Geophysical Research Letters*, *37*(22), 1–5. https://doi.org/10.1029/2010GL045448

Calbet, A. (2001). Mesozooplankton grazing effect on primary production: a global comparative analysis in marine ecosystems. *Limnology and Oceanography* 46 (7), 1824-1830

Carlson, C. A. (2002). Production and Removal Processes. In *Biogeochemistry of Marine Dissolved Organic Matter* (pp. 91–151).

Carlson, C. A., & Ducklow, H. W. (1995). Dissolved organic carbon in the upper ocean of the central equatorial Pacific Ocean, 1992: Daily and finescale vertical variations. *Deep Sea Research Part II: Topical Studies in Oceanography*, *42*(2–3), 639–656. https://doi.org/10.1016/0967-0645(95)00023-J

Carlson, C. A., Ducklow, H. W., Hansell, D. A., & Smith, W. O. (1998). Organic carbon partitioning during spring phytoplankton blooms in the Ross Sea polynya and the Sargasso Sea. *Limnol Oceanogr*, *43*(May), 375–386. https://doi.org/10.4319/lo.1998.43.3.0375

Carlson, C. A., & Hansell, D. A. (2015). Chapter 3: DOM Sources, Sinks, Reactivity, and Budgets. In *Biogeochemistry of Marine Dissolved Organic Matter*. https://doi.org/10.1016/B978-0-12-405940-5.00003-0

Carlson, C. A., Hansell, D. A., Peltzer, E. T., & Smith, W. O. (2000). Stocks and dynamics of dissolved and particulate organic matter in the southern Ross Sea, Antarctica. *Deep-Sea Research Part Ii-Topical Studies in Oceanography*, *47*(15–16), 3201–3225. https://doi.org/10.1016/S0967-0645(00)00065-5

Caron, D. A., Goldman, J. C., Andersen, O. K., & Dennett, M. R. (1985). Nutrient cycling in a microflagellate food chain: II. Population dynamics and carbon cycling. *Marine Ecology Progress Series*, *24*(Harrison 1980), 243–254. https://doi.org/10.3354/meps024243

Carter, L., McCave, I. N., & Williams, M. J. M. (2008). Chapter 4 Circulation and Water Masses of the Southern Ocean: A Review. *Developments in Earth and Environmental Sciences*, *8*(08), 85–114. https://doi.org/10.1016/S1571-9197(08)00004-9

Casciotti, K. L., Sigman, D. M., Hastings, M. G., Bohlke, J. K., & Hilkert, A. (2002). Measurement of the oxygen isotopic composition of nitrate seawater and freshwater using the dentirifier method. *Anal. Chem.*, *74*(19), 4905-4912.

Cassar, N., Laws, E. A., Bidigare, R. R., & Popp, B. N. (2004). Bicarbonate uptake by Southern Ocean phytoplankton. *Global Biogeochemical Cycles*, *18*, 1–10. https://doi.org/10.1029/2003GB002116

Chen, C.-S., Anaya, J. M., Chen, E. Y.-T., Farr, E., & Chin, W. (2015). Ocean Warming – Acidification Synergism Undermines Dissolved Organic Matter Assembly. *PLoS ONE*, *10*(2), 1–9. https://doi.org/10.1371/journal.pone.0118300

Christner, B. C., Priscu, J. C., Achberger, A. M., Barbante, C., Carter, S. P., Christianson, K., … Purcell, A. (2014). A microbial ecosystem beneath the West Antarctic ice sheet. *Nature*, *512*(7514), 310–313. https://doi.org/10.1038/nature13667

Church, M. J., DeLong, E. F., Ducklow, H. W., Karner, M. B., Preston, C. M., & Karl, D. M. (2003). Abundance and distribution of planktonic Archaea and Bacteria in the waters west of the Antarctic Peninsula. *Limnology and Oceanography*, *48*(5), 1893–1902. https://doi.org/10.4319/lo.2003.48.5.1893

Church, M. J., Hutchins, D. A., & Ducklow, H. W. (2000). Limitation of bacterial growth by dissolved organic matter and iron in the Southern Ocean. *Applied and Environmental*

Microbiology, *66*(2), 455–466. https://doi.org/10.1128/AEM.66.2.455-466.2000

Clarke, A., Meredith, M. P., Wallace, M. I., Brandon, M. A., & Thomas, D. N. (2008). Seasonal and interannual variability in temperature, chlorophyll and macronutrients in northern Marguerite Bay, Antarctica. *Deep-Sea Research Part II: Topical Studies in Oceanography*, *55*(18–19), 1988–2006. https://doi.org/10.1016/j.dsr2.2008.04.035

Coale, K. H. (2004). Southern Ocean Iron Enrichment Experiment: Carbon Cycling in High- and Low-Si Waters. *Science*, *304*(5669), 408–414. https://doi.org/10.1126/science.1089778

Cochlan, W. P. (2008). Nitrogen Uptake in the Southern Ocean. *Nitrogen in the Marine Environment*, 569–596. https://doi.org/10.1016/B978-0-12-372522-6.00012-8

Comiso, J. C., Parkinson, C. L., Markus, T., Cavalieri, D. J., & Gersten, R. (2016). Current State of Sea Ice Cover. Retrieved June 29, 2016, from http://neptune.gsfc.nasa.gov/csb/index.php?section=234#southern

Conan, P., Sondergarrd, M., Kragh, T., Pujo-Pay, M., Williams, P. J. B., Markager, S., … Riemann, B. (2007). Partitioning of organic production in marine plankton communities : The effects of inorganic nutrient ratios and community composition on new dissolved organic matter. *Limnol. Oceanogr.*, *52*(2), 753–765.

Constable, A. J., Melbourne-Thomas, J., Corney, S. P., Arrigo, K. R., Barbraud, C., Barnes, D. K. A., … Ziegler, P. (2014). Climate change and Southern Ocean ecosystems I: how changes in physical habitats directly affect marine biota. *Global Change Biology*, *20*(10), 3004–3025. https://doi.org/10.1111/gcb.12623

Convey, P., Chown, S. L., Clarke, A., Barnes, D. K. A., Bokhorst, S., Cummings, V., … Wall, D. H. (2014). The spatial structure of antarctic biodiversity. *Ecological Monographs*, *84*(July 2013), 203–244. https://doi.org/10.1890/12-2216.1

Cook, A. J., Fox, A. . J., Vaughan, D. G., & Ferrigno, J. G. (2005). Retreating glacier fronts on the Antarctic Peninsula over the past half-century. *Science (New York, N.Y.)*, *308*(5721), 541–544. https://doi.org/10.1126/science.1104235

Cook, A. J., Holland, P. R., Meredith, M. P., Murray, T., Luckman, A., & Vaughan, D. G. (2016). Ocean forcing of glacier retreat in the western Antarctic Peninsula. *Science*, *353*(6296), 283–286.

Couto, N. (2017). *Circulation and Heat Transport on the West Antarctic Peninsula continental shelf*. Ph.D. thesis. Rutgers University.

Couto, N., Martinson, D. G., Kohut, J., & Schofield, O. M. E. (2017). Distribution of Upper Circumpolar Deep Water on the warming continental shelf of the West Antarctic Peninsula. *Journal of Geophysical Research: Oceans*, *122*, 5306–5315. https://doi.org/10.1002/2017JC012840.Received

Couto, N., Schofield, O. M. E., & Kohut, J. T. (2016). Comparison between glider-derived geostrophic velocities and shipboard ADCP measurements. *OCEANS 2016 MTS/IEEE Monterey*, 1–5.

Craig, H. (1957). Isotopic standards for carbon and oxygen and correction factors for mass-spectrometric analysis of carbon dioxide. *Geochimica et Cosmochimica Acta*, *12*(1–2), 133–149. https://doi.org/10.1016/0016-7037(57)90024-8

Cyr, F., Tedetti, M., Besson, F., Beguery, L., Doglioli, A. M., Petrenko, A. A., Goutx, M. (2017). A new glider-compatible optical sensor for dissolved organic matter measurements: Test case from the NW Mediterranean Sea. *Frontiers in Marine Science* (4), March, 1-19.

DeVries, T., Roshan, S., & Letscher, R. T. (2018). Accumulation of Dissolved Organic Carbon and Nitrogen in the Global Surface Ocean: A Data-Based Approach. *AGU Fall Meeting*.

Dickson, A., & Goyet, C. (1992). *Handbook of methods for the analysis of the various parameters of the carbon dioxide system in sea water*. *1994*(September), 22. https://doi.org/ORNL/CDIAC-74

DiTullio, G. R., Dunbar, R. B., Leventer, A., Robinson, D. H., Barry, J. P., Arrigo, K. R., … Lizotte, M. P. (2000). Rapid and early export of Phaeocystis antarctica blooms in the Ross Sea, Antarctica. *Nature*, *404*(6778), 595–598. https://doi.org/10.1038/35007061

Doval, M. D., Álvarez-Salgado, X. A., Castro, C. G., & Pérez, F. F. (2002). Dissolved organic carbon distributions in the Bransfield and Gerlache Straits, Antarctica. *Deep-Sea Research Part II: Topical Studies in Oceanography*, *49*(4–5), 663–674. https://doi.org/10.1016/S0967-0645(01)00117-5

Druffel, E. R. M., & Williams, P. M. (1990). Identification of a deep marine source of particulate organic carbon using bomb 14C. *Nature*, *347*(6289), 172–174. https://doi.org/10.1038/347172a0

Duce, R. A., & Tindale, N. W. (1991). Chemistry and biology of iron and other trace metals in the ocean. *Limnol. Oceanogr.*, *36*(8), 1715–1726.

Ducklow, H. W. (2003). Seasonal production and bacterial utilization of DOC in the Ross Sea , Antarctica. *Biogeochemistry of the Ross Sea*, *78*, 143–158. Retrieved from doi: 10.1029/078ARS09

Ducklow, H. W. (2009). *Southern Ocean: Biogeochemistry*. https://doi.org/10.1126/science.1247727

Ducklow, H. W., Baker, K., Martinson, D. G., Quetin, L. B., Ross, R. M., Smith, R. C., … Fraser, W. R. (2007). Marine pelagic ecosystems: the West Antarctic Peninsula. *Philosophical Transactions of the Royal Society B: Biological Sciences*, *362*(1477), 67–94. https://doi.org/10.1098/rstb.2006.1955

Ducklow, H. W., Carlson, C. A., Church, M. J., Kirchman, D. L., Smith, D. C., & Steward, G. (2001). The seasonal development of the bacterioplankton bloom in the Ross Sea, Antarctica 1994-1997. *Deep-Sea Research II*, *48*(19–20), 4199–4221. https://doi.org/10.1016/S0967-0645(01)00086-8

Ducklow, H. W., Clarke, A., Dickhut, R., Doney, S. C., Geisz, H., Kuan Huang, … Fraser, W. R. (2012). The Marine System of the Western Antarctic Peninsula. *Antarctic Ecosystems: An Extreme Environment in a Changing World*, 121–159. Retrieved from http://pal.lternet.edu/docs/bibliography/Public/383lterc.pdf

Ducklow, H. W., Doney, S. C., & Sailley, S. F. (2015). Ecological controls on biogeochemical fluxes in the western Antarctic Peninsula studied with an inverse foodweb model. *Advances in Polar Science*, *26*(2), 122–139. https://doi.org/10.13679/j.advps.2015.2.00122

Ducklow, H. W., Fraser, W. R., Meredith, M. P., Stammerjohn, S. E., Doney, S. C., Martinson, D. G., … Amsler, C. (2013). West Antarctic Peninsula: An Ice-Dependent Coastal Marine Ecosystem in Transition. *Oceanography*, *26*(3), 190–203. https://doi.org/10.5670/oceanog.2013.62

Ducklow, H. W., Myers, K. M. S., Erickson, M., Ghiglione, J. F., & Murray, A. E. (2011). Response of a summertime Antarctic marine -bacterial community to glucose and ammonium enrichment. *Aquatic Microbial Ecology*, *64*(3), 205–220. https://doi.org/10.3354/ame01519

Ducklow, H. W., Purdie, D. A., Williams, P. J., & Davies, J. M. (1986). Bacterioplankton: a

sink for carbon in a coastal marine plankton community. *Science*, *232*(4752), 865–867. https://doi.org/10.1126/science.232.4752.865

Ducklow, H. W., Schofield, O. M. E., Vernet, M., Stammerjohn, S. E., & Erickson, M. (2012a). Multiscale control of bacterial production by phytoplankton dynamics and sea ice along the western Antarctic Peninsula: A regional and decadal investigation. *Journal of Marine Systems*, *98–99*, 26–39. https://doi.org/10.1016/j.jmarsys.2012.03.003

Ducklow, H. W., Stukel, M. R., Eveleth, R., Doney, S. C., Jickells, T., Schofield, O. M. E., … Cassar, N. (2018). Spring – summer net community production, new production, particle export and related water column biogeochemical processes in the marginal sea ice zone of the Western Antarctic Peninsula 2012 – 2014. *Philosophical Transactions of the Royal Society A: Mathematical, Physical and Engineering Sciences*, *376*(3). https://doi.org/10.1098/rsta.2017.0177

Dugdale, R. C., & Goering, J. J. (1967). Uptake of new and regenerated forms of nitrogen in primary productivity. *Limnology and Oceanography*, *12*(2), 196–206. https://doi.org/10.4319/lo.1967.12.2.0196

Emery, W. J., & Meincke, J. (1986). Global water masses: summary and review. *Oceanologica Acta*, *9*(4), 383–391.

Endres, S., Galgani, L., Riebesell, U., Schulz, K., & Engel, A. (2014). Stimulated Bacterial Growth under Elevated pCO2: Results from an Off-Shore Mesocosm Study. *PLoS ONE*, *9*(6), 1–8. https://doi.org/10.1371/journal.pone.0099228

Engel, A., Piontek, J., Grossart, H., Riebesell, U., Schulz, K. G., & Sperling, M. (2014). Impact of CO2 enrichment on organic matter dynamics during nutrient induced coastal phytoplankton blooms. *Journal of Plankton Research*, *36*(3), 641–657. https://doi.org/10.1093/plankt/fbt125

Eppley, R. W., & Peterson, B. J. (1979). Particulate Organic Matter Flux and Planktonic New Production in the Deep Ocean. *Nature*, *282*. https://doi.org/10.1017/CBO9781107415324.004

Epstein, S., & Mayeda, T. (1953). Variation of O-18 content of waters from natural sources. *Geochimica et Cosmochimica Acta*, *4*, 213–224.

Eveleth, R., Cassar, N., Sherrell, R. M., Ducklow, H. W., Meredith, M. P., Venables, H. J., … Li, Z. (2017). Ice melt influence on summertime net community production along the Western Antarctic Peninsula. *Deep-Sea Research Part II: Topical Studies in Oceanography*, *139*, 89–102. https://doi.org/10.1016/j.dsr2.2016.07.016

Fichot, C. G., & Benner, R. (2012). The spectral slope coefficient of chromophoric dissolved organic matter (S275 – 295) as a tracer of terrigenous dissolved organic carbon in river-influenced ocean margins. *Limnol. Oceanogr.*, *57*(5), 1453–1466. https://doi.org/10.4319/lo.2012.57.5.1453

Firing, Y. L., Chereskin, T. K., & Mazloff, M. R. (2011). Vertical structure and transport of the Antarctic Circumpolar Current in Drake Passage from direct velocity observations. *Journal of Geophysical Research: Oceans*, *116*(8), 1–16. https://doi.org/10.1029/2011JC006999

First, M. R., & Hollibaugh, J. T. (2009). The model high molecular weight DOC compound, dextran, is ingested by the benthic ciliate Uronema marinum but does not supplement ciliate growth. *Aquatic Microbial Ecology*, *57*(1), 79–87. https://doi.org/10.3354/ame01338

Fisher, T. R., & Rochelle-Newall, E. (2002). Production of chromophoric dissolved organic matter fluorescence in marine and estuarine environments: an investigation into the role of phytoplankton. *Marine Chemistry*, *77*(1), 7–21. Retrieved from

http://linkinghub.elsevier.com/retrieve/pii/S030442030100072X

Foldvik, A., & Gammelsrød, T. (1988). Notes on Southern-Ocean Hydrography, Sea-Ice And Bottom Water Formation. *Palaeogeography Palaeoclimatology Palaeo-Ecology*, *67*(1–2), 3–17.

Fraser, W. R., Patterson-Fraser, D. L., Ribic, C. A., Schofield, O. M. E., & Ducklow, H. W. (2013). A Nonmarine Source of Variability in Adelie Penguin Demography. *Oceanography*, *26*(3), 207–209. https://doi.org/10.5670/oceanog.2011.65

Fripiat, F., Sigman, D. M., Masse, G., & Tison, J.-L. (2015). High turnover rates indicated by changes in the fixed N forms and their stable isotopes in Antarctic landfast sea ice. *Journal of Geophysical Research: Oceans*, *120*, 3079–3097. https://doi.org/10.1002/2014JC010299.Received

Fripiat, François, Meiners, K. M., Vancoppenolle, M., Papadimitriou, S., Thomas, D. N., Ackley, S. F., … Tison, J.-L. (2017). Macro-nutrient concentrations in Antarctic pack ice: Overall patterns and overlooked processes. *Elem Sci Anth*, *5*(0), 13. https://doi.org/10.1525/elementa.217

Garibotti, I. A., Vernet, M., Ferrario, M. E., Smith, R. C., Ross, R., & Quetin, L. B. (2003). Phytoplankton spatial distribution patterns along the western Antarctic Peninsula (Southern Ocean). *Marine Ecology Progress Series*, *261*, 21–39. https://doi.org/10.3354/meps261021

Garibotti, I. A., Vernet, M., Smith, R. C., & Ferrario, M. E. (2005). Interannual variability in the distribution of the phytoplankton standing stock across the seasonal sea-ice zone west of the Antarctic Peninsula. *Journal of Plankton Research*, *27*(8), 825–843. https://doi.org/10.1093/plankt/fbi056

Garzio, L. M., & Steinberg, D. K. (2013). Microzooplankton grazing along the Western Antarctic Peninsula Deep-Sea Research I Microzooplankton community composition along the Western Antarctic Peninsula. *Deep-Sea Research Part I*, *77*(October 2014), 36–49. https://doi.org/10.1016/j.dsr.2013.03.001

Gasol, J. M., & Del Giorgio, P. A. (2000). Using flow cytometry for counting natural planktonic bacteria and understanding the structure of planktonic bacterial communities. *Scientia Marina*, *64*(2), 197–224. https://doi.org/10.3989/scimar.2000.64n2197

Gasol, J. M., Zweifel, U. L. I., Peters, F., Fuhrman, J. A., & Hagstroem, A. (1999). Significance of Size and Nucleic Acid Content Heterogeneity as Measured by Flow Cytometry in Natural Planktonic Bacteria. *Applied and Environmental Microbiology*, *65*(10), 4475–4483.

Ghiglione, J. F., & Murray, A. E. (2012). Pronounced summer to winter differences and higher wintertime richness in coastal Antarctic marine bacterioplankton. *Environmental Microbiology*, *14*(3), 617–629. https://doi.org/10.1111/j.1462-2920.2011.02601.x

Gobler, C. J., & Sañudo-Wilhelmy, S. a. (2003). Cycling of colloidal organic carbon and nitrogen during an estuarine phytoplankton bloom. *Limnology and Oceanography*, *48*(6), 2314–2320. https://doi.org/10.4319/lo.2003.48.6.2314

Goldberg, S. J., Carlson, C. A., Hansell, D. A., Nelson, N. B., & Siegel, D. A. (2009). Temporal dynamics of dissolved combined neutral sugars and the quality of dissolved organic matter in the Northwestern Sargasso Sea. *Deep-Sea Research I*, *56*, 672–685. https://doi.org/10.1016/j.dsr.2008.12.013

Goldman, J. C., Caron, D. A., & Dennett, M. R. (1987). Regulation of gross growth efficiency and ammonium regeneration in bacteria by responses of marine organisms. *Limnology and Oceanography*, *32*(6), 1239–1252.

Goldman, J. C., & Dennett, M. R. (1991). Ammonium regeneration and carbon utilization by marine bacteria grown on mixed substrates. *Marine Biology*, *109*(3), 369–378. https://doi.org/10.1007/BF01313502

Goldman, J. C., & Dennett, M. R. (2000). Growth of marine bacteria in batch and continuous culture under carbon and nitrogen limitation. *Limnol. Oceanogr.*, *45*(4), 789–800.

Gomes, A., Gasol, J. M., Estrada, M., Franco-Vidal, L., Díaz-Pérez, L., Ferrera, I., & Morán, X. A. G. (2015). Heterotrophic bacterial responses to the winter-spring phytoplankton bloom in open waters of the NW Mediterranean. *Deep-Sea Research Part I: Oceanographic Research Papers*, *96*, 59–68. https://doi.org/10.1016/j.dsr.2014.11.007

Granéli, E., Carlsson, P., & Legrand, C. (1999). The role of C, N and P in dissolved and particulate organic matter as a nutrient source for phytoplankton growth, including toxic species. *Aquatic Ecology*, *33*(1), 17–27. https://doi.org/10.1023/A:1009925515059

Gruber, N., Gloor, M., Mikaloff Fletcher, S. E., Doney, S. C., Dutkiewicz, S., Follows, M. J., … Takahashi, T. (2009). Oceanic sources, sinks, and transport of atmospheric CO2. *Global Biogeochemical Cycles*, *23*(1), 1–21. https://doi.org/10.1029/2008GB003349

Hall, J. A., & Safi, K. (2001). The impact of in situ Fe fertilisation on the microbial food web in the Southern Ocean. *Deep-Sea Research Part II: Topical Studies in Oceanography*, *48*(11–12), 2591–2613. https://doi.org/10.1016/S0967-0645(01)00010-8

Hansell, D. A. (2013). Recalcitrant Dissolved Organic Carbon Fractions. *Annual Review of Marine Science*, *5*(1), 120717164858000. https://doi.org/10.1146/annurev-marine-120710-100757

Hansell, D. A. (2002). DOC in the Global Ocean Carbon Cycle. *Biogeochemistry of Marine Dissolved Organic Matter*, 685–715. https://doi.org/10.1016/B978-012323841-2/50017-8

Hansell, D. A., & Carlson, C. A. (1998). Deep-ocean gradients in the concentration of dissolved organic carbon. *Nature*, *395*, 263–266. https://doi.org/10.1890/0012-9623(2008)89[19:DOC]2.0.CO;2

Hansell, D. A., Carlson, C. A., Repeta, D. J., & Schlitzer, R. (2009). Dissolved Organic Matter in the Ocean - a controversy stimulates insights. *Oceanography*, *22*(4).

Hansell, D. A., & Peltzer, E. T. (1998). Spatial and temporal variations of total organic carbon in the Arabian Sea. *Deep-Sea Research II*, *45*(10–11), 2171–2193.

Harrison, W. G. (1980). Nutrient regeneration and primary production in the sea. In Primary productivity in the sea. *Brookhaven Symp. Biol. 3 1. Plenum.*, 433–460.

Hauri, C., Doney, S. C., Takahashi, T., Erickson, M., Jiang, G., & Ducklow, H. W. (2015). Two decades of inorganic carbon dynamics along the West Antarctic Peninsula. *Biogeosciences*, *12*(22), 6761–6779. https://doi.org/10.5194/bg-12-6761-2015

Henley, S. F. (2013). *Climate-induced changes in carbon and nitrogen cycling in the rapidly warming Antarctic coastal ocean*. University of Edinburgh.

Henley, S. F., Annett, A. L., Ganeshram, R. S., Carson, D. S., Weston, K., Crosta, X., … Clarke, A. (2012). Factors influencing the stable carbon isotopic composition of suspended and sinking organic matter in the coastal Antarctic sea ice environment. *Biogeosciences*, *9*(3), 1137–1157. https://doi.org/10.5194/bg-9-1137-2012

Henley, S. F., Jones, E. M., Venables, H. J., Meredith, M. P., Firing, Y. L., Dittrich, R., … Dougans, J. (2018). Macronutrient and carbon supply, uptake and cycling across the Antarctic Peninsula shelf during summer. *Philosophical Transactions of the Royal Society A: Mathematical, Physical and Engineering Sciences*, *376*. https://doi.org/10.1098/rsta.2017.0168

Henley, S. F., Schofield, O. M. E., Hendry, K. R., Schloss, I. R., Steinberg, D. K., Moffat, C., … Meredith, M. P. (2019). Variability and change in the west Antarctic Peninsula marine system: research priorities and opportunities. *Progress in Oceanography*, *173*(February), 208–237. https://doi.org/10.1016/j.pocean.2019.03.003

Henley, S. F., Tuerena, R. E., Annett, A. L., Fallick, A. E., Meredith, M. P., Venables, H. J., … Ganeshram, R. S. (2017). Macronutrient supply, uptake and recycling in the coastal ocean of the west Antarctic Peninsula. *Deep-Sea Research Part II: Topical Studies in Oceanography*, *139*(October 2016), 58–76. https://doi.org/10.1016/j.dsr2.2016.10.003

Hernando, M., Schloss, I. R., Malanga, G., Almandoz, G. O., Ferreyra, G. A., Aguiar, M. B., & Puntarulo, S. (2015). Effects of salinity changes on coastal Antarctic phytoplankton physiology and assemblage composition. *Journal of Experimental Marine Biology and Ecology*, *466*, 110–119. https://doi.org/10.1016/j.jembe.2015.02.012

Heukelem, L. Van, & Thomas, C. S. (2001). Computer-assisted high-performance liquid chromatography method development with applications to the isolation and analysis of phytoplankton pigments. *Journal of Chromatography A*, *910*, 31–49.

Hobbs, W. R., Massom, R. A., Stammerjohn, S., Reid, P., Williams, G., & Meier, W. (2016). A review of recent changes in Southern Ocean sea ice, their drivers and forcings. *Global and Planetary Change*, *143*, 228–250. https://doi.org/10.1016/j.gloplacha.2016.06.008

Hofmann, E. E., Klinck, J. M., Lascara, C. M., & Smith, D. A. (1996). *Water mass distribution and circulation west of the Antarctic Peninsula and including Bransfield Strait*. (May), 61–80. https://doi.org/10.1029/AR070p0061

Holmes, R. M., Aminot, A., Kérouel, R., Hooker, B. A., & Peterson, B. J. (1999). A simple and precise method for measuring ammonium in marine and freshwater ecosystems. *Canadian Journal of Fisheries and Aquatic Sciences*, *56*(10), 1801–1808. https://doi.org/10.1139/f99-128

Hood, E., Fellman, J., Spencer, R. G. M., Hernes, P. J., Edwards, R., Damore, D., & Scott, D. (2009). Glaciers as a source of ancient and labile organic matter to the marine environment. *Nature*, *462*(7276), 1044–1047. https://doi.org/10.1038/nature08580

Hopkinson Jr., C. S., & Vallino, J. J. (2005). Efficient export of carbon to the deep ocean through dissolved organic matter. *Letters to Nature*, *433*(January), 715–717.

Hubberten, U., Laral, R. J., & Kattnerl, G. (1995). Refractory organic compounds in polar waters : Relationship between humic substances and amino acids in the Arctic and Antarctic. *Journal of Marine Research*, *53*, 137–149. https://doi.org/10.1357/0022240953213322

Hutchins, D. A. (1998). Iron-limited diatom growth and Si:N uptake ratios in a coastal upwelling regime. *Nature*, *393*(June), 65–68. https://doi.org/10.1038/31203

Jiang, H., Hu, Y., Ye, S. (2019). A highly sensitive in-situ CDOM sensor based on frequency spectrum shiftes m-sequence modulation. *IEEE Transactions on Instrumentation and Measurement* (9456)c,

Jiao, N., Azam, F., & Sanders, S. (2011). Microbial Carbon Pump in the Ocean. *Science*, (October).

Jiao, N., Herndl, G. J., Hansell, D. A., Benner, R., Kattner, G., Wilhelm, S. W., … Azam, F. (2010). Microbial production of recalcitrant dissolved organic matter: long-term carbon storage in the global ocean. *Nature Reviews. Microbiology*, *8*(8), 593–599. https://doi.org/10.1038/nrmicro2386

Junk, G., & Svec, H. J. (1958). The absolute abundance of the nitrogen isotopes in the atmosphere and compressed gas from various sources. *Geochimica et Cosmochimica*

Acta, *14*(3), 234–243. https://doi.org/10.1016/0016-7037(58)90082-6

Kähler, P., Bjornsen, P. K., Lochte, K., & Antia, A. (1997). Dissolved organic matter and its utilization by bacteria during spring in the Southern Ocean. *Deep-Sea Research Part II: Topical Studies in Oceanography*, *44*(1–2), 341–353. https://doi.org/10.1016/S0967-0645(96)00071-9

Kähler, P., & Koeve, W. (2001). Marine dissolved organic matter: Can its C:N ratio explain carbon overconsumption? *Deep-Sea Research Part I: Oceanographic Research Papers*, *48*(1), 49–62. https://doi.org/10.1016/S0967-0637(00)00034-0

Karl, D. M., & Björkman, K. M. (2015). Chapter 5: Dynamics of Dissolved Organic Phosphorus. In *Biogeochemistry of Marine Dissolved Organic Matter* (Second Edi). https://doi.org/10.1016/B978-0-12-405940-5.00005-4

Karl, D. M., Christian, J. R., & Dore, J. E. (1996). Microbial oceanography in the region west of the Antarctic peninsula: microbial dynamics, nitrogen cycle and carbon flux. *Foundations for Ecological Research West of the Antarctic Peninsula.*, *70*, 303–332.

Karl, D. M., Tilbrook, B. D., & Tien, G. (1991). Seasonal coupling of organic matter production and particle flux in the western Bransfield Strait, Antarctica. *Deep Sea Research*, *38*, 1097–1126.

Kawasaki, N., & Benner, R. (2006). Bacterial release of dissolved organic matter during cell growth and decline: Molecular origin and composition. *Limnology and Oceanography*, *51*(5), 2170–2180. https://doi.org/10.4319/lo.2006.51.5.2170

Kim, H., Doney, S. C., Iannuzzi, R. A., Meredith, M. P., Martinson, D. G., & Ducklow, H. W. (2016). Climate forcing for dynamics of dissolved inorganic nutrients at Palmer Station, Antarctica: An interdecadal (1993–2013) analysis. *Journal of Geophysical Research G: Biogeosciences*, *121*(9), 2369–2389. https://doi.org/10.1002/2015JG003311

Kim, H., & Ducklow, H. W. (2016). A Decadal (2002–2014) Analysis for Dynamics of Heterotrophic Bacteria in an Antarctic Coastal Ecosystem: Variability and Physical and Biogeochemical Forcings. *Frontiers in Marine Science*, *3*(November), 1–18. https://doi.org/10.3389/fmars.2016.00214

Kim, H., Ducklow, H. W., Abele, D., Barlett, E. M. R., Buma, A. G. J., Meredith, M. P., … Schloss, I. R. (2018). Inter-decadal variability of phytoplankton biomass along the coastal West Antarctic Peninsula. *Philosophical Transactions of the Royal Society A: Mathematical, Physical and Engineering Sciences*, *376*.

Kiørboe, T., & Jackson, G. A. (2001). Marine snow, organic solute plumes, and optimal chemosensory behavior of bacteria. *Limnology and Oceanography*, *46*(6), 1309–1318. https://doi.org/10.4319/lo.2001.46.6.1309

Kirchman, D. L., Morán, X. A. G., & Ducklow, H. W. (2009). Microbial growth in the polar oceans - role of temperature and potential impact of climate change. *Nature Reviews Microbiology*, *7*(6), 451–459. https://doi.org/10.1038/nrmicro2115

Klinck, J. M., Hofmann, E. E., Beardsley, R., Salihoglu, B., & Howard, S. (2004). Water-mass properties and circulation on the west Antarctic Peninsula Continental Shelf in Austral Fall and Winter 2001. *Deep-Sea Research Part II: Topical Studies in Oceanography*, *51*(17–19), 1925–1946. https://doi.org/10.1016/j.dsr2.2004.08.001

Knap, A., Michaels, A., Close, A., Ducklow, H. W., & Dickson, A. (1996). *Protocols for the Joint Global Ocean Flux studies (JGOFS) core measurements (JGOFS Report Nr. 19), Reprint of the IOC Manuals and Guides No. 29, UNESCO 1994 ed*. (19), vi + 170 pp.

Knapp, A., Sigman, D. M., Lipschultz, F. (2005). N isotopic composition of dissolved organic nitrogen and nitrate at the Bermuda Atlantic Time-Series Study site. Global Biogeochemical Cycles, 19(1).

Koch, B. P., Kattner, G., Witt, M., & Passow, U. (2014). Molecular insights into the microbial formation of marine dissolved organic matter: recalcitrant or labile? *Biogeosciences*, *11*(15), 4173–4190. https://doi.org/10.5194/bg-11-4173-2014

Kohut, J. T., Winsor, P., Statscewich, H., Oliver, M. J., Fredj, E., Couto, N., … Fraser, W. (2018). Variability in summer surface residence time within a West Antarctic Peninsula biological hotspot. *Philosophical Transactions of the Royal Society A: Mathematical, Physical and Engineering Sciences*, *376*. https://doi.org/10.1098/rsta.2017.0165

Kozlowski, W. A., Deutschman, D., Garibotti, I., Trees, C., & Vernet, M. (2011). An evaluation of the application of CHEMTAX to Antarctic coastal pigment data. *Deep-Sea Research Part I: Oceanographic Research Papers*, *58*(4), 350–364. https://doi.org/10.1016/j.dsr.2011.01.008

Kujawinski, E. B., Longnecker, K., Barott, K. L., Weber, R. J. M., & Soule, M. C. K. (2016). Microbial Community Structure Affects Marine Dissolved Organic Matter Composition. *Frontiers in Marine Science*, *3*(April), 1–15. https://doi.org/10.3389/fmars.2016.00045

Lachlan-Cope, T. A., Connolley, W. M., & Turner, J. (2001). The Role of the Non-Axisymmetric Antarctic Orography in forcing the Observed Pattern of Variability of the Antarctic Climate. *Geophysical Research Letters*, *28*(21), 4111–4114.

Lafrenière, M., & Sharp, M. (2004). The Concentration and Fluorescence of Dissolved Organic Carbon (DOC) in Glacial and Nonglacial Catchments: Interpreting Hydrological Flow Routing and DOC Sources. *Arctic, Antarctic, and Alpine Research*, *36*(2), 156–165. https://doi.org/10.1657/1523-0430(2004)036[0156:TCAFOD]2.0.CO;2

Lancelot, C., Billen, G., Veth, C., Becquevort, S., & Mathot, S. (1991). Modelling carbon cycling through phytoplankton and microbes in the Scotia—Weddell Sea area during sea ice retreat. *Marine Chemistry*, *35*(1–4), 305–324. https://doi.org/10.1016/S0304-4203(09)90024-X

Lechtenfeld, O. J., Kattner, G., Flerus, R., McCallister, S. L., Schmitt-Kopplin, P., & Koch, B. P. (2014). Molecular transformation and degradation of refractory dissolved organic matter in the Atlantic and Southern Ocean. *Geochimica et Cosmochimica Acta*, *126*, 321–337. https://doi.org/10.1016/j.gca.2013.11.009

Lenton, A., Tilbrook, B., Law, R., Bakker, D. C. E., Doney, S. C., Gruber, N., … Takahashi, T. (2013). Sea-air CO2 fluxes in the Southern Ocean for the period 1990-2009. *Biogeosciences Discussions*, *10*(1), 285–333. https://doi.org/10.5194/bgd-10-285-2013

Letscher, R. T., Moore, J. K., Teng, Y. C., & Primeau, F. (2015). Variable C : N : P stoichiometry of dissolved organic matter cycling in the Community Earth System Model. *Biogeosciences*, *12*(1), 209–221. https://doi.org/10.5194/bg-12-209-2015

Letscher, Robert T., Hansell, D. A., & Kadko, D. (2011). Rapid removal of terrigenous dissolved organic carbon over the Eurasian shelves of the Arctic Ocean. *Marine Chemistry*, *123*(1–4), 78–87. https://doi.org/10.1016/j.marchem.2010.10.002

Li, Y.-H., & Peng, T.-H. (2002). Latitudinal change of remineralization ratios in the oceans and its implication for nutrient cycles. *Global Biogeochemical Cycles*, *16*(4), 77-1-77–16. https://doi.org/10.1029/2001gb001828

Lizotte, M. P. (2006). The Contributions of Sea Ice Algae to Antarctic Marine Primary Production1. *American Zoologist*, *41*(1), 57–73. https://doi.org/10.1668/0003-1569(2001)041[0057:tcosia]2.0.co;2

Loginova, A. N., Borchard, C., Meyer, J., Hauss, H., Kiko, R., & Engel, A. (2015). Effects of nitrate and phosphate supply on chromophoric and fluorescent dissolved organic matter in the Eastern Tropical North Atlantic: a mesocosm study. *Biogeosciences*, 6897–6914. https://doi.org/10.5194/bg-12-6897-2015

Loginova, A. N., Thomsen, S., & Engel, A. (2016). Chromophoric and fluorescent dissolved organic matter in and above the oxygen minimum zone off Peru. *Journal of Geophysical Research: Oceans*, *121*, 7973–7990. https://doi.org/10.1002/2016JC011906.Received

Long, M. C., Thomas, L. N., & Dunbar, R. B. (2012). Control of phytoplankton bloom inception in the Ross Sea, Antarctica, by Ekman restratification. *Global Biogeochemical Cycles*, *26*(1), 1–14. https://doi.org/10.1029/2010GB003982

Long, R. A., & Azam, F. (2001). Microscale patchiness of bacterioplankton assemblage richness in seawater. *Aquatic Microbial Ecology*, *26*(2), 103–113. https://doi.org/10.3354/ame026103

López-Sandoval, D., Fernández, A., & Maranón, E. (2011). Dissolved and particulate primary production along a longitudinal gradient in the Mediterranean Sea. *Biogeosciences*, *8*(815–825).

Lourey, M. J., Trull, T. W., & Tilbrook, B. (2004). Sensitivity of δ13C of Southern Ocean suspended and sinking organic matter to temperature, nutrient utilization, and atmospheric CO2. *Deep-Sea Research Part I: Oceanographic Research Papers*, *51*(2), 281–305. https://doi.org/10.1016/j.dsr.2003.10.002

Luria, C., Ducklow, H., & Amaral-Zettler, L. (2014). Marine bacterial, archaeal and eukaryotic diversity and community structure on the continental shelf of the western Antarctic Peninsula. *Aquatic Microbial Ecology*, *73*(2), 107–121. https://doi.org/10.3354/ame01703

Luria, Catherine M., Amaral-Zettler, L. A., Ducklow, H. W., Repeta, D. J., Rhyne, A. L., & Rich, J. J. (2017). Seasonal Shifts in Bacterial Community Responses to Phytoplankton-Derived Dissolved Organic Matter in the Western Antarctic Peninsula. *Frontiers in Microbiology*, *8*(November), 1–13. https://doi.org/10.3389/fmicb.2017.02117

Lyons, W. B., Welch, K. A., & Doggett, J. K. (2007). Organic carbon in Antarctic snow. *Geophysical Research Letters*, *34*(2), 2–5. https://doi.org/10.1029/2006GL028150

Mackey, M. D., Mackey, D. J., Higgins, H. W., & Wright, S. W. (1996). CHEMTAX - a Program for Estimating Class Abundances From Chemical Markers: Application To HPLC measurements of phytoplankton. *Marine Ecology Progress Series*, *144*, 265–283.

Malinsky-Rushansky, N. Z., & Legrand, C. (1996). Excretion of dissolved organic carbon by phytoplankton of different sizes and subsequent bacterial uptake. *Mar Ecol Prog Ser*, *132*(February), 249–255. https://doi.org/10.3354/meps132249

Malits, A., Christaki, U., Obernosterer, I., & Weinbauer, M. G. (2014). Enhanced viral production and virus-mediated mortality of bacterioplankton in a natural iron-fertilized bloom event above the Kerguelen Plateau. *Biogeosciences*, *11*(23), 6841–6853. https://doi.org/10.5194/bg-11-6841-2014

Marañón, E., Cermeno, P., & Perez, V. (2005). Continuity in the photosynthetic production of dissolved organic carbon from eutrophic to oligotrophic waters. *Mar Ecol Prog Ser*, *299*, 7–17.

Marshall, G. J., Orr, A., van Lipzig, N. P. M., & King, J. C. (2006). The impact of a changing Southern Hemisphere Annular Mode on Antarctic Peninsula summer temperatures. *Journal of Climate*, *19*(20), 5388–5404. https://doi.org/10.1175/JCLI3844.1

Martin, J. H. (1990). Glacial - Interglacial CO2 change: The Iron Hypothesis. *Paleoceanography*, *5*(1), 1–13.

Martinson, D. G., & McKee, D. C. (2012). Transport of warm upper circumpolar deep water

onto the Western Antarctic Peninsula Continental Shelf. *Ocean Science*, *8*(4), 433–442. https://doi.org/10.5194/os-8-433-2012

Martinson, D. G., Stammerjohn, S. E., Iannuzzi, R. A., Smith, R. C., & Vernet, M. (2008). Western Antarctic Peninsula physical oceanography and spatio–temporal variability. *Deep Sea Research Part II: Topical Studies in Oceanography*, *55*(18–19), 1964–1987. https://doi.org/10.1016/j.dsr2.2008.04.038

Martiny, A. C., Pham, C. T. A., Primeau, F. W., Vrugt, J. A., Moore, J. K., Levin, S. A., & Lomas, M. W. (2013). Strong latitudinal patterns in the elemental ratios of marine plankton and organic matter. *Nature Geoscience*, *6*(4), 279–283. https://doi.org/10.1038/ngeo1757

McKnight, D. M., Andrews, E. D., Spaulding, S. A., & Aiken, G. R. (1994). Aquatic fulvic acids in algal-rich antarctic ponds. *Limnology and Oceanography*, *39*(8), 1972–1979. https://doi.org/10.4319/lo.1994.39.8.1972

Medeiros, P. M., Seidel, M., Powers, L. C., Dittmar, T., Hansell, D. A., & Miller, W. L. (2015). Dissolved organic matter composition and photochemical transformations in the northern North Pacific Ocean. *AGU Publications. Geophysical Research Letters*, *42*, 863–870. https://doi.org/10.1002/2014GL062663.Received

Meiners, K. M., & Michel, C. (2016). Chapter 17: Dynamics of nutrients, dissolved organic matter and exopolymers in sea ice. In *Sea Ice: Third Edition* (pp. 415–432). https://doi.org/10.1002/9781118778371.ch17

Meredith, M. P., Brandon, M. A., Wallace, M. I., Clarke, A., Leng, M. J., Renfrew, I. A., … King, J. C. (2008). Variability in the freshwater balance of northern Marguerite Bay, Antarctic Peninsula: Results from δ18O. *Deep-Sea Research Part II: Topical Studies in Oceanography*, *55*(3–4), 309–322. https://doi.org/10.1016/j.dsr2.2007.11.005

Meredith, M. P., & King, J. C. (2005). Rapid climate change in the ocean west of the Antarctic Peninsula during the second half of the 20th century. *Geophysical Research Letters*, *32*(19), 1–5. https://doi.org/10.1029/2005GL024042

Meredith, M. P., Stammerjohn, S. E., Venables, H. J., Ducklow, H. W., Martinson, D. G., Iannuzzi, R. A., … Barrand, N. E. (2016). Changing distributions of sea ice melt and meteoric water west of the Antarctic Peninsula. *Deep-Sea Research Part II: Topical Studies in Oceanography*, *139*, 1–18. https://doi.org/10.1016/j.dsr2.2016.04.019

Meredith, M. P., Venables, H. J., Clarke, A., Ducklow, H. W., Erickson, M., Leng, M. J., … Van Den Broeke, M. R. (2013). The freshwater system west of the Antarctic peninsula: Spatial and temporal changes. *Journal of Climate*, *26*(5), 1669–1684. https://doi.org/10.1175/JCLI-D-12-00246.1

Meredith, M. P., Wallace, M. I., Stammerjohn, S. E., Renfrew, I. A., Clarke, A., Venables, H. J., … Leng, M. J. (2010). Changes in the freshwater composition of the upper ocean west of the Antarctic Peninsula during the first decade of the 21st century. *Progress in Oceanography*, *87*(1–4), 127–143. https://doi.org/10.1016/j.pocean.2010.09.019

Mitchell, B. G., & Holm-Hansen, O. (1991). Observations and Modeling of the Antarctic Phytoplankton Crop in Relation to Mixing Depth. *Deep Sea Research Part A. Oceanographic Research Paperssearch*, *38*(8), 981–1007.

Moffat, C., Beardsley, R. C., Owens, B., & van Lipzig, N. (2008). A first description of the Antarctic Peninsula Coastal Current. *Deep-Sea Research Part II: Topical Studies in Oceanography*, *55*(3–4), 277–293. https://doi.org/10.1016/j.dsr2.2007.10.003

Molina, V., Morales, C. E., Farías, L., Cornejo, M., Graco, M., Eissler, Y., & Cuevas, L. A. (2012). Potential contribution of planktonic components to ammonium cycling in the coastal area off central-southern Chile during non-upwelling conditions. *Progress in Oceanography*, *92–95*, 43–49. https://doi.org/10.1016/j.pocean.2011.07.006

Moline, M. A. (1998). Photoadaptive response during the development of a coastal Antarctic diatom bloom and relationship to water column stability. *Limnol. Oceanogr.*, *43*(1), 146–153.

Moline, M. A., Claustre, H., Frazer, T. K., Schofield, O. M. E., & Vernet, M. (2004). Alteration of the food web along the Antarctic Peninsula in response to a regional warming trend. *Global Change Biology*, *10*(12), 1973–1980. https://doi.org/10.1111/j.1365-2486.2004.00825.x

Moline, M. a, & Prezelin, B. B. (1996). Long-term monitoring and analyses of physical factors regulating variability in coastal Antarctic phytoplankton composition over seasonal and interannual timescales. *Marine Ecology Progress Series*, *145*, 143–160. https://doi.org/Doi 10.3354/Meps145143

Møller, E. F. (2005). Sloppy feeding in marine copepods: prey-size-dependent production of dissolved organic carbon. *Journal of Plankton Research*, *27*, 27–35.

Montes-Hugo, M., Martinson, D. G., Stammerjohn, S. E., & Schofield, O. M. E. (2009). Recent Changes in Phytoplankton Communities Associated with Rapid Regional Climate Change Along the Western Antarctic Peninsula. *Science*, *323*(March).

Mopper, K., & Kieber, D. J. (2002). Photochemistry and the Cycling of Carbon, Sulfur, Nitrogen and Phosphorus. *Biogeochemistry of Marine Dissolved Organic Matter*, 455–489. https://doi.org/10.1016/B978-012323841-2/50011-7

Moran, M. A., & Zepp, R. G. (2000). UV Radiation Effects on Microbes and Microbial Processes. In D. L. Kirchman (Ed.), *Microbial Ecology of the Oceans* (pp. 201–228). New York.

Morán, X. A. G., Gasol, J. M., Pedrós-Alió, C., & Estrada, M. (2001). Dissolved and particulate primary production and bacterial production in offshore Antarctic waters during austral summer: Coupled or uncoupled? *Marine Ecology Progress Series*, *222*, 25–39. https://doi.org/10.3354/meps222025

Moreau, S., Mostajir, B., Belanger, S., Schloss, I., Vancoppenolle, M., Demers, S., & Ferreyra, G. A. (2015). Climate change enhances primary production in the western Antarctic Peninsula. *Global Change Biology*, *21*, 2191–2205. https://doi.org/10.1111/gcb.12878

Mostofa, K. M. G., Liu, C., Mottaleb, M. A., Wan, G., Ogawa, H., Vione, D., … Wu, F. (2013). Dissolved Organic Matter in Natural Waters. In *Photobiogeochemistry of Organic Matter. Principles and Practices in Water Environments*. https://doi.org/10.1007/978-3-642-32223-5

Mulholland, M. R., Glibert, P. M., Berg, G. M., Van Heukelem, L., Pantoja, S., & Lee, C. (1998). Extracellular amino acid oxidation by microplankton : a cross-ecosystem comparison. *Aquatic Microbial Ecology*, *15*(July), 141–152.

Mulholland, M. R., Lee, C., & Glibert, P. M. (2003). Extracellular enzyme activity and uptake of carbon and nitrogen along an estuarine salinity and nutrient gradient. *Marine Ecology Progress Series*, *258*(August), 3–17.

Müller-Niklas, G., Stefan, S., Kaltenböok, E., & Herndl, G. J. (1994). Organic content and bacterial metabolism in amorphous aggregations of the northern Adriatic Sea. *Limnology and Oceanography*, *39*(1), 58–68. https://doi.org/10.4319/lo.1994.39.1.0058

Murphy, J., & Riley, J. R. (1962). A modified single solution method for the determination of phosphate in natural waters. *Analytica Chimica Acta*, *27*, 31–36.

Myklestad, S. M. (2001). Dissolved Organic Carbon from Phytoplankton. In *The Handbook of Environmental Chemistry* (Volume 5D, pp. 111–148).

Nagata, T. (2000). Production mechanisms of dissolved organic matter. In *Microbial ecology of the oceans* (pp. 121–152).

Nagata, T., & Kirchman, D. L. (1999). Bacterial Mortality : A Pathway for the Formation of Refractory. *Microbial Biosystems: New Frontiers: Proceedings of the 8th International Symposium on Microbial Ecology*, *1*, 153–158.

Nichols, C. M., Bowman, J. P., & Guezennec, J. (2005). Effects of incubation temperature on growth and production of exopolysaccharides by an antarctic sea ice bacterium grown in batch culture. *Applied and Environmental Microbiology*, *71*(7), 3519–3523. https://doi.org/10.1128/AEM.71.7.3519-3523.2005

Nikrad, M. P., Cottrell, M. T., & Kirchman, D. L. (2014). Uptake of dissolved organic carbon by gammaproteobacterial subgroups in coastal waters of the West Antarctic Peninsula. *Applied and Environmental Microbiology*, *80*(11), 3362–3368. https://doi.org/10.1128/AEM.00121-14

Norkko, A., Thrush, S. F., Cummings, V. J., Gibbs, M. M., Andrew, N. L., Norkko, J., & Schwarz, A. M. (2007). Trophic structure of coastal Antarctic food webs associated with changes in sea ice and food supply. *Ecology*, *88*(11), 2810–2820. Retrieved from http://www.ncbi.nlm.nih.gov/pubmed/18051650

Norrman, B., Zwelfel, U. L., Hopkinson, C. S., & Fry, B. (1995). Production and utilization of dissolved organic carbon during an experimental diatom bloom. *Limnol. Oceanogr.*, *40*(5), 898–907.

Ogawa, H, Fukuda, R., & Koike, I. (1999). Vertical distributions of dissolved organic carbon and nitrogen in the Southern Ocean. *Deep Sea Research Part I: Oceanographic Research Papers*, *46*, 1809–1826. https://doi.org/10.1016/S0967-0637(99)00027-8

Oliver, J. L., Barber, R. T., Smith, W. O., & Ducklow, H. W. (2004). The heterotrophic bacterial response during the Southern Ocean Iron Experiment (SOFeX). *Limnology and Oceanography*, *49*(6), 2129–2140. https://doi.org/10.4319/lo.2004.49.6.2129

Opsahl, S., Benner, R., & Amon, R. M. W. (1999). Major flux of terrigenous dissolved organic matter through the Arctic Ocean. *Limnology and Oceanography*, *44*(8), 2017–2023. https://doi.org/10.4319/lo.1999.44.8.2017

Ortega-Retuerta, E., Reche, I., Pulido-Villena, E., Agustí, S., & Duarte, C. M. (2008). Exploring the relationship between active bacterioplankton and phytoplankton in the Southern Ocean. *Aquatic Microbial Ecology*, *52*(1), 99–106. https://doi.org/10.3354/ame01216

Ortega-Retuerta, E., Reche, I., Pulido-Villena, E., Agustí, S., & Duarte, C. M. (2010). Distribution and photoreactivity of chromophoric dissolved organic matter in the Antarctic Peninsula (Southern Ocean). *Marine Chemistry*, *118*(3–4), 129–139. https://doi.org/10.1016/j.marchem.2009.11.008

Osterholz, H., Singer, G., Wemheuer, B., Daniel, R., Simon, M., Niggemann, J., & Dittmar, T. (2016). Deciphering associations between dissolved organic molecules and bacterial communities in a pelagic marine system. *The ISME Journal*, *10*(7), 1–14. https://doi.org/10.1038/ismej.2015.231

Östlund, H. G., & Hut, G. (1984). Arctic Ocean Water Mass Balance From Isotope Data. *Journal of Geophysical Research*, *89*(C4), 6373–6381. https://doi.org/10.1029/JC089iC04p06373

Owens, N. J. P. (1988). Natural Variations in 15N in the Marine Environment. *Advances in Marine Biology*, *24*(C), 389–451. https://doi.org/10.1016/S0065-2881(08)60077-2

Pedulli, M., Bisagni, J. J., Ducklow, H. W., Beardsley, R., & Pilskaln, C. (2014). Estimates of potential new production (PNP) for the waters off the western Antarctic Peninsula

(WAP) region. *Continental Shelf Research*, *84*, 54–69. https://doi.org/10.1016/j.csr.2014.05.011

Perl, J. (2009). The SDU (CHORS) Method. The Third SeaWiFS HPLC Analysis Round-Robin Experiment (SeaHARRE-3). *NASA*, 89–91.

Piquet, A. M. T., Bolhuis, H., Meredith, M. P., & Buma, A. G. J. (2011). Shifts in coastal Antarctic marine microbial communities during and after melt water-related surface stratification. *FEMS Microbiology Ecology*, *76*(3), 413–427. https://doi.org/10.1111/j.1574-6941.2011.01062.x

Pollard, R., Treguer, P., & Read, J. (2006). Quantifying nutrient supply to the Southern Ocean. *Journal of Geophysical Research: Oceans*, *111*(5), 1–9. https://doi.org/10.1029/2005JC003076

Pomeroy, L., leB. Williams, P., Azam, F., & Hobbie, J. (2007). The Microbial Loop. *Oceanography*, *20*(2), 28–33. https://doi.org/10.5670/oceanog.2007.45

Pomeroy, L. R., & Wiebe, W. J. (2001). Temperature and substrate as interacting limiting factors. *Aquatic Microbial Ecology*, *23*, 187–204. https://doi.org/10.3354/ame023187

Post, A. L., Meijers, A. J. S., Fraser, A. D., & Raymond, B. (2014). Chapter 1: Environmental Setting. In C. De Broyer, P. Koubbi, H. J. Griffiths, B. Raymond, D. Udekem d'Acoz, A. P. Van de Putte, … Y. Ropert-Coudert (Eds.), *Biogeographic Atlas of the Southern Ocean.* (1st ed., pp. 46–64). Scientific Committee on Antarctic Research.

Prézelin, B. B., Hofmann, E. E., Mengelt, C., & Klinck, J. M. (2000). The linkage between Upper Circumpolar Deep Water (UCDW) and phytoplankton assemblages on the west Antarctic Peninsula continental shelf. *Journal of Marine Research*, *58*(2), 165–202. https://doi.org/10.1357/002224000321511133

Rafter, P. A., Difiore, P. J., & Sigman, D. M. (2013). Coupled nitrate nitrogen and oxygen isotopes and organic matter remineralization in the Southern and Pacific Oceans. *Journal of Geophysical Research: Oceans*, *118*(10), 4781–4794. https://doi.org/10.1002/jgrc.20316

Raphael, M. N., Marshall, G. J., Turner, J., Fogt, R. L., Schneider, D., Dixon, D. A., … Hobbs, W. R. (2016). The Amundsen sea low: Variability, change, and impact on Antarctic climate. *Bulletin of the American Meteorological Society*, *97*(1), 111–121. https://doi.org/10.1175/BAMS-D-14-00018.1

Raymond, P. A., McClelland, J. W., Holmes, R. M., Zhulidov, A. V., Mull, K., Peterson, B. J., … Gurtovaya, T. Y. (2007). Flux and age of dissolved organic carbon exported to the Arctic Ocean: A carbon isotopic study of the five largest arctic rivers. *Global Biogeochemical Cycles*, *21*(4), 1–9. https://doi.org/10.1029/2007GB002934

Redfield, A. C. (1958). The Biological Control of Chemical Factors in the Environment. *Sigma Xi, The Scientific Research Society*, *46*(3), 205–221. https://doi.org/10.2307/27828530

Reinthaler, T., Van Aken, H., Veth, C., Arístegui, J., Robinson, C., Williams, P. M., … Herndl, G. J. (2006). Prokaryotic respiration and production in the meso- and bathypelagic realm of the eastern and western North Atlantic basin. *Limnology & Oceanography*, *51*(3), 1262–1273. https://doi.org/10.4319/lo.2006.51.3.1262

Repeta, D. J. (2015). Chapter 2: Chemical Characterization and Cycling of Dissolved Organic Matter. In *Biogeochemistry of Marine Dissolved Organic Matter* (Second Edi). https://doi.org/10.1016/B978-0-12-405940-5.00002-9

Riebesell, U., Schloss, I., & Smetacek, V. (1991). Aggregation of algae released from melting sea ice: implications for seeding and sedimentation. *Polar Biology*, *11*(4), 239–248. https://doi.org/10.1007/BF00238457

Riedel, A., Michel, C., & Gosselin, M. (2006). Seasonal study of sea-ice exopolymeric substances on the Mackenzie shelf: Implications for transport of sea-ice bacteria and algae. *Aquatic Microbial Ecology*, *45*(2), 195–206. https://doi.org/10.3354/ame045195

Rijstenbil, J. W., Mur, L. R., Wijnholds, J. A., & Sinke, J. J. (1989). Impact of a temporal salinity decrease on growth and nitrogene metabolism of the marine diatom Skeletonema costatum in continuous cultures*. *Marine Biology*, *101*, 121–129.

Romera-Castillo, C., Sarmento, H., Alvarez-Salgado, X., Gasol, J. M., & Marrase, C. (2010). Production of chromophoric dissolved organic matter by marine phytoplankton. *Limnol. Oceanogr.*, *55*(1), 446–454.

Rozema, P. D., Venables, H. J., van de Poll, W. H., Clarke, A., Meredith, M. P., & Buma, A. G. J. (2016). Interannual variability in phytoplankton biomass and species composition in northern Marguerite Bay (West Antarctic Peninsula) is governed by both winter sea ice cover and summer stratification. *Limnology and Oceanography*, 235–252. https://doi.org/10.1002/lno.10391

Rozema, Patrick D., Biggs, T., Sprong, P. A. A., Buma, A. G. J., Venables, H. J., Evans, C., … Bolhuis, H. (2016). Summer microbial community composition governed by upper-ocean stratification and nutrient availability in northern Marguerite Bay, Antarctica. *Deep Sea Research Part II: Topical Studies in Oceanography*, 1–16. https://doi.org/10.1016/j.dsr2.2016.11.016

Saba, G. K., Fraser, W. R., Saba, V. S., Iannuzzi, R. A., Coleman, K. E., Doney, S. C., … Schofield, O. M. E. (2014). Winter and spring controls on the summer food web of the coastal West Antarctic Peninsula. *Nature Communications*, *5*, 4318. https://doi.org/10.1038/ncomms5318

Saba, G.K., Steinberg, D. K., & Bronk, D. A. (2009). Effects of diet on release of dissolved organic and inorganic nutrients by the copepod Acartia tonsa. *Marine Ecology Progress Series*, *386*, 147–161.

Saba, G.K., Steinberg, D. K., & Bronk, D. A. (2011). The relative importance of sloppy feeding, excretion, and fecal pellet leaching in the release of dissolved carbon and nitrogen by Acartia tonsa copepods. *Journal of Experimental Marine Biology 2 Ecology*, *404*, 47–56.

Sallée, J.-B., Matear, R. J., Rintoul, S. R., & Lenton, A. (2012). Localized subduction of anthropogenic carbon dioxide in the Southern Hemisphere oceans. *Nature Geoscience*, *5*(8), 579–584. https://doi.org/10.1038/ngeo1523

Sanders, R., & Jickells, T. (2000). Total organic nutrients in Drake Passage. *Deep-Sea Research Part I: Oceanographic Research Papers*, *47*(6), 997–1014. https://doi.org/10.1016/S0967-0637(99)00079-5

Santoso, A., England, M. H., & Hirst, A. C. (2006). Circumpolar Deep Water Circulation and Variability in a Coupled Climate Model. *Journal of Physical Oceanography*, *36*, 1523–1552. https://doi.org/10.1175/JPO2930.1

Sarmento, H., Romera-Castillo, C., Lindh, M., Pinhassi, J., Sala, M. M., Gasol, J. M., … Taylor, G. T. (2013). Phytoplankton species-specific release of dissolved free amino acids and their selective consumption by bacteria. *Limnology and Oceanography*, *58*(3), 1123–1135. https://doi.org/10.4319/lo.2013.58.3.1123

Schlitzer, R. (2017). *Ocean Data View 4*. Retrieved from http://odv.awi.de

Schoemann, V., Becquevort, S., Stefels, J., Rousseau, V., & Lancelot, C. (2005). Phaeocystis blooms in the global ocean and their controlling mechanisms: A review. *Journal of Sea Research*, *53*(1-2 SPEC. ISS.), 43–66. https://doi.org/10.1016/j.seares.2004.01.008

Schofield, O. M. E., Brown, M., Kohut, J., Nardelli, S., Saba, G., Waite, N., & Ducklow, H. W. (2018). Changing upper ocean mixed layer depth and phytoplankton productivity along the West Antarctic Peninsula. *Philosophical Transactions of the Royal Society A: Mathematical, Physical and Engineering Sciences*, *376*. https://doi.org/10.1098/rsta.2017.0173

Schofield, O. M. E., Miles, T. N., Alderkamp, A. C., Lee, S., Haskins, C., Rogalsky, E., … Yager, P. L. (2015). In situ phytoplankton distributions in the Amundsen Sea Polynya measured by autonomous gliders. *VIMS Article*, *827*.

Schofield, O. M. E., Saba, G., Coleman, K., Carvalho, F., Couto, N., Ducklow, H. W., … Waite, N. (2017). Decadal variability in coastal phytoplankton community composition in a changing West Antarctic Peninsula. *Deep Sea Research Part I: Oceanographic Research Papers*, *124*(April), 42–54. https://doi.org/10.1016/j.dsr.2017.04.014

Selz, V., Lowry, K. E., Lewis, K. M., Joy-Warren, H. L., Van De Poll, W., Nirmel, S., … Arrigo, K. R. (2018). Distribution of Phaeocystis antarctica-dominated sea ice algal communities and their potential to seed phytoplankton across the western Antarctic Peninsula in spring. *Marine Ecology Progress Series*, *586*, 91–112. https://doi.org/10.3354/meps12367

Serebrennikova, Y. M. (2005). *Ammonium distribution and dynamics in relation to biological production and physical environment in the Marguerite Bay Region of the West Antarctic Peninsula*.

Serebrennikova, Y. M., & Fanning, K. A. (2004). Nutrients in the Southern Ocean GLOBEC region: Variations, water circulation, and cycling. *Deep-Sea Research Part II: Topical Studies in Oceanography*, *51*(17–19), 1981–2002. https://doi.org/10.1016/j.dsr2.2004.07.023

Shen, Y., & Benner, R. (2018). Mixing it up in the ocean carbon cycle and the removal of refractory dissolved organic carbon. *Scientific Reports*, 1–9. https://doi.org/10.1038/s41598-018-20857-5

Sherr, E. B., & Sherr, B. F. (1988). Role of microbes in pelagic food webs: A revised concept. *Limnology and Oceanography*, *33*(5), 1225–1227. https://doi.org/10.4319/lo.1988.33.5.1225

Sherr, E. B., Sherr, B. F., & Longnecker, K. (2006). Distribution of bacterial abundance and cell-specific nucleic acid content in the Northeast Pacific Ocean. *Deep-Sea Research Part I: Oceanographic Research Papers*, *53*(4), 713–725. https://doi.org/10.1016/j.dsr.2006.02.001

Sigman, D., Karsh, K., & Casciotti, K. (2009a). Ocean Process Tracers: Nitrogen Isotopes in the Ocean. *Encyclopedia of Ocean Sciences*, (Ms 632), 4138–4153. https://doi.org/10.1006/rwos.2001.0172

Sigman, D. M., Altabet, M. A., McCorkle, D. C., François, R., & Fischer, G. (2000). The d15N of nitrate in the Southern Ocean: Nitrogen cycling and circulation in the ocean interior. *Journal of Geophysical Research*, *105*, 19599. https://doi.org/10.1029/2000JC000265

Sigman, D. M., & Casciotti, K. L. (2001). Nitrogen Isotopes in the Ocean. *Encyclopedia of Ocean Sciences*, (1997), 40–54. https://doi.org/10.1016/B978-012374473-9.00632-9

Sigman, D. M., Casciotti, K. L., Andreani, M., Barford, C., Galanter, M., & Böhlke, J. K. (2001). A bacterial method for the nitrogen isotopic analysis of nitrate in seawater and freshwater. *Analytical Chemistry*, *73*(17), 4145–4153. https://doi.org/10.1021/ac010088e

Sigman, D. M., Hain, M. P., & Haug, G. H. (2010). The polar ocean and glacial cycles in atmospheric CO2 concentration. *Nature*, *466*(7302), 47–55. https://doi.org/10.1038/nature09149

Sinninghe Damsté, J. S., Rampen, S., Irene, W., Rijpstra, C., Abbas, B., Muyzer, G., & Schouten, S. (2003). A diatomaceous origin for long-chain diols and mid-chain hydroxy methyl alkanoates widely occurring in quaternary marine sediments: Indicators for high-nutrient conditions. *Geochimica et Cosmochimica Acta*, *67*(7), 1339–1348. https://doi.org/10.1016/S0016-7037(02)01225-5

Sipler, R. E., & Bronk, D. A. (2015). Chapter 4: Dynamics of Dissolved Organic Nitrogen. In *Biogeochemistry of Marine Dissolved Organic Matter* (Second Edi). https://doi.org/10.1016/B978-0-12-405940-5.00004-2

Smart, S. M., Fawcett, S. E., Thomalla, S. J., Weigand, M. A., Reason, C. J. C., & Sigman, D. M. (2015). Isotopic evidence for nitrification in the Antarctic winter mixed layer. *AGU Publications. Global Biogeochemical Cycles*, *29*, 427–445. https://doi.org/10.1002/2014GB005013.Received

Smith, D. A., Hofmann, E. E., Klinck, J. M., & Lascara, C. M. (1999). Hydrography and circulation of the West Antarctic Peninsula Continental Shelf. *Deep-Sea Research Part I: Oceanographic Research Papers*, *46*(6), 925–949. https://doi.org/10.1016/S0967-0637(98)00103-4

Smith, D. C., & Azam, F. (1992). A simple, economical method for measuring bacterial protein synthesis rates in seawater using tritiated-leucine. *Marine Microbial Food Webs*, *6*(2), 107–114.

Smith, R. C., Baker, K. S., Fraser, W. R., Hofmann, E. E., Karl, D. M., Klinck, J. M., … Vernet, M. (1995). The Palmer LTER: A Long-Term Ecological Research Program At Palmer Station, Antarctica. *Oceanography*, *8*(3), 77–86.

Smith, R. C., Stammerjohn, S. E., & Baker, K. S. (1996). Surface Air Temperature Variations in the Western Antarctic Peninsula Region. *Foundations for Ecological Research West of the Antarctic Peninsula.*, *70*, 105–121.

Smith, W. O., & Comiso, J. C. (2008). Influence of sea ice on primary production in the Southern Ocean: A satellite perspective. *Journal of Geophysical Research: Oceans*, *113*(5), 1–19. https://doi.org/10.1029/2007JC004251

Soendergaard, M., Williams, P. M., Cauwet, G., Riemann, B., Robinson, C., Terzic, S., … Worm, J. (2000). Net accumulation and flux of dissolved organic carbon and dissolved organic nitrogen in marine plankton communities. *Limnology and Oceanography*, *45*(5), 1097–1111. https://doi.org/10.4319/lo.2000.45.5.1097

Stammerjohn, S. E., Martinson, D. G., Smith, R. C., & Iannuzzi, R. A. (2008). Sea ice in the western Antarctic Peninsula region: Spatio-temporal variability from ecological and climate change perspectives. *Deep-Sea Research Part II: Topical Studies in Oceanography*, *55*(18–19), 2041–2058. https://doi.org/10.1016/j.dsr2.2008.04.026

Stammerjohn, S. E., Martinson, D. G., Smith, R. C., Yuan, X., & Rind, D. (2008). Trends in Antarctic annual sea ice retreat and advance and their relation to El Niño–Southern Oscillation and Southern Annular Mode variability. *Journal of Geophysical Research*, *113*(C03S90), 1–20. https://doi.org/10.1029/2007JC004269

Stedmon, C. A., Thomas, D. N., Papadimitriou, S., Granskog, M. A., & Dieckmann, G. S. (2011). Using fluorescence to characterize dissolved organic matter in Antarctic sea ice brines. *Journal of Geophysical Research: Biogeosciences*, *116*(3), 1–9. https://doi.org/10.1029/2011JG001716

Stefels, J., Jones, E. M., Webb, A. L., van Leeuwe, M. A., Meredith, M. P., Henley, S. F., & Venables, H. J. (2018). Impact of sea-ice melt on dimethyl sulfide (sulfoniopropionate) inventories in surface waters of Marguerite Bay, West Antarctic Peninsula. *Philosophical Transactions of the Royal Society A: Mathematical, Physical and Engineering Sciences*, *376*(2122), 20170169. https://doi.org/10.1098/rsta.2017.0169

Steinberg, D. K., & Saba, G. K. (2008). Nitrogen Consumption and Metabolism in Marine Zooplankton. In *Nitrogen in the Marine Environment*. https://doi.org/10.1016/B978-0-12-372522-6.00026-8

Straza, T. R. A., Cottrell, M. T., Ducklow, H. W., & Kirchman, D. L. (2009). Geographic and phylogenetic variation in bacterial biovolume as revealed by protein and nucleic acid staining. *Applied and Environmental Microbiology*, *75*(12), 4028–4034. https://doi.org/10.1128/AEM.00183-09

Straza, T. R. a., Ducklow, H. W., Murray, A. E., & Kirchman, D. L. (2010). Abundance and single-cell activity of bacterial groups in Antarctic coastal waters. *Limnology and Oceanography*, *55*(6), 2526–2536. https://doi.org/10.4319/lo.2010.55.6.2526

Stubbins, A., Niggemann, J., & Dittmar, T. (2012). Photo-lability of deep ocean dissolved black carbon. *Biogeosciences*, *9*(5), 1661–1670. https://doi.org/10.5194/bg-9-1661-2012

Stukel, M. R., Asher, E. C., Couto, N., Schofield, O. M. E., Strebel, S., Tortell, P., & Ducklow, H. W. (2015). The Imbalance of New and Export Production in the Western Antarctic Peninsula, a potentially “leaky” ecosystem. *Global Biogeochemical Cycles*, *29*, 1400–1420. https://doi.org/10.1002/2015GB005211.Received

Stukel, M. R., & Ducklow, H. W. (2017). Stirring Up the Biological Pump: Vertical Mixing and Carbon Export in the Southern Ocean. *Global Biogeochemical Cycles*, *31*(9), 1420–1434. https://doi.org/10.1002/2017GB005652

Tagliabue, A., Sallée, J.-B., Bowie, A. R., Lévy, M., Swart, S., & Boyd, P. W. (2014). Surface-water iron supplies in the Southern Ocean sustained by deep winter mixing. *Nature Geoscience*, *7*(March), 314–320. https://doi.org/10.1038/NGEO2101

Takahashi, T., Sutherland, S. C., Wanninkhof, R., Sweeney, C., Feely, R. A., Chipman, D. W., … de Baar, H. J. W. (2009). Climatological mean and decadal change in surface ocean pCO2, and net sea-air CO2 flux over the global oceans. *Deep-Sea Research Part II: Topical Studies in Oceanography*, *56*(8–10), 554–577. https://doi.org/10.1016/j.dsr2.2008.12.009

Tang, K. W., Smith, W. O., Elliott, D. T., & Shields, A. R. (2008). Colony size of Phaeocystis antarctica (Prymnesiophyceae) as influenced by zooplankton grazers. *Journal of Phycology*, *44*(6), 1372–1378. https://doi.org/10.1111/j.1529-8817.2008.00595.x

Team, R. C. (2017). *R: A Language and Environment for Statistical Computing*. Vienna, Austria: R Foundation for Statistical Computing.

Thomas, D. N., Kattner, G., Engbrodt, R., Giannelli, V., Kennedy, H., Haas, C., & Dieckmann, G. S. (2001). Dissolved organic matter in Antarctic sea ice. *Annals of Glaciology*, *33*, 297–303. https://doi.org/10.3189/172756401781818338

Thomas, D. N., Kennedy, H., Kattner, G., Gerdes, D., Dieckmann, G. S., & Gough, C. (2001b). Biogeochemistry of platelet ice: its influence on particle flux under fast ice in the Weddell Sea, Antarctica. In *Ecological Studies in the Antarctic Sea Ice Zone* (pp. 169–179).

Tranvik, L. J. (1993). Microbial transformation of labile dissolved organic matter into humic-like matter in seawater. *FEMS Microbiol Ecol*, *12*(3), 177–183. https://doi.org/10.1016/0168-6496(93)90013-W

Treger, P., & Jaques, G. (1992). Dynamics of nutrients and phytoplankton, and fluxes of carbon, nitrogen, and silicon in the Antartic Ocean. *Polar Biology*, *12*, 149–162. https://doi.org/10.1007/BF00238255

Tremblay, L., Caparros, J., Leblanc, K., & Obernosterer, I. (2015). Origin and fate of particulate and dissolved organic matter in a naturally iron-fertilized region of the

Southern Ocean. *Biogeosciences*, *12*(2), 607–621. https://doi.org/10.5194/bg-12-607-2015

Trimborn, S., Hoppe, C. J. M., Taylor, B. B., Bracher, A., & Hassler, C. (2015). Physiological characteristics of open ocean and coastal phytoplankton communities of Western Antarctic Peninsula and Drake Passage waters. *Deep-Sea Research Part I: Oceanographic Research Papers*, *98*, 115–124. https://doi.org/10.1016/j.dsr.2014.12.010

Trull, T. W., Davies, D., & Casciotti, K. (2008). Insights into nutrient assimilation and export in naturally iron-fertilized waters of the Southern Ocean from nitrogen, carbon and oxygen isotopes. *Deep-Sea Research Part II: Topical Studies in Oceanography*, *55*(5–7), 820–840. https://doi.org/10.1016/j.dsr2.2007.12.035

Tuerena, R., Henley, S. F., Dougans, J., Tait, A., Fallick, T., & Ganeshram, R. S. (2015). *Measuring the Stable Isotopic Composition of Nitrogen and Oxygen in Dissolved Inorganic Nitrate using the Denitrifier Method*.

Turner, J., Lu, H., White, I., King, J. C., Phillips, T., Hosking, J. S., … Deb, P. (2016). Absence of 21st century warming on Antarctic Peninsula consistent with natural variability. *Nature*, *535*(7612), 1–1. https://doi.org/10.1038/nature18645

Turner, J., Maksym, T., Phillips, T., Marshall, G. J., & Meredith, M. P. (2013). The impact of changes in sea ice advance on the large winter warming on the western Antarctic Peninsula. *International Journal of Climatology*, *861*(March 2012), 852–861. https://doi.org/10.1002/joc.3474

Van den Meersche, K., Middelburg, J. J., Soetaert, K., Rijswijk, P. Van, Boschker, H. T. S., & Heip, C. H. R. (2004). Carbon-nitrogen coupling and algal-bacterial interactions during an experimental bloom : Modeling a 13 C tracer experiment. *Limnol. Oceanogr.*, *49*(3), 862–878.

Van Wessem, J. M., Reijmer, C. H., Van De Berg, W. J., Van Den Broeke, M. R., Cook, A. J., Van Ulft, L. H., & Van Meijgaard, E. (2015). Temperature and wind climate of the Antarctic Peninsula as simulated by a high-resolution Regional Atmospheric Climate Model. *Journal of Climate*, *28*(18), 7306–7326. https://doi.org/10.1175/JCLI-D-15-0060.1

Vaughan, D. G., Marshall, G. J., Connolley, W. M., Parkinson, C. L., Mulvaney, R., Hodgson, D. A., … Turner, J. (2003). Recent Rapid Regional Climate Warming on the Antarctic Peninusla. *Climate Change*, *60*, 243–274. https://doi.org/10.1017/S0016756800021464

Venables, H. J., Clarke, A., & Meredith, M. P. (2013). Wintertime controls on summer stratification and productivity at the western Antarctic Peninsula. *Limnology and Oceanography*, *58*(3), 1035–1047. https://doi.org/10.4319/lo.2013.58.3.1035

Verdugo, P. (2011). Marine Microgels. *Annual Review of Marine Science*, *4*, 375–400. https://doi.org/10.1016/B978-0-12-405940-5.00009-1

Vernet, M., Martinson, D. G., Iannuzzi, R. A., Stammerjohn, S. E., Kozlowski, W., Sines, K., … Garibotti, I. A. (2008). Primary production within the sea-ice zone west of the Antarctic Peninsula: I-Sea ice, summer mixed layer, and irradiance. *Deep-Sea Research Part II: Topical Studies in Oceanography*, *55*(18–19), 2068–2085. https://doi.org/10.1016/j.dsr2.2008.05.021

Vila-Costa, M., Gasol, J. M., Sharma, S., & Moran, M. A. (2012). Community analysis of high- and low-nucleic acid-containing bacteria in NW Mediterranean coastal waters using 16S rDNA pyrosequencing. *Environmental Microbiology*, *14*(6), 1390–1402. https://doi.org/10.1111/j.1462-2920.2012.02720.x

Wang, X. M., Yang, G. P., Lopez, D., Ferreyra, G., Lemarchand, K., & Xie, H. X. (2010). Late autumn to spring changes in the inorganic and organic carbon dissolved in the water

column at Scholaert Channel, West Antarctica. *Antarctic Science*, *22*(2), 145–156. https://doi.org/Doi 10.1017/S0954102009990666

Ward, B. B., & Bronk, D. A. (2001). Net nitrogen uptake and DON release in surface waters: Importance of trophic interactions implied from size fractionation experiments. *Marine Ecology Progress Series*, *219*, 11–24. https://doi.org/10.3354/meps219011

Waser, N. A. D., Harrison, P. J., Nielsen, B., Calvert, S. E., & Turpin, D. H. (1998). Nitrogen isotope fractionation during the uptake and assimilation of nitrate, nitrite, ammonium, and urea by a marine diatom. *Limnol. Oceanogr.*, *43*(2), 215–224.

Wear, E. K., Carlson, C. A., James, A. K., Brzezinski, M. A., Windecker, L. A., & Nelson, C. E. (2015). Synchronous shifts in dissolved organic carbon bioavailability and bacterial community responses over the course of an upwelling-driven phytoplankton bloom. *Limnology and Oceanography*, *60*(2), 657–677. https://doi.org/10.1002/lno.10042

Wedborg, M., Hoppema, M., & Skoog, A. (1998). On the relation between organic and inorganic carbon in the Weddell Sea. *Journal of Marine Systems*, *17*(1–4), 59–76. https://doi.org/10.1016/S0924-7963(98)00029-3

Weitz, J., & Wilhelm, S. (2012). Ocean viruses and their effects on microbial communities and biogeochemical cycles. *F1000 Biology Reports*, *8*(September), 2–9. https://doi.org/10.3410/B4-17

Wetz, M. S., & Wheeler, P. A. (2003). Production and partitioning of organic matter during simulated phytoplankton blooms. *Limnology and Oceanography*, *48*(5), 1808–1817. https://doi.org/10.4319/lo.2003.48.5.1808

Wheeler, P. a., Watkins, J. M., & Hansing, R. L. (1997). Nutrients, organic carbon and organic nitrogen in the upper water column of the Arctic Ocean: implications for the sources of dissolved organic carbon. *Deep Sea Research Part II: Topical Studies in Oceanography*, *44*(8), 1571–1592. https://doi.org/10.1016/S0967-0645(97)00051-9

Whitehouse, M. J., Atkinson, A., Rees, A. P., & Georgia, S. (2011). Close coupling between ammonium uptake by phytoplankton and excretion by Antarctic krill , Euphausia superba. *Deep-Sea Research Part I*, *58*(7), 725–732. https://doi.org/10.1016/j.dsr.2011.03.006

Wiebinga, C. J., Baar, H. J. W. De, Yamashita, Y., Tsukasaki, A., Nishida, T., & Tanoue, E. (1998). Determination of the distribution of dissolved organic carbon in the Indian sector of the Southern Ocean. *Marine Chemistry*, *61*(3–4), 185–201. https://doi.org/10.1016/S0304-4203(98)00014-0

Wilhelm, S. W., Suttle, C. A., & Wilhelm, W. (1999). Viruses and Nutrient Cycles the aquatic food webs. *BioScience*, *49*(10), 781–788.

Williams, P. J. (1995). Evidence for the seasonal accumulation of carbon-rich dissolved organic material, its scale in comparison with changes in particulate material and the consequential effect on net C/N assimilation ratios. *Marine Chemistry*, *51*(1), 17–29. https://doi.org/10.1016/0304-4203(95)00046-T

Williams, T. J., Long, E., Evans, F., Demaere, M. Z., Lauro, F. M., Raftery, M. J., … Cavicchioli, R. (2012). A metaproteomic assessment of winter and summer bacterioplankton from Antarctic Peninsula coastal surface waters. *The ISME Journal*, *6*(10), 1883–1900. https://doi.org/10.1038/ismej.2012.28

Wing, A. S. R., Mcleod, R. J., Leichter, J. J., Frew, R. D., Lamare, M. D., Wing, S. R., … Lamare, M. D. (2012). Sea ice microbial production supports Ross Sea benthic communities : influence of a small but stable subsidy Published by : Wiley on behalf of the Ecological Society of America Stable URL : http://www.jstor.org/stable/23143912 REFERENCES Linked references. *Ecology*, *93*(2), 314–323.

Wright, S. W., van den Enden, R. L., Pearce, I., Davidson, A. T., Scott, F. J., & Westwood, K. J. (2010). Phytoplankton community structure and stocks in the Southern Ocean (30-80°E) determined by CHEMTAX analysis of HPLC pigment signatures. *Deep-Sea Research Part II: Topical Studies in Oceanography*, *57*(9–10), 758–778. https://doi.org/10.1016/j.dsr2.2009.06.015

Young, J. N., Goldman, J. A. L., Kranz, S. A., Tortell, P. D., & Morel, F. M. M. (2015). Slow carboxylation of Rubisco constrains the rate of carbon fixation during Antarctic phytoplankton blooms. *New Phytologist*, *205*(1), 172–181. https://doi.org/10.1111/nph.13021

Zhang, G., Liang, S., Shi, X., & Han, X. (2015). Dissolved organic nitrogen bioavailability indicated by amino acids during a diatom to dinoflagellate bloom succession in the Changjiang River estuary and its adjacent shelf. *Marine Chemistry*, *176*, 83–95. https://doi.org/10.1016/j.marchem.2015.08.001

Zlotnik, I., & Dubinsky, Z. (1989). The effect of light and temperature on DOC excretion by phytoplankton. *Limnol. Oceanogr.*, *34*(5), 831–839.

Zubkov, M. V., Fuchs, B. M., Burkill, P. H., & Amann, R. (2001). Comparison of Cellular and Biomass Specific Activities of Dominant Bacterioplankton Groups in Stratified Waters of the Celtic Sea. *Applied and Environmental Microbiology*, *67*(11), 5210–5218. https://doi.org/10.1128/AEM.67.11.5210

8. Appendix

Table 1: List of all analyses included in this thesis, the method and where the analyses were conducted. Analysis in bold font were conducted by the author Ribanna Dittrich.

Parameter	Method	Institute of Analysis
DOC / TDN	**High Temperature Combustion**	**School of GeoSciences University of Edinburgh**
POC:N, δ^{13}C-POC, δ^{15}N -PN	**High temperature combustion with isotope mass spectrometry**	**School of GeoSciences, University of Edinburgh**
$\delta^{15}N\text{-}NO_3^-$	**Denitrifier method, IRMS**	**School of GeoSciences, University of Edinburgh**
PAL LTER NO_3^-, PO_4^-, $SiOH_4^-$	Segmented flow injection analysis	Ducklow laboratory, Lamont Doherty Earth Observatory
RaTS NO_3^-, PO_4^-, $SiOH_4^-$	Segmented flow injection analysis	Plymouth Marine Laboratory
Primary production	*In situ* ^{14}C incubation	Schofield Group, on-board *Laurence M. Gould*
Bacterial Abundance	Flow Cytometry following Gasol and del Giorgio 2000	Ducklow group, on-board *Laurence M. Gould*
Bacterial Production	^{3}H-leucine incorporation modified from Smith and Azam 1992	Ducklow group, on-board *Laurence M. Gould*
$\delta^{18}O_{H2O}$	Equilibration method following Epstein and Mayeda (1953) / mass spectrometry	NERC Isotope Geosciences Laboratory at the British Geological Survey
Dissolved Inorganic Carbon	Coulometry following Knap et al., (1996)	Ducklow laboratory, Lamont-Doherty Earth Observatory
Phytoplankton pigmentation	High-performance liquid chromatography	Faculty of Science and Engineering, University of Groningen

Table 2.1: Full-depth profiles of all parameters used in analyses of chapter 3 from RaTS season 2013/14. DOM, POM and inorganic nutrients are stated in µmol x L^{-1}, chlorophyll a in mg m^{-3}.

Date	Depth	DOC	DON	DOC	DOP	POC	PON	POC	POP	Chla	NO_3^-	NO_2^-	NH_4^+	PO_4^-	$SI(OH)_4^-$
16/11/2013	5	49.15	4.97	9.89		4.34	0.63	6.89	0.15		26.81	0.11	-	1.87	70.03
16/11/2013	15	42.16	10.13	4.16		4.25	0.65	6.54	0.14		26.69	0.08	0.72	1.91	70.74
16/11/2013	40	41.92	-	-		2.51	0.42	5.98	0.22		29.15	0.04	-	2.04	74.52
19/11/2013	5	47.36	7.23	6.55		3.54	0.51	6.94	0.14		27.75	0.11	0.25	1.93	72.13
19/11/2013	15	44.95	6.67	6.74		3.80	0.65	5.85	0.14		28.00	0.09	-	1.96	73.18
19/11/2013	40	47.42	6.09	7.79		2.44	0.36	6.78	0.31		29.48	0.04	-	2.05	75.88
19/11/2013	100	42.91	6.50	6.60		1.10	0.12	9.17	0.11		31.78	0.01	-	2.27	86.99
25/11/2013	0	51.28	6.92	7.41		4.55	0.71	6.41	0.07		28.22	0.08	0.25	1.95	72.97
25/11/2013	5	48.56	5.16	9.40		4.25	0.69	6.16	0.11		28.43	0.10	-	1.96	74.60
25/11/2013	15	42.10	4.80	8.76		4.29	0.75	5.72	0.12		28.95	0.07	0.23	2.02	77.72
25/11/2013	25	40.36	5.38	7.50		4.08	0.68	6.00	0.24		29.06	0.07	-	2.04	76.19
25/11/2013	40	62.44	4.80	13.01		3.73	0.62	6.02	0.39		29.55	0.07	-	2.05	80.44
28/11/2013	0	40.54	7.18	5.65		4.87	0.84	5.80	0.09		24.53	0.08	0.28	1.75	68.36
28/11/2013	15	40.42	6.72	6.01		5.66	1.02	5.55	0.16		26.99	0.09	0.24	1.93	73.40
02/12/2013	0	44.83	4.93	9.09		5.74	1.07	5.36	0.13		27.02	0.12	0.39	1.87	72.21
02/12/2013	5	41.98	7.90	5.31		5.49	1.05	5.23	0.15		25.57	0.12	-	1.79	71.29
02/12/2013	15	45.83	4.09	11.21		6.70	1.21	5.54	0.14		27.61	0.11	0.44	1.89	73.60
02/12/2013	25	42.40	7.09	5.98		6.29	1.17	5.38	0.20		26.10	0.10	-	1.85	73.53
02/12/2013	40	42.94	6.64	6.47		5.86	1.03	5.69	0.47		28.31	0.06	-	1.97	76.24
05/12/2013	0	43.12	5.65	7.63		7.14	1.35	5.29	0.14		26.19	0.18	0.19	1.77	71.48
05/12/2013	15	42.73	4.71	9.07		8.65	1.73	5.00	0.20		26.41	0.12	0.16	1.80	73.10
09/12/2013	0	45.97	5.14	8.94		19.77	3.86	5.12	0.29		23.17	0.20	0.66	1.56	68.75
09/12/2013	5	48.21	5.60	8.61		24.47	4.81	5.09	0.29		23.17	0.20	-	1.56	68.75
09/12/2013	25	45.56	5.43	8.39		14.82	2.76	5.37	1.41		23.93	0.08	-	1.63	70.49
09/12/2013	40	41.16	7.15	5.76		11.93	2.21	5.40	1.09		25.98	0.06	-	1.80	73.23
13/12/2013	5	53.86	3.68	14.64		68.42	12.55	5.45	5.62		13.14	0.21	-	0.80	60.77
13/12/2013	15	48.51	-	-		21.49	4.18	5.14	2.85		23.15	0.09	0.27	1.50	68.16
13/12/2013	25	43.09	4.96	8.69		12.19	2.17	5.62	1.36		26.02	0.06	-	1.73	71.29
13/12/2013	40	43.93	5.17	8.50		5.92	1.04	5.69	0.78		28.03	0.06	-	1.91	75.43
19/12/2013	0	88.65	8.46	10.48		166.26	18.79	8.85	-		0.04	0.01	-	0.03	28.63
24/12/2013	0	76.09	5.83	13.06		119.72	10.18	11.76	1.77		0.05	0.00	-	0.03	0.56
24/12/2013	5	55.08	6.41	8.59		117.22	14.86	7.89	13.02		2.85	0.07	-	0.11	2.37
24/12/2013	15	50.27	8.02	6.27		50.95	7.77	6.56	9.23		16.14	0.11	-	1.15	41.88
24/12/2013	25	60.02	5.87	10.22		12.21	2.03	6.01	3.27		25.48	0.09	-	1.80	69.51
24/12/2013	40	55.03	5.73	9.60		6.54	0.94	6.96	0.26		29.14	0.08	-	2.06	78.98
28/12/2013	0	54.35	4.52	12.02		78.95	10.53	7.50	1.16		0.96	0.06	-	0.01	9.90
28/12/2013	5	57.69	6.59	8.75		51.55	7.89	6.53	6.56		11.77	0.12	-	0.66	39.00
28/12/2013	15	48.01	5.72	8.39		45.55	7.45	6.11	3.26		16.44	0.12	-	0.96	47.26
28/12/2013	25	41.09	5.15	7.98		-	-	-	1.37		26.93	0.10	-	1.83	69.38
28/12/2013	40	53.87	5.56	9.69		6.29	0.79	7.96	0.26		29.47	0.10	-	2.04	77.39
30/12/2013	15	45.04	4.24	10.62		24.16	3.61	6.69	4.87		24.50	0.10	1.11	1.67	63.42
30/12/2013	100	42.78	-	-		1.64	0.23	7.13	0.11		38.33	0.09	-	2.78	103.12
06/01/2014	0	52.40	4.76	11.01		48.41	5.78	8.38	0.40		0.05	0.00	0.24	0.01	3.07
06/01/2014	5	50.33	5.74	8.77		50.55	8.10	6.24	1.99		6.25	0.12	-	0.26	16.73
06/01/2014	15	43.85	4.76	9.21		27.94	4.89	5.71	4.61		18.62	0.12	1.26	1.29	43.07
06/01/2014	25	48.36	7.00	6.91		19.69	3.36	5.86	2.45		22.47	0.11	-	1.62	56.28
06/01/2014	40	40.97	-	-		8.10	1.24	6.53	0.83		27.45	0.12	-	2.02	73.29
08/01/2014	5	51.43	5.84	8.81		37.46	6.26	5.98	-		0.48	0.03	-	0.04	6.89
15/01/2014	0	66.28	4.63	14.32		9.78	1.97	4.96	0.14		22.21	0.14	1.38	1.56	59.02
15/01/2014	5	45.94	5.72	8.03		9.43	1.96	4.81	0.12		23.35	0.14	-	1.65	62.66
15/01/2014	15	54.39	4.52	12.03		6.03	1.29	4.67	0.13		25.83	0.15	1.81	1.91	70.66
15/01/2014	25	56.85	7.52	7.56		6.84	1.44	4.75	0.17		24.66	0.14	-	1.78	65.98
15/01/2014	40	45.06	6.28	7.18		5.02	1.05	4.78	0.30		28.40	0.15	-	2.07	75.51

Table 2.1 cont'd: Full-depth profiles of all parameters used in analyses of chapter 3 from RaTS season 2013/14. Temperature in °C, density in kg m^{-3}, MLD in meters, sea-ice cover in scores from 1 to 10 with 10 – 100% sea-ice cover. %sim=%sea ice meltwater, %met = %meteoric meltwater (glacial), %cdw = % circumpolar deepwater

Date	Depth	Temper-ature	Density	Salinity	MLD	SeaIce	%sim	%met	%cdw
16/11/2013	5	-1.58	27.08	33.65	8	8	-	-	-
16/11/2013	15	-1.54	27.24	33.84	-	-	-0.14	2.37	97.77
16/11/2013	40	-1.39	27.31	33.94	-	-	-	-	-
19/11/2013	5	-1.49	27.20	33.80	23	4	-	-	-
19/11/2013	15	-1.53	27.22	33.82	-	-	-0.22	2.48	97.74
19/11/2013	40	-1.43	27.29	33.91	-	-	-	-	-
19/11/2013	100	-0.57	27.45	34.14	-	-	-	-	-
25/11/2013	0	-1.24	27.23	33.85	53	1	-0.23	2.42	97.81
25/11/2013	5	-1.26	27.24	33.85	-	-	-	-	-
25/11/2013	15	-1.18	27.25	33.88	-	-	-0.06	2.19	97.87
25/11/2013	25	-1.11	27.26	33.89	-	-	-	-	-
25/11/2013	40	-1.04	27.27	33.91	-	-	-	-	-
28/11/2013	0	-1.16	27.13	33.72	10	2	-0.24	2.79	97.44
28/11/2013	15	-0.93	27.19	33.81			-0.17	2.49	97.68
02/12/2013	0	-0.76	27.05	33.65	11	4	-0.08	2.88	97.21
02/12/2013	5	-0.68	27.09	33.69	-	-	-	-	-
02/12/2013	15	-0.80	27.13	33.74	-	-	0.16	2.41	97.44
02/12/2013	25	-1.04	27.18	33.79	-	-	-	-	-
02/12/2013	40	-1.15	27.24	33.87	-	-	-	-	-
05/12/2013	0	0.03	26.87	33.47	2	5	-0.55	3.76	96.79
05/12/2013	15	-0.73	27.10	33.70			-0.19	2.80	97.39
09/12/2013	0	0.51	26.78	33.38	8	6	-	-	-
09/12/2013	5	0.51	26.78	33.38	-	-	-	-	-
09/12/2013	25	-0.75	27.13	33.75	-	-	-	-	-
09/12/2013	40	-1.15	27.22	33.84	-	-	-	-	-
13/12/2013	5	0.38	26.87	33.49	1	6	-	-	-
13/12/2013	15	-0.72	27.08	33.68	-	-	-0.13	2.81	97.32
13/12/2013	25	-1.04	27.16	33.77	-	-	-	-	-
13/12/2013	40	-1.14	27.24	33.86	-	-	-	-	-
19/12/2013	0	-	-	-	-	1	-	-	-
24/12/2013	0	0.69	26.09	32.54	2	3	1.46	4.85	93.70
24/12/2013	5	0.13	26.46	32.97	-	-	-	-	-
24/12/2013	15	-0.39	26.91	33.49	-	-	-0.26	3.48	96.78
24/12/2013	25	-0.84	27.08	33.68	-	-	-	-	-
24/12/2013	40	-1.14	27.24	33.87	-	-	-	-	-
28/12/2013	0	1.19	26.32	32.86	2	3	0.66	4.55	94.79
28/12/2013	5	0.32	26.81	33.41	-	-	-	-	-
28/12/2013	15	-0.96	27.01	33.59	-	-	-0.03	3.01	97.02
28/12/2013	25	-1.25	27.16	33.76	-	-	-	-	-
28/12/2013	40	-1.15	27.28	33.91	-	-	-	-	-
30/12/2013	15	-0.95	27.07	33.66	1	3	-0.45	3.14	97.31
30/12/2013	100	-0.21	27.49	34.21	-	-	-	-	-
06/01/2014	0	2.48	26.25	32.89	1	4	-0.85	5.66	95.19
06/01/2014	5	1.03	26.70	33.33	-	-	-	-	-
06/01/2014	15	-0.42	26.95	33.54	-	-	0.24	2.92	96.84
06/01/2014	25	-0.74	27.05	33.64	-	-	-	-	-
06/01/2014	40	-1.11	27.21	33.83	-	-	-	-	-
08/01/2014	5	-	-	-	-	3	-	-	-
15/01/2014	0	-0.50	27.00	33.59	5	3	-	-	-
15/01/2014	5	-0.63	27.04	33.64	-	-	-	-	-
15/01/2014	15	-0.82	27.10	33.71	-	-	0.21	2.48	97.32
15/01/2014	25	-0.92	27.15	33.76	-	-	-	-	-
15/01/2014	40	-1.07	27.26	33.89	-	-	-	-	-

Table 2.1 cont'd: Full-depth profiles of all parameters used in analyses of chapter 3 from RaTS season 2013/14. DOM, POM and inorganic nutrients are stated in µmol x L^{-1}, chlorophyll a in mg m^{-3}.

Date	Depth	DOC	DON	DOC/DON	POC	PON	POC/PON	Chla	NO_3^-	NO_2^-	NH_4^+	PO_4^-	$SI(OH)_4^-$
18/01/2014	15	53.05	4.44	11.95	30.18	5.49	5.50	14.85	10.51	0.08	0.62	0.64	33.27
18/01/2014	100	43.82	5.20	8.43	-	-	-	1.08	32.63	0.16	-	2.31	90.85
21/01/2014	0	52.97	4.56	11.62	28.71	5.38	5.34	0.63	0.36	0.04	0.49	0.09	21.20
21/01/2014	5	58.22	5.91	9.85	46.81	8.63	5.42	3.70	0.09	0.03	-	0.10	22.36
21/01/2014	15	49.43	-	-	46.33	8.14	5.69	12.34	7.67	0.06	0.60	0.42	29.75
21/01/2014	25	55.05	8.26	6.66	37.74	6.56	5.75	10.30	9.22	0.07	-	0.55	33.10
21/01/2014	40	56.13	5.17	10.86	14.36	2.49	5.77	2.65	22.17	0.12	-	1.53	61.41
24/01/2014	15	62.96	4.98	12.64	36.19	7.29	4.96	12.24	5.94	0.05	1.42	0.39	26.32
27/01/2014	0	56.14	5.52	10.17	28.15	5.01	5.62	1.03	0.20	0.02	2.05	0.20	18.43
27/01/2014	5	59.32	8.13	7.30	35.72	6.42	5.56	2.50	0.32	0.03	-	0.18	18.80
27/01/2014	15	72.57	5.77	12.58	48.08	8.80	5.46	14.92	1.78	0.05	0.58	0.16	22.36
27/01/2014	25	50.50	6.19	8.16	45.24	9.37	4.83	12.66	4.06	0.06	-	0.29	25.44
27/01/2014	40	71.67	-	-	17.41	3.20	5.44	3.48	14.72	0.11	-	1.05	48.98
30/01/2014	15	56.00	7.61	7.36	60.56	10.77	5.62	-	1.99	0.05	0.48	0.12	19.94
03/02/2014	0	55.47	5.74	9.66	35.37	5.27	6.71	-	0.07	0.01	0.21	0.04	14.94
03/02/2014	5	61.72	7.83	7.88	55.23	-	-	-	0.06	0.03	-	0.06	13.66
03/02/2014	15	57.70	4.84	11.92	53.86	5.04	10.69	-	1.64	0.05	0.87	0.13	18.56
03/02/2014	25	61.54	6.93	8.88	33.83	6.14	5.51	-	5.99	0.07	-	0.47	29.08
03/02/2014	40	60.16	6.99	8.61	8.85	1.57	5.64	-	18.75	0.11	-	1.48	54.86
03/02/2014	75	59.18	-	-	2.59	0.43	6.02	-	38.67	0.18	-	2.95	121.52
06/02/2014	15	67.34	5.82	11.57	59.63	9.96	5.99	-	0.64	0.03	-	0.06	16.47
10/02/2014	0	63.14	4.70	13.43	45.36	7.00	6.48	1.50	1.54	0.05	0.23	0.09	17.48
10/02/2014	5	51.14	5.09	10.05	49.10	8.09	6.07	5.37	3.05	0.06	-	0.15	21.10
10/02/2014	15	52.68	-	-	22.69	3.97	5.72	8.01	13.50	0.09	2.10	0.98	44.93
14/02/2014	0	61.16	3.38	18.09	45.43	8.10	5.61	5.39	9.52	0.11	1.41	0.51	36.92
14/02/2014	5	48.69	5.67	8.59	31.80	5.98	5.32	13.30	10.76	0.10	-	0.69	39.43
14/02/2014	15	63.17	4.92	12.84	31.27	5.64	5.54	12.28	10.74	0.10	0.84	0.68	38.99
14/02/2014	25	57.48	6.01	9.56	28.87	-	-	13.45	12.23	0.10	-	0.81	42.81
14/02/2014	40	55.93	6.00	9.32	28.14	5.33	5.28	10.25	14.24	0.10	-	0.93	47.65
17/02/2014	0	53.36	4.58	11.65	9.15	1.65	5.55	0.22	12.44	0.09	2.82	1.01	38.20
17/02/2014	5	49.52	7.95	6.23	9.42	1.83	5.15	0.25	12.51	0.09	-	1.02	38.72
17/02/2014	15	52.59	5.03	10.46	10.35	2.05	5.05	0.69	12.59	0.09	2.62	1.01	39.01
17/02/2014	25	46.95	8.01	5.86	9.74	1.79	5.44	2.28	12.69	0.09	-	1.03	38.45
17/02/2014	40	51.70	7.60	6.80	9.63	1.89	5.10	2.63	13.72	0.09	-	1.07	41.02
19/02/2014	0	47.45	7.94	5.98	8.45	1.55	5.45	-	12.54	0.10	-	1.02	38.82
19/02/2014	5	49.76	6.65	7.48	9.34	1.91	4.89	-	12.50	0.10	-	1.03	39.15
19/02/2014	15	60.12	7.16	8.40	11.80	2.35	5.02	-	12.55	0.09	-	1.02	39.34
19/02/2014	25	55.48	7.05	7.87	8.00	1.53	5.23	-	12.99	0.10	-	1.04	39.02
19/02/2014	40	48.67	7.63	6.38	6.43	1.22	5.27	-	14.10	0.10	-	1.15	44.11
19/02/2014	75	44.38	-	-	4.20	0.86	4.88	-	30.16	0.12	-	2.27	84.59
19/02/2014	130	50.15	5.61	8.94	-	-	-	-	34.91	0.11	-	2.50	96.00
21/02/2014	15	49.92	5.42	9.21	9.49	1.83	5.19	1.43	12.93	0.10	2.45	1.02	38.82
25/02/2014	15	51.21	6.26	8.18	11.65	2.22	5.25	1.79	16.82	0.11	-	1.27	50.88
25/02/2014	100	41.01	5.24	7.83	2.63	0.41	6.41	0.09	34.35	0.10	-	2.48	99.82
27/02/2014	0	52.59	4.72	11.14	11.96	2.36	5.07	0.40	15.00	0.12	2.10	1.11	44.81
27/02/2014	5	44.68	6.59	6.78	16.97	3.09	5.49	0.51	14.96	0.12	-	1.08	44.18
27/02/2014	15	61.66	4.48	13.76	14.45	2.74	5.27	2.05	15.05	0.12	2.20	1.08	45.06
27/02/2014	25	49.42	8.17	6.05	16.91	3.31	5.11	4.22	15.22	0.12	-	1.09	44.57

Table 2.1 cont'd: Full-depth profiles of all parameters used in analyses of chapter 3 and 5 from RaTS season 2013/14. Temperature in °C, density in kg m^{-3}, MLD in meters, sea-ice cover in scores from 1 to 10 with 10 – 100% sea-ice cover. %sim = % sea ice meltwater, %met = %meteoric meltwater, %cdw = %circumpolar deepwater.

Date	Depth	Temper-ature	Density	Salinity	MLD	SeaIce	%sim	%met	%cdw
18/01/2014	15	-0.55	26.40	32.85	8	2	-	-	-
18/01/2014	100	-0.52	27.41	34.10	-	-	-	-	-
21/01/2014	0	2.01	26.12	32.68	3	2	2.761	3.393	93.846
21/01/2014	5	0.84	26.23	32.72	-	-	-	-	-
21/01/2014	15	-0.35	26.43	32.90	-	-	2.282	3.139	94.579
21/01/2014	25	-0.37	26.52	33.01	-	-	-	-	-
21/01/2014	40	-0.71	27.00	33.58	-	-	-	-	-
24/01/2014	15	-0.39	26.40	32.86	4	1	2.673	2.941	94.386
27/01/2014	0	1.12	26.18	32.69	3	1	1.935	4.034	94.031
27/01/2014	5	0.75	26.25	32.75	-	-	-	-	-
27/01/2014	15	0.63	26.31	32.81	-	-	2.385	3.342	94.273
27/01/2014	25	0.60	26.32	32.83	-	-	-	-	-
27/01/2014	40	-0.40	26.78	33.32	-	-	-	-	-
30/01/2014	15	-	-	-	-	4	2.399	3.218	94.383
03/02/2014	0	-	-	-	-	5	-	-	-
03/02/2014	5	-	-	-	-	5	-	-	-
03/02/2014	15	-	-	-	-	5	-	-	-
03/02/2014	25	-	-	-	-	-	-	-	-
03/02/2014	40	-	-	-	-	-	-	-	-
03/02/2014	75	-	-	-	-	-	-	-	-
06/02/2014	15	-	-	-	-	1	-	-	-
10/02/2014	0	-0.20	25.97	32.33	1	6	1.292	5.579	93.129
10/02/2014	5	0.11	26.35	32.82	-	-	-	-	-
10/02/2014	15	-0.21	26.62	33.14	-	-	1.08	3.414	95.506
14/02/2014	0	-0.15	26.51	33.01	30	1	1.146	3.737	95.117
14/02/2014	5	-0.09	26.52	33.02	-	-	-	-	-
14/02/2014	15	-0.11	26.53	33.03	-	-	1.343	3.513	95.144
14/02/2014	25	-0.12	26.54	33.05	-	-	-	-	-
14/02/2014	40	-0.33	26.68	33.21	-	-	-	-	-
17/02/2014	0	-0.15	26.38	32.85	13	1	1.837	3.644	94.519
17/02/2014	5	-0.15	26.38	32.85	-	-	-	-	-
17/02/2014	15	-0.20	26.46	32.94	-	-	1.823	3.39	94.787
17/02/2014	25	-0.20	26.52	33.01	-	-	-	-	-
17/02/2014	40	-0.25	26.57	33.08	-	-	-	-	-
19/02/2014	0	-	-	-	-	2	-	-	-
19/02/2014	5	-	-	-	-	2	-	-	-
19/02/2014	15	-	-	-	-	2	-	-	-
19/02/2014	25	-	-	-	-	-	-	-	-
19/02/2014	40	-	-	-	-	-	-	-	-
19/02/2014	75	-	-	-	-	-	-	-	-
19/02/2014	130	-	-	-	-	-	-	-	-
21/02/2014	15	-0.12	26.44	32.92	8	1	2.446	2.973	94.581
25/02/2014	15	-0.50	26.78	33.32	8	1	-	-	-
25/02/2014	100	-0.04	27.49	34.23		-	-	-	-
27/02/2014	0	-0.16	26.53	33.03	39	2	1.358	3.515	95.127
27/02/2014	5	-0.17	26.54	33.04	-	-	-	-	-
27/02/2014	15	-0.16	26.55	33.05	-	-	1.293	3.506	95.201
27/02/2014	25	-0.16	26.55	33.05	-	-	-	-	-

Table 3.1: Full-depth profiles of all parameters used in analyses of chapter 3 from RaTS season 2014/15. DOM, POM and inorganic nutrients are stated in µmol x L^{-1}, chlorophyll a in mg m^{-3}.

Date	Depth	DOC	DON	DOC:DO	POC	PON	POC:PN	Chla	NO_3^-	NO_2^-	NH_4^+	PO_4^-	$SI(OH)_4$
10/11/2014	15	43.46	4.85	8.96	2.77	0.47	5.89	0.110	26.25	0.18	0.28	1.83	70.12
10/11/2014	50	42.87	5.04	8.51	1.87	0.28	6.68	0.342	27.07	0.16	-	1.88	71.23
14/11/2014	0	41.63	5.55	7.50	3.10	0.45	6.89	0.101	25.58	0.09	0.18	1.78	65.89
14/11/2014	15	54.24	4.64	11.69	3.21	0.50	6.42	0.169	26.27	0.08	0.32	1.80	66.92
14/11/2014	50	41.82	6.66	6.28	1.68	0.22	7.64	0.292	27.20	0.06	-	1.88	69.82
18/11/2014	5	43.46	4.80	9.05	-	-	-	0.050	26.64	0.15	-	1.84	67.82
18/11/2014	15	55.90	6.38	8.76	4.01	0.64	6.27	0.058	26.64	0.13	0.29	1.84	67.21
18/11/2014	30	45.82	4.65	9.85	-	-	-	0.070	27.84	0.03	-	1.92	71.38
22/11/2014	15	43.54	5.57	7.82	3.79	0.68	5.57	0.131	25.94	0.09	-	1.80	69.99
25/11/2014	0	42.59	5.60	7.61	4.28	0.68	6.29	0.054	25.45	0.15	0.30	1.80	69.77
25/11/2014	15	41.46	5.68	7.30	3.89	0.68	5.72	0.135	26.14	0.10	0.35	1.83	68.87
25/11/2014	40	41.26	5.46	7.56	2.98	0.54	5.52	0.412	26.97	0.08	-	1.89	72.11
04/12/2014	0	43.26	6.70	6.46	11.42	2.01	5.68	0.237	23.16	0.13	0.46	1.64	66.92
04/12/2014	15	48.20	4.44	10.86	12.02	2.16	5.56	0.784	23.58	0.11	0.96	1.67	65.80
09/12/2014	0	44.47	6.37	6.98	7.75	1.43	5.42	0.210	19.81	0.16	-	1.39	60.53
09/12/2014	5	44.05	5.45	8.09	9.15	1.70	5.38	0.342	22.55	0.14	-	1.57	63.97
09/12/2014	15	44.23	4.83	9.16	9.89	1.94	5.10	1.055	22.64	0.11	-	1.58	64.92
09/12/2014	40	42.86	7.05	6.08	4.66	0.85	5.48	1.185	23.76	0.08	-	1.66	62.55
12/12/2014	15	47.50	5.14	9.24	11.77	2.22	5.30	0.544	22.29	0.10	0.59	1.54	65.94
16/12/2014	0	44.99	5.92	7.60	4.66	0.79	5.90	0.164	24.65	0.11	-	1.73	69.31
16/12/2014	5	45.57	6.75	6.76	5.52	1.00	5.52	0.179	24.22	0.10	-	1.71	67.54
16/12/2014	15	42.44	5.49	7.73	6.35	1.15	5.52	0.265	24.63	0.10	-	1.71	68.80
16/12/2014	30	42.76	7.04	6.07	6.09	1.08	5.64	0.764	24.62	0.10	-	1.75	68.82
19/12/2014	15	44.31	5.78	7.67	24.10	4.34	5.55	3.583	20.67	0.12	-	1.36	64.78
22/12/2014	15	48.46	4.75	10.20	34.40	6.54	5.26	5.676	17.63	0.13	0.45	1.16	61.03
13/01/2015	0	79.66	7.08	11.26	22.54	4.24	5.32	0.870	0.18	0.02	0.34	0.10	37.86
13/01/2015	5	53.81	6.08	8.85	36.65	6.23	5.88	6.146	0.51	0.02	-	0.06	38.31
13/01/2015	15	65.39	7.26	9.01	71.42	12.12	5.89	17.703	0.63	0.03	0.28	0.14	39.86
13/01/2015	40	56.78	7.23	7.85	15.04	2.57	5.85	4.151	19.29	0.15	-	1.44	60.33
13/01/2015	75	40.88	6.91	5.92	3.59	0.56	6.41	0.707	27.58	0.21	-	1.99	77.82
17/01/2015	0	-	-	-	-	-	-	0.386	1.02	0.04	-	0.19	47.52
17/01/2015	5	-	-	-	-	-	-	0.716	-	-	-	-	-
17/01/2015	15	-	-	-	-	-	-	10.296	16.54	0.06	-	1.22	63.70
17/01/2015	40	-	-	-	-	-	-	2.075	26.03	0.17	-	1.89	72.71
20/01/2015	0	-	-	-	-	-	-	1.803	-	-	-	-	-
20/01/2015	5	-	-	-	65.90	11.23	5.87	7.091	5.33	0.08	-	0.40	45.74
20/01/2015	15	-	-	-	44.03	7.81	5.64	9.224	9.04	0.10	0.89	0.66	49.66
20/01/2015	40	-	-	-	13.87	2.30	6.03	2.012	24.52	0.20	-	1.81	69.33
24/01/2015	0	-	-	-	31.74	5.75	5.52	4.220	9.94	0.15	0.19	0.56	51.89
24/01/2015	5	-	-	-	-	-	-	10.671	-	-	-	-	-
24/01/2015	15	-	-	-	42.40	8.04	5.27	6.454	12.30	0.14	0.55	0.83	54.88
24/01/2015	40	-	-	-	24.35	4.53	5.38	3.823	15.35	0.14	-	1.12	58.78
02/02/2015	0	-	-	-	12.24	1.89	6.48	0.279	18.70	0.16	0.38	1.22	53.83
02/02/2015	5	-	-	-	14.54	2.66	5.47	0.414	19.17	0.16	-	1.23	52.66
02/02/2015	15	-	-	-	16.04	2.99	5.36	2.032	19.61	0.16	0.59	1.24	53.32
02/02/2015	40	-	-	-	10.00	1.88	5.32	1.763	20.97	0.16	-	1.44	55.63
02/02/2015	75	54.19	6.36	8.52	7.31	1.59	4.60	1.662	21.63	0.18	-	1.57	61.53
07/02/2015	0	-	-	-	-	-	-	0.829	-	-	-	-	-
07/02/2015	5	-	-	-	33.55	6.13	5.47	3.056	16.32	0.18	-	0.96	52.79
07/02/2015	15	-	-	-	30.90	5.68	5.44	4.997	17.51	0.17	0.44	1.06	53.45
07/02/2015	40	-	-	-	19.41	3.66	5.30	3.547	19.23	0.17	-	1.27	55.61

Table 3.1 cont'd: Full-depth profiles of all parameters used in analyses of chapter 4 from RaTS season 2014/15. Temperature in °C, density in kg m^{-3}, MLD in meters, sea-ice cover in scores from 1 to 10 with 10 – 100% sea-ice cover. %sim = % sea ice meltwater, %met = %meteoric meltwater, %cdw = %circumpolar deepwater.

Date	Depth	Temper-ature	Density	Salinity	MLD	Sea ice	%sim	%met	%cdw
10/11/2014	15	-1.57	27.08	33.65	28	6	-0.272	3.041	97.231
10/11/2014	50	-1.57	27.15	33.73		-	-	-	-
14/11/2014	0	-1.62	27.03	33.59	33	8	-0.215	3.174	97.041
14/11/2014	15	-1.62	27.05	33.60	-	-	-0.058	3.007	97.051
14/11/2014	50	-1.57	27.10	33.67	-	-	-	-	-
18/11/2014	5	-1.55	27.06	33.63	28	5	-	-	-
18/11/2014	15	-1.58	27.07	33.63	-	-	0.182	2.726	97.092
18/11/2014	30	-1.55	27.11	33.69	-	-	-	-	-
22/11/2014	15	-1.60	27.08	33.65	23	5	-0.127	2.935	97.192
25/11/2014	0	-1.51	26.99	33.53	6	5	0.022	3.144	96.834
25/11/2014	15	-1.55	27.08	33.65	-	-	-0.334	3.095	97.239
25/11/2014	40	-1.42	27.15	33.74	-	-	-	-	-
04/12/2014	0	-0.84	26.99	33.57	18	4	-0.954	3.827	97.127
04/12/2014	15	-1.03	27.04	33.61		4	0.044	2.895	97.061
09/12/2014	0	-1.10	26.58	33.05	2	4	0.793	3.94	95.267
09/12/2014	5	-0.87	26.77	33.29	-	-	-	-	-
09/12/2014	15	-0.76	26.97	33.54	-	-	-0.267	3.355	96.912
09/12/2014	40	-1.31	27.06	33.63	-	-	-	-	-
12/12/2014	15	-0.85	26.91	33.47	5	6	-0.048	3.385	96.663
16/12/2014	0	-1.02	27.02	33.59	35	1	-1.977	4.566	97.411
16/12/2014	5	-1.06	27.03	33.60	-	-	-	-	-
16/12/2014	15	-1.06	27.03	33.61	-	-	0.061	2.898	97.041
16/12/2014	30	-1.11	27.05	33.63	-	-	-	-	-
19/12/2014	15	-0.80	26.89	33.44	14	1	-0.099	3.504	96.595
22/12/2014	15	-0.87	26.89	33.44	1	3	0.041	3.398	96.561
13/01/2015	0	1.34	25.86	32.31	1	3	2.947	4.361	92.692
13/01/2015	5	0.73	26.40	32.93	-	-	-	-	-
13/01/2015	15	-0.13	26.69	33.23	-	-	0.366	3.756	95.878
13/01/2015	40	-0.99	26.95	33.52	-	-	-	-	-
13/01/2015	75	-1.26	27.18	33.78	-	-	-	-	-
17/01/2015	0	1.71	26.07	32.60	4	2	-2.45	7.83	94.62
17/01/2015	5	1.16	26.16	32.66	-	-	-	-	-
17/01/2015	15	-0.50	26.78	33.32	-	-	-	-	-
17/01/2015	40	-1.23	27.03	33.60	-	-	-	-	-
20/01/2015	0	0.13	26.52	33.04	6	2	-	-	-
20/01/2015	5	0.00	26.56	33.08	-	-	-	-	-
20/01/2015	15	-0.36	26.71	33.24	-	-	0.322	3.75	95.928
20/01/2015	40	-1.35	27.07	33.64	-	-	-	-	-
24/01/2015	0	-0.22	26.57	33.08	6	1	0.22	4.301	95.479
24/01/2015	5	-0.12	26.61	33.14	-	-	-	-	-
24/01/2015	15	-0.36	26.70	33.24	-	-	0.48	3.646	95.874
24/01/2015	40	-0.65	26.83	33.38	-	-	-	-	-
02/02/2015	0	0.04	26.61	33.14	16	2	-0.831	4.974	95.857
02/02/2015	5	0.04	26.64	33.18	-	-	-	-	-
02/02/2015	15	-0.07	26.65	33.19	-	-	1.223	3.183	95.594
02/02/2015	40	-0.35	26.78	33.33	-	-	-	-	-
02/02/2015	75	-0.66	26.89	33.46	-	-	-	-	-
07/02/2015	0	-0.16	26.51	33.01	2	4	1.259	3.69	95.051
07/02/2015	5	-0.05	26.60	33.12	-	-	-	-	-
07/02/2015	15	-0.08	26.63	33.16	-	-	1.376	3.141	95.483
07/02/2015	40	-0.21	26.68	33.22	-	-	-	-	-

Table 4.1: Full-depth profiles of all parameters used in analyses of chapter 4 from RaTS season 2015/16. DOM, POM and inorganic nutrients are stated in µmol x L^{-1}, chlorophyll a in mg m^{-3}.

Date	Depth	DOC	DON	DOM C:N	POC	PON	POM C:N	Chla	NO_3^-	NO_2^-	NH_4^+	PO_4^-	$I(OH)_4^-$
10/11/2015	0	-	-	-	-	-	-	0.04	-	-	-	-	-
10/11/2015	5	-	-	-	-	-	-	0.06	-	-	-	-	-
10/11/2015	15	-	-	-	-	-	-	0.08	22.94	0.21	-	1.90	62.55
10/11/2015	40	-	-	-	-	-	-	0.18	-	-	-	-	-
12/11/2015	0	-	-	-	-	-	-	0.06	-	-	-	-	-
12/11/2015	5	-	-	-	-	-	-	0.06	-	-	-	-	-
12/11/2015	15	-	-	-	-	-	-	0.08	29.37	0.10	-	2.06	86.19
12/11/2015	40	-	-	-	-	-	-	0.10	-	-	-	-	-
18/11/2015	0	-	-	-	-	-	-	0.04	-	-	-	-	-
18/11/2015	5	-	-	-	-	-	-	0.05	-	-	-	-	-
18/11/2015	15	-	-	-	-	-	-	0.05	28.06	0.08	-	1.94	82.20
18/11/2015	40	-	-	-	-	-	-	0.15	-	-	-	-	-
26/11/2015	0	-	-	-	-	-	-	0.04	-	-	-	-	-
26/11/2015	5	-	-	-	-	-	-	0.04	-	-	-	-	-
26/11/2015	15	-	-	-	-	-	-	0.06	-	-	-	-	-
26/11/2015	40	-	-	-	-	-	-	0.22	-	-	-	-	-
01/12/2015	0	-	-	-	-	-	-	0.04	-	-	-	-	-
01/12/2015	5	-	-	-	-	-	-	0.04	28.67	0.09	-	1.94	84.23
01/12/2015	15	-	-	-	-	-	-	0.05	28.19	0.11	-	1.94	84.47
01/12/2015	40	-	-	-	-	-	-	0.08	-	-	-	-	-
13/12/2015	0	-	-	-	-	-	-	0.06	-	-	-	-	-
13/12/2015	5	-	-	-	-	-	-	0.06	-	-	-	-	-
13/12/2015	15	-	-	-	-	-	-	0.09	28.46	0.12	-	1.93	85.98
13/12/2015	40	-	-	-	-	-	-	0.26	-	-	-	-	-
17/12/2015	0	-	-	-	-	-	-	0.09	-	-	-	-	-
17/12/2015	5	-	-	-	-	-	-	0.13	26.95	0.14	-	1.84	84.35
17/12/2015	15	-	-	-	-	-	-	0.26	27.02	0.11	-	1.86	84.88
17/12/2015	30	-	-	-	-	-	-	0.78	28.01	0.09	-	1.91	83.55
17/12/2015	40	-	-	-	-	-	-	1.07	-	-	-	-	-
21/12/2015	0	-	-	-	-	-	-	0.14	-	-	-	-	-
21/12/2015	5	-	-	-	-	-	-	0.22	-	-	-	-	-
21/12/2015	15	-	-	-	-	-	-	0.30	27.26	0.10	-	1.88	86.42
21/12/2015	40	-	-	-	-	-	-	1.16	-	-	-	-	-
02/01/2016	0	-	-	-	-	-	-	0.59	-	-	-	-	-
02/01/2016	5	-	-	-	-	-	-	0.74	-	-	-	-	-
02/01/2016	15	-	-	-	-	-	-	1.01	27.57	0.10	-	1.81	80.36
02/01/2016	40	-	-	-	-	-	-	0.85	-	-	-	-	-
05/01/2016	0	-	-	-	19.11	3.84	4.98	0.51	22.57	0.08	0.51	1.51	74.16
05/01/2016	5	-	-	-	23.95	4.94	4.85	0.87	21.82	0.08	-	1.48	74.13
05/01/2016	15	-	-	-	27.65	6.09	4.54	4.55	22.91	0.08	0.27	1.53	75.94
05/01/2016	25	-	-	-	16.08	3.41	4.72	3.39	23.48	0.08	-	1.59	75.61
05/01/2016	40	-	-	-	9.11	2.06	4.42	1.75	24.26	0.08	-	1.69	75.56
05/01/2016	70	-	-	-	7.90	1.48	5.34	1.25	25.93	0.09	-	1.80	79.05

Table 4.1 cont'd: Full-depth profiles of all parameters used in analyses of chapter 4 from RaTS season 2015/16. Temperature in °C, density in kg m^{-3}, MLD in meters, sea-ice cover in scores from 1 to 10 with 10 – 100% sea-ice cover. %sim = % sea ice meltwater, %met = %meteoric meltwater, %cdw = %circumpolar deepwater.

Date	Depth	Temper-ature	Density	Salinity	MLD	seaice	%sim	%met	%cdw
10/11/2015	0	-1.46	27.00	33.55	5	3	0.07	3.03	96.90
10/11/2015	5	-1.54	27.04	33.60	-	-	-	-	-
10/11/2015	15	-1.46	27.12	33.70	-	-	-0.72	3.23	97.49
10/11/2015	40	-1.21	27.31	33.94	-	-	-	-	-
12/11/2015	0	-	27.14	33.72	21	3	-0.25	2.79	97.46
12/11/2015	5	-	27.14	33.73	-	-	-	-	-
12/11/2015	15	-	27.15	33.74	-	-	-0.04	2.57	97.47
12/11/2015	40	-	27.36	34.01	-	-	-	-	-
18/11/2015	0	-1.41	27.02	33.58	23	8	-0.36	3.28	97.08
18/11/2015	5	-1.62	27.06	33.62	-	-	-	-	-
18/11/2015	15	-1.55	27.07	33.63	-	-	-0.58	3.31	97.27
18/11/2015	40	-1.40	27.16	33.75	-	-	-	-	-
26/11/2015	0	-0.93	27.09	33.68	31	7	-0.73	3.29	97.43
26/11/2015	5	-0.95	27.09	33.68	-	-	-	-	-
26/11/2015	15	-0.98	27.09	33.69	-	-	-0.28	2.91	97.37
26/11/2015	40	-1.14	27.16	33.76	-	-	-	-	-
01/12/2015	0	-0.97	27.08	33.67	17	7	-1.17	3.67	97.50
01/12/2015	5	-0.94	27.12	33.72	-	-	-	-	-
01/12/2015	15	-1.00	27.12	33.72	-	-	-0.39	2.90	97.49
01/12/2015	40	-1.40	27.26	33.88	-	-	-	-	-
13/12/2015	0	-0.70	26.96	33.54	6	1	-	-	-
13/12/2015	5	-0.74	27.01	33.59	-	-	-	-	-
13/12/2015	15	-0.92	27.05	33.63	-	-	-	-	-
13/12/2015	40	-1.13	27.24	33.86	-	-	-	-	-
17/12/2015	0	-0.74	26.67	33.18	2	1	-	-	-
17/12/2015	5	-0.76	26.79	33.33	-	-	-	-	-
17/12/2015	15	-0.68	26.96	33.54	-	-	-	-	-
17/12/2015	30	-0.89	27.07	33.66	-	-	-	-	-
17/12/2015	40	-1.05	27.15	33.75	-	-	-	-	-
21/12/2015	0	0.47	26.75	33.35	3	8	-0.30	3.92	96.38
21/12/2015	5	-0.30	26.87	33.45	-	-	-	-	-
21/12/2015	15	-0.86	27.04	33.62	-	-	-0.55	3.32	97.23
21/12/2015	40	-1.03	27.23	33.86	-	-	-	-	-
02/01/2016	0	-0.82	26.98	33.55	11	0	-	-	-
02/01/2016	5	-0.84	26.98	33.56	-	-	-	-	-
02/01/2016	15	-0.75	27.12	33.73	-	-	-0.96	3.32	97.63
02/01/2016	40	-0.84	27.20	33.83	-	-	-	-	-
05/01/2016	0	-0.59	26.62	33.12	4	6	0.28	4.12	95.60
05/01/2016	5	-0.55	26.68	33.20	-	-	-	-	-
05/01/2016	15	-0.63	26.80	33.35	-	-	0.04	3.65	96.32
05/01/2016	25	-0.67	26.90	33.46	-	-	-	-	-
05/01/2016	40	-0.72	26.94	33.52	-	-	-	-	-
05/01/2016	70	-0.78	27.02	33.60	-	-	-	-	-

Table 4.1 cont'd: Full-depth profiles of all parameters used in analyses of chapter 4 from RaTS season 2015/16. DOM, POM and inorganic nutrients are stated in µmol x L^{-1}, chlorophyll a in mg m^{-3}.

Date	Depth	DOC	DON	DOM C:N	POC	PON	POM C:N	Chla	NO_3^-	NO_2^-	NH_4^+	PO_4^-	$I(OH)_4^-$
07/01/2016	0	-	-	-	33.73	7.03	4.80	0.64	20.06	0.09	0.13	1.29	74.65
07/01/2016	5	-	-	-	-	-	-	0.85	-	-	-	-	-
07/01/2016	15	48.45	6.29	7.70	23.67	5.11	4.63	-	21.77	0.08	0.25	1.45	75.30
07/01/2016	40	-	-	-	6.13	1.37	4.47	1.05	25.60	0.09	0.18	1.80	80.25
11/01/2016	0	-	-	-	29.01	6.39	4.54	0.28	16.20	0.14	-	1.06	71.14
11/01/2016	5	-	-	-	36.47	7.76	4.70	0.62	16.28	0.13	0.47	1.05	71.67
11/01/2016	15	-	-	-	25.45	5.42	4.70	2.20	20.42	0.08	-	1.34	74.91
11/01/2016	25	-	-	-	9.86	2.09	4.72	1.32	22.65	0.08	-	1.65	75.42
11/01/2016	40	-	-	-	4.69	0.87	5.39	0.75	25.65	0.09	-	1.82	77.09
11/01/2016	70	-	-	-	6.66	1.32	5.05	0.24	31.39	0.14	-	2.17	88.32
14/01/2016	0	56.90	4.60	12.37	19.45	3.62	5.37	3.75	13.93	0.14	0.68	0.86	68.69
14/01/2016	15	51.29	2.27	22.59	19.35	3.11	6.22	4.76	16.44	0.12	4.14	1.07	70.21
14/01/2016	40	44.51	5.66	7.86	2.48	0.41	6.05	0.46	29.03	0.10	-	2.02	88.74
21/01/2016	0	55.46	5.85	9.48	33.66	6.56	5.13	2.52	7.40	0.15	0.58	0.38	65.23
21/01/2016	15	50.29	4.75	10.59	28.54	5.35	5.33	2.12	22.72	0.07	0.97	1.48	78.12
21/01/2016	40	42.27	4.73	8.94	1.95	0.27	7.22	0.23	30.49	0.12	-	2.11	90.91
01/02/2016	0	56.33	5.82	9.68	32.85	6.13	5.36	-	10.00	0.11	1.15	0.68	64.67
01/02/2016	15	52.16	4.87	10.71	43.39	8.12	5.34	-	11.29	0.11	1.25	0.77	65.36
01/02/2016	40	50.52	6.46	7.82	29.10	5.49	5.30	-	15.55	0.11	-	1.11	71.29
09/02/2016	0	51.30	4.55	11.27	26.40	4.79	5.51	1.66	11.73	0.11	2.21	0.92	66.91
09/02/2016	15	57.55	6.21	9.27	33.76	6.02	5.61	5.15	12.30	0.11	2.02	1.00	67.09
09/02/2016	40	55.98	7.38	7.59	33.93	6.08	5.58	5.16	13.47	0.12	-	1.09	68.69
15/02/2016	0	55.70	3.39	16.43	31.05	5.78	5.37	1.92	11.60	0.11	3.65	0.88	66.83
15/02/2016	15	48.61	2.47	19.68	17.88	3.36	5.32	1.15	14.59	0.12	3.96	1.13	70.02
15/02/2016	40	48.58	8.36	5.81	15.52	2.93	5.30	2.12	17.88	0.12	-	1.40	73.74
25/02/2016	0	52.55	3.37	15.59	28.27	4.93	5.73	1.11	11.07	0.12	2.10	0.92	65.09
25/02/2016	15	62.69	4.96	12.64	32.47	5.72	5.68	3.08	11.59	0.12	2.58	0.97	63.69
25/02/2016	40	54.26	8.01	6.77	17.79	3.21	5.54	1.25	14.52	0.12	-	1.24	70.12
01/03/2016	0	51.09	2.87	17.80	21.82	3.91	5.58	-	16.40	0.13	5.47	1.33	70.93
01/03/2016	15	49.20	1.14	43.16	20.95	3.55	5.90	-	16.43	0.13	6.56	1.34	69.71
01/03/2016	40	46.99	6.32	7.44	15.38	2.75	5.59	-	18.88	0.13	-	1.49	75.47
04/03/2016	15	58.37	-	-	20.31	3.66	5.55	1.72	14.39	0.13	3.00	1.19	66.45
10/03/2016	0	71.00	4.01	17.71	17.77	3.52	5.05	1.48	15.24	0.13	3.88	1.24	66.85
10/03/2016	15	48.69	2.74	17.77	14.38	2.76	5.21	1.50	15.50	0.13	4.09	1.27	68.24
10/03/2016	40	46.14	6.29	7.34	13.14	2.58	5.09	1.51	15.65	0.13	-	1.28	69.06
18/03/2016	0	50.93	4.02	12.67	18.64	3.57	5.22	1.20	14.78	0.12	3.07	1.18	69.49
18/03/2016	15	60.07	3.32	18.09	16.24	3.13	5.19	1.63	15.23	0.12	2.97	1.23	68.86
18/03/2016	40	45.85	9.18	4.99	10.36	1.95	5.31	0.78	16.61	0.13	-	1.37	69.02

Table 4.1 cont'd: Full-depth profiles of all parameters used in analyses of chapter 4 from RaTS season 2015/16. Temperature in °C, density in kg m^{-3}, MLD in meters, sea-ice cover in scores from 1 to 10 with 10 – 100% sea-ice cover. %sim = % sea ice meltwater, %met = %meteoric meltwater, %cdw = %circumpolar deepwater.

Date	Depth	Temper-ature	Density	Salinity	MLD	seaice	%sim	%met	%cdw
07/01/2016	0	-0.30	26.64	33.16	13	2	-0.74	4.80	95.95
07/01/2016	5	-0.42	26.66	33.17	-	-	-	-	-
07/01/2016	15	-	-	-	-	-	-0.13	3.88	96.25
07/01/2016	40	-0.75	26.99	33.57	-	-	-	-	-
11/01/2016	0	1.10	26.36	32.91	3	1	0.72	4.37	94.91
11/01/2016	5	0.20	26.49	33.01	-	-	-	-	-
11/01/2016	15	-0.64	26.74	33.27	-	-	0.22	3.74	96.05
11/01/2016	25	-0.67	26.87	33.42	-	-	-	-	-
11/01/2016	40	-0.78	26.98	33.55	-	-	-	-	-
11/01/2016	70	-0.87	27.32	33.97	-	-	-	-	-
14/01/2016	0	0.54	26.26	32.74	4	3	0.45	5.09	94.47
14/01/2016	15	-0.11	26.58	33.09	-	-	0.55	3.97	95.48
14/01/2016	40	-1.03	27.12	33.72	-	-	-	-	-
21/01/2016	0	0.22	25.79	32.14	1	5	3.15	4.64	92.21
21/01/2016	15	-1.00	26.84	33.38	-	-	0.35	3.32	96.33
21/01/2016	40	-0.97	27.23	33.86	-	-	-	-	-
01/02/2016	0	-	-	-	-	2	-	-	-
01/02/2016	15	-	-	-	-	-	-	-	-
01/02/2016	40	-	-	-	-	-	-	-	-
09/02/2016	0	-0.26	26.52	33.02	31	2	0.79	4.00	95.21
09/02/2016	15	-0.38	26.55	33.05	-	-	0.96	3.78	95.26
09/02/2016	40	-0.44	26.57	33.07	-	-	-	-	-
15/02/2016	0	-0.15	26.23	32.66	6	2	1.22	4.69	94.10
15/02/2016	15	-0.35	26.50	32.99	-	-	0.62	4.23	95.15
15/02/2016	40	-0.63	26.68	33.20	-	-	-	-	-
25/02/2016	0	-0.42	26.35	32.79	18	3	1.28	4.26	94.46
25/02/2016	15	-0.52	26.39	32.84	-	-	1.48	3.97	94.55
25/02/2016	40	-0.41	26.52	33.00	-	-	-	-	-
01/03/2016	0	-	-	-	-	0	-	-	-
01/03/2016	15	-	-	-	-	-	-	-	-
01/03/2016	40	-	-	-	-	-	-	-	-
04/03/2016	15	-0.70	26.51	32.98	30	1	1.10	3.86	95.05
10/03/2016	0	-0.67	26.50	32.96	46	2	1.15	3.86	94.98
10/03/2016	15	-0.64	26.51	32.98	-	-	1.03	3.91	95.07
10/03/2016	40	-0.64	26.53	33.00	-	-	-	-	-
18/03/2016	0	-0.86	26.38	32.81	20	0	-	-	-
18/03/2016	15	-0.90	26.40	32.84	-	-	-	-	-
18/03/2016	40	-0.82	26.51	32.98	-	-	-	-	-

Table 5: HPLC phytoplankton-pigmentation contribution to total phytoplankton biomass in % for all three RaTS seasons.

Date	Prasino-phytes	Chloro-phytes	Dinofla-gellates	Crypto-phytes	Hapto-phytes	Diatoms
19/11/2013	15.65	4.71	0.03	0.73	27.30	51.58
25/11/2013	4.96	0.00	0.01	0.07	22.70	72.26
28/11/2013	0.00	0.55	0.01	7.43	17.00	75.00
02/12/2013	1.34	1.98	0.01	9.31	16.17	71.18
05/12/2013	0.48	2.78	0.00	3.53	17.07	76.15
13/12/2013	1.67	0.72	0.13	0.58	5.10	91.79
24/12/2013	0.21	0.00	0.00	0.00	1.03	98.76
28/12/2013	0.32	0.00	0.00	0.00	1.54	98.14
30/12/2013	0.01	0.00	0.12	0.00	1.16	98.71
06/01/2014	0.47	0.00	0.00	0.00	1.14	98.39
15/01/2014	3.01	0.04	0.00	0.62	10.28	86.05
18/01/2014	1.17	0.00	0.31	1.92	13.07	83.53
21/01/2014	1.10	0.00	0.43	0.83	12.01	85.63
24/01/2014	1.68	0.00	0.46	1.31	12.53	84.02
27/01/2014	2.99	0.00	0.99	2.59	10.99	82.44
30/01/2014	1.24	0.00	0.60	0.84	6.23	91.10
03/02/2014	1.42	0.19	0.70	0.05	3.85	93.79
06/02/2014	1.28	0.53	0.91	6.84	6.20	84.24
10/02/2014	1.05	0.30	0.33	3.98	4.01	90.33
14/02/2014	0.77	0.12	0.31	4.69	5.09	89.03
17/02/2014	2.28	3.70	0.74	32.09	27.90	33.29
19/02/2014	3.91	2.66	0.94	38.74	29.34	24.41
21/02/2014	7.78	4.76	1.35	8.11	39.80	38.19
25/02/2014	1.51	0.47	0.32	6.94	15.22	75.55
27/02/2014	3.06	1.26	0.78	4.66	5.95	84.29

Date	Prasino-phytes	Chloro-phytes	Dinofla-gellates	Crypto-phytes	Hapto-phytes	Diatoms
10/11/2014	18.40	2.54	0.81	3.94	46.65	27.66
14/11/2014	9.43	3.88	0.78	2.67	30.56	52.67
18/11/2014	15.34	3.51	0.74	2.85	32.63	44.92
22/11/2014	6.25	2.04	0.02	0.38	21.15	70.16
25/11/2014	4.76	1.95	0.32	0.00	17.78	75.20
04/12/2014	4.71	2.08	0.59	2.01	16.28	74.34
09/12/2014	2.93	1.48	0.32	0.03	22.71	72.53
12/12/2014	1.37	1.17	0.53	1.11	21.10	74.72
16/12/2014	3.94	1.08	0.00	0.00	10.41	84.56
19/12/2014	0.92	0.00	0.42	0.01	2.78	95.87
13/01/2015	6.82	0.00	0.02	4.91	4.69	83.56
17/01/2015	0.29	0.00	0.00	0.07	5.49	94.15
20/01/2015	2.30	0.01	0.00	11.71	3.23	82.75
24/01/2015	1.14	0.00	0.00	3.99	1.86	93.02
02/02/2015	6.36	2.25	0.66	4.39	5.14	81.20
07/02/2015	2.57	0.61	0.26	0.57	1.58	94.41
11/02/2015	1.27	0.00	0.40	5.24	1.57	91.51
17/02/2015	0.49	0.11	0.24	1.40	1.14	96.62
21/02/2015	1.22	0.04	0.37	1.05	1.64	95.68
27/02/2015	0.60	0.00	0.27	2.34	0.80	95.99

Table 5 cont'd

Date	Prasino-phytes	Chloro-phytes	Dinofla-gellates	Crypto-phytes	Hapto-phytes	Diatoms
10/11/2015	1.84	8.03	0.40	0.01	51.30	38.42
12/11/2015	1.24	5.36	0.00	0.00	53.23	40.17
18/11/2015	4.37	11.26	0.00	0.04	38.42	45.91
26/11/2015	5.54	19.64	0.01	0.16	35.98	38.66
01/12/2015	2.11	17.06	0.00	0.05	39.19	41.59
13/12/2015	3.94	26.64	0.82	0.04	26.65	41.91
17/12/2015	2.10	30.06	0.03	1.89	24.77	41.15
21/12/2015	2.25	27.19	0.01	2.61	21.28	46.66
02/01/2016	3.34	13.41	0.00	1.63	11.61	70.01
05/01/2016	2.59	13.00	0.07	1.67	4.44	78.23
07/01/2016	1.61	1.86	0.10	0.54	2.07	93.82
11/01/2016	0.39	1.36	0.01	1.62	2.49	94.13
14/01/2016	1.74	0.00	0.07	3.67	2.15	92.36
21/01/2016	0.10	2.92	0.00	0.41	3.71	92.87
01/02/2016	0.36	3.61	0.40	2.46	5.01	88.16
09/02/2016	0.34	3.81	1.23	2.49	2.58	89.55
15/02/2016	0.84	1.62	0.00	63.84	2.51	31.18
25/02/2016	1.58	10.37	1.44	44.97	2.58	39.06

Table 6: DOM and inorganic nutrients measured in sea-ice cores collected at the RaTS site in 2014. All concentrations stated in µmol x L^{-1}

Date	Site	Depth	DON	DOC	DOC:DON	NO_3^-	$Si(OH)_4^-$	PO_4^-	NO_2^-
04/11/2014	HC1	5-20cm	3.75	37.00	11.49	0.14	0.69	0.11	0.03
04/11/2014	HC1	20-35cm	4.46	55.14	14.42	0.14	1.14	0.23	0.02
04/11/2014	HC1	35-49cm	8.75	165.20	22.01	0.12	4.89	0.36	0.03
08/11/2014	HC1	5-20cm	3.38	43.40	14.99	1.11	1.37	0.17	0.03
08/11/2014	HC1	20-35cm	4.76	36.98	9.06	2.77	6.20	0.39	0.04
08/11/2014	HC1	35-50cm	9.95	94.42	11.07	1.45	8.89	0.88	0.03
08/11/2014	HC1	50-76cm	4.07	85.75	24.59	0.02	3.71	0.07	0.02
12/11/2014	HC2	0-5cm	25.40	197.10	9.05	9.13	5.35	1.86	0.07
12/11/2014	HC2	5-15cm	1.90	42.26	25.88	0.09	0.14	0.08	0.02
12/11/2014	HC2	15-30cm	4.35	33.47	8.97	0.06	0.41	0.11	0.02
12/11/2014	HC2	30-48cm	4.15	133.90	37.59	-0.01	1.62	0.20	0.02
12/11/2014	HC2	48-74cm	5.19	70.62	15.86	0.02	1.96	0.06	0.02
18/11/2014	HC2	5-20cm	3.36	29.88	10.36	0.41	1.36	0.16	0.03
18/11/2014	HC2	20-35cm	7.69	100.75	15.29	0.58	2.85	0.49	0.04
18/11/2014	HC2	35-53cm	13.77	326.90	27.69	0.03	2.38	1.20	0.02
18/11/2014	HC2	53-80cm	3.07	53.17	20.20	0.00	5.65	0.06	0.02
24/11/2014	HC3	0-5cm	107.99	771.70	8.33	13.61	13.80	6.52	0.09
24/11/2014	HC3	5-15cm	4.42	48.79	12.89	0.35	1.08	0.11	0.04
24/11/2014	HC3	15-30cm	3.18	42.57	15.60	0.23	1.62	0.10	0.03
24/11/2014	HC3	30-45cm	3.65	120.10	38.38	0.03	3.45	0.09	0.03
24/11/2014	HC3	45-70cm	4.23	93.37	25.73	0.05	2.66	0.08	0.04
29/11/2014	HC3	0-9cm	41.15	308.20	8.73	9.35	8.25	2.84	0.06
29/11/2014	HC3	9-24cm	3.44	37.11	12.57	0.38	1.31	0.12	0.04
29/11/2014	HC3	24-39cm	5.76	70.35	14.25	0.49	2.68	0.27	0.05
29/11/2014	HC3	39-54cm	7.99	389.40	56.83	0.05	7.86	0.44	0.05
29/11/2014	HC3	54-75cm	4.17	63.41	17.72	0.00	4.69	0.05	0.03
03/12/2014	HC4	35-50cm	6.70	294.30	51.26	0.03	5.05	0.42	0.04
06/12/2014	HC4	5-20cm	4.74	45.23	11.13	0.22	1.90	0.12	0.04
06/12/2014	HC4	20-35cm	6.38	72.97	13.34	0.13	1.56	0.16	0.05
06/12/2014	HC4	35-50cm	4.59	129.70	32.95	0.02	4.51	0.12	0.04
06/12/2014	HC4	50-75cm	3.05	66.04	25.22	0.02	3.34	0.04	0.04
12/12/2014	HC4	5-20cm	5.80	71.26	14.32	0.24	2.12	0.22	0.03
12/12/2014	HC4	20-35cm	3.39	60.52	20.82	0.05	1.87	0.12	0.03
12/12/2014	HC4	35-50cm	5.69	239.70	49.17	0.02	4.85	0.27	0.03
12/12/2014	HC4	50-76cm	4.47	54.27	14.16	0.04	2.86	0.05	0.03
18/12/2014	HC4	5-20cm	6.42	42.13	7.65	0.18	1.04	0.11	0.03
18/12/2014	HC4	20-35cm	4.90	37.19	8.86	0.09	1.01	0.10	0.02
18/12/2014	HC4	35-50cm	5.72	41.76	8.51	0.08	1.24	0.06	0.03
22/12/2014	HC4	0-5cm	160.55	1037.00	7.53	1.30	8.12	1.06	0.07
22/12/2014	HC4	20-35cm	12.30	178.30	16.90	0.06	2.29	0.70	0.04
22/12/2014	HC4	35-50cm	10.45	226.53	25.28	0.03	2.96	0.48	0.03
22/12/2014	HC4	50-65cm	4.62	48.32	12.20	0.09	0.89	0.06	0.03

Table 7.1: Full-depth profiles of all parameters used in analyses of chapter 4 from PAL LTER research cruise LMG1701. DOM, POM are stated in µmol x L^{-1}, chlorophyll-a concentrations in mg m^{-3}, PP (primary production) in mg C m^{-3} d^{-1}, bacterial abundance, HNA, LNA in cells L^{-1} and bacterial activity in pmol leu L^{-1} hr^{-1}. Depth in meters.

Station	Depth	DOC	DON	DOC:DON	POC	PN	POC:PN	PP	chla	Bacterial Abundance	Bacterial Activity	HNA	LNA
600.040	1300	42.95	5.59	8.96	-	-	-	-	-	-	-	-	-
600.040	700	-	-	-	-	-	-	-	-	-	-	-	-
600.040	320	-	-	-	-	-	-	-	-	-	-	-	-
600.040	200	-	-	-	-	-	-	-	-	-	-	-	-
600.040	125	43.72	4.40	11.59	-	-	-	-	-	-	-	-	-
600.040	100	44.32	4.70	11.00	6.66	0.20	38.09	-	0.013	2.80E+08	0.73	1.90E+08	8.05E+07
600.040	75	48.56	6.10	9.28	2.28	0.22	12.02	-	0.034	3.04E+08	1.62	1.99E+08	9.79E+07
600.040	50	47.08	5.26	10.44	6.22	0.31	23.74	2.890	0.115	4.13E+08	3.86	2.75E+08	1.28E+08
600.040	40	47.66	5.39	10.31	6.39	0.44	16.97	9.226	0.216	5.68E+08	5.69	4.16E+08	1.39E+08
600.040	30	50.16	4.91	11.91	7.01	0.65	12.57	14.771	0.256	8.90E+08	14.68	6.58E+08	2.11E+08
600.040	5	49.81	7.57	7.67	-	-	-	46.756	0.482	7.86E+08	56.22	5.38E+08	2.32E+08
600.040	0	54.97	5.87	10.92	30.97	5.18	6.98	36.562	1.115	6.58E+08	69.55	4.24E+08	2.30E+08
600.100	593	43.50	4.40	11.53	-	-	-	-	-	-	-	-	-
600.100	500	-	-	-	-	-	-	-	-	-	-	-	-
600.100	400	-	-	-	-	-	-	-	-	-	-	-	-
600.100	300	-	-	-	-	-	-	-	-	-	-	-	-
600.100	200	47.24	3.80	14.50	-	-	-	-	-	4.68E+08	0.75	3.87E+08	7.24E+07
600.100	100	57.03	3.75	17.74	-	-	-	-	0.138	5.56E+08	3.57	4.14E+08	1.32E+08
600.100	65	46.63	4.75	11.45	3.34	0.40	9.87	-	0.138	5.56E+08	3.57	4.14E+08	1.32E+08
600.100	50	45.30	5.56	9.50	26.33	1.55	19.84	2.914	0.280	6.44E+08	6.80	4.91E+08	1.44E+08
600.100	40	46.18	5.90	9.13	18.79	1.30	16.86	3.590	0.589	8.28E+08	15.84	6.61E+08	1.58E+08
600.100	30	49.38	5.54	10.39	16.30	2.20	8.63	4.709	1.349	8.17E+08	24.54	6.47E+08	1.58E+08
600.100	10	52.24	4.98	12.23	27.30	4.07	7.83	2.720	1.834	6.89E+08	43.92	5.63E+08	1.22E+08
600.100	0	54.32	5.13	12.35	46.57	4.18	12.99	17.826	1.378	7.88E+08	52.56	6.58E+08	1.23E+08
600.200	3040	42.45	5.15	9.61	-	-	-	-	-	-	-	-	-
600.200	2500	-	-	-	-	-	-	-	-	-	-	-	-
600.200	1500	-	-	-	-	-	-	-	-	-	-	-	-
600.200	500	-	-	-	-	-	-	-	-	-	-	-	-
600.200	250	37.04	-	-	-	-	-	-	-	-	-	-	-
600.200	100	45.85	4.40	12.15	5.73	0.24	27.77	-	0.494	2.64E+08	1.27	1.71E+08	8.20E+07
600.200	70	47.57	6.52	8.51	4.22	0.53	9.21	-	0.599	4.59E+08	4.77	2.87E+08	1.58E+08
600.200	50	53.74	4.55	13.77	10.12	0.97	12.12	2.454	0.400	6.73E+08	8.19	3.91E+08	2.63E+08
600.200	40	44.73	6.32	8.25	12.04	1.33	10.57	4.253	0.437	8.96E+08	11.37	4.83E+08	3.88E+08
600.200	25	60.22	5.09	13.80	15.22	1.57	11.30	2.219	0.283	7.05E+08	14.95	4.13E+08	2.69E+08
600.200	10	50.69	4.06	14.56	11.71	1.49	9.16	2.324	0.340	4.82E+08	12.28	2.92E+08	1.73E+08
600.200	0	47.41	4.47	12.37	11.05	1.25	10.31	11.738		4.52E+08	11.49	2.76E+08	1.59E+08

Table 7.1 cont'd

Station	Depth	DOC	DON	DOC:DON	POC	PN	POC:PN	PP	chla	Bacterial Abundance	Bacterial Activity	HNA	LNA
500.200	2672	43.39	3.98	12.71	-	-	-	-	-	-	-	-	-
500.200	2000	41.32	3.92	12.29	-	-	-	-	-	-	-	-	-
500.200	1000	42.21	3.84	12.82	-	-	-	-	-	-	-	-	-
500.200	500	-	-	-	-	-	-	-	-	-	-	-	-
500.200	200	41.57	4.80	10.10	-	-	-	-	-	-	-	-	-
500.200	90	47.21	5.33	10.33	5.05	0.52	11.30	-	-	4.72E+08	3.50	3.87E+08	8.09E+07
500.200	75	40.50	5.10	9.26	2.99	0.42	8.23	-	0.318	5.52E+08	3.92	4.34E+08	1.12E+09
500.200	60	42.83	5.62	8.89	7.39	0.66	13.13	3.413	0.481	6.40E+08	5.12	4.84E+08	1.48E+08
500.200	45	46.11	5.69	9.45	11.33	1.14	11.64	3.998	0.652	9.98E+08	10.05	6.92E+08	2.83E+08
500.200	25	50.76	4.03	14.69	12.33	1.56	9.19	4.095	0.643	1.03E+09	17.79	7.17E+08	2.81E+08
500.200	10	48.01	4.64	12.07	10.63	1.52	8.14	2.408	0.494	1.03E+09	18.28	7.32E+08	2.72E+08
500.200	0	46.94	4.21	13.00	11.97	1.95	7.17	18.083	0.532	1.08E+09	17.29	7.60E+08	2.85E+08
500.100	424	40.86	1.85	25.76	-	-	-	-	-	-	-	-	-
500.100	375	-	-	-	-	-	-	-	-	-	-	-	-
500.100	280	-	-	-	-	-	-	-	-	-	-	-	-
500.100	200	-	-	-	-	-	-	-	-	-	-	-	-
500.100	150	42.41	3.98	12.43	-	-	-	-	-	-	-	-	-
500.100	100	44.02	2.03	25.29	2.86	0.27	12.28	-	-	3.32E+08	1.11	2.26E+08	9.23E+07
500.100	70	43.29	4.02	12.56	2.76	0.26	12.55	-	0.029	3.46E+08	3.39	2.27E+08	1.08E+08
500.100	50	57.20	5.87	11.36	6.01	0.41	16.88	1.642	0.023	3.28E+08	3.06	2.02E+08	1.19E+08
500.100	30	44.33	4.52	11.44	8.40	0.80	12.20	6.169	0.680	4.73E+08	8.79	3.07E+08	1.60E+08
500.100	20	44.69	5.17	10.08	11.80	1.26	10.93	3.036	0.821	5.94E+08	10.62	3.94E+08	1.89E+08
500.100	10	51.83	4.65	13.00	22.98	4.05	6.62	8.782	1.561	4.27E+08	46.14	2.62E+08	1.59E+08
500.100	0	51.40	5.16	11.62	28.83	5.14	6.55	16.669	1.448	4.58E+08	46.55	2.89E+08	1.61E+08
500.060	290	43.56	4.49	11.31	-	-	-	-	-	-	-	-	-
500.060	200	-	-	-	-	-	-	-	-	-	-	-	-
500.060	150	-	-	-	-	-	-	-	-	-	-	-	-
500.060	125	-	-	-	-	-	-	-	-	-	-	-	-
500.060	100	40.58	3.91	12.10	-	-	-	-	-	-	-	-	-
500.060	80	42.87	5.44	9.19	2.41	0.33	8.39	-	0.233	3.49E+08	2.80	2.42E+08	9.66E+07
500.060	50	51.31	5.47	10.94	4.32	0.71	7.08	-	-	4.16E+08	9.35	2.61E+08	1.51E+08
500.060	45	55.25	1.70	37.90	8.58	0.96	10.39	8.230	0.706	4.63E+08	14.08	3.00E+08	1.59E+08
500.060	35	47.04	5.56	9.87	7.64	0.92	9.73	12.515	0.636	5.54E+08	11.39	3.46E+08	1.97E+08
500.060	25	44.89	7.61	6.88	14.21	2.30	7.21	43.958	2.795	5.74E+08	34.33	4.05E+08	1.61E+08
500.060	10	56.02	4.34	15.05	37.76	7.33	6.01	37.340	1.210	5.24E+08	50.94	2.90E+08	2.26E+08
500.060	0	54.71	4.31	14.80	38.68	7.48	6.03	######	2.004	5.40E+08	50.96	2.88E+08	2.45E+08

Table 7.1 cont'd

Station	Depth	DOC	DON	DOC:DON	POC	PN	POC:PN	PP	chla	Bacterial Abundance	Bacterial Activity	HNA	LNA
400.040	270	43.61	3.70	13.75	-	-	-	-	-	-	-	-	-
400.040	225	-	-	-	-	-	-	-	-	-	-	-	-
400.040	200	-	-	-	-	-	-	-	-	-	-	-	-
400.040	150	-	-	-	-	-	-	-	-	-	-	-	-
400.040	125	43.35	3.72	13.59	-	-	-	-	-	-	-	-	-
400.040	100	41.79	4.33	11.26	2.08	0.20	12.42	-	-	4.51E+08	5.24	3.46E+08	9.01E+07
400.040	80	42.02	3.46	14.16	2.42	0.31	8.99	-	0.088	4.35E+08	3.00	3.19E+08	9.96E+07
400.040	50	42.34	3.95	12.50	5.02	0.34	17.15	2.397	0.190	4.89E+08	5.76	3.40E+08	1.32E+08
400.040	35	57.86	4.36	15.48	4.02	0.38	12.38	4.259	0.295	5.95E+08	11.07	4.27E+08	1.51E+08
400.040	20	-	-	-	8.51	1.01	9.82	6.208	0.889	9.82E+08	46.84	7.52E+08	2.12E+08
400.040	10	52.06	6.53	9.30	-	-	-	5.360	1.380	1.30E+09	183.82	1.09E+09	2.04E+08
400.040	0	56.92	7.88	8.42	-	-	-	61.298	0.907	1.61E+09	426.50	1.39E+09	2.11E+08
400.100	337	41.20	4.65	10.33	-	-	-	-	-	-	-	-	-
400.100	320	37.14	4.17	10.39	-	-	-	-	-	-	-	-	-
400.100	265	-	-	-	-	-	-	-	-	-	-	-	-
400.100	175	-	-	-	-	-	-	-	-	-	-	-	-
400.100	140	38.57	3.41	13.19	-	-	-	-	-	-	-	-	-
400.100	100	45.11	3.35	15.70	1.97	0.26	8.67	-	-	3.17E+08	0.86	2.18E+08	8.99E+07
400.100	70	44.52	4.73	10.98	2.57	0.34	8.72	-	0.213	4.57E+08	3.35	2.89E+08	1.55E+08
400.100	50	45.46	5.10	10.40	5.20	0.52	11.57	2.288	0.277	7.69E+08	10.07	4.72E+08	2.79E+08
400.100	30	44.83	4.19	12.48	9.16	1.07	9.97	7.434	0.767	7.98E+08	16.59	5.14E+08	2.71E+08
400.100	20	51.89	5.34	11.33	23.35	3.81	7.14	13.147	1.817	1.05E+09	100.93	7.92E+08	2.47E+08
400.100	10	60.47	3.65	19.32	26.50	4.46	6.92	55.136	1.583	1.00E+09	92.14	7.65E+08	2.26E+08
400.100	0	45.62	4.53	11.74	26.78	4.52	6.91	18.953	1.783	1.09E+09	97.31	8.14E+08	2.55E+08
400.200	2700	43.84	4.59	11.14	-	-	-	-	-	-	-	-	-
400.200	2000	-	3.73	-	-	-	-	-	-	-	-	-	-
400.200	800	-	-	-	-	-	-	-	-	-	-	-	-
400.200	350	-	-	-	-	-	-	-	-	-	-	-	-
400.200	200	43.25	4.05	12.45	-	-	-	-	-	-	-	-	-
400.200	100	42.02	4.52	10.84	1.23	0.16	9.02	-	-	2.82E+08	1.83	1.84E+08	8.90E+07
400.200	75	48.71	4.96	11.45	1.81	0.22	9.45	-	0.128	2.78E+08	2.59	1.82E+08	9.13E+07
400.200	60	45.88	3.79	14.12	2.88	0.29	11.72	3.757	0.294	2.89E+08	3.08	1.85E+08	9.87E+07
400.200	40	45.56	4.52	11.75	6.17	0.96	7.46	9.071	0.598	8.60E+08	13.89	4.93E+08	3.41E+08
400.200	30	47.88	3.45	16.18	22.31	3.93	6.62	41.837	1.502	6.33E+08	21.73	3.97E+08	2.17E+08
400.200	10	45.84	2.90	18.43	23.31	4.40	6.18	33.197	0.964	5.44E+08	17.43	3.36E+08	1.88E+08
400.200	0	47.83	4.49	12.42	23.20	4.37	6.19	30.501	1.266	5.49E+08	17.54	3.41E+08	1.87E+08

Station	Depth	DOC	DON	DOC:DON	POC	PN	POC:PN	PP	chl*a*	Bacterial Abundance	Bacterial Activity	HNA	LNA
300.200	3023	38.87	5.53	8.20	-	-	-	-	-	-	-	-	-
300.200	1500	-	3.18	-	-	-	-	-	-	-	-	-	-
300.200	750	-	-	-	-	-	-	-	-	-	-	-	-
300.200	500	-	-	-	-	-	-	-	-	-	-	-	-
300.200	275	42.01	4.52	10.84	-	-	-	-	-	-	-	-	-
300.200	100	50.39	-	-	2.22	0.36	7.22	-	-	3.52E+08	2.51	2.22E+08	1.20E+08
300.200	85	41.37	5.62	8.58	2.70	0.43	7.32	-	0.234	3.69E+08	4.19	2.29E+08	1.29E+08
300.200	70	40.48	5.62	8.40	3.92	0.49	9.25	4.934	0.317	4.41E+08	4.79	2.76E+08	1.57E+08
300.200	50	46.50	7.12	7.62	5.17	0.77	7.79	6.085	0.212	6.49E+08	6.49	3.43E+08	2.90E+08
300.200	30	-	-	-	2.67	0.43	7.27	6.453	0.144	5.25E+08	8.46	3.13E+08	1.97E+08
300.200	10	42.99	5.32	9.42	5.04	0.85	6.89	2.273	0.087	2.67E+08	4.40	1.55E+08	1.03E+08
300.200	0	45.93	5.02	10.67	3.89	0.68	6.70	16.559	0.113	2.70E+08	3.81	1.60E+08	1.02E+08
300.100	470	44.16	4.53	11.37	-	-	-	-	-	-	-	-	-
300.100	425	-	-	-	-	-	-	-	-	-	-	-	-
300.100	350	-	-	-	-	-	-	-	-	-	-	-	-
300.100	270	37.39	4.12	10.58	-	-	-	-	-	-	-	-	-
300.100	200	39.99	3.92	11.90	-	-	-	-	-	-	-	-	-
300.100	100	41.13	3.32	14.45	2.05	0.23	10.48	-	-	3.14E+08	6.31	2.03E+08	1.01E+08
300.100	80	43.92	4.72	10.85	2.57	0.40	7.44	-	0.008	3.92E+08	1.93	2.39E+08	1.40E+08
300.100	50	46.32	5.12	10.55	3.01	0.46	7.62	2.285	0.248	8.00E+08	6.01	4.33E+08	3.45E+08
300.100	40	-	-	-	18.09	3.46	6.09	50.094	1.901	9.68E+08	23.99	6.17E+08	3.28E+08
300.100	30	48.35	4.62	12.20	24.84	4.48	6.46	46.478	2.071	8.34E+08	30.26	5.63E+08	2.49E+08
300.100	15	48.19	4.72	11.91	17.00	3.25	6.10	37.359	0.912	8.60E+08	39.42	5.94E+08	2.50E+08
300.100	0	52.61	3.92	15.65	15.13	2.88	6.12	33.816	0.379	8.92E+08	29.60	6.08E+08	2.61E+08
300.040	523	41.89	3.88	12.59	-	-	-	-	-	-	-	-	-
300.040	400	-	-	-	-	-	-	-	-	-	-	-	-
300.040	300	-	-	-	-	-	-	-	-	-	-	-	-
300.040	200	-	-	-	-	-	-	-	-	-	-	-	-
300.040	150	42.41	4.82	10.26	-	-	-	-	-	-	-	-	-
300.040	110	45.08	3.82	13.76	2.41	0.33	8.42	-	-	3.76E+08	3.13	2.65E+08	1.01E+08
300.040	80	38.13	8.32	5.34	3.18	0.54	6.85	-	0.179	8.09E+08	8.36	4.91E+08	2.96E+08
300.040	50	45.82	5.02	10.64	4.24	0.72	6.90	5.332	0.271	9.10E+08	15.06	5.92E+08	2.99E+08
300.040	30	44.82	6.02	8.68	9.83	1.70	6.74	6.036	0.149	1.04E+09	74.06	7.98E+08	2.28E+08
300.040	15	60.41	5.42	13.00	28.72	5.28	6.34	6.286	13.065	2.64E+09	211.57	2.37E+09	2.42E+08
300.040	10	50.91	4.92	12.07	95.56	16.39	6.80	2.256	14.777	2.69E+09	194.18	2.42E+09	2.41E+08
300.040	0	-	-	-	98.62	16.84	6.83	17.189	16.973	2.74E+09	168.28	2.48E+09	2.32E+08

Table 7.1 cont'd

Table 7.1 cont'd

Station	Depth	DOC	DON	DOC:DON	POC	PN	POC:PN	PP	chla	Bacterial Abundance	Bacterial Activity	HNA	LNA
200.040	730	40.99	2.92	16.37	-	-	-	-	-	-	-	-	-
200.040	600	-	-	-	-	-	-	-	-	-	-	-	-
200.040	450	-	-	-	-	-	-	-	-	-	-	-	-
200.040	360	-	-	-	-	-	-	-	-	-	-	-	-
200.040	200	40.79	3.92	12.13	-	-	-	-	-	-	-	-	-
200.040	100	43.32	6.12	8.25	1.31	0.17	9.01	-	-	3.47E+08	1.44	2.43E+08	9.21E+07
200.040	75	42.10	6.22	7.89	1.05	0.14	8.47	-	0.089	2.64E+08	2.19	1.86E+08	6.93E+07
200.040	60	43.38	5.02	10.08	2.06	0.23	10.39	2.127	0.157	3.22E+08	3.33	2.21E+08	9.16E+07
200.040	40	47.32	4.42	12.48	1.90	0.23	9.76	45.431	0.217	5.40E+08	6.79	3.87E+08	1.39E+08
200.040	25	47.10	4.42	12.43	3.41	0.49	8.11	41.295	0.374	6.19E+08	13.19	4.51E+08	1.52E+08
200.040	15	-	-	-	3.85	0.63	7.08	35.683	0.516	7.18E+08	17.74	5.32E+08	1.70E+08
200.040	0	46.91	4.12	13.28	14.81	2.59	6.66	27.095	0.866	4.35E+08	112.11	3.02E+08	1.24E+08
200.000	662	40.14	3.61	12.97	-	-	-	-	-	-	-	-	-
200.000	500	-	-	-	-	-	-	-	-	-	-	-	-
200.000	400	-	-	-	-	-	-	-	-	-	-	-	-
200.000	300	-	-	-	-	-	-	-	-	-	-	-	-
200.000	250	39.06	3.92	11.62	-	-	-	-	-	-	-	-	-
200.000	100	42.43	4.32	11.45	1.33	0.19	8.24	-	-	4.17E+08	2.01	2.90E+08	1.09E+08
200.000	75	44.05	4.12	12.47	1.96	0.29	7.90	-	0.15	4.97E+08	3.33	3.18E+08	1.63E+08
200.000	45	43.73	6.92	7.37	2.85	0.48	6.96	7.305	0.31	5.75E+08	9.68	3.94E+08	1.69E+08
200.000	30	42.51	5.12	9.68	5.69	1.01	6.58	15.646	0.37	9.42E+08	26.95	7.06E+08	2.18E+08
200.000	20	45.93	9.92	5.40	11.43	2.05	6.50	24.478	0.53	1.43E+09	121.54	1.21E+09	2.01E+08
200.000	10	58.28	10.52	6.46	22.12	4.07	6.34	58.797	1.12	2.88E+09	408.52	2.68E+09	1.97E+08
200.000	0	57.64	8.62	7.80	20.41	3.78	6.30	66.724	1.21	3.10E+09	414.83	2.90E+09	1.98E+08

Table 7.1 cont'd

Station	Depth	DOC	DON	DOC:DON	POC	PN	POC:PN	PP	chl*a*	Bacterial Abundance	Bacterial Activity	HNA	LNA
200.100	415	41.87	4.61	10.59	-	-	-	-	-	-	-	-	-
200.100	360	-	-	-	-	-	-	-	-	-	-	-	-
200.100	270	-	-	-	-	-	-	-	-	-	-	-	-
200.100	175	-	-	-	-	-	-	-	-	-	-	-	-
200.100	125	40.58	4.12	11.49	-	-	-	-	-	-	-	-	-
200.100	100	38.85	3.42	13.25	1.35	0.20	7.97	-		3.13E+08	1.18	2.27E+08	7.32E+07
200.100	85	44.22	5.22	9.88	2.37	0.37	7.54	-	0.090	4.05E+08	2.18	2.74E+08	1.20E+08
200.100	50	45.89	-		3.05	0.48	7.47	3.746	0.271	1.07E+09	9.89	6.18E+08	4.21E+08
200.100	30	46.90	5.52	9.91	9.94	1.89	6.12	11.781	0.709	1.18E+09	66.23	8.15E+08	3.42E+08
200.100	17	54.64	8.12	7.85	18.50	3.56	6.06	33.230	1.036	1.28E+09	151.29	1.02E+09	2.44E+08
200.100	10	55.77	5.32	12.23	18.21	3.49	6.09	46.074	1.337	1.31E+09	142.32	1.07E+09	2.19E+08
200.100	0	58.45	5.42	12.58	21.52	4.19	6.00	53.314	1.493	1.33E+09	153.72	1.10E+09	2.11E+08
200.200	3643	-	4.64	-	-	-	-	-	-	-	-	-	-
200.200	3000	-	-	-	-	-	-	-	-	-	-	-	-
200.200	1500	-	5.15	-	-	-	-	-	-	-	-	-	-
200.200	700	-	-	-	-	-	-	-	-	-	-	-	-
200.200	370	49.18	4.42	12.98	-	-	-	-	-	-	-	-	-
200.200	170	44.47	4.52	11.47	1.33	0.17	8.98	-	-	3.45E+08	0.36	2.14E+08	1.16E+08
200.200	100	41.41	4.12	11.72	1.60	0.26	7.14	-	0.171	4.20E+08	1.64	2.72E+08	1.29E+08
200.200	70	46.68	4.52	12.04	4.43	0.76	6.77	13.069	0.269	4.49E+08	1.71	2.95E+08	1.35E+08
200.200	60	44.02	4.42	11.61	3.92	0.67	6.79	12.299	0.291	8.55E+08	5.92	5.93E+08	2.34E+08
200.200	30	46.43	4.72	11.47	5.08	0.94	6.33	9.191	0.148	7.31E+08	7.36	4.20E+08	2.94E+08
200.200	10	47.93	5.82	9.60	3.57	0.63	6.64	6.811	0.076	3.59E+08	3.95	1.86E+08	1.61E+08
200.200	0	51.85	4.42	13.68	5.36	1.06	5.91	7.181	0.101	3.29E+08	3.65	1.70E+08	1.47E+08

Table 7.2: Full-depth profiles of all parameters used in analyses of chapter 4 from PAL LTER research cruise LMG1701. Inorganic nutrients are stated in µmol x L^{-1}, Temperature in °C, Density anomaly in kg m^{-3}, Depth and MLD in meters. SIRD (sea ice retreat days) in days, %SIM = % of sea ice meltwater, %MET= % of meteoric meltwater (glacial), %CDW=% of Circumpolar Deepwater

Station	Depth	NO_3^-	PO_4^-	$Si(OH)_4^-$	Salinity	Temperature	Density anomaly	MLD	SIRD < 15 %	%SIM	%MET	%CDW
600.040	1300	31.83	2.16	88.29	34.69	1.40	27.78	8	22	-0.2	0.3	99.9
600.040	700	33.16	2.19	88.73	34.68	1.33	27.77	8	22	-0.3	0.4	99.9
600.040	320	33.12	2.19	86.97	34.63	1.06	27.74	8	22	-0.3	0.5	99.8
600.040	200	33.02	2.15	82.49	34.58	0.89	27.71	8	22	-0.3	0.7	99.6
600.040	125	32.73	2.15	78	34.47	0.41	27.64	8	22	-0.7	1.3	99.4
600.040	100	32.73	2.13	79.36	34.39	0.25	27.59	8	22	-0.5	1.4	99.1
600.040	75	30.36	2.02	74.24	34.22	-0.19	27.46	8	22	-0.6	2.0	98.7
600.040	50	30.37	2.03	74.95	34.05	-0.26	27.31	8	22	-0.4	2.3	98.1
600.040	40	32.07	2.15	78.66	33.89	-0.66	27.20	8	22	-0.5	2.8	97.7
600.040	30	30.26	2.08	79.06	33.75	-0.83	27.02	8	22	0.0	2.8	97.2
600.040	5	19.55	1.39	70.58	33.14	2.44	26.41	8	22	1.5	3.4	95.1
600.040	0	16.8	1.17	68.87	32.98	1.95	26.40	8	22	1.7	3.6	94.6
600.100	593	33.46	2.25	95.13	34.70	1.40	27.78	29	48	-0.3	0.3	100
600.100	500	33.05	2.18	91.13	34.70	1.39	27.78	29	48	0.2	0.0	99.9
600.100	400	33.38	2.19	89.64	34.69	1.34	27.77	29	48	-0.5	0.5	100
600.100	300	33.11	2.18	83.36	34.65	1.18	27.75	29	48	-0.4	0.6	99.9
600.100	200	33.4	2.18	83	34.60	0.90	27.73	29	48	-0.5	0.8	99.7
600.100	100	32.6	2.11	77.53	34.32	-0.08	27.56	29	48	-0.3	1.4	98.9
600.100	65	27.94	1.88	69.15	34.02	0.00	27.32	29	48	-0.2	2.2	98.0
600.100	50	26.03	1.78	67.91	33.88	0.43	27.21	29	48	-0.1	2.5	97.6
600.100	40	22.93	1.57	65.64	33.85	1.06	27.14	29	48	0.2	2.4	97.4
600.100	30	21.92	1.43	63.16	33.78	1.34	26.95	29	48	0.3	2.5	97.2
600.100	10	19.93	1.25	65.6	33.65	2.31	26.87	29	48	0.3	2.9	96.8
600.100	0	19.92	1.26	64.71	33.65	2.31	26.87	29	48	0.1	3.0	96.9
600.200	3040	33.3	2.2	119.53	34.70	0.45	27.84	34	-38	-0.9	0.8	100
600.200	2500	33.21	2.19	113.89	34.71	0.49	27.84	34	-38	-1.0	0.9	100
600.200	1500	32.81	2.12	100.98	34.72	0.94	27.82	34	-38	-0.5	0.4	100
600.200	500	33.1	2.1	80.13	34.72	1.77	27.76	34	-38	-0.1	0.1	100
600.200	250	34.43	2.21	74.72	34.64	1.87	27.69	34	-38	0.2	0.1	99.7
600.200	100	32.96	2.12	63.39	34.22	-0.34	27.49	34	-38	-0.3	1.7	98.6
600.200	70	30.15	1.99	57.63	34.06	-0.82	27.38	34	-38	-0.6	2.4	98.2
600.200	50	27.66	1.72	46.52	33.97	-0.15	27.28	34	-38	-0.1	2.3	97.8
600.200	40	26.17	1.6	42.08	33.91	0.95	27.17	34	-38	-0.5	2.7	97.7
600.200	25	25.57	1.49	37.45	33.88	1.92	27.08	34	-38	-0.3	2.7	97.6
600.200	10	25.38	1.5	33.72	33.87	2.20	27.05	34	-38	-0.1	2.5	97.5
600.200	0	25.35	1.52	34.28	33.87	2.21	27.05	34	-38	-0.1	2.6	97.6

Table 7.2 cont'd

Station	Depth	NO_3^-	PO_4^-	$Si(OH)_4^-$	Salinity	Temperature	Density anomaly	MLD	SIRD < 15 %	% SIM	% MET	% CDW
500.200	2672	33.19	2.18	115.91	34.70	0.42	27.85	35	114	-0.9	0.8	100
500.200	2000	32.95	2.16	110.25	34.71	0.54	27.85	35	114	-0.7	0.6	100
500.200	1000	32.63	2.13	95.1	34.73	1.17	27.82	35	114	-0.3	0.2	100
500.200	500	32.73	2.12	83.72	34.73	1.65	27.78	35	114	0.0	0.0	100
500.200	200	34.3	2.21	75.93	34.56	1.21	27.69	35	114	0.1	0.4	99.5
500.200	90	29.17	1.95	58.77	34.09	-0.97	27.44	35	114	-0.9	2.6	98.3
500.200	75	28.52	1.92	58.39	34.07	-0.89	27.41	35	114	-0.8	2.5	98.3
500.200	60	27.53	1.8	51.51	34.03	-0.51	27.35	35	114	-0.7	2.6	98.1
500.200	45	26.47	1.65	47.86	33.97	0.37	27.25	35	114	-0.5	2.6	97.9
500.200	25	25.58	1.45	37.14	33.90	1.77	27.11	35	114	-0.4	2.7	97.7
500.200	10	25.25	1.45	37.03	33.90	1.81	27.11	35	114	-0.1	2.5	97.6
500.200	0	25.24	1.45	36.85	33.91	1.80	27.11	35	114	-0.4	2.7	97.7
500.100	424	32.97	2.18	91.3	34.71	1.42	27.79	13	51	-0.4	0.4	100
500.100	375	33.05	2.17	90.31	34.71	1.43	27.78	13	51	-0.2	0.2	100
500.100	280	33.36	2.18	89.51	34.70	1.45	27.77	13	51	0.0	0.1	99.9
500.100	200	33.53	2.18	88.24	34.64	1.29	27.74	13	51	-0.1	0.4	99.8
500.100	150	33.19	2.21	83.19	34.53	0.85	27.69	13	51	0.0	0.6	99.4
500.100	100	33.45	2.2	81.47	34.26	-0.37	27.51	13	51	0.0	1.4	98.7
500.100	70	31.69	2.11	78.31	34.05	-0.61	27.36	13	51	0.2	1.8	98.0
500.100	50	28.4	1.89	69.87	33.93	-0.49	27.23	13	51	0.1	2.2	97.7
500.100	30	25.45	1.73	67.67	33.79	-0.04	27.12	13	51	-0.2	2.9	97.4
500.100	20	23.61	1.58	63.9	33.76	0.47	26.98	13	51	0.4	2.5	97.1
500.100	10	18.81	1.16	62.7	33.59	2.70	26.83	13	51	-0.1	3.3	96.7
500.100	0	18.13	1.1	62.84	33.61	2.68	26.83	13	51	0.1	3.1	96.8
500.060	290	33.38	2.18	89.41	34.67	1.23	27.76	23	14	-0.4	0.5	99.9
500.060	200	33.55	2.22	89.56	34.61	1.01	27.73	23	14	-0.4	0.7	99.8
500.060	150	33.29	2.2	83.53	34.51	0.54	27.66	23	14	-0.2	0.8	99.4
500.060	125	33.31	2.21	83.17	34.40	0.16	27.61	23	14	-0.5	1.3	99.1
500.060	100	33.14	2.21	80.59	34.25	0.01	27.50	23	14	-0.7	2.0	98.8
500.060	80	32.01	2.11	75.93	34.09	0.00	27.37	23	14	-1.0	2.6	98.4
500.060	50	25.56	1.71	58.23	33.91	0.00	27.20	23	14	-1.0	3.2	97.8
500.060	45	24.15	1.57	56.13	33.85	0.54	27.17	23	14	-1.0	3.3	97.7
500.060	35	24.6	1.65	63.34	33.76	0.14	27.06	23	14	-0.4	3.1	97.3
500.060	25	18.15	1.21	53.88	33.69	1.56	26.85	23	14	-0.1	3.1	97.0
500.060	10	15.99	0.99	64.05	33.49	2.90	26.69	23	14	0.2	3.4	96.4
500.060	0	15.83	0.98	65.93	33.49	2.90	26.69	23	14	0.5	3.2	96.3

Table 7.2 cont'd

Station	Depth	NO_3^-	PO_4^-	$Si(OH)_4^-$	Salinity	Temperature	Density anomaly	MLD	SIRD < 15 %	% SIM	% MET	% CDW
400.040	270	33.35	2.21	89.62	34.70	1.41	27.78	13	20	0.0	0.1	99.9
400.040	225	27.69	2.04	71.15	34.64	1.24	27.74	13	20	0.0	0.3	99.7
400.040	200	34.09	2.23	86.77	34.61	1.14	27.72	13	20	-0.8	1.0	99.8
400.040	150	33.69	2.24	85.73	34.54	0.84	27.66	13	20	-0.9	1.3	99.6
400.040	125	34.22	2.28	85.77	34.46	0.55	27.61	13	20	-1.0	1.6	99.4
400.040	100	33.8	2.22	83.77	34.33	0.05	27.54	13	20	-1.0	1.9	99.1
400.040	80	33.21	2.18	78.66	34.16	-0.48	27.45	13	20	-0.8	2.3	98.5
400.040	50	31.09	2.09	76.56	33.95	-0.78	27.20	13	20	-0.7	2.8	97.9
400.040	35	30.41	2.03	71.81	33.67	-0.77	27.04	13	20	-0.1	3.2	97.0
400.040	20	23.24	1.59	67.73	33.54	0.32	26.75	13	20	0.2	3.3	96.5
400.040	10	19.44	1.36	67.5	33.20	1.18	25.97	13	20	0.7	3.8	95.5
400.040	0	10.75	0.8	61.82	32.83	1.80	25.97	13	20	0.9	4.7	94.3
400.100	337	33.51	2.22	93.1	34.71	1.52	27.78	30	50	-0.6	0.5	100
400.100	320	33.28	2.22	95.27	34.71	1.52	27.78	30	50	0.2	-0.1	99.9
400.100	265	33.68	2.17	85.93	34.70	1.56	27.76	30	50	0.0	0.1	99.9
400.100	175	33.95	2.21	84.37	34.61	1.23	27.71	30	50	-0.3	0.6	99.7
400.100	140	34.42	2.21	81.38	34.50	0.69	27.66	30	50	-0.5	1.1	99.4
400.100	100	33.31	2.2	82.32	34.29	-0.17	27.52	30	50	-0.8	1.9	98.9
400.100	70	29.94	2	69.16	33.95	-1.03	27.31	30	50	-0.7	2.8	97.9
400.100	50	26.64	1.79	60.97	33.84	-0.54	27.19	30	50	-0.6	3.0	97.5
400.100	30	24.36	1.64	64.79	33.66	0.04	26.85	30	50	0.1	3.0	96.9
400.100	20	19.14	1.2	62.04	33.49	2.01	26.76	30	50	0.2	3.4	96.4
400.100	10	18.79	1.18	63.1	33.49	2.15	26.76	30	50	0.4	3.3	96.3
400.100	0	18.8	1.19	63.97	33.49	2.15	26.76	30	50	0.1	3.5	96.4
400.200	2700	33.28	2.18	108.52	34.70	0.41	27.85	38	117	-0.9	0.8	100
400.200	2000	33.14	2.2	109.77	34.71	0.58	27.84	38	117	-0.7	0.6	100
400.200	800	32.66	2.12	91.35	34.73	1.33	27.81	38	117	-0.3	0.2	100
400.200	350	33.22	2.14	77.67	34.71	1.84	27.75	38	117	0.1	0.0	99.9
400.200	200	34.19	2.2	77.51	34.57	1.19	27.69	38	117	-0.1	0.5	99.6
400.200	100	30.91	2.08	64.03	34.15	-1.03	27.45	38	117	-0.9	2.4	98.5
400.200	75	29.81	1.98	61.56	34.10	-1.04	27.40	38	117	-0.4	2.2	98.3
400.200	60	29.4	1.94	61.16	34.08	-0.95	27.38	38	117	-1.3	2.9	98.4
400.200	40	26.76	1.74	54.66	33.98	0.22	27.20	38	117	-0.7	2.7	98.0
400.200	30	23.12	1.25	47.41	33.92	1.61	27.13	38	117	-0.8	3.0	97.8
400.200	10	22.57	1.22	48.49	33.92	2.14	27.10	38	117	-0.8	2.9	97.8
400.200	0	22.51	1.21	48.1	33.92	2.15	27.09	38	117	-0.8	3.0	97.8

Table 7.2 cont'd

Station	Depth	NO_3^-	PO_4^-	$Si(OH)_4^-$	Salinity	Temperature	Density anomaly	MLD	SIRD < 15 %	%SIM	%MET	%CDW
300.200	3023	33.55	2.22	120	34.71	0.40	27.86	19	116	-1.0	0.9	100
300.200	1500	33.01	2.14	98.22	34.72	1.01	27.83	19	116	-0.5	0.4	100
300.200	750	32.74	2.1	82.42	34.73	1.62	27.79	19	116	-0.1	0.1	100
300.200	500	32.82	2.11	78.05	34.72	1.92	27.75	19	116	0.2	-0.1	99.9
300.200	275	34.52	2.21	73.85	34.65	2.02	27.69	19	116	0.2	0.1	99.7
300.200	100	31.6	2.05	60.32	34.17	-0.92	27.49	19	116	-0.5	2.0	98.5
300.200	85	30.17	1.99	58.52	34.12	-1.05	27.44	19	116	-0.5	2.1	98.3
300.200	70	29.31	1.94	57.79	34.09	-0.97	27.39	19	116	-1.0	2.6	98.4
300.200	50	28.01	1.81	50.14	34.04	-0.51	27.33	19	116	-1.1	2.8	98.2
300.200	30	25.36	1.61	38.84	33.92	0.54	27.19	19	116	-0.2	2.5	97.7
300.200	10	24.15	1.56	33.6	33.83	2.03	27.05	19	116	-0.1	2.7	97.4
300.200	0	24.03	1.57	33.19	33.83	2.11	27.04	19	116	0.0	2.6	97.4
300.100	470	32.81	2.18	95.52	34.73	1.31	27.80	25	54	-0.4	0.3	100
300.100	425	32.85	2.15	88.79	34.72	1.51	27.79	25	54	-0.3	0.3	100
300.100	350	32.83	2.12	83.07	34.72	1.61	27.77	25	54	-0.3	0.3	100
300.100	270	33.45	2.17	80.78	34.70	1.77	27.75	25	54	-0.3	0.3	100
300.100	200	34.01	2.18	79.37	34.64	1.61	27.71	25	54	-0.3	0.5	99.8
300.100	100	32.45	2.11	70.66	34.21	-0.88	27.49	25	54	-1.2	2.5	98.7
300.100	80	30.72	2.06	68.88	34.07	-1.06	27.42	25	54	-0.9	2.6	98.3
300.100	50	28.34	1.86	60.42	33.98	-0.32	27.32	25	54	-0.8	2.8	98.0
300.100	40	23.67	1.31	52.78	33.89	1.37	27.21	25	54	-0.3	2.7	97.7
300.100	30	22.29	1.26	53.23	33.87	1.63	27.13	25	54	-0.5	2.9	97.6
300.100	15	22.39	1.35	53.42	33.81	1.83	27.04	25	54	-0.4	3.0	97.4
300.100	0	22.27	1.34	54.07	33.81	1.83	27.03	25	54	-1.0	3.5	97.5
300.040	523	32.64	2.16	94.62	34.72	1.36	27.80	14	51	-0.6	0.5	100
300.040	400	33.31	2.2	94.6	34.71	1.41	27.78	14	51	-0.5	0.4	100
300.040	300	33.33	2.19	88.35	34.68	1.46	27.76	14	51	-0.5	0.5	100
300.040	200	34.39	2.27	87.79	34.57	0.99	27.71	14	51	-0.3	0.7	99.6
300.040	150	33.51	2.2	83.41	34.42	0.33	27.62	14	51	-0.5	1.3	99.2
300.040	110	32.69	2.11	70.19	34.17	-0.81	27.48	14	51	-0.8	2.3	98.6
300.040	80	27.47	1.84	66.73	33.87	-0.29	27.21	14	51	-0.5	2.9	97.6
300.040	50	25.73	1.75	64.23	33.67	-0.37	27.05	14	51	-0.2	3.2	97.0
300.040	30	21.83	1.5	63.51	33.40	1.43	26.73	14	51	0.4	3.5	96.1
300.040	15	6.21	0.32	57.92	32.86	1.34	26.30	14	51	0.3	5.2	94.6
300.040	10	3.32	0.19	56.13	32.80	1.37	26.25	14	51	0.2	5.4	94.4
300.040	0	0.77	0.1	52.02	32.64	1.32	26.13	14	51	0.5	5.6	93.9

Table 7.2 cont'd

Station	Depth	NO_3^-	PO_4^-	$Si(OH)_4^-$	Salinity	Temperature	Density anomaly	MLD	SIRD < 15 %	% SIM	% MET	% CDW
200.040	730	33.11	2.21	99.84	34.72	1.22	27.81	14	5	-0.6	0.5	100
200.040	600	33.45	2.23	99.76	34.72	1.32	27.80	14	5	-0.3	0.3	100
200.040	450	33.19	2.19	91.11	34.71	1.39	27.78	14	5	-0.3	0.3	100
200.040	360	33.81	2.23	92.6	34.69	1.40	27.77	14	5	-0.2	0.3	99.9
200.040	200	34.32	2.24	86.13	34.57	0.98	27.70	14	5	-0.8	1.1	99.7
200.040	100	33.1	2.2	84.21	34.03	-0.72	27.34	14	5	-0.6	2.5	98.1
200.040	75	32.03	2.13	84.1	33.80	-1.19	27.19	14	5	-1.0	3.5	97.5
200.040	60	30.73	2	79.81	33.69	-1.52	27.11	14	5	-1.5	4.2	97.3
200.040	40	30.14	1.99	77.08	33.60	-1.70	27.04	14	5	-1.6	4.5	97.1
200.040	25	29.65	1.94	74.71	33.54	-1.71	26.97	14	5	-1.3	4.5	96.8
200.040	15	29.05	1.92	73.76	33.52	-1.71	26.63	14	5	-1.4	4.6	96.8
200.040	0	19.33	1.23	66.65	32.96	1.08	26.40	14	5	0.8	4.4	94.8
200.000	662	33.08	2.18	94.03	34.72	1.33	27.80	9	6	-0.3	0.3	100
200.000	500	33.21	2.19	95.26	34.72	1.38	27.79	9	6	-0.3	0.3	100
200.000	400	33.5	2.21	91.67	34.71	1.41	27.78	9	6	-0.4	0.4	100
200.000	300	33.56	2.16	87.71	34.69	1.45	27.77	9	6	-0.3	0.3	99.9
200.000	250	33.68	2.2	86.59	34.67	1.43	27.75	9	6	0.1	0.1	99.8
200.000	100	33.19	2.16	77.96	34.17	-0.75	27.48	9	6	-0.8	2.3	98.6
200.000	75	30.18	2.01	72.7	33.88	-1.20	27.26	9	6	-0.9	3.2	97.7
200.000	45	27.88	1.86	71.03	33.62	-1.08	27.04	9	6	-1.0	4.0	97.0
200.000	30	27.61	1.87	72.62	33.63	-1.12	26.98	9	6	-1.1	4.0	97.0
200.000	20	25.52	1.78	69.38	33.46	-0.92	26.91	9	6	-0.5	4.1	96.4
200.000	10	13.65	0.84	61.97	32.89	2.38	26.25	9	6	0.9	4.6	94.5
200.000	0	13.61	0.85	61.99	32.89	2.43	26.25	9	6	0.9	4.6	94.5
200.100	415	33.81	2.27	100.71	34.71	1.39	27.79	11	56	-0.4	0.4	100
200.100	360	33.89	2.23	92.78	34.70	1.40	27.78	11	56	-0.7	0.7	100
200.100	270	26.16	1.77	56.66	34.68	1.39	27.76	11	56	-0.4	0.4	99.9
200.100	175	35.02	2.28	86.35	34.56	0.96	27.68	11	56	-0.4	0.8	99.6
200.100	125	34.24	2.24	84.55	34.40	0.30	27.59	11	56	-0.6	1.4	99.2
200.100	100	34.14	2.24	88.25	34.23	-0.09	27.49	11	56	-0.3	1.7	98.6
200.100	85	31.22	2.04	68.32	34.13	-0.87	27.40	11	56	-0.9	2.4	98.4
200.100	50	33.88	2.24	91.31	33.86	-0.19	27.20	11	56	-0.5	2.9	97.6
200.100	30	22.17	1.49	62.21	33.71	1.15	26.99	11	56	-0.5	3.4	97.2
200.100	17	18.55	1.17	62.71	33.51	2.93	26.83	11	56	-0.2	3.7	96.6
200.100	10	17.95	1.15	63.16	33.20	2.57	26.53	11	56	0.5	4.0	95.5
200.100	0	17.57	1.11	62.11	33.20	2.57	26.50	11	56	0.3	4.1	95.5
200.200	3643	33.66	2.24	123.94	34.70	0.41	27.86	32	125	-1.0	0.9	100
200.200	3000	33.47	2.21	115.07	34.70	0.50	27.85	32	125	-0.9	0.8	100
200.200	1500	32.73	2.13	93.05	34.73	1.22	27.82	32	125	-0.5	0.4	100
200.200	700	33.08	2.12	79.59	34.72	1.88	27.76	32	125	0.1	0.0	99.9
200.200	370	34.39	2.23	72.42	34.64	2.05	27.68	32	125	0.1	0.1	99.7
200.200	170	35.78	2.28	60.71	34.43	1.86	27.53	32	125	0.5	0.5	99.1
200.200	100	32.86	2.11	49.79	34.11	0.00	27.40	32	125	0.4	1.5	98.1
200.200	70	29.99	1.96	43.91	33.98	-0.96	27.33	32	125	-0.1	2.3	97.9
200.200	60	29.27	1.94	43.13	33.95	-1.11	27.31	32	125	0.2	2.1	97.7
200.200	30	25.7	1.69	37.31	33.83	0.41	27.07	32	125	-0.3	2.8	97.5
200.200	10	25.14	1.63	31.84	33.82	1.90	27.03	32	125	-0.3	2.9	97.5
200.200	0	25.45	1.64	32.26	33.82	1.91	27.03	32	125	-0.1	2.7	97.4

Table 8: PAL LTER (chapter 4) depth-integrated standing stocks of organic carbon and nitrogen, Chla and bacterial abundance. Maximum rates of primary production (PP) and leucine incorporation. All values are calculated for the top 50m. Stations in italics are interpolated as there was no sample collected at 50m depth.

Station	Depth (m)	DOC (mmol C m^{-2})	DON (mmol N m^{-2})	POC (mmol C m^{-2})	TOC (mmol C m^{-2})	PN (mmol N m^{-2})	TON (mmol N m^{-2})	PP (mg m^{-3} day^{-1})	Chl a (mg m^{-2})	Leucine (pmol L^{-1} hr^{-1})	Bacterial abundance	$\delta^{18}O$ (‰)
600.200	50	2602	251	631	3233	70	385	11.74	19.78	14.95	3.34E+10	
500.200	*50*	*2396*	*270*	*562*	*2958*	*71*	*372*	*18.08*	*26.62*	*18.28*	*4.99E+10*	
400.200	*50*	*2329*	*294*	*875*	*3205*	*158*	*403*	*41.84*	*46.32*	*21.73*	*3.02E+10*	
300.200	50	2234	237	200	1540	33	397	16.56	6.86	8.46	2.24E+10	
200.200	*50*	*2346*	*251*	*221*	*2567*	*40*	*352*	*12.30*	*9.71*	*7.36*	*3.01E+10*	
600.100	50	2484	253	1207	3691	136	470	17.83	54.32	61.93	3.80E+10	
500.100	50	2459	181	678	3137	95	409	16.67	57.20	41.49	2.29E+10	
400.100	50	2479	226	822	3301	127	417	55.14	60.47	57.18	4.56E+10	
300.100	50	1953	271	875	2828	163	398	50.09	52.61	62.66	4.37E+10	
200.100	50	2545	301	642	3187	122	418	53.31	58.45	43.60	6.07E+10	
600.040	50	2474	232	700	3174	97	456	46.76	54.97	17.22	3.68E+10	
500.060	50	2548	247	995	3543	81	397	101.95	56.02	69.97	2.65E+10	
400.040	50	1991	248	204	2195	21	357	61.30	57.86	35.30	4.59E+10	
300.040	50	2228	292	1711	3940	297	601	17.19	60.41	331.67	8.76E+10	
200.040	*50*	*1744*	*215*	*235*	*1979*	*37*	*252*	*45.43*	*47.32*	*19.24*	*2.81E+10*	
200.000	*50*	*2408*	*385*	*577*	*2985*	*105*	*551*	*66.72*	*58.28*	*29.81*	*7.85E+10*	

Station	Depth (m)	NO_3^- (mmol N m^{-2})	PO_4^- (mmol P m^{-2})	SiO_4^- (mmol Si m^{-2})	NO_3^- rem (mmol N m^{-2})	PO_4^- rem (mmol P m^{-2})	SiO_4^- rem (mmol Si m^{-2})	S min	Tmax (°C)	Tmin (°C)	MLD (m)	$\delta^{18}O$ (‰)
600.200	50	1293	77	1913	372	33	4063	33.87	2.21	-0.152	34	-0.564
600.100	50	1087	71	3251	586	41	1506	33.65	2.31	0.431	29	-0.599
600.040	50	1337	92	3776	319	18	661	32.98	2.44	-0.829	8	-0.373
500.200	*60*	*1292*	*76*	*2042*	*370*	*33*	*3771*	*33.90*	*1.81*	*-0.506*	*35*	*-0.232*
500.100	50	1181	78	3294	472	31	1271	33.59	2.71	-0.492	13	-0.415
500.060	50	997	65	3004	672	44	1467	33.49	2.90	0.002	23	-0.342
400.200	*50*	*1213*	*70*	*2534*	*452*	*39*	*2895*	*33.92*	*2.15*	*-0.954*	*38*	*-0.303*
400.100	50	1105	72	3153	570	39	1502	33.49	2.15	-0.538	30	-0.363
400.040	50	1228	84	3482	440	27	999	32.83	1.80	-0.784	13	-0.382
300.200	50	1270	82	1948	408	29	4052	33.83	2.11	-0.511	19	-0.347
300.100	50	1160	68	2702	481	41	2074	33.81	1.83	-0.318	25	-0.396
300.040	50	730	49	3014	902	59	1717	32.64	1.43	-0.374	14	-0.257
200.200	*50*	*1311*	*86*	*1815*	*372*	*26*	*4381*	*33.82*	*1.91*	*-1.11*	*32*	*-0.305*
200.100	50	1131	74	3414	560	39	1621	33.20	2.93	-0.187	11	-0.268
200.040	*50*	*1410*	*92*	*3722*	*247*	*18*	*1274*	*32.96*	*1.08*	*-1.71*	*14*	*-0.278*
200.000	*50*	*1175*	*78*	*3423*	*502*	*31*	*1278*	*32.89*	*2.43*	*-1.119*	*9*	*-0.270*